THE UNIVERSITY *of* EDINBURGH

Using Novel Models of Glioma for Cancer Discovery Science

Paul Martin Brennan
BSc (Hons), MB BChir, MRCS

This thesis is submitted in fulfilment of the requirements for the degree of
Doctor of Philosophy
at the University of Edinburgh

2014

Declaration

This thesis has been composed by the candidate.
The work is the candidate's own.
The work has not been submitted for any other degree or professional qualification except as specified.

Paul Brennan

Abstract

The prognosis for patients diagnosed with glioma has changed little over the past two decades. Many therapies that appeared promising in preclinical studies have been unsuccessful in the clinic. In an attempt to address this problem I developed a method for the efficient derivation of glioma primary cultures from fresh human brain tumours. These cultures are enriched for putative cancer stem-like cells that are thought to be responsible for glioma initiation, therapy resistance and recurrence. This mechanism of tumour development is a departure from the traditional multistep model of cancer. It is hoped that preclinical models incorporating glioma stem-like cells will more effectively recapitulate the biology of human disease and so better predict the likely clinical efficacy of inhibitor compounds tested in vitro and in the preclinical setting.

In contrast to the majority of the existing literature, I identified two distinct tumour-derived glioma stem-like cell phenotypes in my primary cultures that I have called 'branched' and 'flat.' The branched cells had similarities to the radial glia-like cells previously described in glioma stem-like cultures. In contrast, the flat cells had mesenchymal-like features. I discuss the implications of these observations for understanding glioma cell biology. I describe the development of high content phenotypic assays that incorporate these putative glioma stem-like cells. I screened inhibitor compounds of the PI3 kinase pathway, which is important in glioma cell behaviour, and identified that PIK75, a drug that targets the p110α catalytic subunit of PI3 kinase, inhibited growth of all the primary cells tested. I examined PIK75 activity in some detail.

In vivo models of glioma are used to validate the findings of in vitro compound screening, so I describe my attempt to develop a novel genetically engineered mouse model designed to initiate glioma formation from the glioma stem-like cell. Surprisingly, these mice actually developed malignant peripheral nerve sheath

tumours and that gave me a novel insight into the pathogenesis of this rare disease. This also informed future work on my long-term goal of generating a genetic model of glioma that recapitulates human disease.

Acknowledgements

I would like to thank my supervisor Margaret Frame for her help, guidance and encouragement throughout this thesis project. I also received helpful advice and assistance from many people in the Edinburgh Cancer Centre and the Institute for Genetics and Molecular Medicine, especially Neil Carragher, Val Brunton, Melanie Rall and Kenneth Macleod. The work would not have been possible without the support given by the Edinburgh Clinical Academic Track programme, in particular from John Iredale, Brian Walker and from the Wellcome Trust who provided funding.

Throughout this study, I have benefited from the input of many scientists from different laboratories around the University of Edinburgh. Siddharthan Chandran and his team, especially Bilada Bilcan, David Hampton, Andrea Serio and David Story provided practical support and guidance in developing my primary glioma culture method. James Ironside, Colin Smith and Diane Ritchie provided technical assistance and diagnostic input into the characterisation of my in vivo model. Eddy Maher, Ariana Carpico and Roddy Murray at the NHS Lothian Cytogenetics Unit, Edinburgh provided technical assistance for the array CGH work. All the genetically engineered mice and subcutaneous xenotransplantation mice were housed and cared for at the Biological Research Facility, Western General Hospital, Edinburgh. The CNP-cre mice were a kind gift from Peter Brophy and Klaus Amin Nave. The orthotopic xenotransplantation experiments were performed in collaboration with Anthony Chalmers and Lesley McPhail at the Beatson Institute for biological sciences, Glasgow.

None of this would have been possible without the tolerance of Mary, my wife.

TABLE OF CONTENTS

LIST OF TABLES

Chapter 1

Chapter 2

Chapter 3

LIST OF FIGURES

Chapter 1

Chapter 2

Chapter 3

Chapter 4

Chapter 5

ABBREVIATIONS

αSMA	Alpha smooth muscle actin
5-ALA	5-aminolaevulinic acid
ABC	ATP-binding cassette
aGGH	Array comparative genomic hybridisation
ANOVA	Analysis of variance
APS	Ammonium persulphate
BCA	Bicinchoninic acid
bFGF	Basic fibroblast growth factor
CAF	Cancer associated fibroblasts
cDNA	complementary DNA
CI	Clonogenic index
CNP	2,3-cyclic nucleotide 3-phosphodiesterase
CNS	Central Nervous System
CNV	Common normal variant
CSC	Cancer Stem Cell
DAB	Diaminobenzidine
ECL	Enhanced chemiluminescence
EGF(R)	Epidermal Growth factor (receptor)
EMT	Epithelial to mesenchymal transition
FCS	Fetal calf serum
GBM	Glioblastoma
GEMM	Genetically engineered mouse model
GFAP	Glial fibrillary acidic protein
GFR	Growth factor reduced
GIC50	Absolute half-maximal effective concentration
HCA	High content analysis
HGF	Hepatocyte growth factor
HIF	Hypoxia Inducible Factor

IC50	50% inhibitory concentration
IDH1	Isocitrate Dehydrogenase 1
iMRI	intraoperative MRI
LICAM	L1 cell adhesion molecule
LOH	Loss of heterozygosity
MAPK	Mitogen-Activated Protein Kinase
MGMT	O6-methylguanine DNA methyltransferase
mmHg	millimetres of mercury
MPNST	Malignant peripheral nerve sheath tumour
MRI	Magnetic resonance imaging
mTOR	Mammalian target of Rapamycin
NF1	Neurofibromatosis type 1
NGS	Normal goat serum
NG2	NG2 chondroitin sulphate proteoglycan
NOD/SCID	Non-obese diabetic/severe combined immunodeficiency
NRG	Neuregulin-1
NSC	Neural stem cells
OD	Optical density
OPC	Oligodendrocyte precursor cell
PBS	Phosphate-buffered saline
PBST	PBS-Tween 20
PCV	Procarbazine-lormustine-vincristine
PDGF	Platelet-derived growth factor
PDGFR	Platelet-derived growth factor receptor
PET	Positron emission tomography
pHH3	Phospho-histone H3
PI3 K	Phosphatidylinositol-3-OH kinase (PI(3)K)
PIP3	Phosphatidyl inositol-3,4,5-triphosphate
PLP	Proteolipid protein
PN	Plexiform neurofibromas

PNST	Peripheral nerve sheath tumour
pO_2	The partial pressure of oxygen
PTEN	Phosphatase and Tensin homolog
RCAS/tv-a	Replication-competent avian sarcoma-leukosis virus
RIN	RNA integrity
RIPA	Radioimmuno-precipitation assay
RNA	Ribonucleic acid
RPM	Revolutions per minute
RPPA	Reverse phase protein micro array
RT-PCR	Reverse transcription polymerase chain reactions
SABG	Senescence-associated beta-galactosidase
SDS	Sodium dodecyl sulphate
SRB	Sulforhodamine B
TBE	Tris/Borate/EDTA
TBS	Tris-buffered saline
TMZ	Temozolomide

Chapter 1. Introduction

Glioma is an aggressive cancer of the central nervous system (CNS) support cells called glia [1]. Despite the best efforts of surgeons and oncologists, it remains one of the most deadly of all cancers. Even with optimal surgery and adjuvant chemoradiotherapy patients can expect to live only a few months after diagnosis [2]. Progress to improve patient survival requires improved treatment options and the development of these in turn requires a greater understanding of the genetic and biochemical drivers of glioma cell proliferation, survival and invasion. My ambition is to better model glioma in the laboratory, improving the selection and testing of therapeutics such that I can then predict positive clinical responses, therefore ultimately improving clinical outcomes.

This introduction is broadly divided into three parts. In the first section I will discuss the management of glioma prevailing in the clinic and explore why this is failing to impact on patient prognosis. I consider the role of surgery and how novel techniques might improve the extent of tumour resection. I will then address the importance of adjuvant chemotherapies and examine some of the limitations of currently available drugs. The focus of this discussion is to identify where innovations in treatment are likely to come from that will improve patient outcomes.

In the second section I examine the drug discovery process in more detail. A key part of preclinical compound screening is the development of in vitro models on which inhibitor efficacy is assayed. The design of these models is informed by theories about the process of glioma development. I will therefore discuss the emergence of the hierarchical theory of tumour initiation that implicates a cell with stem-like properties in the process of tumour formation and explore how this relates to what is known about normal neurogenesis [3].

Finally, I will examine the different types of glioma in vivo models currently available. These models are valuable for validating compound inhibitors selected in vitro, and also for probing the molecular pathways responsible for glioma initiation and development. I will discuss the design of these models and explore how variations in the modelling strategy influence the tumours that form.

1.1 Gliomas

Tumours within the CNS are broadly classified as being primary or secondary in origin (Figure 1.1) [4]. Primary lesions originate from a constituent component of the CNS, such as glial cells or meningeal cells, whereas secondary tumours have metastasised from elsewhere in the body, such as from tumours in the breast, lung or skin. The assignment of a pathological diagnosis to any individual tumour is based clinically on a combination of the location, shape and general appearance of the lesion radiologically, and pathologically based on histological assessment of tissue removed during surgery. The most common primary brain tumour is glioma [4].

Glioma is an aggressive cancer of the CNS support cells called glia [1]. By contrast, meningiomas, tumours of meningeal cells, are usually benign [1]. Less common primary brain tumours include choroid plexus papillomas and central neurocytomas that arise from the choroid plexus cells and neuronal cells, respectively, and also pituitary tumours. There are some tumours that arise in the brain from remnants of the developing brain, including primitive neuroectodermal tumours, of which the most common is medulloblastoma. This thesis will focus on gliomas.

Gliomas occur with an incidence of 4/100,000 of the population, accounting for 2% of all malignant tumours in adults [5]. The average age of onset of the most common glioma, glioblastoma (GBM), is 59 years [6]. As the elderly population increases and becomes generally fitter, the significance of this tumour in clinical practice is likely

Figure 1.1 Basic classification of human brain tumours. Classical MRI images of the most common types of brain tumour are used to illustrate the classification system. The assignment of a pathological diagnosis to each image is based on a combination of the location, shape and general appearance of the lesion. The relationship between the calassical radiological appearance of a type of brain tumour and its actual pathological diagnosis has been established over many years by comparing pre-operative radiological assessment with subsequent histological assessment of tissue removed during surgery. Images courtesy of brainsurgery.net.edu, brown.edu, medilogy.net, wikipedia.com, brain-surgery.com, nnnews.org and umrc.rochster.edu.

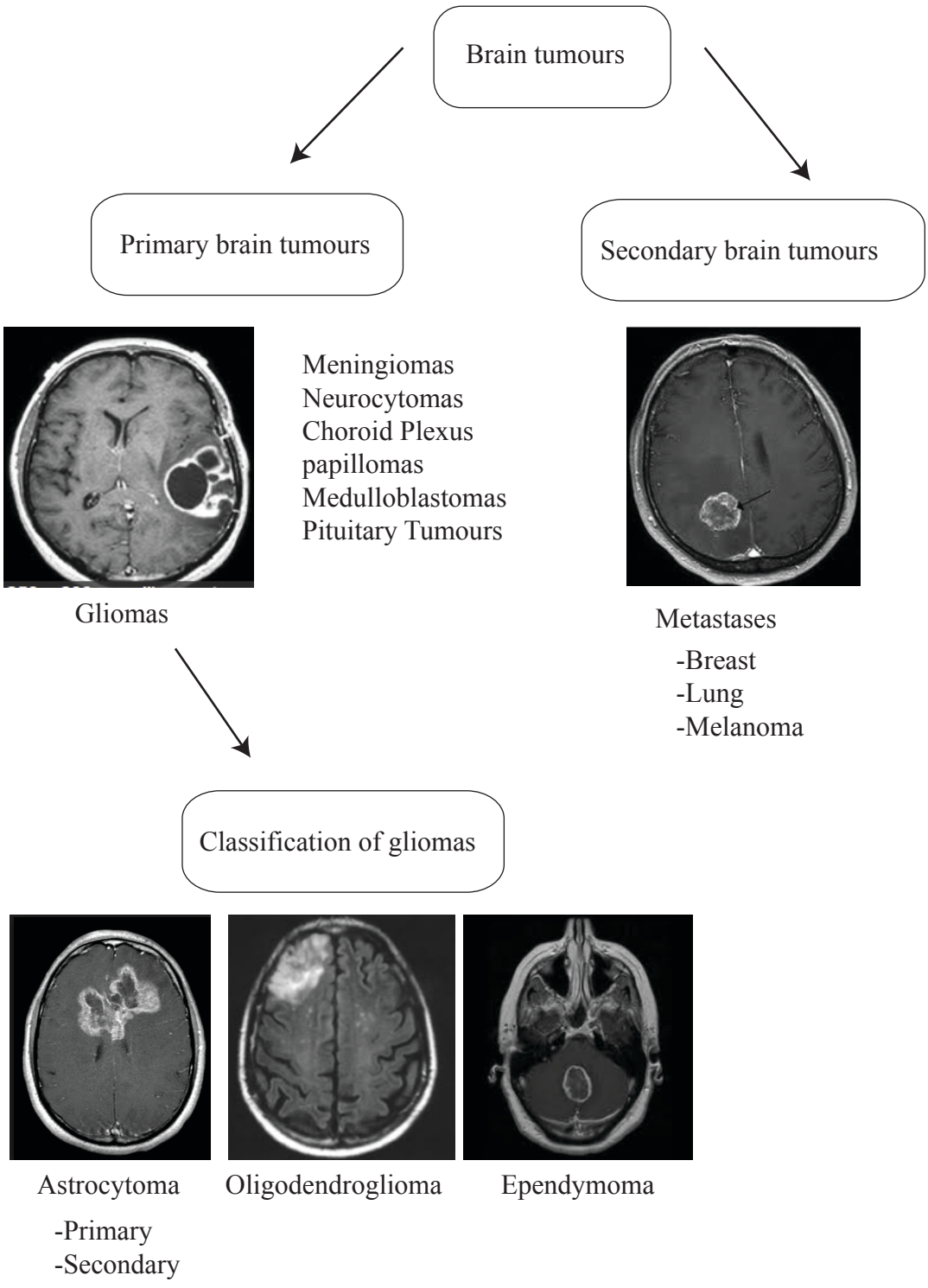

to increase. Age at diagnosis and the medical fitness of a patient are currently the most important determinants of outcome [7]. This is because, as I will discuss below, surgery and adjuvant chemoradiotherapy have failed to significantly impact on patient survival [2].

1.1.1 Glioma Cell Biology and Classification

Gliomas consist of neoplastic and non-neoplastic cells, including vessels, and inflammatory cells [8]. Since the cells that predominate within an individual glioma share phenotypic similarities to one or other of the glial supporting cells of the brain, these tumours are classified as astrocytoma, oligodendroglioma or ependymoma according to the glial cell type that is predominant (astrocyte, oligodendrocyte or ependymal cell) [1, 9].

Astrocytoma is the most common glioma [1]. It is characterised by cells expressing glial fibrillary acidic protein (GFAP), similar to astrocytes. Astrocytes are themselves the most abundant glial cell in the human brain and are named for their star-shaped appearance formed by the processes that envelop neuronal synapses [10]. Astrocytes provide glycogen and lactate to neurons, have a role in repairing brain injury and can signal to neurons through the calcium-dependant release of glutamate. There are three broad types of astrocytes, namely fibrous astrocytes in the white matter, protoplasmic astrocytes in the grey matter, and radial astrocytes that are located adjacent to the ventricles [10]. These radial glial cells have a role in brain development, as I will discuss.

Oligodendrogliomas are the second most common glioma [1]. They are characterised by cells with an oligodendrocyte-like phenotype, although they also contain astrocyte-like tumour cells. Oligodendrocytes provide an insulating myelin sheath composed of 80% lipid and 20% protein. This facilitates rapid saltatory conduction of action potentials down neurons between the nodes of Ranvier formed by the

unmyelinated axon between adjacent oligodendrocyte sheaths; schwann cells perform the same function in the peripheral nervous system [11]. Single oligodendrocytes can myelinate multiple neurons, whereas each schwann cell wraps only one axon [11]. Oligodendrocytes develop from oligodendrocyte precursor cells (OPC) during embryogenesis and early postnatal life. I discuss oligodendrocytes and the OPC in more detail below in relation to mouse models of glioma that target tumour initiation to these cells.

The third type of glioma is an ependymoma. It is much less common than either astrocytomas or oligodendrogliomas, accounting for only about 5% of adult intracranial gliomas [1]. Ependymomas arise from ependymal cells that form a simple ciliated eplithelium-like lining of the ventricular system [12]. Ependymal cells first appear during development with regression of radial glial cells and may actually arise from the terminal differentiation of these cells [12]. Ependymal cells are not themselves thought to be pluripotent, although this is disputed [12, 13]. The ependymal cells are instead thought to support and protect the adjacent subventricular zone (SVZ) where pluripotent cells are located during development and in adult life [12]; I will discuss the SVZ and these pluripotent cells in more detail below. The ependymal cilia may also have a role to maintain patency of the ventricular system and to resist the entry of infectious organisms into the brain [12]. Ependymomas have different clinical manifestations and require different treatment strategies, when compared to astrocytomas and oligodendrogliomas [14]. For example, they occur predominantly in the adult spine, rather than intra-cranially, and are generally benign rather than malignant. Ependymomas are therefore not the focus of either this introduction or thesis.

In addition to their histology, gliomas are also subdivided by tumour grade, an assessment of the aggressiveness of the tumour [1]; grade I tumours are the least aggressive and grade IV tumours are the most aggressive. Glioblastoma (GBM) is the most aggressive (WHO grade IV) of the gliomas [4]. The hallmarks of GBM are

histological features of uncontrolled cellular proliferation, diffuse infiltration, necrosis and vascular proliferation [15]. Although GBMs are generally considered a type of astrocytoma, grade II and III oligodendroglial tumours can also undergo malignant change and take on features leading to the diagnosis of a GBM. When such a lower grade glioma undergoes malignant transformation, the resultant tumour is referred to as a secondary GBM, as I will discuss below; clinically this change is manifest by a new onset rapid tumour growth.

In clinical practice, an assessment of the phenotype of the cells present in a glioma, and the tumour grade, is made during histological examination of formalin-fixed, paraffin embedded tissue after it has been resected at the time of surgery. Implicit in this classification is an assumption that there is a relationship between the histological appearance of the cells in a tumour and development of the glioma itself [16]. However, as I will discuss below, it is unclear whether glioma origin can actually be inferred simply from an assessment of lineage differentiation on a histological slide [16]. Significantly, within the histological classification of gliomas there can be inter-observer variation in diagnosis and so it is perhaps not surprising that the system does not adequately predict tumour behaviour, therapy responsiveness or patient prognosis [16]; for example, the prognosis of patients does not significantly differ simply between those with astrocytic and oligodendroglial histological variants of glioma [2, 17].

There are nevertheless some molecular differences between gliomas classified histologically as astrocytic rather than oligodendroglial and these differences can have implications for patient management. For example, patient outcome correlates with a genetic mutation that is observed in 70% of anaplastic oligodendroglioma; the presence of a deletion of the 1p and 19q chromosomal arms correlates with improved responsiveness to therapy and so improved survival [18]. Not all anaplastic oligodendrogliomas have this mutation and in fact up to 50% of mixed

oligoastrocytomas also have it, so it is not strictly speaking the histological appearance of the tumour that predicts outcome [18].

As similar molecular characteristics are identified, a novel classification of gliomas is emerging based on tumourigenic pathways, rather than histology [16]. These genetic changes are not specific to histological categories of glioma, but do have some correlation with whether or not the glioma is primary or secondary; a malignant glioma is called 'primary' if there is no antecedent history of a lower grade glioma. More than 90% of gliomas are classified as primary tumours (Figure 1.2) [16] [15]. Primary and secondary gliomas appear to have different genetic aetiologies, constitute distinct disease subtypes, and affect patients of different ages (Figure 1.2) [19]. Lower grade tumours tend to affect younger people, are better differentiated than the higher-grade lesions and are more slowly growing, but they still invade surrounding normal brain [19].

The Cancer Genome Atlas consortium performed the most recent and comprehensive assessment of genetic alterations in high-grade gliomas. They identified an average of 47 somatic mutations per tumour [20]. When this data was combined with analysis of copy number alterations, a smaller number of candidate cancer genes was described that are thought most likely to drive glioma formation, including *CDKN2A, p53, EGFR, PTEN, NF1, CDK4, RB1, IDH1, PIK3CA*, and *PIK3R1* [20]. The frequency of these gene mutations in malignant gliomas is illustrated in Table 1.1. The Cancer Genome Atlas team further demonstrated that additional gene members within the signalling pathways affected by these 10 key cancer genes were also commonly mutated in gliomas, such that the TP53 pathway RB1 pathway and PI3 kinase pathways were affected in 64%, 68% and 50% of tumours, respectively [20]. I will discuss the relevant gene members of the PI3 kinase pathway, in particular PIK3CA and PTEN, when I consider drug screening below. Interestingly, in a majority of the 83 tumours the group examined, mutations affected only one gene in any of these three key pathways, although more than one pathway was

Figure 1.2 Characteristic genetic changes that distinguish primary and secondary gliomas. Gliomas are traditionally classified according to the cell type that is predominant on histological examination of tissue removed at surgery. Thus astrocytomas, oligodendrogliomas and ependymomas are dominated by cells with astrocyte-like, oligodendroglial-like and ependymal-like features, respectively. Three MRI images are shown to illustrate these three glioma sub-types. The location and shape of the lesion, along with the clinical history, are used to determine the likely tumour diagnosis from such images. Histological inspection of the tissue removed at operation is required to absolutely confirm such a diagnosis. Importantly though, the histological classification of a glioma does not necessarily inform about the actual tumour cell biology or patient prognosis. As our understanding of the molecular characteristics of glioma grows, a novel classifcation of gliomas is emerging that is distinct from the histological classification. This Figure illustrates the common genetic mutations in astrocytic and oligodendroglial tumours; ependymomas are distinct in their clinical and molecular characteristics from oligodendrogliomas and astrocytomas and are not considered further. Some gliomas present clinically as highly malignant tumours and these are called GBMs. *EGFR* amplification, loss of *PTEN,* and *p16INK4a* mutation all suggest that a GBM is primary and has not arisen from within a lower grade glioma. In contrast, grade II and III astrocytomas or oligodendrogliomas can undergo malignant transformation to form so-called secondary GBMs. *p53* and *IDH1* mutations observed in a GBM are suggestive that such a tumour has arisen secondarily from a lower grade precursor. The deletion of 1p19q is common in anaplastic oligodendrogliomas, so when it is observed in a GBM this also indicates that this tumour has arisen from the malignant transformation of a lower grade tumour.

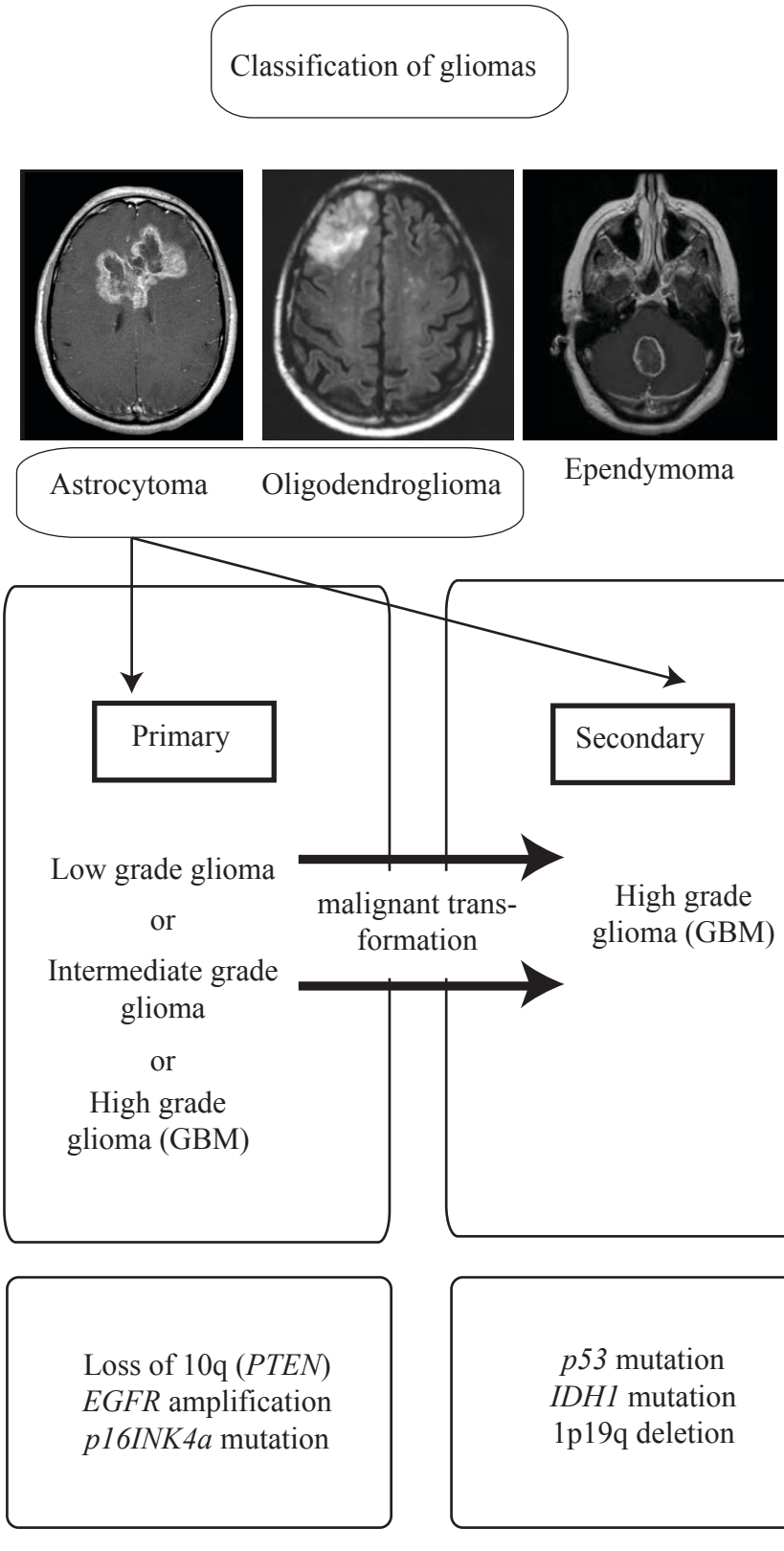
Classification of gliomas
Astrocytoma
Oligodendroglioma
Ependymoma
Primary
Secondary
Low grade glioma
or
Intermediate grade glioma
or
High grade glioma (GBM)
malignant trans-formation
High grade glioma (GBM)
Loss of 10q (PTEN)
EGFR amplification
p16INK4a mutation
p53 mutation
IDH1 mutation
1p19q deletion

Table 1.1 The incidence of individual gene mutations in malignant gliomas. The Cancer Genome Atlas collaboration performed an analysis of the most common genetic alterations in 83 malignant gliomas and determined the genes most important in driving tumour development. The table lists these 10 genes, indicates the proportion of the examined tumours that had alterations in these genes and details whether gene deletion, amplification or point mutation was most common [20].

Gene	Proportion of tumours with alteration (%)	Most common type of genetic alteration
CDKN2A	50	Deletion
p53	40	Point mutation /Deletion
EGFR	37	Amplification
PTEN	30	Point mutation /Deletion
NF1	15	Point mutation
CDK4	14	Amplification
RB1	12	Point mutation/Deletion
IDH1	11	Point mutation
PIK3CA	10	Point mutation
PIK3R1	8	Point mutation

affected in each tumour [20]. This was interpreted as indicating that any gene alteration in a given pathway is functionally equivalent for the purposes of tumourigenesis.

The incidence of specific genetic mutations is different between primary and secondary gliomas. Foe example, loss of the long arm of chromosome 10 (10q) including the *PTEN* gene, and *EGFR* gene amplification, are characteristic of primary GBMs, as is $p16^{INK4a}$ gene deletion. In contrast, *p53* and Isocitrate Dehydrogenase 1 (*IDH1*) gene mutations are most frequent in low-grade gliomas and secondary GBMs, along with the 1p19q deletion described above in oligodendrogliomas [15, 18, 21]. Approximately 70% of low-grade gliomas (grade II and III) and secondary GBMs have an *IDH1* mutation, compared to 12% of gliomas overall [20, 22]. This is important, because the presence of an *IDH1* mutation is associated with a better prognosis when compared to tumours that lack this mutation [22]. *IDH1* encodes a NADP+-dependant Isocitrate dehydrogenase and the mutations observed in glioma eliminate the protein's enzymatic activity [23]. This is thought to impact on the biology of affected glioma cells through an alteration in the cell's CpG island methylator phenotype [24].

Unfortunately, none of these genetic alterations is sufficiently specific to distinguish between primary and secondary GBMs [20]. Moreover, within a single tumour the assessment of the significance of these genetic mutations is complicated by intra-tumoural genetic heterogeneity. For example, expression levels of receptor tyrosine kinase genes such as *EGFR* and *PDGFRα* have been shown to vary between different tumour regions [25, 26]. This underlines the need to model intra-tumoural heterogeneity in vitro, particularly when approaching selection of inhibitor compounds. Nevertheless, the identification of key genetic mutations in glioma has developed our understanding of the cell signalling pathways that may be important in tumourigenesis and this will help guide the search for effective chemotherapeutic agents.

A second molecular classification system for glioma has been developed that is based on gene expression profiles, rather than gene mutations [27]. Within this system malignant gliomas are classified into Proneural, Neural, Classical and Mesenchymal subtypes, based on the expression of signature genes in each group; these subtypes were determined from hierarchical clustering analysis of the gene expression profiles of 202 gliomas [27]. Within the group of genes whose expression characterised each subtype, the key cancer driver genes *EGFR*, *NF1* and *IDH1*/*PDGFRα* were observed to define the Classical, Mesenchymal and Proneural subtypes, respectively, although none of these mutations was exclusive to a particular subtype [27]. In contrast, loss of *PTEN* was observed throughout all the subtypes. Based on functional analysis of the characteristic gene expression profiles, the Mesenchymal subtype of tumour demonstrated a combination of astrocytic and mesenchymal activity, and this was thought to be reminiscent of epithelial to mensenchymal transition observed in some other solid tumours [27]. In contrast, the Proneural tumours demonstrated high expression of oligodendrocytic developmental genes such as *OLIG2* and *NKX2.2*, as well as other developmental genes such as *SOX* family members [27]. The observation that the genes enriched in each subtype relate to distinct neural lineages has been interpreted as suggesting that this may reflect a specific cell of origin [28]. For example, *OLIG2* expression implicates the oligodendrocyte precursor cell, a neural progenitor cell that I discuss later, as a possible initiating cell for Proneural-type gliomas. In support of this hypothesis, when retroviruses expressing PDGF and Cre recombinase were delivered stereotactically to progenitors in the subcortical white matter of mice containing floxed *PTEN* and/or *p53*, GBMs resembling the Proneural subtype were formed [28]; analysis of retroviral expression shortly after intracranial injection indicated that the transfected cells expressed Olig2, consistent with these cells being OPCs.

Unlike the histological and genetic classification systems, this gene expression classification system may provide a molecular rationale for clinically observed outcomes [27]. For example, when gene expression profile subtypes were examined

in the context of the matched patient clinical history and tissue samples, it was observed that tumours with a Mesenchymal profile had a higher fraction of necrosis and that the affected patients had worse outcomes [27]. In contrast, tumours with a Proneural profile tended to be found in younger patients, suggestive of secondary gliomas, and these patients tended to have a longer survival [27]. Within the Proneural subtype of gliomas, further subdividing the tumours by the presence or absence of *p53* and *PTEN* mutations correlates with survival and this approach may also be applicable to the other tumour subtypes [28]. Interestingly, despite having an overall longer survival, patients with Proneural tumours did not appear to benefit from the more aggressive chemo-radiotherapy regimens that improved survival in those with Mesenchymal and Classical tumours [27]. This classification system may therefore be of use in clinical decision making.

This classification system based on gene expression profiling of tumours currently offers the most promise for the development of a clinically relevant tool for prognostication and management in glioma. It may be possible to further enhance its usefulness by integration with other prognostic indicators. For example, the methylation status of the promoter of a single gene, 0-6-methylguanine-DNA methyltransferase (*MGMT*), correlates with responsiveness to chemotherapy [29]. Analysis of methylation status alongside the gene expression profile of an individual glioma may therefore give added value in assessment of the likelihood of responsiveness to therapy. The widespread routine clinical use of the gene expression classification system is currently prohibited by cost, so it has been proposed that a simplified, but no less accurate, assessment of the subtype of a glioma could be made using an immunohistochemical technique [30]. This requires further validation on larger numbers of tumours.

1.2 Current Management of gliomas

1.2.1 Surgery

It is more than a century since the first attempt at surgical resection of a glioma was made, but surgery has added little real value to clinical outcomes during this period; even with optimal surgery and adjuvant chemoradiotherapy the average survival of patients diagnosed with GBM is just 14.6 months [2]. The lack of progress in treating glioma is in stark contrast to the therapeutic advances made in combatting many other cancers over recent years [31].

It is the extensive invasion of glioma cells amongst normal brain tissue that prevents total surgical resection. Even hemi-cerebrectomy, removing the whole half of the brain affected by glioma, cannot prevent tumour recurrence [32]. The brain's lack of a basement membrane structure to arrest cancer cell invasion means that, at diagnosis, glioma cells can be found in parts of the brain distant to the principal lesion [32]. Attempts to remove increasing amounts of glioma tissue surgically at its interface with normal brain tissue risks damaging functioning brain and reducing a patient's quality of life without realistic prospect of improving prognosis [2]. Extensive surgery would only improve a patient's prognosis if it made adjunctive therapies more effective, but unfortunately this is not the case [2]. The limitation that this places on the aggressiveness of surgical resection contributes to the fact that more than 90% of gliomas recur adjacent to the resection cavity, within just a few months of surgery [33]. However, even though complete surgical resection of a glioma is not possible, the development of techniques to safely maximise the extent of tumour resection might result in fewer tumours recurring at the primary resection cavity and perhaps result in a longer disease-free interval [2, 34].

Currently, intra-operative assessment of tumour infiltration into normal brain tissue at the macroscopic edge of the tumour usually depends on visual inspection and

manual palpation, neither of which is particularly robust [35]. However, imaging modalities, such as magnetic resonance imaging (MRI), exist that can aid the surgeon in the assessment of glioma extent and spread. Better still, by combining a radiological assessment of glioma cell invasion into normal brain tissue with functional brain mapping to localize key neurological pathways and structures, the extent of surgical tumour excision can be maximised, because critical brain regions can be identified and safeguarded during surgical resection [36]. These pre-operative imaging strategies can actually also now be used intra-operatively to aid resection at the tumour margin [37]. This is of particular value, because when the cranial vault is opened, drainage of cerebrospinal fluid and removal of brain tissue causes brain shift such that the operative field cannot be accurately correlated to pre-operative imaging [38]. Intra-operative imaging modalities overcome the problem of brain shift, but the images are still not 'live.' In the case of intra-operative MRI (iMRI), for example, the anaesthetized patient must be moved from the operating part of the theatre to the imaging part, and then back again [37]. Moreover, intraoperative imaging is expensive to install and time consuming to operate. Although it has been shown that iMRI increases the volume of tumour resection, this has not yet been correlated with improvement in progression free survival [37]. One reason why these imaging strategies might not translate into improved patient outcomes is because they still cannot identify individual glioma cells that have invaded deep into the brain, and even if they could, surgery would not be a practical technique to remove multiple small foci of abnormal cells from in amongst normal brain tissue. Effective techniques for eradicating these small foci of glioma cells distant from the tumour bulk are likely to be non-surgical. Nevertheless, there are still many novel techniques available in the neurosurgeon's armoury that aim to facilitate tumour visualisation and enhance resection [39]. Some of these strategies overcome the limitations of standard intra-operative imaging that I have described.

One approach is to visualise tumour cells using the characteristics that differentiate them from normal brain cells, such as their metabolism. For example, tumours have

an increased glycolytic metabolism compared to normal tissue and an overexpression of glucose transporters [40]. The positron emission tomography (PET) imaging technique allows regions of increased metabolic activity to be visualised using the glucose mimetic 2-deoxy-2-[^{18}F]fluoro-D-glucose [40]. For this reason, PET is used in pre-operative assessment of tumour spread, particularly for identifying metastatic deposits of cancers other than gliomas [40]. Hand held detectors are now also available that allow translation of PET into the operating theatre. This technology is still limited though by its poor spatial resolution and the need for radiopharmaceuticals that require special handling to avoid radiation exposure to operating room staff [40].

To overcome the problems of using radiopharmaceuticals in surgical practice, other probes are available that can be targeted to tumours and visualised without the need for radioactive tracers. These include ligands that target recognised disease biomarkers. For example, a monoclonal antibody to the $\alpha 5\beta 3$ integrin that is associated with angiogenesis can be conjugated to an optically active reporter such as a fluorophore [41]. When the antibody binds its cellular target it is internalised, resulting in cleavage of the probe and fluorescence activation. A significant challenge remains to demonstrate the sensitivity of such techniques for tumour tissue and their specificity at discriminating tumour from normal tissue.

Instead of using labelled probes at all, another approach has been to exploit the properties of emitted light from tumour tissue itself [42]. This allows direct real-time imaging of the anatomical and chemical characteristics of tumours. This intrinsic fluorescence, called autofluorescence, can be excited when a tissue is activated by ultraviolet, visible or near-infrared radiation [42]. The morphological and biochemical changes that occur when a tissue is affected by cancer alters these fluorescent properties, allowing tumour tissue to be differentiated from normal tissue without the need to administer any exogenous agents [42]. In practical terms, the autofluorescence signal is weak and it has not been possible to apply this technique

into the operating theatre with existing technologies. However, a related technique using 5-aminolevulinic acid (5-ALA) has been developed and is becoming established in the surgical management of gliomas (Figure 1.3) [35].

5-ALA is a compound of the porphyrin synthesis pathway [35]. There is an increased amount of endogenous porphyrin in dysplastic and malignant tissue that results in an increased red autofluorescence [35]. The exogenous administration of 5-ALA augments this autofluorescence effect through accumulation of the fluorescent porphyrin protoporphyrin IX in tumour cells (Figure 1.3) [35]. When visualised using violet–blue illumination through an operating microscope, the tumour cells glow an intense red, whilst normal cells appear blue [35]. This technique obviates the need for labeled probes or additional imaging equipment, because an operating microscope is a standard tool in the operating theatre [35]. In a randomised study of the use of 5-ALA in glioma surgery to enhance surgical resection, the proportion of patients with progression free survival at 6 months significantly improved compared to patients operated on without this surgical adjunct [35]. However, even in this highly selected study population the overall length of patient survival did not improve much beyond 15 months [35]. Nevertheless, a significant factor in favour of the rapid adoption of 5-ALA in UK clinical practice is that it hasn't needed to pass through regulatory processes such as validation by the National Institute for Clinical Effectiveness (NICE). This is because NICE determined that 5-ALA was sufficiently similar to existing products in clinical use whose benefits and risks were well established [43]. This contrasts with the additional regulatory minefields that labelled probes would need to navigate if they are classed as novel medicinal compounds.

1.2.2 Adjunctive therapies for management of glioma

5-ALA is being adopted into routine neurosurgical practice in the UK and this may be the best strategy available currently to maximize the extent of surgical resection of gliomas. However, for the reasons that I have discussed concerning glioma cell

Figure 1.3 Visualisation of glioma invasion using tumour autofluorescence. These images demonstrate how a standard macroscopic assessment of the extent of glioma cell invasion into normal brain surrounding a tumour (top image) can be supplemented by visualisation of the tumour under ultraviolet light after the intravenous administration of the prophyrin synthesis pathway substrate 5-aminolevulinic acid (5-ALA) (bottom image). 5-ALA administration leads to accumulation of the fluorescent porphyrin protoporphyrin IX. Malignant tissue appears purple because of the increased uptake of the substrate compared to normal tissue, which itself appears blue. In the top image the yellow star indicates a region of macroscpically normal brain. The yellow star in the bottom image indicates the same region, but the purple colour demonstrates that this region is actually involved by tumour. Similarly, although the area of necrosis and solid tumour labelled in the bottom image can also be distinguished in white light, the area labelled 'vague' might have been regarded as normal without 5-ALA adminstration and so not resected. Images courtesy of neuorosurgery blog.com.

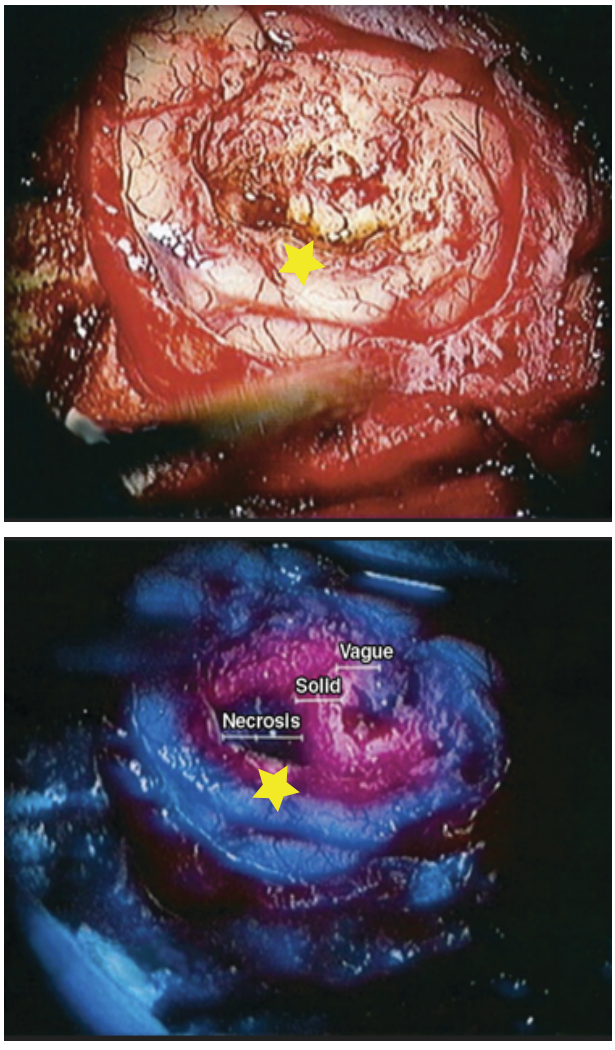

invasion, surgery cannot by itself hope to remove all tumour cells in a brain affected by glioma. It is therefore perhaps futile to search for an entirely surgical solution to the problem of managing gliomas. Effective non-surgical treatment strategies, such as chemotherapy and radiotherapy, are clearly needed. The goal of both adjunctive therapies is to slow the growth and invasion of glioma, and better still to downgrade glioma into a focal disease that is more susceptible to local treatments, such as surgery.

Unfortunately though, the best adjunctive therapies currently available for the management of glioma are fairly ineffective [2]. The current standard of care for adjuvant therapy in glioma is 60 Grays of radiotherapy with concomitant use of the oral alkylating agent Temozolomide (TMZ), then 6 further cycles of TMZ [2]. The use of TMZ with adjuvant radiotherapy is associated with an improved prognosis for patients compared to the use of TMZ alone; 14.6 months versus 12.1 months survival, respectively [2]. This highlights the important role of radiotherapy in glioma cell control after surgery. However, an analysis of radiotherapy in the management of glioma is not a focus of this thesis and will not be discussed further.

TMZ is a prodrug that is rapidly converted into its active form (monomethyl triazeno imidazole carboxamide) in the systemic circulation [44]. DNA damage caused by TMZ-mediated alkylation triggers cell death, unless the tumour cell contains active 0-6-methylguanine-DNA methyltransferase enzyme (MGMT), in which case DNA damage repair can take place [29]. In the presence of intact DNA repair mechanisms the efficacy of TMZ is reduced, and so the 45% of patients whose MGMT gene is inactivated by promoter methylation have an improved prognosis up to 21.7 months on average [29]. However, this implies that the stark reality for the majority of patients with glioma is that there is no effective chemotherapy treatment. The provision of suitable chemotherapy for all glioma patients is therefore a significant unmet clinical need.

TMZ itself replaced the less well-tolerated and less efficacious regimen Procarbazine-Lormustine-Vincristine (PCV) [45, 46]. The other principal chemotherapy agent in current use for treatment of glioma is Carmustine, which is administered direct to the tumour cavity infused into biodegradable wafers to avoid problems of systemic toxicity [47]. Phase III studies in small groups of patients have shown a survival benefit to using Carmustine wafers [48]. Patients who received adjuvant Carmustine survived 14.5 months on average compared to 10.0 months for those who did not [48]. However, surgical contraindications to wafer placement, such as breaching the ventricular ependyma, preclude their use in a large number of patients [49]. Furthermore, up to 28% of patients who receive the wafers develop intracranial infection, which is a significantly higher proportion than in patients who do not receive Carmustine [49]. For these reasons Carmustine wafers do not yet have a clear role in glioma management. Studies comparing TMZ, radiotherapy and Carmustine to the current standard adjuvant therapy regimen of TMZ and radiotherapy alone are awaited.

Other than TMZ and Carmustine wafers there have been no effective treatments for glioma successfully entering into the clinic over the last decade, despite promising data from preclinical studies [50, 51]. One drug that it was hoped would have a significant impact on glioma recurrence and progression based on in vitro and in vivo preclinical studies was Bevacizumab, a humanised monoclonal antibody that targets vascular endothelial growth factor-A, so inhibits angiogenesis [50, 51]. Rapidly dividing tumours such as gliomas are dependant on new blood vessel growth to keep pace with their metabolic needs, so inhibiting blood vessel growth had a clear rationale [50, 51]. Currently, Bevacizumab has approval from the US Food and Drug Administration agency (FDA) for use as a single agent in patients with progressive or recurrent glioma disease who have already received TMZ and radiotherapy [50]. However, although it has been shown in non-randomised studies that Bevacizumab improves progression free survival in 42.6% of patients diagnosed with recurrent GBM, there remains an absence of prospective randomised trials to support the

promising pre-clinical data that suggested it could be a first line therapy for treatment of gliomas [52].

The failure of inhibitor compounds such as Bevacizumab to translate successfully into the clinic from the laboratory suggests that the models on which pre-clinical screens are being performed may not adequately recapitulate human disease. The challenge for drug discovery is therefore to understand the process of glioma initiation and progression so that it can be better modelled in the laboratory and therefore compound screening can be made more predictive of likely chemotherapeutic success in the clinic.

1.3.Glioma drug discovery

If compounds that have shown promise in preclinical studies fail to be of value in the clinic then this is a significant problem both for patients who are left with limited therapy options and also for the drug companies that are spending billions of pounds in an attempt to develop effective therapies [53]. Despite a gradual increase in spend on drug research and development the FDA approved only around 20 new chemical entities for use across all disease categories in the US in 2002/2003 and there is no indication that the situation has improved since then [53]. The total research and development spending per new drug has been calculated at a staggering 4-12 billion dollars, and the average time taken for development is 12 years and 10 months [54]. Only 1 in 9 compounds actually make it through development from first-in-man trials to registration [54]. Unsurprisingly, only 3 out of 10 drugs that do make it to market actually recover the investment made in them [54]. The likely success of any drug in this process varies with the target disease and whilst compounds for cardiovascular problems have a 20% success rate, those targeted at oncology and the CNS have a success rate of only 5% and 8%, respectively [54].

A number of compounds fail at the early clinical trials stage despite the fact that they appeared efficacious in laboratory models; 60% of oncology drugs fail in phase III trials [54]. This is problematic because much of the expense of drug development is incurred by the cost of human trials. One reason for this drug attrition is compound safety and this could actually be identified or even overcome by earlier proof of concept testing in man, as is being advocated in some quarters [54]. Another reason for the low success rate translating compounds from the laboratory into the clinic is that when a new drug is trialled its efficacy is compared against existing therapies [54]. This means that the bar for regulatory approval, in terms of improving patient outcomes, effectively increases over time [54]. Nevertheless, the discrepancy across therapeutic areas in attrition rates of drugs during development suggests that there is actually a methodological problem in pre-clinical drug selection and testing that contributes to failure in clinical trials [54].

A particular problem for CNS drug discovery is the challenge of ensuring compounds of interest actually cross the blood brain barrier (BBB). The BBB consists of endothelial cells lining the cerebral microvasculature that form a selective barrier to the free movement of molecules and compounds between blood and the extracellular fluid of the CNS [55]. This selectivity results from tight junctions between adjacent cells that restrict the para-cellular diffusion of large or hydrophilic molecules that would normally be possible in most other endothelia [55]. Whilst some small (400-500 Dalton) lipophilic agents, such as barbiturates, can nevertheless diffuse freely through the cell's lipid membrane, other molecules, especially hydrophilic molecules such as peptides, must instead rely on specific membrane transport systems; these same transport mechanisms may however also be responsible for the efflux of compounds from a cell if that cell determines they might be harmful [55]. The BBB also contains intracellular and extracellular enzymes that provide a metabolic barrier to entry of compounds [55]. As a consequence of these structural features, the BBB is thought to exclude over 98% of large and small drug molecules from the brain [56].

Interestingly, it is thought that brain tumours may actually modulate the efficacy of the BBB. This is proposed to result from down regulation of the protein Claudin 1, opening up tight junctions, redistributing aquaporin 4 and triggering release of vascular endothelial growth factor, all of which might increase the ability of compounds to cross the BBB [55]. However, whilst this might be predicted to facilitate drug delivery to target tumour cells, is also known that dexamethasone, a steroid routinely administered to patients with glioma to reduce symptomatic brain swelling, actually improves the selectivity of BBB function and so impairs the ability of exogenously administered chemotherapeutics to access the tumour [55]. For the purpose of screening drugs targeted against glioma, it therefore seems prudent to assume that the BBB is probably intact. Moreover, when in vitro studies are translated to in vivo preclinical models, care must be taken to avoid using solvents such as ethanol or DMSO to solubilise the compounds of interest, because they cause BBB disruption, risking a false positive result of the experiment [56].

Modifications to compounds, such as increasing the lipid content, may improve uptake across the BBB, but this also simultaneously increases the removal of a drug from blood, so reducing its availability to cross the BBB [56]. A better approach might therefore be to design drugs that can cross the BBB using native carrier mediated transport systems, and the results of such a strategy are awaited. As well as designing compounds to cross the BBB, attempts have also been made to improve drug delivery to intracranial tumours by usurping the BBB itself. Strategies have included the use of hyperosmolar solutions to open up the BBB, implanting drug-impregnated wafers in the surgical cavity at operation, or leaving a catheter in the cavity at surgery that attaches to an external drug pump [56]. Any invasive strategy for drug delivery risks increasing infection. To date these approaches have not yet significantly improved patient survival in clinical trials [55, 56].

The observed lack of efficacy of compounds in the clinic that appeared effective in the laboratory also suggests that the models used in the preclinical drug screening

may not accurately recapitulate glioma biology. This may be because our understanding of the mechanism of glioma initiation on which these models are predicated is incorrect. A better understanding of the cellular origin of gliomas is therefore crucial to informing the design of more biologically relevant preclinical models which can be used for drug selection. Secondly, it is also possible that the assays of drug efficacy developed using these in vitro and in vivo glioma models may be inadequate. I will explore both these problems in turn.

1.3.1 Models of glioma initiation and development

Gliomas, like other cancers, develop from the clonal expansion of mutated cells [57]. Genetic and epigenetic alterations occur as the cancer progresses, leading to the emergence of clonal diversity, each clone having different survival advantages [58]. These observations underline the need to develop models that recapitulate glioma initiation at an early stage in its development before heterogeneity arises that cannot easily be recapitulated in vitro. Inhibitor compounds selected using models that recapitulate the early stages of tumour initiation and development would target the root cause of gliomas and might therefore be more effective in the clinic than potential drugs selected using other models. The key then is to understand the identity of the cell of glioma origin.

In the traditional, so-called *multistep model* of gliomagenesis, a fully differentiated glial cell undergoes a series of molecular events leading to its neoplastic transformation (Figure 1.4) [59]. These mutations confer a selective advantage on the cell so that it can out compete other cells. Historically, the brain was thought to be a post-mitotic organ so it made sense that only differentiated glia were candidates as the glioma cell of origin [60]. The in vitro glioma models prevailing at the time were serum-grown glioma cell lines derived from human tumours. However, it is now known that cell growth under serum conditions does not reflect the in vivo brain environment and actually promotes the accumulation of non-tumour-derived

Figure 1.4 Models of glioma development. In the traditional multistep model of glioma development a differentiated glial cell undergoes a series of molecular events leading to its neoplastic transformation. In contrast, the cancer stem cell model proposes that the tumour initiating event occurs in a stem-like cell. This cell can undergo symmetrical divisions to produce new stem-like cells or asymmetrical division to produce new stem-like cells and more fate restricted progenitor cells or differentiated cells. The progenitor-like cells in turn produce differentiated cells that will constitute the tumour bulk. Conventional chemotherapies that eradicate differentiated glioma cells leave behind the stem-like cells, leading to tumour recurrence. Glioma stem-like cells will also acquire new mutations in a stepwise manned, so the multistep model is still relevant.

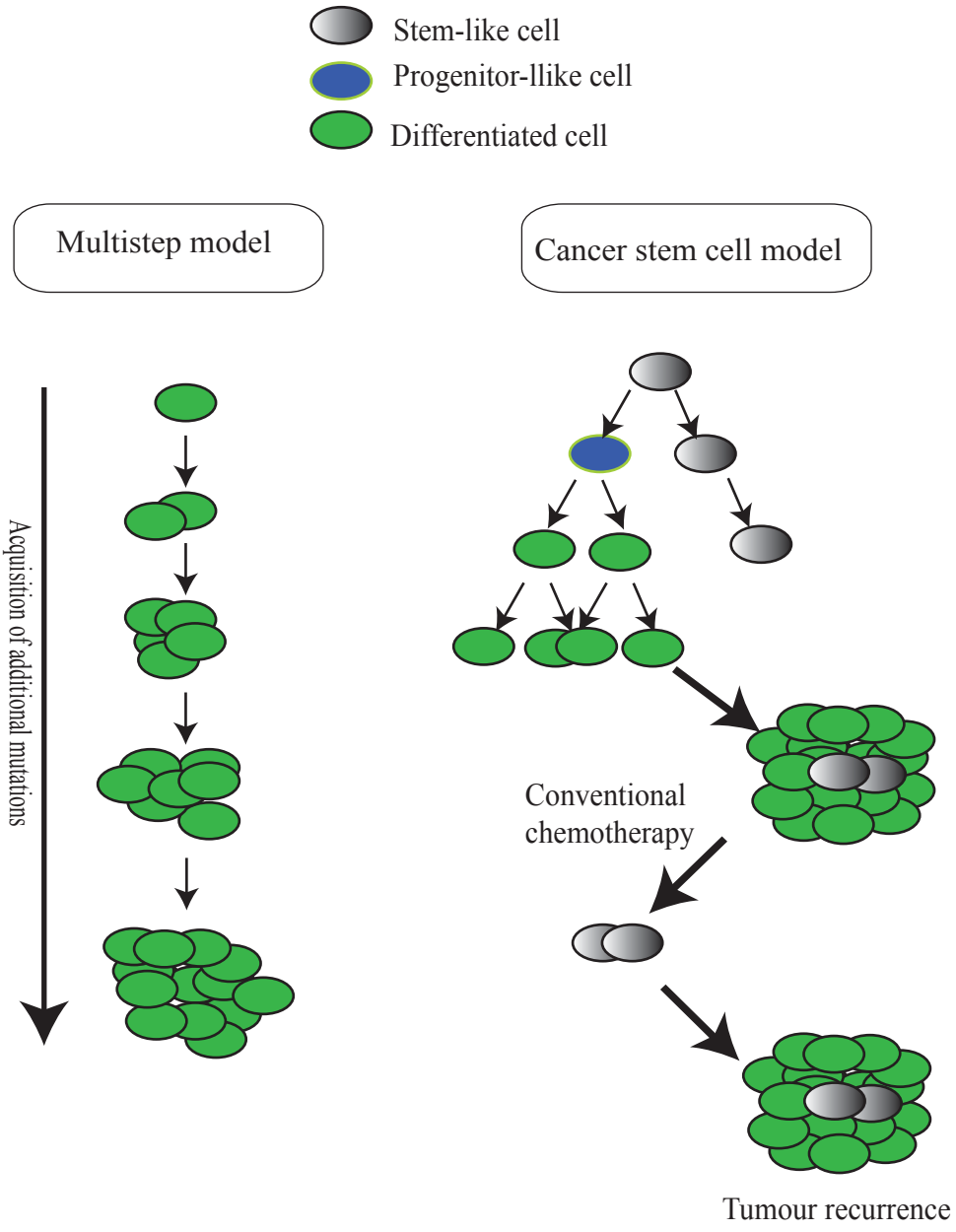

mutations [61]. It is perhaps not surprising then that the use of these serum-grown glioma cell cultures for preclinical compound screening correlates with a time period during which there has been a failure to successfully translate promising drugs from the laboratory into the clinic [50, 51].

Recently, a novel concept of glioma initiation and development has emerged called the *hierarchical* model (Figure 1.4) [3]. This model is based on the so-called cancer stem cell (CSC) hypothesis of tumour development that predicts that cancer cells that share characteristics with normal stem cells, such as self-renewal and differentiation, are responsible for tumour initiation [62]. The concept of CSCs developed from observations made in haematological malignancies and has now been extended to many solid tumours, including glioma [58, 63]. The hierarchical model suggests that not all cells within a tumour have these stem cell-like characteristics, but instead that there is a subpopulation of CSCs that can give rise both to more CSCs and also to mutant differentiated cells in a type of recapitulation of the cellular hierarchy observed in normal tissues [62, 64]. This model is consistent with the cellular heterogeneity that is observed in tumours. Importantly, CSCs are tumourigenic in vivo, in contrast to their differentiated progeny [64].

It is not yet known with certainty whether CSCs within gliomas are derived from differentiated cells that acquire a stem-like phenotype, or from native stem cells in the brain that undergo malignant transformation. However, since stem cells are the most long-lived cell population in a tissue, they therefore have longer to be exposed to genotoxic stresses than their shorter-lived, differentiated progeny [62]. In contrast to normal neural stem cells and progenitor cells, glioma stem-like cells are able to undergo unlimited proliferation [65-67]. It has been suggested that oncogenic mutations might confer this self-renewal potential on premalignant neural progenitors that then become fully malignant following accumulation of further tumourigenic mutations [3, 66]. Therefore, whilst the hierarchical model implicates the CSC as the cell of origin in glioma, this does not necessarily exclude the *multi-*

step model as irrelevant, because CSCs likely emerge through the sequential acquisition of genomic mutations, as described in the *multi-step* model.

The cellular origin of the CSC and the role of the CSC in tumourigenesis have been interrogated through in vitro and in vivo modelling. These models are based on a consideration of the stem cells present in normal human neurogenesis and in the adult human brain that are possible candidates as the glioma cell of origin.

1.3.2 Human neurogenesis

Neurons and the glial supporting cells of the brain were previously thought to derive from separate precursor cells called neuroblasts and radial glial cells, respectively, but are now thought to share a common precursor cell called a neural stem cell [68]. These neural stem cells undergo either symmetric divisions producing two daughter stem cells, or asymmetric divisions to produce one daughter stem cell and one more differentiated cell, such as a multipotent cell rather than a stem cell, or a differentiated cell like a neuron or glial cell. The principle criteria used to define a cell as a stem cell are that it can self renew for an unlimited number of cell divisions through the transient amplification of a population of progenitor cells, and that it is multipotent and can give rise to numerous types of differentiated cells [69]. Stem cells should also generate new cells in response to injury or disease [60].

Neural progenitors arise early in embryogenesis from the ectoderm and are located in a single layer of cells called the ventricular zone; these cells are called neuroepithelial cells and have an elongated appearance with a nucleus that varies in position to give the appearance of a pseudostratified epithelium [70]. During development a marginal zone forms between the ventricular zone and the outer surface of the neural tube. The cells of the ventricular zone now become more fate restricted than neuroepithelial cells and are called radial glial cells [70] (Figure 1.5). The radial glial cell is known as a transit amplifying cell, and has both

Figure 1.5 Embryonic and adult neurogenesis. Neural progenitors called neuroepithelial cells are located in a single layer of cells called the ventricular zone, forming a pseudostratified epithelium. They can divide either assymmetrically to give daughter neurons and a new neuroepithelial cell, or symmetrically to give two neuroepithelial cells. During development a marginal zone forms between the ventricular zone and the outer surface of the neural tube. The cells of the ventricular zone now become more fate restricted and are called radial glial cells. Radial glial cells can also undergo symmetric or asymmetric division, the latter producing a differentiated cell that is usually a neuron, but can be an astrocyte or oligodendrocyte; the differentiated progeny of radial glial cells are located in an intermediate zone between the ventricular zone and marginal zone. Radial glial cells, as well as neuroepithelial cells, also generate another neuronal progenitor called a basal progenitor. These cells leave the ventricular zone and form the subventricular zone, which is a reservoir of neural precursor cells in the adult. Progenitors in this region can divide either symmetrically or asymmetrically, but are thought to produce only neurons and not glia, although this is disputed. In the adult, neural stem cells present during embryogenesis are now also found throughout the subcortical white matter and are thought to function as oligodendrocyte precursor cells. (Figure after Leclerc et. al. 2012)

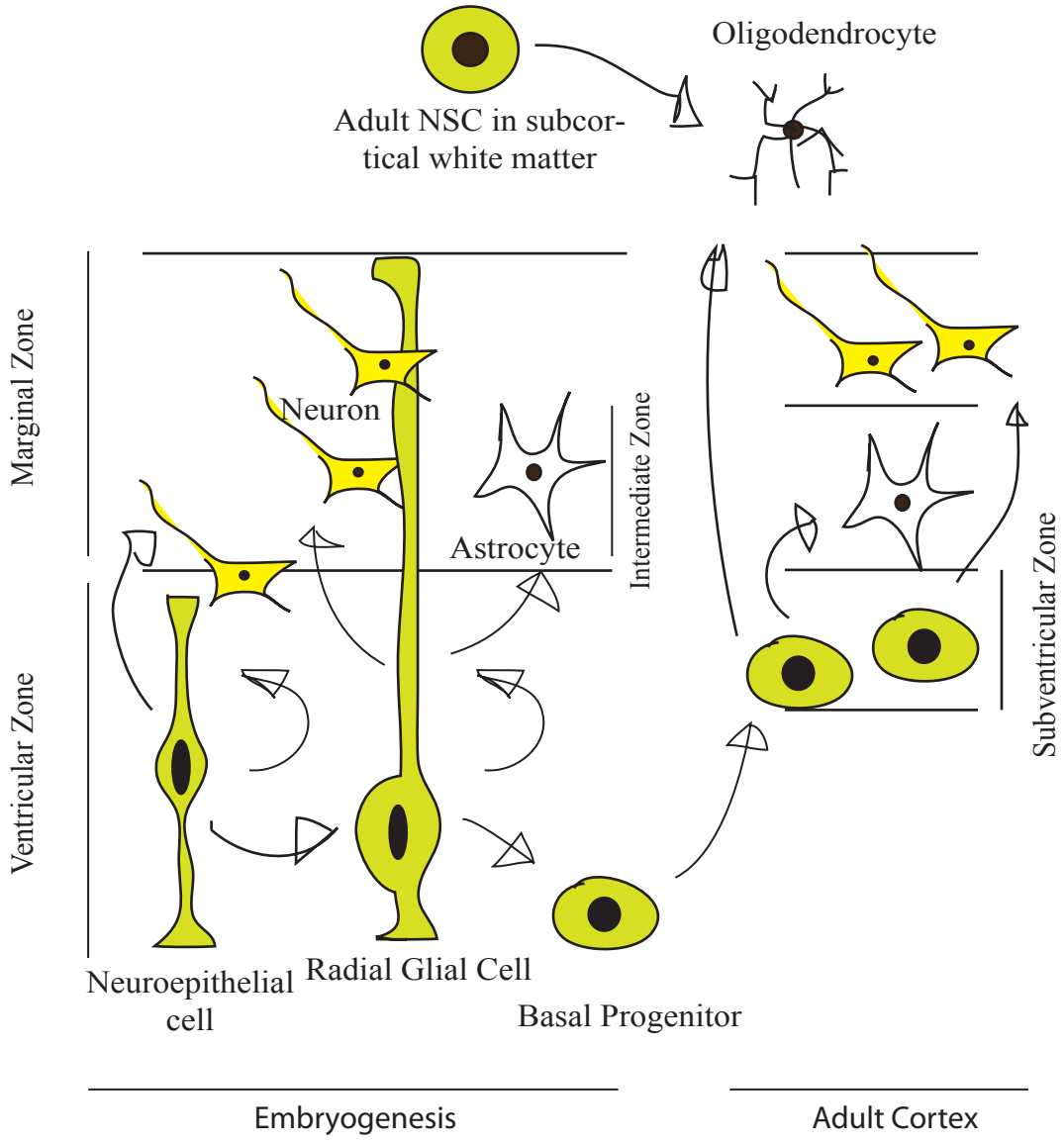

neuroepithelial and astroglial properties. Both neuroepithelial cells and radial glial cells are referred to as neural stem cells and can self-renew; cells that produce only more differentiated or post-mitotic cells when they divide are called neural progenitor cells [71]. Radial glial cells express Nestin like their precursor neuroepithelial cells, whilst astroglial features such as S100B, GFAP and Vimentin expression emerge over time [68]. The radial glial cells are thought to provide some of the same neuronal support function and regulation of metabolic activity that differentiated glial cells provide [68].

Radial glial cells can undergo symmetric division to produce two new radial glial cells, or asymmetric division to produce one radial glial cell and one differentiated cell, which is usually a neuron, but can be an astrocyte or oligodendrocyte; the term 'glia' encompasses both radial glial cells and the differentiated cell known as astrocytes, oligodendrocytes and ependymal cells that I discussed above [68, 70]. The differentiated progeny of radial glial cells are located in the intermediate zone between the ventricular zone and marginal zone [70]. Retroviral labelling studies have also demonstrated that a radial glial cell that produces neurons can then itself transform into an astroglial cell [68]. Radial glial cells, as well as neuroepithelial cells, also generate another neuronal progenitor called a basal progenitor. These cells leave the ventricular zone and form the subventricular zone (SVZ) of the brain [68]. Progenitors in this region can divide either symmetrically or asymmetrically. They are reported to produce only neurons and not glia, but this is disputed [71, 72].

Once neurogenesis is completed during development, it was historically thought that there was little turnover of cells in the adult brain. Whilst it is true that most neural stem and progenitor cells have differentiated into neurons and glia by the end of development, some persist and stem cells can be isolated from the adult human brain that undergo self-renew and differentiation into neuronal, astrocytic and oligodendroglial lineages [71, 73]. Neural stem cells with radial glial characteristics persist in restricted regions of the adult brain, namely the SVZ and the subgranular

layer of the hippocampus [68]. For example, it has been demonstrated that one third of neurons in the human hippocampus are regularly renewed throughout life [74].
Much of what is described about adult mammalian neural stem cells comes from experiments in non-human subjects. The adult neural stem cell in the rodent SVZ can be differentiated into astrocytes, oligodendrocytes and neurons in vitro [13]. In these models the NSC in the SVZ are known as type B cells [13]. These cells will give rise to actively proliferating type C cells that in turn produce immature neuroblasts (type A cells) that migrate to the olfactory bulb [13]. The SVZ B cells have similar morphological characteristics to embryonic radial glial cells and express Nestin and Sox2 [68]. Type B cells also express GFAP and GLAST that are more frequently associated with astrocytes [68]. The radial glial-like adult neural stem cells give rise to basal progenitor-like cells that in turn produce neurons and possibly glial cells (Figure 1.5) [71].

Importantly, stem-like cells that can give rise to new neurons and glia have also been identified in adult human brain removed intra-operatively or at post mortem [72]. These cells reside in the SVZ of the human brain and are radial glia-like, generate neurospheres similar to neural stem cells, and can be differentiated into GFAP-positive astrocytes, O4-positive oligodendrocytes and TuJ1-positive neurons, in a ratio 87.8%:6.5%:5.8%, respectively [72]. Interrogation of the cellular architecture of the SVZ in adult humans has identified that these cells exist as a ribbon of mitotically active cells separated from the ependyma by a gap filled with GFAP-positive processes [72]. These ‘gap’ cells were astrocytic in appearance at the ultrastructural level, staining for both Vimentin and GFAP [72]. This cytoarchitecture is distinct from that described previously in the SVZ of rodents and primates.

Despite differences between rodent and human adult neurogenesis, the key fact is that neural stem or progenitor cells exist in the adult human SVZ. It is a transformation event in these cells that is thought to be responsible for the initiation of at least some gliomas [71, 75]. It has also been proposed that more fate restricted

glial progenitor cells in the subcortical white matter and cortex, such as oligodendrocyte precursor cells, might be responsible for initiation of the Proneural subtype of gliomas (Figure 1.5) [28].

1.3.3 The glioma stem-like cell

The hierarchical model of glioma initiation and development benefits from these observations that the normal brain, rather than being a post-mitotic organ, actually contains stem or progenitor cells that can be grown and differentiated into astrocytes, neurons and oligodendrocytes [75]. The subpopulation of cells in glioma that is thought to have tumour-initiating properties has been shown to resemble these precursor cells, hence why they have been called glioma stem-like cells [66, 75, 76]. The glioma stem-like cells also appear to be regulated by the same cellular pathways as neural stem cells [66, 75, 76]. Furthermore, a role for stem-like cells in gliomagenesis is supported by the observation that the SVZ region of the adult brain rich in progenitor cells and their progeny is also implicated from radiological and pathological studies as the region of glioma origin [59, 77-79]. However, despite these observations supporting a link between glioma stem-like cells and neural progenitors, the precise lineage relationship between these cell types remains uncertain. This is because an alternative explanation is that the stem-like features of this subpopulation of glioma cells are instead acquired during transformation of a differentiated cell [80-82]. It is not yet known which of these cell of origin hypotheses is correct and further in vitro and vivo modelling will be required to interrogate this problem further [83]. I will review some of the evidence supporting a native stem cell origin for the glioma stem-like cell when I discuss in vivo glioma models.

1.3.4 In vitro modelling of the glioma stem-like cell

Glioma stem-like cells with the stem cell-like characteristics of self-renewal and multipotency have been purified from human gliomas using a serum-free culture technique. The serum-free approach to cell culture contrasts with the 'traditional' culture of glioma cell lines in serum-supplemented media even though in vivo the vasculature prevents exposure of cells to serum [61, 75]. When glioma stem-like cells are transplanted into immune deficient mice the tumours that form recapitulate some of the features of the glioma from which they were derived [75]. Significantly, when these primary culture cells were compared with cell lines grown from matched glioma tissue cultured in serum, the glioma stem cell-like primary cultures, but not the serum-grown cell lines, were found to have a genotype, gene expression profile and in vivo biology that closely resembled the tumour from which the cells have been derived [61]. Serum-supplemented media was shown to cause irreversible cell differentiation such that the phenotypic characteristics and genetic aberrations within these repeatedly in vitro passaged cell lines had little resemblance to those found within the corresponding primary human tumour [61]. For these reasons glioma-stem like cells are currently the preferred modality for in vitro studies in glioma, as evidenced by the prevailing literature.

An important first step in modelling and interrogating the glioma stem-like cell in vitro is to develop a tissue culture technique that enriches for these cells rather than the differentiated cell types that dominate existing serum-derived glioma cell lines and gliomas themselves. Key to this is access to abundant fresh human glioma tissue from which primary cultures can be derived. The purification of glioma stem-like cells from human gliomas utilises serum-free tissue culture conditions for the reasons described above [3, 66, 67]. This strategy is itself adapted from the method used to expand and maintain a continuously dividing multi-potent population of progenitor cells from the human embryonic forebrain [65, 67, 84]. Another key component of the glioma stem-like cell culture techniques that have been described is the addition

of basic fibroblast growth factor (bFGF) to prevent cell differentiation and epidermal growth factor (EGF) to support proliferation, which again builds on the in vitro culture of neural stem cells and progenitor cells [61, 85, 86]. With this basic strategy, primary cultures can be reliably derived from human gliomas [65, 87]. The constituent cells in these cultures have stem-like or progenitor-like characteristics and are observed to grow as neurosphere-like collections of cells, similar to neural stem cells; I will subsequently refer to these neurosphere-like structures as glioma-derived spheres [3, 66, 88]. Cells without stem-like or progenitor-like features have more restricted self-renewal capacity and lineage potential, and so tend to adhere to the plastic of the culture dish, differentiate and cease to proliferate [3, 66, 67]. Interestingly though, even within neural stem cell-derived neurospheres originating from normal brain tissue, only approximately 1% of cells are actually stem cells with the ability to self-renew and generate all neural lineages [85, 89]. This suggests that glioma-derived spheres will also contain a heterogeneous population of cells in different stages of differentiation and with different self-renewal capacity.

Cells within glioma-derived spheres been observed to have biological similarities to neural stem cells. For example, glioma stem-like cells stain with antibodies to Nestin, an intermediate filament protein expressed during development in neuroepithelial precursor cells and radial glial cells that is downregulated with differentiation, but re-expressed by reactive astrocytes [90, 91]. Another similarity between glioma stem-like cells and neural stem cells is the ability of both to differentiate into multiple cell lineages. Glioma stem-like cells can differentiate on removal of EGF and bFGF down neuronal and oligodendroglial lineages [87]. The further addition of either Bone Morphogenic Protein 4 (BMP4) or fetal calf serum is necessary for astrocytic differentiation [87]. The differentiation of individual glioma stem-like cells can be assessed after one week using an immunohistochemical technique, with antibodies to GFAP, TUJ-1 or O4 to characterise astrocytic, neuronal and oligodendroglial differentiation, respectively [87]. This in vitro observation appears clinically relevant, because gliomas are themselves a heterogeneous mass of undifferentiated

and differentiated tumour cells, some of which express either neural or glial markers, supporting an hypothesis that the glioma initiating cell does indeed have a multi-potent capacity [3, 66, 67, 88]. Nevertheless, this strategy of assessing multipotency does have its limitations. For example, I described above that GFAP was expressed both by some radial glial cells as well as differentiated astrocytes, so the antibody staining is not specific for differentiated cells. Moreover, individual cells in gliomas and in vitro can actually be 'double-positive' with antibodies to both astrocytic (e.g. GFAP) and neuronal (e.g. neurofilament) proteins, indicating that the process of differentiation is disordered [3, 66, 67, 88]. Furthermore, compared to neural stem cells, the process of differentiation in glioma stem-like cells is generally less efficient, meaning that stem-like cells cannot always be driven to differentiate into all three neural lineages, namely astrocytic, neuronal and oligodendroglial [67]. The differentiation that does occur appears predictable by tumour histology. For example, oligodendroglial differentiation is generally found only in glioma stem-like cells derived from oligodendrogliomas [67]. These observations suggest that glioma stem-like cells in primary culture may have more progenitor-like rather than stem-like abilities. Nevertheless, glioma stem-like cells are capable of self-renewal and a single glioma stem-like cell can be expanded clonally, in similarity to neural stem cells [3, 66, 67, 88]. The frequency of clone formation varies according to the grade of the tumour and is greatest for GBM, perhaps suggesting that these high-grade tumours contain the most stem-like cells [75]. Differentiation inhibits this clonagenic ability, as would be expected from neural stem cell biology [61].

A key requirement of the glioma stem-like cell as a putative tumour-initiating cell is that it has the ability to generate tumours in vivo that recapitulate human gliomas. In fact, it has been demonstrated that implantation of glioma stem-like cells into the brain of immune compromised mice results in the formation of tumours that more accurately replicate the infiltrating growth pattern of human tumours than tumours that form in vivo from the injection of traditional serum-grown glioma cell lines [66, 67]. For example, just 100 glioma stem-like cells purified by their expression of

CD133 were capable of initiating tumour growth in 12-24 weeks when injected into the striatum of immune compromised mice [75]; I will discuss the relevance of CD133 expression below. Therefore, as well as being stem-like, these cells derived from human gliomas in serum-free conditions can also be said to have tumourigenic potential and so fit the criteria for being cancer stem cells [66, 67].

1.3.5. Glioma stem-like cell enrichment

Similar to neural stem cells, glioma stem-like cells have been demonstrated to undergo both symmetric and asymmetric divisions to produce either self-renewal or differentiated cells, respectively [92]. The result is cellular heterogeneity within primary cell cultures. Similar heterogeneity is observed in vivo, but in vitro this could complicate interrogation of a single cell type of interest from within the heterogeneous mix of cells. Attempts have therefore been made to enrich the proportion of stem-like cells, rather than more differentiated cells, in glioma primary culture [55]. The main approach to achieving this has been to sort cells with flow cytometry using antibodies to cell surface makers that have been proposed to be specific to the glioma stem-like cell [93-97]. These markers include CD133, LICAM (L1 cell adhesion molecule), α6 integrin and CD15 [93-103]. Of these, the CD133 antigen is the most commonly described for enriching glioma stem-like cells in primary cultures [93-103].

CD133 is a five transmembrane spanning cell surface marker that can enrich for neural stem cells capable of neurosphere initiation, self-renewal, and multilineage differentiation from normal brain, although its actual function is largely unknown [104]. CD133 is selectively found in the apical plasma membrane of neuroepithelial cells and radial glial cells in the developing brain [69]. CD133 is also found on some cells types outside the CNS including endothelial progenitors, myogenic cells and prostatic epithelial stem cells, as well as cancers of the prostate, colon and lung [93]. In neurosphere cultures CD133 is lost on differentiation [98, 105]. CD133 is also

expressed in glioma tumours and this expression is associated with increasing tumour grade [103]. Early reports suggested that only CD133 positive glioma stem-like cells were capable of self-renewal in vitro and that as few as 100 CD133 positive cells were required to form tumours in immune compromised mice, in contrast to 10,000 unsorted cancer cells [3, 75]. However, CD133 negative cells are actually able to generate CD133 positive cells in vitro and in sufficient numbers CD133 negative cells will even form tumours in vivo [106]. It has also been shown that not all CD133 positive glioma-derived spheres form secondary glioma-derived spheres in vitro and that some glioma stem-like cell cultures have heterogeneous or even absent CD133 expression, correlating with their parent tumour [91, 98, 101]. There is therefore clearly much still to be understood about what role, if any, CD133 antigen expression plays in defining the glioma stem-like cell.

LICAM, also known as CD171, is a transmembrane glycoprotein neural cell adhesion molecule that has a role in the regulation of neuronal cell growth, migration, axonal outgrowth and neurite extension during CNS development [94]. LICAM expression is a poor prognostic indicator in solid cancers such as colorectal cancer where it is thought to protect against drug-induced apoptosis [94]. LICAM is overexpressed in gliomas, but its expression in glioma stem-like cells segregates with CD133 expression, so cell sorting for this protein does not appear to offer much additional value to enrichment using the CD133 antigen alone [94]. However, L1CAM may have a role in glioma stem-like cell survival though activation of DNA damage checkpoint repair and so its knockdown is an interesting potential target for future research [107]

CD15, also known as Lewis X and stage-specific embyonic antigen 1 (SSEA-1), is a carbohydrate adhesion molecule [106, 108]. It mediates phagocytosis and chemotaxis of neutrophils, is a marker of murine pluripotent stem cells, and its expression on so-called Reed-Sternberg cells is diagnostic of Hodgkin disease [108]. In glioma, CD15 selects a subpopulation of cells from a CD133-negative population of glioma stem-

like cells that can form glioma-derived spheres, differentiate down neural lineages and initiate tumourigenesis [92]. However, this antigen has not been identified in all gliomas, so its applicability as a generic tool for the enrichment of stem-like cells is uncertain [92]. Furthermore, CD133 negative cells have independently been shown to form glioma-derived spheres in vitro and tumours in vivo, so the added value of cell sorting with the CD15 antigen is yet to be fully demonstrated [106]. It has been suggested though that combined CD133/CD15 antigen positivity may specifically select cells indicative of a rare variety of malignant glioma that has a mixed astrocytic and primitive/embryonal elements [109]. This antigen may therefore be of use as a diagnostic tool.

The α6 integrin may have more potential as a glioma stem-like cell marker. Integrins are transmembrane receptors that mediate the attachment between a cell and extracellular matrix proteins [97]. The integrin receptor is a heterodimer of an α and β subunit; eighteen α and eight β subunits have been described in mammals and variants of some of the subunits also occur as a result of differential splicing [110]. It is known that in the normal brain α6 integrin forms a heterodimer with either integrin β1 or β4 and interacts with extracellular laminin to regulate normal neural stem cells. It also regulates proliferation and migration of the glioma stem-like cell [92]. Further characterisation of glioma stem-like cells purified by their α6 integrin expression is therefore awaited. Interestingly, inhibition of α6 integrin in glioma stem-like cells using lentiviral delivery of shRNA directed against the α6 integrin impairs self-renewal of cells and glioma formation [92]. Integrin inhibition may therefore be an important future treatment strategy in glioma; the major integrin inhibitor trial to date was of Cilengitide, a selective inhibitor of αvβ3 and α5β5 integrins, but this did not increase overall survival in a recent trial of patients with newly diagnosed GBM containing a methylated MGMT promoter [111].

Another promising approach to glioma stem-like cell purification is the so-called ‘side population’ technique. This is based on the observation that lipophilic dyes

such as Hoechst 33342 are effluxed from stem cells because of expression of ATP-binding cassette (ABC) transporters [112]. Glioma stem-like cells selected in this way have been demonstrated to form larger tumours in xenotransplantation models than the non-side population [112]. This technique for enriching stem-like cells from glioma primary cultures has potential, but further characterisation of the stem-like and glioma initiating characteristics of the purified cells is needed [112].

In practice, it may be that a selection of different markers is required to enrich a cell population with stem-like cells from glioma primary cultures. This may vary depending on the molecular and biological characteristics of the glioma from which a given cell culture has been derived. The expression levels of markers may even change within primary cultures over time, with the cell cycle, or on purification.

1.3.6 The role of oxygen tension in glioma stem-like cell culture

Another key area of interest in the optimisation of glioma stem-like cell culture is whether there is a benefit to deriving and expanding cultures in hypoxic conditions. Hypoxia is important in neural stem cell biology where, for example, it delays or halts senescence and apoptosis [113, 114]. Hypoxia may therefore also have a role in glioma stem-like cells.

Glioma stem-like cell cultures are traditionally incubated in an environment containing approximately 20% oxygen, equivalent to a partial pressure of oxygen (pO_2) of 150 millimetres of mercury (mmHg) [115]. The percentage of oxygen in blood is at most half of this and within the normal brain actually ranges from only 1% to 5% [116, 117]. Intra-tumoural electrode studies have shown a mean tumour pO_2 of 21mmHg, which is approximately 3% O_2 [118]. The mean peri-tumoural tissue pO_2 in this same study was 29.1mmHg, so not significantly different from the reading in the tumour [118]. Standard in vitro incubation of cells at 20% oxygen is therefore clearly non-physiological. This observation has influenced the adoption of

so-called ‘hypoxic’ tissue culture incubation in 3% oxygen conditions, a partial pressure that is actually ‘normoxic’ with respect to the normal human brain and gliomas [101].

Pesudopalisading necrosis and endothelial proliferation are histological characteristics of hypoxia [112, 119]. Both these hallmarks are observed in glioma tissue samples and increase with tumour grade [112, 119]. This supports the hypothesis that hypoxia may have a biological role in glioma development and it is plausible that such a role is facilitated through the action of hypoxia on glioma stem-like cells [112, 119]. Moreover, the genes specifically expressed in an enriched population of glioma stem-like cells in vitro are also enriched in vascular and necrotic niches within glioma tissue, implicating these hypoxic niches as key the location of glioma stem-like cells [112, 120]. Interestingly, the putative glioma stem-like cell marker CD133 has been demonstrated to be enriched in glioma cells cultured in hypoxia, as well as in hypoxic areas of tumour tissue [112]. In hypoxic conditions in vitro it has also been shown that non-stem-like glioma cells can acquire the properties of self-renewal and begin to express genes related to stem cell-like function, a process thought to be regulated by hypoxia-inducible factors [93].

Hypoxia drives tumour progression by initiating adaptive transcriptional responses that regulate tumour angiogenesis, tumour cell metabolism, motility and survival, ultimately promoting a more aggressive tumour phenotype [112]. The transcription factors known as Hypoxia-Inducible Factors (HIFs) play a key role in these events [121]. HIFs are heterodimers composed of a specific alpha subunit and a shared constitutively expressed beta subunit; two mammalian alpha subunits have been described HIF-1α and HIF-2α [121]. Hypoxia stabilises HIF-1α by inhibiting its hydroxylation by prolyl hydroxylase. Hydroxylation of HIF-1α normally leads to its degradation, because this promotes binding of von Hippel-Lindau that is itself part of an E3 ubiquitin ligase complex that facilitates proteosomal degradation [122]. In contrast, stabilisation of HIF-1α results in its translocation to the nucleus, where it

dimerises with HIF-1β to form active HIF-1, leading ultimately to target gene expression.

If hypoxia delays or halts senescence and apoptosis in glioma stem-like cells, as is seen in neural stem cells, then increased HIF-mediated target gene expression may be facilitate this, protecting the pool of cancer stem cells [113, 114]. Interestingly, TP53 enhances the degradation of HIF-1α, so the mutations of *p53* that are common in gliomas contribute to increased HIF-1α expression; HIF-1α expression is also increased by EGFR amplification and by PI3-kinase activation, for example as a result of PTEN loss [122]. Through its role in transcriptional regulation, HIF-1 may directly or indirectly regulate stem cell genes such as Oct4 and Notch, influencing the tumour stem cell phenotype [112]. HIFs may also have a further role in attenuating the ability of BMP4 to induce differentiation of glioma stem-like cells [121].

HIF-2α has also been shown to have a role in the response of glioma to hypoxia [112, 122]. HIF-2α is structurally similar to HIF-1α, but HIF-2α expression appears to be specific to glioma cell biology and no HIF-2α mRNA or protein was expressed in normal neural progenitors [121, 122]. Moreover, whilst HIF-2α expression levels were elevated at up to 5% oxygen levels, as is found in the brain and gliomas, HIF-1α was present only at <1% oxygen levels. HIF-2α is responsible for mediating the regulation of angiogenesis by glioma stem-like cells through VEGF secretion [121]. HIF-2α, but not HIF-1α, expression levels have also been associated with poor prognosis [121]. In fact, HIF-2α expression is able to induce a stem-cell like phenotype in cells without a stem cell-like profile, as characterised by induction of Nanog, c-myc and Oct4 expression [121]. This observation emphasises the potential value of HIF-2α as a therapeutic target, and in fact, knockdown of HIF-2α supresses the stem-like gene expression profile characteristic of glioma stem-like cells [112, 121].

In gliomas, hypoxia appears to have a role in promoting resistance to current therapies, firstly through upregulation of genes including erythropoietin and VEGF that promote radiation resistance, and secondly through an impaired ability for DNA damage to occur because of the reduced availability of oxygen for free radical formation, limiting the efficacy of some chemotherapy agents [114, 123, 124]. Hypoxia, acting through HIFs, also induces the expression of the ATP-binding cassette transporters that are thought to confer drug resistance in glioma stem-like cells [112].

If hypoxia has such an important role in glioma stem-like cell biology, then it needs to be modelled in vitro. During in vitro culture the oxygen tension at the cellular level depends not only on the atmospheric partial pressure of oxygen, but also on the depth of media and the density of cells. This importance of the density of cells therefore raises an important question as to whether glioma primary cultures should be propagated as glioma-derived spheres or as monolayers [116]. The initial descriptions of glioma stem-like cell culture were of glioma-derived spheres that were similar to the neurospheres seen in neural stem cell culture [66]. Glioma-derived spheres have a three-dimensional shape and so cells in the centre of the spheres will be subject to a markedly different oxygen tension than the cells around the periphery. This might influence growth of the glioma stem-like cells. An alternative approach is therefore to propagate glioma stem-like cells as monolayers where all cells have a more uniform exposure to the prevailing culture media oxygen conditions [65-67]. Such monolayer cultures have been demonstrated to maintain glioma stem-like cells in their stem-like state and are now the preferred method for propagation of these cells in vitro [67]. These cultures are also more reliable for developing inhibitor compound assays, as I will discuss below [67].

1.3.7 Glioma stem-like cell therapy resistance

The culture of glioma stem-like cells from human patients provides an in vitro model in which inhibitor compound screening can be performed. The goal is to identify therapies that will translate successfully into the clinic. As I discussed previously, stem-like cells are thought to better recapitulate the biology of human disease than serum-grown glioma cell lines, because they have a genetic profile that more closely resembles the tumour from which they were derived. Glioma stem-like cells, but not the differentiated glioma cells observed in serum-supplemented media, are also thought to be responsible for glioma initiation, propagation and treatment resistance, emphasising the need to model them in vitro [75, 125]. Glioma stem-like cells might therefore be better than serum-grown glioma cell lines at selecting inhibitors in vitro that will subsequently be effective in the clinic [125, 126].

An important way in which glioma stem-like cells are proposed to recapitulate human disease is that they are thought to be the population of cells responsible for resistance to current therapies [125, 126]. For example, glioma stem-like cells generally have a better capacity for DNA-damage repair and activation of survival pathways than more differentiated cells and this contributes to resistance to chemo-radiotherapies [125, 126]. Another mechanism of chemotherapy resistance in glioma stem-like cells is the increased expression and activity of O-6-methylguanine-DNA methyltransferase (MGMT) [125]. The therapeutic activity of TMZ depends on its ability to alkylate and methylate DNA, so cells that have increased levels of MGMT are better able to repair DNA damage and are more resistant to this drug [29]. TMZ may actually also increase the stem-like characteristics of glioma cells, especially those cells that have lost the Phosphatase and Tensin Homologue (*PTEN*) gene [126]; mutation of the *PTEN* gene is a common finding in gliomas [127]. Other mechanisms of resistance in glioma stem-like cells include the expression of transporters such as the BRCP1 ABC transporter that facilitate efflux of

chemotherapy drugs [112, 128]. These transporters are expressed in higher concentrations on glioma stem-like cells than other glioma cells [112, 128].

These observations suggest that glioma stem-like cells are the source of resistance to current glioma therapies. This could explain why many inhibitor compounds that appeared to be effective in preclinical studies based on traditional serum-grown glioma cell lines have failed to translate successfully into the clinic [67, 129]. Therapies deemed effective against serum-grown glioma cells lines target the bulk of differentiated cells within the glioma mass, but may not be effective against the sub-population of glioma stem-like cells [51]. The glioma stem-like cells that remain are then responsible for tumour regrowth and clinical recurrence. If therapies are instead selected based on their efficacy against glioma stem-like cells then they may have more efficacy in the clinic. Support for the potential usefulness of a glioma stem-like cell model rather than a traditional serum-grown glioma cell line approach to compound screening has been demonstrated recently [130]. An in vitro model of high passage traditional serum-grown glioma cells had previously supported a role for the small molecule tyrosine kinase inhibitor Imatinib through inhibition of the Platelet-Derived Growth Factor (PDGF) receptor tyrosine kinase, but this effect had not been clinically reproducible [130]. An in vitro model of glioma stem-like cells was therefore used to evaluate the role of PDGF signalling and inhibition [130]. The results predicted the lack of therapeutic efficacy of PDGF receptor inhibition that had been observed in the clinic [130]. This underlines the potential importance of accurate disease modelling based on the glioma stem-like cell.

1.3.8 Screening for compound inhibitors of glioma stem-like cells

Modelling the stem-like cell subpopulation of glioma provides an opportunity to screen for inhibitors that can overcome the resistance mechanisms that I have described above. It is also important that the assays against which potential drugs are screened have biological end points that are relevant to the natural history of the

disease [131]. For example, proliferative assays based solely on assessment of total protein content, such as the sulforhodamine B colorimetric assay, do not differentiate between cell cycle arrest and apoptosis as the mechanism of reduced proliferation [132, 133]. Such a distinction is important, because arrested cells can re-enter the cell cycle when the inhibitor is removed and contribute to tumour recurrence [134]. The assays should also permit compounds to be tested both singly and in combination. This is because inhibition of individual targets is unlikely to be a successful strategy as cells are able to dynamically adapt and activate redundant cell signalling pathways, leading ultimately to tumour recurrence [135, 136]. For any compound found to be efficacious against glioma cells in vitro or in vivo, evidence should be sought that the actual mechanism of action modulates a target (or targets) in a disease relevant pathway. This is necessary to reduce the likelihood that the compound would be poorly tolerated by patients because of toxicity caused by off-target effects. This might be achieved, for example, by using a relevant biomarker that identifies an on target effect [137]. An alternative approach is to make a proteomic profiling of cells subjected to compound treatment [137]. If multiple proteins can be assessed simultaneously, for example by using a reverse phase protein microarray approach, then response to a single agent across multiple signalling pathways can be analysed [138]. Such a strategy can be used to confirm the on target activity of a compound, but has the additional advantage of also being able to identify activation of other signalling pathways, therefore guiding the design of combinatorial therapies.

It is clear from this discussion that the actual conduct of in vitro compound screening is perhaps as important as ensuring the model used accurately recapitulates human disease. To conduct preclinical drug assessment to the standards that I have outlined, in a timely and efficient manor across several different primary cultures requires a suite of assays that assess multiple and distinct biological processes. This can be achieved through a process known as high content phenotypic analysis that is of increasing interest to both pharmaceutical companies and academics [137].

1.3.9 High content phenotypic analysis

Efficient and effective drug discovery requires that model systems can be used to screen compounds, or combinations of compounds, rapidly and reliably [137]. Assays should provide a robust and reproducible representation of a biologically relevant event following administration of an inhibitor without relying on preconceptions of cellular targets of the compound [137]. Drug discovery has traditionally been target-directed based on the perceived importance of a given target in the biology of the disease of interest [139]. However, target-validation often lacks a clear definition as to the criteria that need to be fulfilled for a target to be considered validated. This makes it difficult to predict whether compounds selected against a given target are likely to be effective [139].

In contrast to a target directed approach to compound selection and validation, high content phenotypic analysis quantifies cellular phenotype responses to an inhibitor in an unbiased way [137]. This approach is necessary because cellular pathways have multiple readouts and cross talk to other pathways [139]. High content phenotypic analysis has become possible because of the availability of technologies that allow the rapid interrogation of multiple biological systems in parallel [137]. The assessment of drug efficacy therefore no longer needs to be based on the binary success or failure of a single assay [137]. High content phenotypic analysis utilises automated microscopes and image analysis algorithms to carry out phenotypic multiparametric cellular analysis across multiple cells in an unbiased, target agnostic, fully automated and quantitative fashion [139]. Automation removes the potential imaging bias of an individual researcher and allows a large number of images to be collected, in contrast with the traditional strategy of applying imaging subjectively on a small scale, limiting both the quality and throughput [137]. It also allows analyses to be performed on live cells, allowing the temporal assessment of biological efficacy, and several modes of action, to be screened concomitantly [137]. This reduces the likelihood of false positives in terms of drug efficacy [137]. The

likelihood of identifying a biological response to an inhibitor in vitro that will be clinically relevant can be further enhanced by performing multiple experiments in parallel over a series of compound concentrations, or by comparing different compounds with related mechanisms of action [137].

High content phenotypic assays offer an approach to inhibitor compound screening that might improve on the high attrition rates of current glioma drug discovery [137, 139]. There is support for the use of high content phenotypic analysis in compound screening of glioma stem-like cells in the existing literature [129, 130]. For example, in one screen of 1000 inhibitor compounds using a live imaging assay, 14 compounds were identified that had a significant cytotoxic effect on glioma stem-like cells [98]. The translation of this research into clinical trials is awaited.

1.3.10 Identifying targets for compound inhibition

As I discussed above, the Cancer Genome Atlas group identified 10 key genes in glioma from analysis of over 200 tumours [20]. These genes affected three key signalling pathways, namely the TP53, RB1 and PI3 kinase pathways [20]. In a majority of the tumours that they examined only one gene in any of these three key pathways was mutated, although more than one pathway was affected in each tumour [20]. This was interpreted as indicating that any gene alteration in a given pathway is functionally equivalent for the purposes of tumourigenesis. This suggests that these three pathways are likely important targets for inhibitor compounds. By contrast, the current chemotherapy of choice in the clinic for glioma, TMZ, has a non-specific cytotoxic action through DNA damage mechanisms [2, 45]. There is therefore a need to screen inhibitor compounds targeting the TP53, RB1 and PI3 kinase pathways in glioma stem-like cell models. There are also other signalling pathways that have been demonstrated to be deranged in gliomas, including the Mitogen-Activated Protein Kinase (MAPK) pathway (Table 1.2) [20, 140].

Table 1.2 Summary of pathways implicated in the pathogenesis of glioma. Genes commonly mutated or over-expressed in gliomas in each of these pathways are indicated [20, 141-143].

Pathways	Genes commonly mutated/over-expressed in glioma
PI3 kinase	*PTEN, EGFR, ERBB2, PDGFRA, MET, NF1, MET*
Notch signalling	*DII-3, Hash-1*
TP53	*TP53, $p14^{ARF}$, MDM2*
RB1	*$p16^{INK4a}$, CDK4, RB1*
RAF/MEK/ERK	*ERK*

Inhibitor compounds have already been trialled both in preclinical and clinical studies against multiple targets in these pathways (Table 1.3). As I have already discussed, the majority of these therapies have failed to demonstrate significant clinical efficacy despite appearing promising in the laboratory, possibly because the preclinical models on which their efficacy was assessed did not adequately recapitulate human disease as they were based on serum-grown glioma cell lines [144]. Other reasons why these compounds may have failed in the clinic include heterogeneity of expression of the inhibitor's molecular target in the tumour, compound-induced activation of redundant signalling pathways, or failure to identify a biologically relevant endpoint for evaluation of the drug [144]. It may also be that tumour tissue concentrations of the compound of interest have been too low in human subjects, perhaps because of the blood brain barrier. I have already discussed strategies by which some of these problems can be addressed in preclinical compound screening design.

Of the key somatic mutations identified in glioma, including *PTEN, Nf1, EGFR, IDH1* and *ErbB2*, one of the most significant for glioma cell biology is *PTEN* [27]. The *PTEN* gene is located at 10q23.3 and encodes a tyrosine phosphatase, phosphatidylinositol-3,4,5-trisphosphate 3-phosphatase, with a lipid phosphatase activity that targets phosphatidyl inositol-3,4,5-triphosphate (PIP3) (Figure 1.6) [127]. PIP3 is a component of the phosphatidylinositol 3-kinase (PI3 kinase) pathway [127]. The PI3 kinases are lipid kinases that can be activated by a wide range of receptor tyrosine kinases, such as EGFR, resulting in the phosphorylation of phophatodylinositol-4,5,-bisphosphate (PIP2) and generating PIP3. PIP3 recruits Akt, a protein serine/threonine kinase, and phosphoinositide-dependent kinase-1 (PDK1) to the plasma membrane (Figure 1.6) [145]. In combination, PDK1 phosphorylates Akt at its threonine 308 residue, leading to its partial activation [145]. Full activation occurs through phosphorylation of Akt's serine 473 residue by the TORC2 complex of mammalian target of Rapamycin (mTOR) protein kinase [145].

Table 1.3 Compounds in current use in pre-clinical studies, clinical trials or clinical practice in the management of glioma. The molecular entity against which these compounds are targeted is indicated [143].

Therapy targets	Compounds
DNA	Temozolomide
EGFR	Gefitinib, Erlotinib, Nimotuzumab, Lapatinib
PDGFR	Sorafenib
VEGFR, Raf, PDGFR	Bevacizumab, Vatalanib, Cediranib
Integrins avb3, a5b5	Cilengitide
Notch 1	GSI RO4929097
VEGF	Afllibercept
Ribonucleotide reductase	Hydroxyurea
Bcr-able, c-KIT, PDGFR	Imatinib
Ras	Tipifarnib
mTOR	Temsirolimus, Rapamycin, Everolimus
HDAC	Vorinostat, Valproic acid, Depsipeptide
Farnesyltransferase	Tipifarnib, Ionafarnib
VEGFR, EGFR, RET	Vandetanib
VEGFR-2, PDGFR, c-KIT	Sunitinib maleate
Src, Abl	Dasatinib
TGF-b2	AP 12009
Ubiquitin-proteosome	Bortezomib
Topoisomerase 1	Irinotecan
Protein Kinase C	Enzastaurin
poly-ADP ribose polymerase	Veliparib, Iniparib
PDGFR, c-KIT, Bcr-ABL	Tandutinib
Hepatocyte growth factor	AMG 102
FLT1/KDR	Cediranib

Figure 1.6 PTEN and the PI3 kinase pathway, with common compound inhibitors. This Figure provides an illustration of the importance of the PTEN protein in the PI3 kinase pathway. PI3 kinases, such as the class I PI3 kinase illustrated, are activated by tyrosine kinases such as EGFR. This leads to phosphorylation of phophatodylinositol-4,5,-bisphosphate (PIP2), generating phophatodylinositol-3,4,5,-bisphosphate (PIP3). PIP3 is localised on the cell membrane and recruits Akt in addition to PDK1. In combination with Akt, PDK1 phosphorylates and activates Akt at its threonine 308 residue. Full activation of Akt occurs with phosphorylation of its serine 437 residue by the TORC2 complex of the mamallian target of Rapamycin (mTOR) protein kinase. Akt in its activated state has many important roles including in cell proliferation and migration. PTEN protein has a tumour supressor activity, because its phosphatase activity converts PIP3 back to PIP2, so reducing the activation of Akt. Indicated in the square boxes are compound inhibitors targeted against EGFR, PI3 kinase, PDK1, mTOR and Akt.

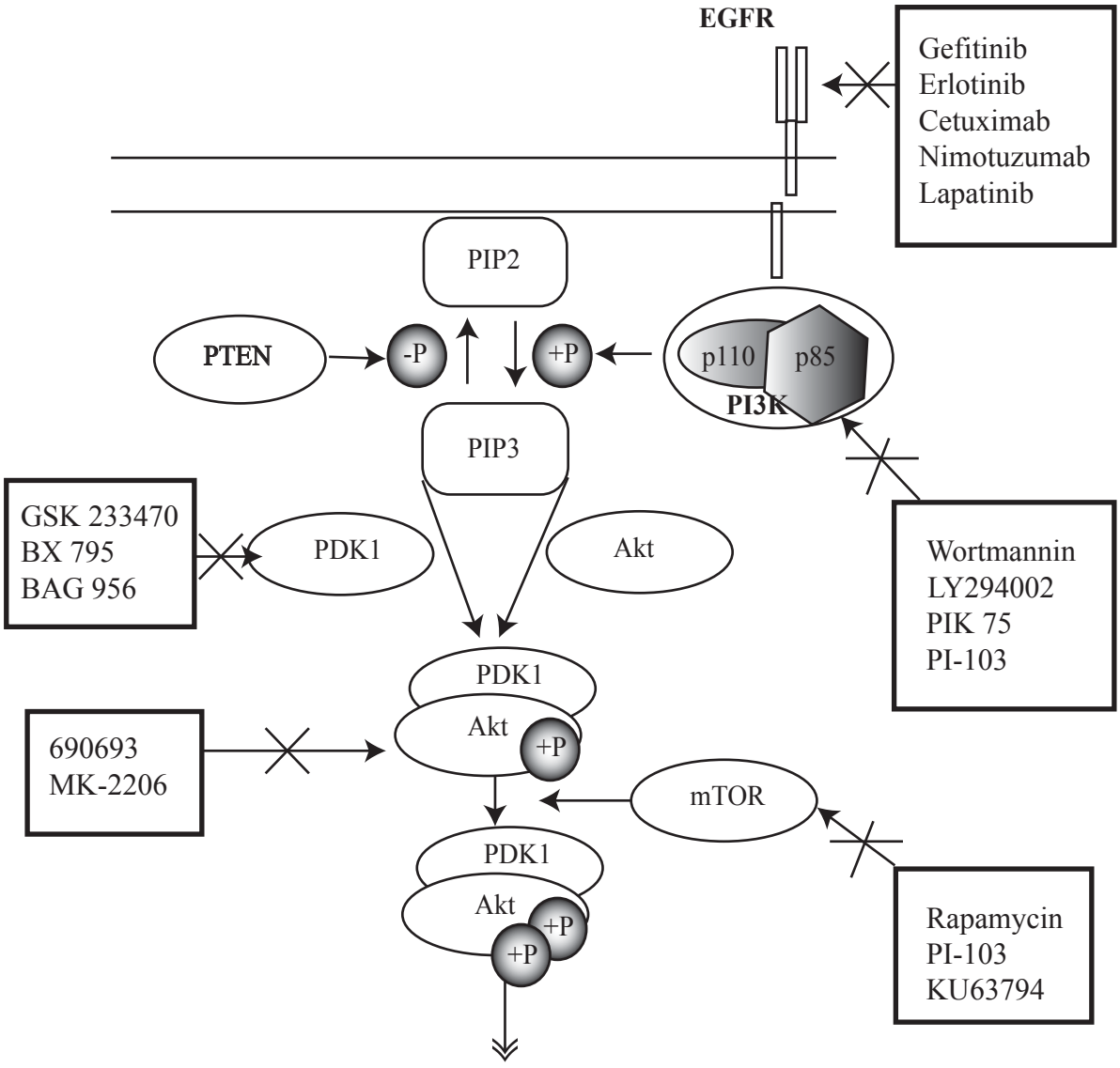

Activation of Akt in turn leads to phosphorylation of proteins involved in the regulation of cell growth, differentiation, adhesion, migration and survival [145] [146]. The PTEN protein converts PIP3 back to phosphatidylinositol 4,5-bisphosphate, so negatively regulating the PI3 kinase pathway and downgrading these events [127]. PTEN inactivation therefore results in persistent pathway and cellular activation [147].

Loss of heterozygosity (LOH) on the long arm of chromosome 10, a region that includes the *PTEN* locus, is the most frequent mutation in both primary and secondary GBMs (60-90%) [148]. Forty-four percent of GBMs have homozygous somatic *PTEN* mutations [148]. The frequency with which *PTEN* loss occurs in gliomas suggests that it is an early event in the process of tumour initiation. Moreover, in both clinical and preclinical trials *PTEN* deletion has been directly associated with therapy resistance that correlates with adverse clinical outcomes, perhaps because the PI3 kinase pathway regulates ABC transporters, which in turn contribute to chemotherapy resistance in glioma stem-like cells [126] [149]. Conversely, overexpression of wild-type *PTEN* suppresses growth in *PTEN*-mutated serum-derived glioma cell lines [126, 150].

If glioma stem-like cells are responsible for tumour initiation and *PTEN* loss is an early event in glioma development, then it follows that *PTEN* mutations may occur in glioma stem-like cells. Interestingly, PTEN is already known to have an important role in neural stem cell biology, because *PTEN* loss is associated with increased proliferation and self-renewal of these cells [146, 151]. Furthermore, in an array comparing normal fetal neural stem cells to glioma stem-like cells, *PTEN* was the most significantly down-regulated gene in the glioma cells [67]. Additional evidence of a key role for *PTEN* loss in glioma stem-like cells comes from in vivo modelling. For example, it has been observed that both low and high-grade gliomas are formed when homozygous loss of *PTEN* and *Ink4a/Arf* alleles were targeted to mouse neural stem cells [152]. Glioma-like tumours also formed when *PTEN, p53 and Nf1* loss

was targeted to neural progenitor cells via Nestin promoter-driven expression of cre recombinase [153]. These in vitro and in vivo studies support the hypothesis that *PTEN* loss in glioma stem-like cells is important in glioma cell biology and in the initiation of gliomagenesis.

Activation of the PI3 kinase pathway can also occur through mechanisms other than *PTEN* loss, for example from overexpression of the tyrosine kinase receptor EGFR that occurs in 50-60% of patients with glioma [154, 155]. This augments the effect of *PTEN* loss on glioma development [156]. Despite this role for EGFR, inhibitors of the EGFR tyrosine kinase are yet to make an impact in the clinic, even though they have demonstrated success in other solid tumours such as lung cancer [157]. This is thought to be because the loss of PTEN function, which often co-exists with EGFR over-expression, results in persistent PI3-kinase pathway activation that is independent of EGFR signalling [157]. It has also been observed that EGFR mutations in GBM are manifest in the extracellular domain of the tyrosine kinase receptor, compared to mutations in the kinase domain of the receptor that are predominant in lung cancer. Inhibitors specific to this extracellular domain, so-called type 3 EGFR kinase inhibitors such as lapatinib, may therefore be more effective in GBM than the inhibitors that have been trialled to date [154].

Another mechanism of PI3 kinase activation implicated in glioma development is mutation in a specific isoform of the p110 catalytic subunit of PI3 kinase [145, 147, 158]. The p110 catalytic subunit of PI3 kinase has a number of different isoforms that are divided into three classes (I-III) according to their substrate specificity, structure and regulation [145]. The class I group of PI3 kinases has two subgroups, 1A containing p110α, p110β and p110γ, and subgroup IB containing p110δ. Class II PI3 kinases consist of a single p110-like catalytic subunit, whilst class III PI3 kinases regulate mTOR [145]. It is the p110α catalytic subunit that is of particular interest, because the gene encoding it, *PIK3CA*, is mutated in some high-grade gliomas, generally in the absence of *PTEN* mutations [158, 159]. These mutations are thought

to increase the activity of PI3 kinase, activating the downstream signalling pathway described above [158]. Several compound inhibitors have been developed that selectively target individual PI3 kinase isoforms, replacing the earlier non-specific PI3 kinase inhibitors such as Wortmannin and LY294002 [104][158, 160, 161]. These new compounds include specific inhibitors of the p110α isoform, such as PIK75 and PI-103 [161]. PI-103 has additional downstream action against the mTOR complex and has been shown to be effective against traditional serum-grown glioma cell lines in an in vivo model, but not glioma stem like cells [161]. Compounds have also been developed that inhibit Akt, such as 690693 and MK-2206 [162]. However, Akt is also important in many other cellular processes, including glucose metabolism, and so a side of effect to these compounds is insulin resistance and diabetes [162].

The evidence that supports a central role for *PTEN* loss and subsequent PI3 kinase pathway activation in glioma indicates that restoring regulation of the pathway in glioma stem-like cells using inhibitor compounds could be an important strategy for improving the prognosis of a large proportion of patients with glioma. The compounds that have already been screened against this pathway in glioma have been tested on in vitro models incorporating serum-grown glioma cells (Figure 1.6). Future studies should therefore focus on screening compounds against glioma stem-like cells.

1.4 In vivo glioma modelling

In vivo models, similar to in vitro models, should recapitulate the development of human gliomas as closely as possible. These models can be used to validate inhibitor compounds selected through in vitro screening, but the design of in vivo models also permits direct interrogation of mechanisms of tumour formation, such as the role of glioma stem-like cells. The two principal types of in vivo models are the

xenotransplantation model and the genetically engineered mouse model (GEMM). In xenotransplantation models tumour cells are transplanted into an immune compromised host, whereas in GEMMs the mouse genome is directly manipulated with the aim of initiating tumour formation spontaneously [83]. I will discuss these different in vivo technologies and explore how these models can inform understanding of the origin of human gliomas.

1.4.1 Xenotransplantation models

In xenotransplantation models glioma cell lines, glioma stem-like cells, or freshly dissociated tumour cells, are injected either subcutaneously into the flank (heterotopic), or directly into the brain (orthotopic) of immune compromised mice. Serial imaging is required to assess tumour growth and drug responsiveness in orthotopic xenotransplantation models. In heterotopic xenotransplantation models the tumour is assessed simply with caliper measurement of the subcutaneous injection site. These models have been widely used in pre-clinical drug testing, not least because of their ease and low cost [163]. However, there are a number of limitations of this model that are evident by the significant failure of many compounds that appeared effective in pre-clinical studies to make an impact in actual clinical trials [163]. Significant amongst these limitations is that the important role that the immune system plays in tumour-host interaction is excluded by the immune compromised status of the mice. Furthermore, notwithstanding the lack of an intact immune system, transplanted human cells will behave differently in a murine microenvironment than in a human host [164, 165]. For example, cells may proliferate that would not do so in a more normal microenvironment, and vice versa, such that the model risks simply selecting for tumour cells most capable of adapting to the murine microenvironment, rather than cells most important to glioma development in humans [164, 165]. It has actually been shown that the specific strain of immune compromised mice used influences tumour formation, underlining the fact that factors unrelated to the particular tumour cells under analysis can influence

tumour growth in these xenotransplantation models [166]. For example, human melanoma cancer cells only infrequently initiate tumour formation when transplanted into non-obese diabetic/severe combined immunodeficiency (NOD/SCID) mice, but the frequency of tumourigenic cells increases in more immunosuppressed mice such as NOD/SCID mice lacking the interleukin-2 gamma receptor [166]. Simply performing the assay over a longer time period, or co-injecting cells with Matrigel, can also increase tumour formation by some cancer cell lines [166]. If the apparent tumourigenicity of cell lines and cells from primary cultures can be modified by such changes in the growth conditions than then this calls into question the ability of this model to accurately recapitulate human disease.

The biological usefulness of xenotransplantation can be optimised if cells are transplanted into an orthotopic rather than heterotopic environment [167]. This gives transplanted cells a more appropriate environment in which to proliferate. Orthotopic xenotransplantation can still be problematic though. For example, serum-grown human glioma cell lines transplanted orthotopically into murine brains generally form masses that compress rather than diffusely invade the surrounding tissue, unlike the tumours from which the cells were derived [168]. In contrast, glioma stem-like cells in orthotopic xenotransplantation models form tumours that better recapitulate the histology of human tumours [169]. However, even freshly dissociated human tumour cells serially passaged using xenotransplantation undergo changes in their gene expression profile over time, becoming more phenotypically malignant but less invasive [169]. In contrast, the invasiveness of actual human gliomas increases with increasing tumour grade, which is a marker of malignancy [1].

There are other reasons why xenotransplantation models may be suboptimal for compound screening. For example, the traditional serum-grown glioma cell lines most often utilised in these models tend to have very high tumour cell growth fractions and rapid doubling times [163]. This makes them more susceptible to cytotoxic therapies that target rapidly dividing cells than human tumours where the

growth fraction is only 10-15% and the doubling time months to years [163]. Another problem with xenotransplantation models may be that investigators have tended to utilise concentrations of drugs that represent the maximum tolerated dose for mice rather than humans [163]. The maximum tolerated dose is often greater in mice than in humans, making it difficult to subsequently reproduce results from animal studies in the clinic because of drug toxicity [163]. The use of drug concentrations in mice that are clinically equivalent to the maximum tolerated dose in humans might therefore make the xenotransplantation models more predictive of clinical efficacy [163]; this concept is also applicable to compound testing in GEMMs. The limitations of xenotransplantation models may explain why compounds that appeared to have potent activity against glioma cells in preclinical in vivo studies have generally transpired to be of limited efficacy in the clinic [163]. Nevertheless, proponents of xenotransplantation models highlight that the alternative in vivo model, GEMMs, are not without their own limitations, as I will discuss [163].

Aside from their role in drug screening, orthotopic xenotransplantation models have also acquired an important role in the characterisation of glioma stem-like cells. The ability of glioma stem-like cells to recapitulate the appearance of the tumour from which they were derived in a xenotransplantation model has been described as a cardinal feature of the cancer stem cell hypothesis [3, 65, 67]. The first reports of glioma stem-like cells described that only the CD133 positive fraction of cells initiated tumour formation in NOD-SCID mouse brains [3, 65, 67]. However, as I have discussed, it has now been shown that CD133 negative cells also have stem-like characteristics and form tumours in xenotransplantation models [3, 106]. The xenotransplantation model is widely used for validating the tumour initiating properties of glioma stem-like cells, but the limitations of this model that I described for drug screening still apply. If the xenotransplantation model reflects human glioma biology so poorly, this raises a question as to how valuable this assay really is in interrogating the tumourigenic potential of glioma stem-like cells.

1.4.2 Genetically engineered mouse models

The limitations of the xenotransplantation model raises a question as to what other in vivo models might better recapitulate human disease and therefore be more predictive of the likely clinical success during drug screening. GEMMs employ germ line or somatic genetic modifications to predispose animals to spontaneously develop gliomas in the context of an intact immune system. The development of tumours within a more normal microenvironment, albeit a murine rather than human microenvironment, should better model human glioma formation than xenotransplantation models [83]. GEMMs also allow theories on the cell of glioma origin to be directly tested [170].

The use of GEMMs for validating compound inhibitor efficacy requires that this approach be shown to be better at predicting the likely clinical success of potential drugs than xenotransplantation models. However, the usefulness of GEMMs in the preclinical testing of drugs has not been extensively tested to date, perhaps because this type of model is more time consuming and expensive to generate than xenotransplantation assays. Nevertheless, where xenotransplantation models and GEMMs have been directly compared, for example in trials of the peroxisome proliferator-activated receptor-γ agonist thiazolidinediones, the GEMM better predicted the subsequent outcome of clinical studies [171]. However, there have also been some disappointments where compounds efficacious in a GEMM have subsequently failed to live up to expectations of their efficacy in the clinic [163, 171].

There are some difficulties in the utilisation of GEMMs for compound screening that may explain a failure to predict clinical drug efficacy. For example, the spontaneous nature of tumour development in GEMMs means that it can be uncertain exactly where or when a tumour will form in the target organ [83, 163]. Even with serial

non-invasive imaging, for example using MRI, lesions might be overlooked. This problem could be overcome by attempts currently in progress to augment visualisation of intra-cranial tumours with the development of genetically engineered bioluminescent reporter mice that permit dividing cells to be tracked in situ [107]. However, these mice will still require serial imaging, which is costly and time consuming [107]. Even with adequate tumour imaging, it is not clear exactly what type of tumour response to compound inhibition should be interpreted as evidence of efficacy against the target glioma stem-like cells. In preclinical models, as in the clinic, efficacy is usually assessed by reduction in tumour bulk [171]; in xenotransplantation models the end point may simply be survival, but serial imaging could also be used. Assessing reduction in tumour size is logical in a model of glioma where the cell responsible for tumour growth and recurrence constitutes the bulk of the lesion. However, the hierarchical model predicts that glioma stem-like cells account for only a subpopulation of cells in the tumour [125]. Successful eradication of this small population of glioma stem-like cells might therefore not actually be apparent simply by assessing a reduction in overall tumour bulk. Attempts to specifically assay changes in the number of glioma stem-like cells to determine inhibitor efficacy will require identification of a specific and sensitive marker of these cells, which remains to be achieved [83].

Another potential difficulty in expecting GEMM-mediated compound screening to be predictive of clinical drug efficacy is that although tumours form spontaneously in GEMMs, similar to the situation in humans, GEMM-derived gliomas may not necessarily recapitulate the biology of human disease. For example, the tumours in GEMMs might grow at a faster rate than human gliomas [126]. Furthermore, in GEMMs, in contrast to human tumours, the oncogenic drivers necessary to precipitate tumour formation are usually present in every cell [107]. This increases the liklihood that tumours form, perhaps in multiple foci and often without the additional stochastic events required for tumour formation in humans [107][126].

One strategy to mitigate at least one of these problems is to restrict oncogene expression to a particular cell lineage or time point in development.

At their simplest, GEMMs are generated by expressing chosen genetic mutations, so-called transgenes, in the mouse germ line [172]. In these 'knock out' models the transgenes will be present in every cell in the animal, which does not reflect the situation in the majority of human tumours. A better option is to express the mutant gene(s) under a constitutive murine promoter that restricts expression to a specific cell type, such as the glioma-initiating cell [172]. Such spatial control of transgene expression is possible using cre-lox technology where short target *Lox* sequences are placed flanking either side of the gene of interest [172]. Cre recombinase, derived from the bacteriophage P1, recombines these sequences, leading to the removal of the intervening genetic data [172]. Depending on the placement of the *Lox* sequences the result is either deletion or activation of the gene. Cell specific expression of this effect is achieved by integrating the cre recombinase enzyme into the murine genome so its expression is under control of a native promoter expressed in a particular cell type [172]. Some promoters will only be expressed at particular time points in development, or in the adult mouse, but expression of transgenes can be further temporally controlled by combining the cre recombinase with a drug-inducible element so that the enzyme is only expressed when the appropriate drug, such as Tamoxifen, is administered [172].

An alternative to cre-lox technology for controlling transgene expression in GEMMs is the RCAS/tv-a model where replication-competent avian sarcoma-leukosis (RCAS) retroviruses containing the transgene of interest are delivered stereotactically into the brain region of interest [173]. The transgenes are targeted to cells engineered to expresses the viral vector receptor (tv-a) under the control of a cell specific promoter [173]. Spatial expression is augmented by the stereotactic localisation of the injection. However, tumours arising in GEMMs generated with either a cre-lox or RCAS/tv-a approach are still somewhat removed from the single

cell event that we understand underlies the initiation of gliomagenesis in humans; only in rare cancer-predisposing syndromes in humans are the predispoding genetic mutations present in all cells or a cell type [8].

Existing GEMM of Gliomas have been generated using a wide range of genetic modifications, inluding inactivation of *TP53*, *NF1*, *PTEN* and *Rb* in target cells such as astrocytes, neural stem cells or neural progenitor cells [174]. Analysis of the tumours produced in some of these mice has demonstrated cell expression of differentiation markers that is similar to that observed in human gliomas. For example, in the GEMM produced by injection of an adenovirus containing Cre recombinase into the lateral ventricle of mice carrying floxed p53 and PTEN genes, the resultant gliomas express the stem cell markers GFAP, PDGFRα, Nestin, as well as the transit amplifying cell markers Sox2 and Olig2, similar to human anaplastic oligoastrocytomas [174].

There is a variation in the penetrance and histology of gliomas that arise in the spectrum of existing GEMMs and this suggests that there are still gaps in our understanding of the process of gliomagenesis (Table 1.4) [83]. Targeting progenitor cells for transgene expression using different promoters with apparently identical primary mutations can give rise to a range of gliomas from anaplastic astrocytomas to oligodendrogliomas [174]. For example, activation of Akt and Ras in Nestin-expressing progenitor cells results in the growth of glioblastomas, but the same mutations in GFAP-expressing cells do not [175]. However, when PTEN and TP53 are inactivated in GFAP-expressing cells then malignant gliomas do form [175]. The different efficacies of tumourigenesis in these models may be explained by the relative susceptibilities of the target cell population to the effect of the mutated gene. This emphasizes the importance of the genetic mutations rather than tumour histology to understanding the pathogenesis of glioma, underscoring that a molecular approach to glioma classification may be more useful than the traditional histological nomenclature.

Table 1.4 Available GEMMs and the tumour subtypes associated with them. The mutant transgenes incorporated into the model are given, along with details of the GEMM design, including the promoter used to drive the Cre recombinase, if relevant. The histological phenotype of the tumours that arise in these models is indicated, along with the penetrance of the tumours at a time point given in brackets [83, 176]. (KO - knock out model, Astro – astrocytoma, variable –variable tumour histology, HG – high grade glioma, TG – non-conditional transgenic other than knock out)

Transgenes	Design	Phenotype	Penetrance
Nf1+/–; *p53*+/–	Conventional KO	Astro/variable	92% (6 months)
Nf1+/–; *p53*+/–	Conventional and GFAP-Cre	Astro/variable	100% (5–10 months)
Nf1+/–; *p53*+/–; *Pten*–/–	Conventional and GFAP-Cre	Astro/HG	100% (5–8 months)
$GFAPT_{121}$	TG	Astro/LG	100% (10–12 months)
$GFAPT_{121}$; *Pten*–/–	Conditional KO (MSCV-Cre)	Astro/HG	100% (6 months)
GFAP-V^{12}*Ras*	TG	Astro/HG	100% (0.5–3 months)
GFAP-V^{12}*Ras; EGFRvIII*	TG; adenovirus	Oligo/HG	100% (3 months)
GFAP-V^{12}*Ras; Pten*–/–	Conventional KO	Astro/HG	100% (6 weeks)
S100-v-erbB	TG	Oligo/LG	60% (12 months)
S100-v-erbB; Ink4a/Arf–/–	Conventional KO	Oligo/HG	100% (12 months)
S100-v-erbB; p53+/–	Conventional KO	Oligo/variable	100% (12 months)

PDGF-B	MoMuLV	Oligo/variable	40% (10 months)
kRas; Akt	RCAS	Astro/variable	25% (3 months)
kRas; Pten−/−	RCAS	Astro/variable	60% (3 months)
kRas; Akt; Ink4a/Arf−/−	RCAS and conventional KO	Astro/variable	20%–50% (3 months)
PDGF-B	RCAS	Oligo/variable	60%–100% (3 months)
PDGF-B; Ink4a/Arf−/−; Pten−/−	RCAS and conventional KO;	Oligo/HG	60%–100% (3 months)
FIG-ROS; Ink4a/Arf/−	Adeno-Cre and conventional KO	Astro/variable	100% (3 months)
Nf1+/−^{GFAP}CKO	GFAP-Cre	Optic glioma	100% (3 months)
PTEN-/-; Ink41/Arf /-; K-Ras^{v12}	Lentiviral GFAP-Cre	Astro/HG	31%
P53-/-; Ink41/Arf-/-; K-Ras ^{v12}	Lentiviral GFAP-Cre,	Astro/HG	80%
Ink41/Arf-/-; K-Ras ^{v12}	Lentiviral CMV-Cre	Astro/HG	100%
Ink41/Arf-/-; K-Ras ^{v12}	Lentiviral GFAP-Cre,	Astro/HG	35%
P53-/-; Ink41/Arf /-; K-Ras ^{v12}	Lentiviral CMV-Cre	Astro/HG	100%

Significantly, it has been demonstrated that there is correlation between the gene expression profiles of at least some GEMM tumours and the gene expression profiles of the Proneural,/Classical/Mesenchymal classification system described for human gliomas [174, 177]. For example, the gene expression profile of tumours in the floxed p53/PTEN knockout described above correlated with the Proneural subgroups of gliomas [174]. Such a correlation supports the view that GEMMs have a clinical relevance that makes them useful models for preclinical inhibitor compound screening. Moreover, whilst both GEMMs and xenotransplantation models have limitations in their applicability to human glioma cell biology, there is a necessity for in vivo testing of compounds and overall GEMMs have more advantages than xenotransplantation models for this purpose.

1.4.3 Targeting tumour initiation to the glioma stem-like cell

As well as serving as tools to screen potential drugs, the design of GEMMs can also allow theories on the cell of glioma origin and the process of glioma development to be directly tested [170]. The emergence of the hierarchical model of gliomagenesis creates an opportunity to develop GEMMs where tumour initiation is directed to the glioma stem-like cell.

Both cre-lox and RCAS/tv-a technologies have been used in the development of existing glioma GEMMs, as detailed in Table 1.4 [83]. These models have utilised various different strategies for directing transgene expression to the suspected glioma cell of origin [83]. It is possible that different subgroups of human gliomas may actually arise from tumour initiation in different cell types, or in cells in differing states of differentiation [27]. The two most commonly used promoters to drive cre recombinase or tv-a expression in existing GEMMs are those belonging to the *Nestin* and *GFAP* genes, both of which strategies have resulted in GEMMs in which infiltrative astrocytomas occur [83]. It is not clear though how well these promoters actually specify the glioma-initiating cell. For example, although GFAP-expressing

progenitor cells can differentiate to neurons and oligodendrocytes throughout the central nervous system, GFAP is also expressed in differentiated astrocytes [178, 179]. However, in a GEMM where p53 and PTEN were selectively deleted in the GFAP-positive cells of the SVZ, tumours resembling gliomas formed [175]. In contrast, in GFAP-positive cells outside the SVZ presumed to be differentiated astrocytes, deletion of these genes did not result in tumour formation [175]. Whilst the authors acknowledge that differentiated astrocytes have been implicated in glioma formation in other in vivo models, this work nonetheless suggests an important role for GFAP-expressing cells in the SVZ in glioma initiation. However, GFAP-targeted transgene expression does not always result in tumour formation with mutations common to human glioma, such as Akt and Ras, and it remains to be clarified whether there are other glioma-initiating cells either inside or outwith the SVZ [175].

Nestin is an intermediate filament protein expressed during development in neuroepithelial precursor cells and radial glial cells, and is downregulated with differentiation [90]. Its expression persists in the adult brain in precursor cells found in the SVZ. It is also re-expressed by reactive astrocytes found in the periphery of brain injury, for example secondary to ischaemia, possibly because of a recapitulation of developmental processes that facilitate brain repair [90]. Nestin is also expressed in proliferating endothelial cells as well as in tissues outside the CNS such as cells within the pancreatic ducts [90, 180-183].

These observations raise the possibility that *GFAP* and *Nestin* promoter-mediated transgene expression may lack specificity for the glioma-initiating cell, or that there is more than one type of glioma-initiating cell. This in turn could explain variations in the incidence of tumour formation in GEMM breeding populations (penetrance) and the time to appearance of tumours (latency), both within and between models (Table 1.4) [83]. For example, only 26% of mice develop gliomas in a RCAS/tv-a model utilising *K-Ras* and *Akt* transgenes targeted to GFAP-expressing cells [173].

This low penetrance could be problematic and costly if utilising such models for preclinical drug testing. Poor tumour penetrance in a GEMM may also indicate that the model does not account for a pivotal genetic event important in the process of tumour initiation. However, a highly penetrant tumour could result from dominant oncogenes or loss of tumour suppressors such that few of the secondary genetic or epigenetic events seen in human tumours actually occur in the model. Therefore a model with 'moderate' penetrance of glioma formation might actually be desirable, because it implies that the engineered genetic event that initiates tumour formation in the GEMM is followed by the stochastic accumulation of additional mutations as the tumour develops.

1.4.4 The oligodendrocyte precursor cell as the glioma cell of origin

A possible strategy to improve the low penetrance of glioma formation associated with some transgenes is to use a different promoter to drive cre recombinase expression. One such potential target for transgene expression is the oligodendrocyte precursor cell (OPC). Despite its name the OPC has a multi-potential state in the adult both in vitro and in vivo, although it does predominantly differentiate into oligodendrocytes in the perinatal period [79, 184-190]. A slowly dividing population of OPCs produced in the perinatal period from neural stem cells remains widely distributed throughout the adult brain [191, 192]. Approximately 5-8% of glial cells in the adult brain are OPCs whose processes are observed to contact neuronal nodes of Ranvier and synapses, suggesting a possible neuronal regulatory role for the cells [193]. Adult OPCs are unipolar or bipolar cells that can differentiate into either astrocytes or oligodendrocytes [193]. Another source of OPCs in the adult is the GFAP-expressing astrocytes within the SVZ called type B cells, although this is disputed [71, 79]. These SVZ cells predominantly generate neurones, but can also function as OPCs that produce oligodendrocytes as characterised by Olig 2 and PDGFRα expression [79].

A potential role for the OPC as a glioma-initiating cell is supported by observations made in humans and in vivo models of gliomas [79, 188-191]. Many types of human gliomas, not just oligodendrogliomas, contain regions with an oligodendroglial phenotype, supporting a central role for the OPC in tumour formation [186]. Furthermore, NG2 chondroitin sulphate proteoglycan (NG2) is expressed by OPCs and has been demonstrated using immunohistochemistry and western blotting techniques in oligodendrogliomas and some glioblastomas [194]. In addition, an analysis of gliomas developing in GEMMs utilising *GFAP* or *Nestin* promoter-specific transgene expression identified that a majority of these tumours were also positive for NG2 [185]. In a separate study, the OPC, but not other neural-stem cell-derived lineages, was implicated as the glioma cell of origin based on phenotypic and transcriptome analysis of tumours in a GEMM [136]. This was demonstrated using a mosaic analysis with a double marker-based lineage tracing system to observe the cell of origin in two cre-lox models of glioma that utilised either *GFAP* or *Nestin* promoter-driven cre recombinase with *p53*/*Nf1* mutations [136].

Adult OPCs can be identified by their expression of the platelet derived growth factor alpha receptor (PDGFRα) and the proliferation and migration of adult OPCs within normal brain is induced by the mitogen Platelet Derived Growth Factor (PDGF) [195][152][196, 197]. PDGF A and B isoforms create either homodimers or heterodimers that can bind PDGFRα [198]. In support of a role for the OPC in glioma initiation it is therefore intriguing that the PDGFR is constitutively activated in more than 80% of oligodendrogliomas, in 50% - 100% of astrocytomas, and that it increases with tumour grade and predicts survival [27, 197, 199, 200]. However, it is interesting to note that within a single human glioma amplification of PDGFRα actually varies across different tumour regions, suggesting that mutation in this gene might not actually be an early event in glioma formation [25].

The role of PDGF in glioma initiation has previously been modelled in vivo where PDGF expression was controlled by *Nestin* or *GFAP* promoters [201].

Oligodendroglioma-like tumours were identified in 40-60% of these mice [201]. In a different GEMM *PDGFB* expression was targeted specifically to myelinating OPCs expressing the 2,3-cyclic nucleotide 3-phosphodiesterase (*Cnp*) gene [185]. The specificity of *Cnp* gene expression to the OPC makes it ideal for examining glioma initiation in the OPC [185]. The *Cnp* promoter itself consists of two separate promoter regions, *Cnp1* and *Cnp2*. The former encodes the CNP1 protein, which is mainly active after birth, whereas the latter regulates transcription of CNP2 that is active both in the embryonic brain and postnatally [185]. CNP itself is one of the earliest myelin-specific proteins to be synthesized by developing oligodendrocytes, but is also maintained in mature oligodendrocytes throughout life [185, 202]. Thirty-three percent of the mice in this *Cnp* model developed low-grade gliomas at 12 weeks of age [185]. The low penetrance of tumour formation in this model may reflect the fact, as I described above, that PDGFRα gene amplification is not an early event in glioma initiation and so overexpression of *PDGFB* may not be sufficient by itself to drive gliomagenesis [25]. Nevertheless, *Cnp* may still be a useful promoter to target expression of other transgenes to the glioma-initiating cell.

1.5 Summary and thesis aims

The emergence of the hierarchical model implicating a stem-like cell in glioma initiation, development and treatment resistance has changed the direction of glioma research in the laboratory. Similarly, the observation that human tumours can be subdivided on the basis of their gene expression profiles has major implications for the clinic, because for the first time we have a classification system that correlates with patient outcome. The challenge now exists to bridge the gap between the laboratory and the clinic by identifying inhibitor compounds that target the glioma stem-like cell and can be translated effectively into patients, perhaps targeting treatment based on the gene expression profile of individual gliomas.

Work correlating glioma stem-like cell biology with tumour subtypes based on gene expression profiles has begun to suggest that the characteristics of the tumour cell of origin may vary between tumours, although the precise nature of each tumour initiating cell is still not known. This underlines the fact that an important challenge to meet in order to achieve the goal of identifying effective therapies for glioma is to adequately model the cellular heterogeneity that exists both within individual gliomas and also between tumours. One of the obstacles to addressing this question is the need to have access to large amounts of fresh, patient-derived material to ensure that the whole spectrum of different types of human glioma can be interrogated. Fortunately, as a neurosurgeon I have such access to such a wealth of tissue. I can therefore aim to establish a panel of in vitro glioma stem-like cell cultures within which I can make a detailed examination of the molecular heterogeneity present, interrogate the pathogenesis of tumour initiation and assess factors that might predict treatment efficacy.

Unfortunately, despite glioma stem-like cells having been described now for several years, the majority of therapeutic compound screening continues to be performed on traditional serum-derived glioma cell lines. This is possibly because of the technical challenges of adapting drug screening methods for use with glioma stem-like cells. Drug screening with glioma stem-like cells is vital though to address the specific question of whether inhibitors against the PI3 kinase pathway, which is identified as central to glioma stem cell biology, are efficacious. To adequately address this question in the context of the intra- and inter-tumoural cellular heterogeneity that I have referred to, protocols need to be developed that allow these experiments to be performed in a high throughout fashion with assay endpoints that are relevant to human cancers; total protein assays are inadequate and instead assays should focus on cell death, cell cycle arrest and cell invasion. I aim to develop these necessary assays to interrogate the efficacy of inhibitor compounds in glioma stem-like cells from a spectrum of human gliomas.

Inhibitor compounds that are efficacious in vitro must be trialled using in vivo models before they can be translated into pre-clinical trials. Both xenotransplantation models and GEMMs have their advantages and disadvantages for these experiments, but a significant attraction of GEMMs is the opportunity to study the spontaneous development of glioma and assess the efficacy of inhibitor compounds in an immune competant microenvironment. Potenital drugs for use against gliomas have not been systematically tested in GEMM of glioma. It has been proposed that rather than seeking to create a single GEMM that perfectly recapitulates all aspects of human glioma formation, a better approach might be to study compound efficacy across a panel of different GEMMs that incorporate varying facets of glioma cell biology. To this end I propose to generate a novel GEMM that would target tumour initiation to the OPC, which, as I have discussed, may be the tumour initiating cell for the Proneural subtype of gliomas. A high penetrance GEMM of malignant glioma developing from an OPC does not currently exist.

Aims

- To develop a reliable protocol for the enrichment and expansion of glioma stem-like cells from patient-derived glioma tissue.

- To use these in vitro cultures to interrogate the intra- and inter-tumoural molecular heterogeneity of the glioma stem-like cell.

- To develop high throughput in vitro assays with biologically relevant therapeutic end points such as cell death, cell cycle arrest and cell invasion to screen inhibitor compounds against the PI3 kinase pathway in glioma stem-like cells.

- To develop a novel GEMM of glioma targeting mutant transgenes to the OPC as the potential glioma-initiating cell.

2. MATERIALS AND METHODS

2.1 Materials

2.1.1 Animal experiments

Supplier: Charles River, Kent, UK

CD-1 nude mice

2.1.2 Cell culture plastic ware

Supplier: BD Biosciences, Oxford, UK

Falcon tissue culture dishes (60 mm, 90 mm, 120 mm)

Cell strainers (40 and 70μm)

Supplier: Corning, Sigma Aldrich, Gillingham, UK

Cell culture flasks (T25, T75, T150)

96-well, 24-well, 6-well plates

Supplier: Thermo Scientific, Langenselbold, Germany.

Mr Frosty Cryo 1ºC freezing container

Supplier: VWR International Ltd, Leicestershire, UK

Black polystyrene 96-well plate

2.1.3 Cell culture reagents

Supplier: BD Biosciences, Oxford, UK

Growth factor-reduced Matrigel

Supplier: ECRC Central Services

Sterile PBS

Sterile PBS/1mM EDTA

Supplier: Invitrogen Life Sciences Ltd, Paisley, UK

Accutase

Advanced DMEM F12

B27

DMEM

Fetal calf serum

L-Glutamine 200mM

N2

RNA later

Trypan blue stock solution

Trypsin solution 2.5%

Supplier: Qiagen, Crawley, UK

RNA extraction kit

Supplier: R&D systems, Abingdon, UK

Basic fibroblast growth factor (bFGF)

Epidermal growth factor (EGF)

Supplier: Roche, Welwyn Garden City, UK

DNAse 1

Supplier: Sigma Chemical Co, Poole, UK

Dimethyl sulphoxide (DMSO)

Heparin

Soybean trypsin inhibitor

Paraformaldehyde

2.1.4 Cell viability assays

Supplier: Cambridge Bioscience, Cambridge, UK

NucView caspase detection system

Supplier: Invitrogen, Paisley, UK

Hoechst 33342 DNA binding dye

Supplier: Sigma Chemical Co, Poole, UK

Staurosporine

Taxol

Supplier: Stratech Scientific Ltd, Newmarket, UK

Non-PI3 kinase pathway inhibitors (Table 2.1)

Supplier: Symansis, Timaru, NZ

PI3 kinase pathway inhibitors (Table 2.2)

2.1.5 Flow-activated cell sorting

Supplier: ebioscience, Hatfield, UK

APC-conjugated CD133 antibody

Supplier: Sigma Chemical Co, Poole, UK

Propidium iodide (PI)

2.1.6 Immunofluorescence

Supplier: Invitrogen, Paisley, UK

Anti-mouse/rabbit Alexa Fluor® conjugated secondary antibodies

DAPI (4',6-diamidino-2-phenylindole)

Supplier: Sigma Chemical Co, Poole, UK

Formaldehyde

Supplier: Vector Laboratories Ltd,

Vectashield mounting medium with DAPI

2.1.7 Immunohistochemistry

Supplier: DAKO ltd, Ely, UK

DAKO Envision kit™ (mouse and rabbit)

Supplier: Sigma Chemical Co, Poole, UK

Hydrochloric acid

Sodium citrate

Toludine Blue O

Supplier: Thermo Scientific, Langenselbold, Germany

DPX mounting media

2.1.8 Inverse invasion assays

Supplier: Corning, Sigma Aldrich, Gillingham, UK

Transwells

Supplier: Invitrogen, Paisley, UK

Calcein-AM

Supplier: Nutacon, Leimuiden, Netherlands

Purecol

2.1.9 Microscopy

Supplier: National Institute of Health, Bethseda, USA

ImageJ software

Supplier: Olympus UK Ltd, Hertfordshire, UK

Olympus FV1000 Confocal microscope

Olympus ScanR/CellR microscope

2.1.10 Molecular biology techniques

Supplier: Acros Organics, Loughborough, UK

Tween 20

Supplier: Agilent, Berkshire, UK

2100 Bioanalyzer

Supplier: Ambio, Life-Sciences, UK

Turbo DNA-free kit

Supplier: Bell Laboratories, New Jersey, USA

R statistical package version 2.14.2

Supplier: Bioline Reagents ltd., London, UK

Agarose gel

DNA Hyperladder 1

Supplier: Bio-Rad, Hertfordshire, UK

DNA Engine® thermal cycler

Supplier: Illumina, Essex, UK

TotalPrep RNA Amplification Kit

Human HT12 Expression BeadChips.

Supplier: Invitrogen, Paisley, UK

Blood DNA extraction kit

SuperScript First-Strand Synthesis System

Sytox® Green

Supplier: New England Biolabs, Hertfordshire, UK

Hyperladder IV molecular weight ladder

Taq 2x master mix

Supplier: Qiagen, Crawley, UK

RNeasy mini-kit

DNeasy Blood and Tissue Kit

RNALater

Supplier: Roche Nimblegene, Waldkraiburg, Germany

Human CGH 12x135K Whole-Genome Tiling v3.0 array

SignalMap version 1.9.0.05.

Phosphatase inhibitor cocktail

cOmplete ULTRA Tablets

Supplier: Sigma Chemical Co, Poole, UK

Agarose

Ethidium bromide

Supplier: Thermo Scientific, Delaware, USA

Nanodrop 1000 spectrophotometer

Superfrost Plus slides

Supplier: Vector labs, Peterborough, UK

Immedge hydrophobic barrier pen

2.1.11 Primary antibodies

Supplier: Cell Signalling Technologies, Hitchin, UK

Anti-Akt monoclonal antibody

Anti-phospho-Akt-S473 monoclonal antibody

Anti-Cyclin B1 monoclonal antibody

Anti-Erk monoclonal antibody

Anti-phospho-Erk monoclonal antibody

Anti-phospho-Histone H3-Serine 10 monoclonal antibody

Anti-S6 monoclonal antibody

Anti-phospho-S6 monoclonal antibody

Supplier: DAKO

Anti-S100B monoclonal antibody

Anti-GFAP monoclonal antibody

Supplier: Millipore, Abingdon, UK

Anti-Olig 2 monoclonal antibody

Anti-Nestin monoclonal antibody

Supplier: Sigma Chemical Co, Poole, UK

Anti-β-actin monoclonal antibody

Anti-Beta III tubulin monoclonal antibody

Supplier: Thermo Fisher Scientific, Loughborough, UK

Anti-Ki67 monoclonal antibody

2.1.12 Western Blotting

Supplier: Biohit, Ellsmere Port, Cheshire, UK

BP800 spectrophotometer

Supplier:ECRC Central Supplies

ECL reagent

Supplier: GE Healthcare, Little Chalfont, UK

High molecular weight rainbow markers

Supplier: Genetic Research Instrumentation, Dunmow, UK

Atto protein electrophoresis apparatus

Supplier: Jencons, Leighton Buzzard, UK

Wet blotting apparatus

Supplier: Licor, Cambridge, UK

Odyssey Blocking buffer

Supplier: Millipore, Watford, UK

Re-blot plus mild antibody stripping solution

Phosphate-buffered saline (PBS) tablets

Supplier: New England Biolabs, Hertfordshire, UK

Anti-mouse/horseradish peroxidase conjugate

Anti-rabbit/horseradish peroxidase conjugate

Supplier: Thermo Scientific, Delaware, USA

Micro BCA protein assay kit

Supplier: Schleicher and Schuell, London, UK

Nitrocellulose membrane

Supplier: Sigma Chemical Co, Poole, UK

Ammonium persulphate (APS)

0.1% (v/v) aprotinin

Bovine serum albumin (BSA)

NP-40

2mM phenylmethylsulponyl fluoride

Sodium deoxycholate

Sodium fluoride

Sodium orthovanadate

TEMED

Triton X-100

Tween 20

Supplier: Whatman, Maidstone, UK

3MM filter paper

2.1.13 Zeptosens reverse phase protein microarray

Supplier: Zeptosens, Witterswil, Switzerland

ZeptoMARK protein microarray chips

Spotting buffer

CSBL spotting buffer

CAB1 and CAB2 buffers

2.2 Stock solutions and buffers

2.2.1 Cell culture media

Glioma stem-like cell Expansion Media:

1% B27 (10x)	(400µl)
0.5% N2 (100x)	(200µl)
1% Glutamax 100mM	(400µl)
1% Penicillin/Streptomycin	(400µl)
1% Fungizone	(400µl)

EGF 10ng/ml	(20μl)
basic FGF 10ng/ml	(400μl)
Heparin 5ug/ml	(40μl)
Advanced DMEM:F12 (1:1)	(to total volume 40ml)

Glioma cell lines

GCCM: 10% FCS in DMEM
1% Penicillin/Streptomycin
1% Glutamate

U87: 15% FCS in DMEM
1% Penicillin Streptavidin
1% Glutamate

U251: 10% FCS in Advanced DMEM F12 (1:1)
1% Penicillin Streptavidin
1% Glutamate

Trypsin solution

0.25% trypsin in sterile PBS/1mM EDTA

2.2.2 Immunohistochemistry

Scots Tap Water

3.5g sodium bicarbonate
20g magnesium sulphate
to 1000 ml water

2.2.3 Inverse invasion assay

Collagen gel (pH 7.4)

Purecol

10% 10 x PBS

10% NaOH

2.2.4 Polymerase chain reaction

TBE – 5X:

54g Tris Base

27.5g Boric acid

20ml 0.5M EDTA

to 1000ml water

2.2.5 Protein extraction and western blotting

Blocking buffer

0.2% Tween 20 in Tris Base Solution

5% bovine serum albumin

PBS–Tween 20 (PBST)

1X PBS

0.1% (v/v) Tween 20

Radioimmuno-precipitation assay (RIPA) buffer

50mM Tris/HCl, pH 7.4	(25ml of 1M)
150mM NaCl	(15ml 5M)
1% sodium deoxycholate	(5g)
1% NP40	(5ml)
0.1% sodium dodecyl sulphate (SDS)	(0.5g)

to 500ml water

Inhibitors made up fresh immediately prior to use

10μM sodium orthovanadate	(10μl)
500μM sodium fluoride	(10μl)
1mM phenylmethanesulphonylfluoride (PMSF)	(20μl)
10μg/ml aprotinin	(10μl)
10μg/ml leupeptin	(10μl)
10μg/ml benzamidine	(10μl)
to 10ml in RIPA	

Running gel -10%

4.43ml 30% acrylamide
5ml Tris pH 8.8
3.9ml H_2O
130μl 10% SDS
125μl 10% APS
6.6μl TEMED

Sample buffer – 2x

800μl 2-mercaptoethanol
1.3ml Tris pH 6.8
2ml glycerol
5ml 10% SDS
1.3ml H_2O
Bromophenol to colour

Stacker gel

1.07ml 30% acrylamide
0.83ml Tris pH 6.8
4.67ml H_2O

70µl 10% SDS

70µl 10% APS

20µl TEMED

Tank Buffer – 10x

50mM Tris Base	(60.4g)
50mM glycine	(288g)
0.1% SDS	(20g)

to 2000ml water

Transfer Buffer

50mM Tris Base	(60.4g)
40mM glycine	(230g)
0.04% SDS	(4g)
20% methanol	(400ml)

to 2000ml water

Wash Buffer

0.2% Tween 20 in Tris Base Solution

2.2.6 Sulforhodamine B Assay

10mM Tris Base Buffer (pH 10.5)

1.21g of tris base

2M NaOH to pH 10.5

to 1000ml in water

2.2.7 Zeptosens reverse protein array

Lysis buffer

1% Triton X-100	(2.5ml)

50mM HEPES, pH 7.4	(2.98g)
150mM NaCl	(2.19g)
1.5mM MgCl2	(0.36g)
1mM EGTA	(0.1g)
100mM NaF	(1.05g)
10mM Na pyrophosphate	(1.12g)
1mM Na_3VO_4	(46.0g)
10% glycerol	(25ml)
phosphatase inhibitor cocktail tablets	
to 250ml water	

4x SDS sample buffer (pH 6.8)

40% Glycerol	(4ml)
8% SDS	(0.8g)
0.25M Tris-HCL	(2.5ml)
to 10ml in water	

2.3 Methods

2.3.1 Glioma primary cell culture

2.3.1.1 Generation of stem-like primary culture cells

The development and refinement of this protocol is discussed in more detail in Chapter 3.

Tumour tissue (≥1cm^3) was collected from eligible patients undergoing craniotomy for therapeutic management of a suspected glioma at the Department of Clinical Neurosciences, Western General Hospital, Edinburgh. All patients gave informed signed consent. The South East Scotland Research Ethics committee approved the study (LREC 2004/4/16). The region of tumour sampling was determined from pre-operative imaging and macroscopic inspection, avoiding areas of frank necrosis. Tumour samples were collected into Advanced DMEM F12 (1:1) media on ice then transferred to a primary tissue culture hood where the tissue was rinsed once in warm PBS. Each sample was divided to give adjacent sections for tissue culture, snap freezing for storage at minus 80°C, fixation in 2% paraformaldehyde, and preservation in RNA Later. All tissue was processed within one hour of harvest from the brain.

Tumour for tissue culture was removed to a dry 60mm culture dish and chopped finely using a scalpel blade. The chopped tissue was dissociated in 0.8% trypsin at 37ºC for ten minutes, agitating gently intermittently. An equal volume of soybean trypsin inhibitor was then added and the mixture transferred to a 15ml falcon tube. 40µl of recombinant DNAse 1 was added to prevent DNA from lysed cells sticking the intact cells together and interfering with subsequent filtration. The tube was inverted 10 times, then the mixture was filtered through a 70µm filter and the resulting single cell suspension centrifuged at 1300rpm for 4 minutes at room

temperature. The supernatant was discarded and the pellet resuspended in 10ml *expansion media* in an upright T25 flask. The flask was maintained in a dry 5% CO_2 incubator at 37°C in 21% oxygen, and fed every 3-5 days. For experiments performed in parallel in hypoxic (3% oxygen) and normoxic (21% oxygen) conditions the resuspended pellet was split between two T25 flasks and one flask immediately transferred to each of a hypoxic or normoxic incubator. All experiments were performed in a 21% oxygen atmosphere unless otherwise stated.

2.3.1.2 Expansion of primary culture cells

After a few days (1-5 days) free-floating glioma-derived spheres were visible in culture. These spheres continued to grow in size and after 10-14 days the glioma-derived spheres were aspirated from the culture medium and transferred to a new T25 flask. These flasks had been coated for 30 minutes at 37°C with growth factor reduced-Matrigel (GFR-Matrigel) diluted 1:80 in Advanced DMEM F12; the GFR-Matrigel was removed and the flasks washed twice with warm PBS prior to use. Flasks were maintained in the incubator in a horizontal position. Glioma-derived spheres adhered to the coated flasks. Cells then grew out from these spheres and proliferated. Flasks were fed every 3-5 days by replenishing 50% of the expansion media. When the adherent primary cultures reached approximately 80% confluence, media was aspirated, the cells washed with warm PBS and then Accutase added (1ml per T75 flask). Flasks were incubated at 37°C for approximately three minutes until the cells detached, then cells were collected into Advanced DMEM:F12 and the mixture centrifuged at 1300rpm for 3 minutes at room temperature. The supernatant was discarded, the pellet resuspended in fresh expansion media and then plated onto a GFR Matrigel-coated flask.

2.3.1.3 Purification of glioma stem-like cells using CD133 antigen

Primary culture cells were passaged and one million cells counted using the technique described below (Section 2.3.1.5). Cell labelling was performed on ice with an APC-conjugated CD133 antibody according to the manufacturer's protocol. First, the cell pellet was resuspended in PBS, then mixed with CD133 antibody diluted in flow cytometry staining buffer to a final volume of 100µl. The mixture was pulse vortexed. The antibody and cells were incubated together in the dark for 15 minutes, washed in PBS three times, pelleting the cells at 1300rpm for 3 minutes between each wash. Cells were resuspended in PBS and transferred on ice to the Fluorescence Activated Cell Sorting (FACS) facility at the Human Genetics Unit, Institute for Genetics and Molecular Medicine, Edinburgh, who performed the cell sorting. Shortly before sorting, cells were incubated with propidium iodide (1µg/ml) to allow determination of cell viability. An aliquot of cells not labelled with the CD133 antibody were used as a negative control. CD133 positive and negative cell populations were sorted and collected into expansion media, then plated onto GFR-Matrigel-coated flasks, as described above. After 2 passages, CD133 positive and negative primary cultures from each tumour were subjected to repeat flow cytometric cell sorting for the CD133 antigen to establish the purity of the expanded cell populations for this putative glioma stem-like cell marker.

2.3.1.4 Storage of primary cell cultures

Primary culture cell pellets were banked for storage in 1ml of 10% DMSO: 90% Advanced DMEM F12 (1:1) in cryovials after the cells had been harvested from flasks with Accutase as described above, centrifuged at 1300 rpm for 3 minutes at room temperature and the supernatant removed. Cryovials were then transferred to a cooled Mr Frosty Cryo 1ºC freezing container at -80ºC. After at least 24 hours the cryovials were transferred to liquid nitrogen for long-term storage.

2.3.1.5 Cell counting

The number of viable cells in a given volume of media was counted using a trypan blue exclusion test. An equal volume of cell suspension and 1X trypan blue was mixed together and a small quantity inspected in a haemocytometer at 20x magnification. Cells that excluded the dye were alive and the number of such cells was counted per unit area. This same method was used for counting serum-grown glioma cell lines.

2.3.2 Serum-grown glioma cell line culture

U251, GCCM and U87 traditional serum-grown glioma cell lines were a kind gift from the Beatson Institute, Glasgow. The media conditions of each cell line were optimized for growth on uncoated-plastic flasks and are detailed in section 2.2.1. Cell lines were passaged when approximately 80% confluent. Media was aspirated and the adherent cells washed in warm PBS. Flasks were incubated with 0.25% trypsin (1ml for T75) for approximately 5 minutes at 37ºC until the cells detached. Cells were collected in FCS, the mixture centrifuged at 1300rpm for 3 minutes, the supernatant discarded and the pellet resuspended in fresh media.

2.3.3 Characterisation of glioma primary cultures and glioma tissue

2.3.3.1 Sulforhodamine B Assay

The number of cells in adherent primary culture during a period of cellular proliferation was determined using a modified-Sulforhodamine B (SRB) assay of total protein [133]. Total protein was used as a proxy for cell number. Primary culture cells were grown on GFR Matrigel-coated 96 well plates. For each glioma stem-like cell, the time from plating to log-phase growth was determined using a

series of 96 well plates. One plate from each set was fixed at time zero then another plate was fixed every 24 hours until all the plates had been fixed. Each of seven identical plates contained cells from each primary culture seeded in 6 wells. This experiment was also repeated at different cell densities to optimise the time course to log-phase growth. All experiments in 96 well plates were performed only in the middle 60 wells of the plate, whilst the outside rim of wells was filled with 200µl of PBS to avoid cell drying. Cells were fixed at the time points described by addition of 50µl of cold 25% trichloroacetic acid (TCA) for at least 1 hour at 4ºC. The supernatant was then discarded and the plates washed with water, before being allowed to air dry. Fifty microlitres of 0.4% SRB solution (w/v) in 1% acetic acid was added to each well and incubated for 30 minutes at room temperature. Unbound dye was removed by washing with 1% acetic acid, followed by air-drying. Bound stain was solubilized with 150µl of 10mM Tris Base buffer (pH 10.5) per well. After one hour, binding of the dye was quantified by determining the optical density (OD) of each well at 540nm using a microplate reader. SRB binds proteins stoichiometrically so the amount of bound dye, and therefore the OD, is directly proportional to the amount of protein [133]. OD values were normalised to a DMSO control and a proliferation curve plotted using GraphPad Prism software version 4.00 for Windows (GraphPad Software, San Diego California USA).

2.3.3.2 Colony forming assay

A defined number of primary culture cells were plated in 100µl of expansion media in each of the central 60 wells of an uncoated 96 well plate. The outside rim of wells was filled with 200µl PBS to avoid cell drying The numbers of glioma-derived spheres forming per well were counted manually with a brightfield microscope at 20x magnification after 7 days. The experiment was repeated with a gradually reducing number of cells per microliter until no glioma-derived spheres formed. The clonogenic index of each primary culture was calculated as a ratio of the number of glioma-derived spheres formed to the number of cells per microliter plated.

2.3.3.3 Immunofluorescence microscopy

Five thousand cells were plated onto autoclaved and acid washed coverslips that had been coated for 30 minutes with a 50μl drop of GFR Matrigel in the centre. The GFR Matrigel was aspirated, the site gently washed with PBS so as not to wet the uncoated part of the coverslip and the coverslip then placed in an uncoated 24 well plate before addition of the cells. Each aliquot of 5000 cells was placed on the area of Matrigel coating in 40μl of expansion media. Cells were allowed to adhere for 60 minutes at 37°C, then 500μl of expansion media was added to each well. After 12 hours, cells adherent to the coverslips were fixed in 2% paraformaldehyde (pH 7.5) for 8 minutes at room temperature. Cells were washed three times with PBS and permeabilised with 0.2% Triton X-100 in PBS for 20 minutes. Coverslips were blocked in 3% normal goat serum (NGS) for 10 minutes. They were then removed from the 24 well plate and placed onto a tray in a humidified container followed by incubation with primary antibody (Table 2.1) diluted in 0.2% Triton X-100: 3% NGS (1:1) for one hour at room temperature. After washing three times in PBS, each coverslip was incubated for 30 minutes at room temperature with an appropriate secondary fluorophore-conjugated antibody (1:000) diluted in 0.2% Triton X-100: 3% NGS (1:1). All coverslips were kept in the dark from this point onwards to preserve the fluorescent signal. After incubation, the secondary antibody was removed with three PBS washes and then the coverslip stained with Bisbenzimide (1:5000) for seven minutes to visualize nuclei. Slides were mounted in Fluorsave onto SuperFrost Plus microscope slides, then stored in the dark at 4°C. The primary antibody was omitted to test non-specific binding of the secondary antibody. Imaging was performed with a Zeiss Axiovision fluorescent/brightfield microscope. At least five fields at 20x power were examined from each of three coverslips per primary culture for every antibody examined. Images were analysed using AxioVision software.

Table 2.1 Primary antibody dilutions for immunofluorescence microscopy.

Primary antibody	Dilution
Beta-III tubulin	1:1000
GFAP	1:500
Nestin	1:500
Olig 2	1: 500

2.3.3.4 Western blotting

To determine the expression levels of proteins in primary culture cells lysates were prepared and analysed by western blotting. Glioma primary cultures were seeded onto 60mm culture dishes and grown to approximately 80% confluence. The media was aspirated and dishes were washed twice with ice-cold PBS, then the PBS aspirated to dryness. Plates were snap frozen on dry ice and stored at -80ºC until lysis, at which time they were thawed on ice.

Dishes were lysed with 100µl of RIPA buffer on ice for 15 minutes. Lysates were cleared by centrifugation at 13000 rpm for 15 minutes at 4°C. The supernatant was transferred to a fresh 1.5ml tube. The protein concentration was determined using a Micro Bicinchoninic Acid (BCA) protein assay kit according to the manufacturer's instructions. Absorbance was measured with a BP800 spectrophotometer at 562nm.

A total of 20µg of protein from each sample was made up to an equal volume with RIPA buffer, then denatured in *sample buffer* at 95°C for 3 minutes, before collection with brief centrifugation. Samples were resolved on 10% gel at 180V, 230mA, and 30W for 70 minutes, then transferred to a nitrocellulose membrane in *transfer buffer* at 100V 400mA 50W for 70 minutes. Five microlitres of pre-stained molecular weight rainbow protein marker was loaded into the first well of each gel to allow the molecular weight of the sample proteins to be determined.

Membranes were blocked in *blocking buffer* for 1 hour at room temperature with gentle agitation. Subsequently, membranes were probed with a primary antibody diluted 1:1000 in blocking buffer: PBS (1:1). After overnight incubation at 4ºC with agitation, membranes were washed three times with PBST. HRP-conjugated secondary antibodies (1:5000) were used for detection. Visualisation was by enhanced chemiluminescence (ECL). Briefly, bound antibodies were detected by exposure of the membrane to blue-light sensitive autoradiography film following

washing in ECL solution. The film was developed using an AGFA Curix 60 processor. Membranes were then rinsed with PBST and distilled water before stripping with Reblot plus mild antibody solution. After washing with distilled water stripped membranes were probed with a second primary antibody, as described previously.

2.3.3.5 DNA and RNA analysis

DNA was extracted from pelleted primary culture cells or snap-frozen glioma tissue using the DNeasy Blood and Tissue Kit according to the manufacturer's instructions. DNA was isolated from human blood using the Invitrogen DNA extraction kit, according to the manufacturer's instructions. Eluted DNA was stored at -20°C. The concentration and purity of each sample was tested using a NanoDrop 1000 spectrophotometer.

RNA was extracted from tumour tissue and primary culture cell pellets using the RNeasy mini-kit according to the manufacturer's protocol. Contaminating DNA was removed from the eluted RNA using a Turbo DNA-free kit, according to the manufacturer's protocol. The concentration of RNA was determined using a NanoDrop spectrophotometer. Samples were stored at -80°C.

2.3.3.5.1 Array comparative genomic hybridization

Array comparative genomic hybridisation (array CGH) was performed to identify copy number changes in DNA samples from glioma tissues and matched primary cultures using the NimbleGen human CGH 12x135K Whole-Genome Tiling v3.0 array. Hybridisation was performed by Ariana Carpico, (Cytogenetics Unit, NHS Lothian, Edinburgh), according to the manufacturer's instructions. The concentration of each DNA sample ranged from 20-200ng/μl. The output data files were analysed using SignalMap version 1.9.0.05.

2.3.3.5.2 Gene expression microarray analysis

Amplification and hybridization of RNA from glioma tissue and matched primary cultures was performed by Dr Colm Nestor, Human Genetics Unit, Edinburgh. RNA integrity (RIN) was assessed using an Agilent 2100 Bioanalyzer (samples used had RIN score of ≥9.0). RNA was amplified and biotinylated using an Illumina TotalPrep RNA Amplification Kit and subsequently hybridized to Illumina human HT12 version 3 Expression BeadChip. Array processing was performed at the Wellcome Trust Clinical Research Facility in Edinburgh.

Bioinformatic analysis was performed using R version 2.14.2. The data was normalized and hierarchical clustering was performed using *Euclidian distance* and *Ward* algorithms. Based on the clustering results the fold change differences in gene expression levels between the clusters were determined and the significance of the differences calculated using a student t-test corrected for multiple testing, and by a Wilcoxon signed-rank test. The gene expression profiles from the resultant clusters were compared with other published data sets using an identical number of genes from each group. The intersect of different gene lists was determined using the following command:

```
x <- scan("c:/file1.txt", what="character", list(id="a"))
y <- scan("c:/file2.txt", what="character", list(id="b"))
intersect(x,y)
```

2.3.3.5.3 Reverse Transcription Polymerase Chain Reaction

Reverse transcription polymerase chain reactions (RT-PCR) were performed on primary culture lysates to validate the findings of the gene expression microarray analysis. One microgram of RNA from each sample was reverse transcribed using the SuperScript First-Strand Synthesis System, according to the manufacturer's

protocol. cDNA samples were stored at -20°C. Reverse transcription polymerase chain reactions (RT-PCR) were performed on the cDNA using Taq 2x master mix and primers (Table 2.2). All primers were deigned by colleagues Dr Tesh Patel or Dr Bilada Bilcan. The primer mix was prepared from forward and reverse primer stocks; 2µl of forward primer (100µM) and 2µl reverse primer (100µM) were mixed with 196µl of nuclease-free water. Samples were made up on cooled PCR blocks in PCR tubes. The following reaction was performed in a DNA thermal cycler:

1. 95°C 5 minutes
2. 95°C 30 seconds
3. 57°C 30 seconds
4. 72°C 30 seconds
5. Repeat steps 2-4 a further 29 times
6. 70°C 10 minutes

PCR products were separated on a 1.6% agarose gel at 120mV for 15 to 20 minutes and ethidium bromide used to visualise the products under ultraviolet light. The DNA Hyperladder 1 was used to size the fragments. A negative control containing primers but no cDNA was included for each analysis. At the start of the experiment, sample cDNA content was normalised amongst the samples using primers to the house keeping gene actin.

2.3.4 The tumourigenic potential of glioma stem-like cells

Immune-compromised mice were housed in filter cages at the Biological Research Facility, Western General Hospital, Edinburgh. All procedures were performed according to Home Office project license conditions. Transgenic mice were housed in cages under standard conditions. All mice were fed with standard feed.

Table 2.2 Primer sequences for polymerase chain reactions.

Target	Direction	5' sequence
Actin	F	GTTACAGGAAGTCCCTTGCCATCC
	R	CACCTCCCCTGTGTGGACTTGGG
Fibronectin	F	CAGTGGGAGACCTCGAGAAG
	R	CACTGTGAGAGCAGGAGCAT
GFAP	F	ATCGAGAAGGTTCGCTTCCTG
	R	TGTTGGCGGTGAGTTGATCG
Nestin	F	GGCGCACCTCAAGATGTCC
	R	CTTGGGGTCCTGAAAGCTG
Olig 2	F	GGACAAGCTAGGAGGCAGTG
	R	ATGGCGATGTTGAGGTCGTG
Sox 2	F	ATGTCCCAGCACTACCAGAG
	R	GCACCCCTCCCATTTCCC
S100B	F	TGGCCCTCATCGACGTTTTC
	R	CACTCTTTCCATGACTTTGTCC
Vimentin	F	CCCTCACCTGTGAAGTGGAT
	R	CTCAATGTCAAGGGCCATCT

2.3.4.1 Xenotransplantation

The tumourigenic potential of primary culture cells was assayed with heterotopic and orthotopic transplantation experiments in CD-1 nude mice.

2.3.4.1.1 Heterotopic xenotransplantation

Primary culture cells were passaged, counted as described previously, and 5 x 10^6 cells resuspended in sterile HBSS made up in a 50:50 mix with Matrigel to a total volume of 200ul. One hundred microliters of this cell suspension was injected subcutaneously into the right flank of CD-1 nude mice. Tumours were monitored for growth and measurements taken twice weekly using callipers. Two measurements perpendicular to each other were made across the tumour's maximum dimensions and used to calculate tumour volume with the equation 0.5*(measurement 1)*(measurement 2)*(measurement 2). The mice were monitored for any sign of distress. The experiment was terminated when then tumours began to decrease in size after two months. The tumours were then excised and fixed in 2% paraformaldehyde for histological examination.

2.3.4.1.2 Orthotopic xenotransplantation

Our collaborators at the Beatson Institute for Cancer Research, Glasgow, performed these experiments using my glioma primary cultures. Briefly, primary cultures were passaged, counted as described, and resuspended in 150ul of PBS to give the desired final concentration. The cell suspension was cooled to 4°C and kept on ice prior to injection. CD-1 nude mice were anaesthetized, and an incision made through the midline of the scalp along its length. A burr hole was made 3mm caudally and 2mm laterally to the bregma on the right. A stereotaxic frame was placed to position the needle against the dura and advance 3mm into the brain. Five microliters of cells in suspension were injected at 2ul/minute and the needle left in situ for a further 5

minutes to ensure no reflux of the cells. The scalp was closed with tissue glue. Mice were monitored for any sign of distress. Three groups of four mice were each injected with cells from one of three primary cultures. The head of each mouse was imaged at 12 and 20 weeks using MRI, where possible with gadolinium contrast, for any evidence of tumour growth. All mice were euthanized at 20 weeks and the brains fixed in 2% paraformaldehyde before being subjected to serial sectioning around the needle insertion site to identify any histological evidence of tumour growth.

2.3.5 Cell viability, cell invasion and proteomic assays

2.3.5.1 Inhibitor screening

I tested a panel of glioma stem-like cell primary cultures with compounds from a PI3 kinase array (Symansis, Timaru, New Zealand), and a selection of other kinase inhibitors chosen to target pathways known to be important in glioma (Table 2.3). The inhibitor array consisted of serial compound dilutions in vehicle (DMSO) ranging from 1-50mM to 1-50μM. All other inhibitor compounds were solubilized in DMSO and diluted from stock concentrations across an eight point half-log dose range from 10mM to 1μM in order to prepare a master inhibitor plate at 1000 times the final desired concentrations (Table 2.4).

Cells were seeded onto the central 60 wells of a 96 well plate, as described earlier for the SRB assay and allowed to proliferate for 48 hours before being fed with fresh media. Compounds were then added at 1:1000 dilutions to give a final dose range of 10μM to 1nM. Media and DMSO controls were included on each plate and used to normalize the experimental results.

Table 2.3 Inhibitor compounds.

Compound Name	Target
PIK75	P110alpha
TGX-221	P110beta
PIK294	P110delta
AS252424	P110gamma
LY294002	PI3 kinase
PI-103	PI3 kinase, DNA-PK, mTOR
Rapamycin	mTOR
KU63794	mTOR
690693	Akt
SB 431542	Smad
Vismodegib (GDC-0449)	Hedgehog pathway
Raf265 derivative	RAF and VEGFR kinase inhibitor
TGX-221	PI-3K p11b subunit
Sorafenib	VEGFR, PDGFR,RAF/MEK/ERK cascade
CHIR-99021	GSK-3
Barasertib (AZD 1152-HQPA)	Aurora Kinase B

Table 2.4 Preparation of eight-point half-log dose range of inhibitor compounds.

Lane	1	2	3	4
Dilution	Stock	15µl of 1 in 35µl DMSO	5µl of 1 in 45µl DMSO	5µl of 3 in 45µl DMSO
Concentration	10mM	3mM	1mM	0.3mM

Lane	5	6	7	8	9
Dilution	5µl of 4 in 45µl DMSO	5µl of 5 in 45µl DMSO	5µl of 6 in 45µl DMSO	5µl of 7 in 45µl DMSO	5µl of 8 in 45µl DMSO
Concentration	0.1mM	0.03mM	0.01mM	0.003mM	0.001mM

After 48 hours cells were fixed and total protein analysed with the SRB assay, as described earlier. All dose points were performed in triplicate on each plate and at least duplicates were made of each plate. The OD reading at each inhibitor concentration was averaged and plotted against the log 10 of the inhibitor concentration. A non-linear regression analysis of this data was performed and a variable slope sigmoidal response determined using Graph Pad prism software. The absolute half maximal inhibitor concentration (GIC50) was calculated by constraining the resultant sigmoidal response curves between 0 and 100% inhibition, provided some inhibition of cell proliferation had occurred.

2.3.5.2 Cell death assay

Cell death and cell cycle assays were performed on primary cultures to establish the mechanism of any inhibitor-related dose-dependent reduction in total protein content.

An early event in apoptosis is the activation of caspase 3. The activity of this enzyme can be assayed using the fluorogenic caspase 3 substrate NucView. NucView consists of an enzyme substrate moiety linked to a nucleic acid dye. The initially non-fluorescent probe is cleaved by caspase 3 activated in the process of apoptosis releasing a high-affinity DNA dye that subsequently translocates into the nucleus, staining it green. Imaging can therefore identify apoptotic cells with green nuclei compared to non-apoptotic cells whose nuclei are only blue from Hoechst-staining. However, cell death can also occur independently of apoptosis and caspase activation. Such cells can be detected using Sytox Green. Sytox Green is a high-affinity DNA dye that easily passes through the plasma membranes of dead cells, but not of living cells.

Cells were seeded onto GFR-Matrigel-coated black polystyrene 96-well plates at a density of 10,000 cells per well and cultured for 48 hours before compounds were added in the same dilution ranges as described above for the inhibitor assays. After a

further 48 hours live imaging was performed. Prior to live imaging, cells were incubated in 0.2µg/ml NucView for 1h at 37°C, or 0.25mM Sytox Green at room temperature for 1 hour. In both assays Hoechst 33342 DNA binding dye was also added 20 minutes prior to imaging to a final concentration of 0.5µg/ml for nuclear visualisation. Plates were imaged using scan^R image analysis software on an Olympus microscope with a 10x objective. During the period of imaging cells were maintained at 37°C in 5% CO_2. Experiments were performed in triplicate at each dose point, with each replicate plate containing three wells at each inhibitor concentration. The number of NucView or Sytox Green-positive nuclei was determined as a proportion of the total number of nuclei at each inhibitor concentration. The average number of green nuclei across the triplicate wells in each experiment was calculated and the significance of any change across the inhibitor concentration range determined with an analysis of variance (ANOVA) test.

2.3.5.3 Cell cycle assays

Plates were prepared as described above for the cell cycle assay. Forty-eight hours after addition of the inhibitor compounds cells were fixed in 4% Paraformaldehyde, washed in PBS and incubated in blocking buffer (PBS containing 1.1% BSA, 0.2% Triton X 100) for 30 minutes. Primary antibodies to the cell cycle proteins Cyclin B1 and phospho-histone H3 (pHH3) were diluted in blocking buffer and incubated with the cells for 1 hour at room temperature (Table 2.5). After washing three times in PBS, an appropriate fluorescent-labelled secondary was added at a dilution of 1:1000 in blocking buffer along with 0.5 µg/ml Hoechst 33342 to allow nuclear visualisation. Imaging was performed on an Olympus microscope using a 20x objective. From these images the distribution of cells in G1, S and G2/M phases of the cell cycle was analysed based on DNA content using scan^R analysis software. The percentage of pHH3 positive nuclei and Cyclin B positive cells was also determined.

Table 2.5 Cell cycle assay primary antibodies.

Antibody	Dilution
Mouse anti-Cyclin B1	1:300
Rabbit anti-pHH3	1:1000
AlexaFluor 488 donkey anti-mouse	1:500
AlexaFluor Cy5 goat anti-rabbit	1:500

2.3.5.4 Inverse invasion assays

The ability of primary culture cells to invade in three dimensions was tested with a modified inverse invasion assay. The development of this assay is described in more detail in Chapter 4. Fifty thousand cells were seeded onto the underside of an inverted 8µm pore-size Transwell filter into which 100µl of type I collagen or GFR Matrigel diluted 1:1 with PBS had previously been set. The Transwell inserts were then covered with the base of a 24-well tissue culture plate, making contact with each cell suspension droplet, and the plate then incubated in an inverted state for 4 hours to allow cell attachment. The filter was then rinsed in media three times to remove non-adherent cells and the Transwells placed in their non-inverted state into a fresh well of a 24 well plate in 500µl of media, with 500µl media also added to the top of the Transwell. The media was based on standard expansion media supplemented with growth factors and inhibitors according to the particular experiment, as described in Chapter 4. The Transwells loaded with cells were incubated for 5 days at 37°C. Transwells were then removed into new wells and incubated with 1ml of 4µm Calcein for 1h at 37°C to allow visualization of cell nuclei, which was performed using an Olympus FV1000 confocal microscope. Horizontal Z-sections through the gel were taken at 15µm intervals starting from the underside of the filter and proceeding upwards through the gel using a 20x objective. The maximum distance of cell invasion was determined from analysis of a Z-section stack of images using 'Image J' software. The maximum distance of invasion was defined as the maximum distance of any cell from the chamber filter. Cells were considered to have invaded when they were visualised more than 45µm from the filter. Montage images of invasion were created using Image J software. Experiments were run in duplicate and at least four Z-section stacks were imaged per Transwell chamber. An average of the results for each set of replicates was calculated and plotted as a box plot along with the 95% confidence intervals to compare the invasion of different primary cultures cells and also to assess the effect of compound inhibitors.

2.3.5.5 Reverse phase protein microarray assay

Reverse phase protein microarray (RPPA) platforms allow the simultaneous measurement of protein expression levels in a large number of biological samples [203]. Multiplexing is achieved by probing multiple arrays spotted with the same protein lysate using different antibodies, simultaneously. By analysing the change in protein expression levels across samples from the same primary culture treated with different inhibitor concentrations, the changes in signalling pathways can be mapped. This technique has been validated to demonstrate that its findings correlate with a standard western blotting technique (Figure 2.1) [204]. With an RPPA approach it is possible to analyse a large number of protein lysates and antibodies more quickly than a standard western blotting technique. It is also possible to analyse lysates with a smaller protein concentration than is possible with a standard western blotting technique. I therefore used the RPPA technique in preference to western blotting for analysing changes in pathway signalling in response to inhibitor compounds in my putative glioma stem-like cells, which I describe in Chapter 4.

One million primary culture cells were grown on a GFR Matrigel-coated 100mm cell culture plate until they reached approximately 80% confluence. The inhibitor compound was added at the concentration of interest to the existing media and the cells returned to the incubator for 30 minutes at 37°C. The media was aspirated, cells washed with ice cold PBS, and the plates snap frozen on dry for storage -80°C. Subsequent lysate preparation proceeded according to the MD Anderson protocol (http://www.mdanderson.org). Cells were allowed to thaw on ice and 100µl of lysis buffer was added to each plate and incubated for 20 minutes, before collection into a microcentrifuge tubes. Tumour tissue was homogenised with ceramic beads and lysis buffer added at 1ml per 40mg of tissue. Samples were placed on a slow turning holder for 30 minutes. The lysate was aspirated, centrifuged at 14,000 rpm for 10 minutes at 4°C and the supernatant collected. Protein concentration was determined using the Bradford protein assay and sample concentrations adjusted to 2mg/ml.

Figure 2.1 Validation of reverse phase protein microarray with Western blotting technique. Total Src levels and Src activation, as demonstrated by phosphorylation at the tyrosine 416 residue, was determined across a half-log concentration range of the Src tyrosine kinase inhibitor AZD0424 in the breast cell line MDA-MB-231. The bar chart shows the results of the experiment performed using a reverse phase protein microarray approach and these are compared to the western blotting technique across the same dose range shown. Data courtesy of Dr Neil Carragher.

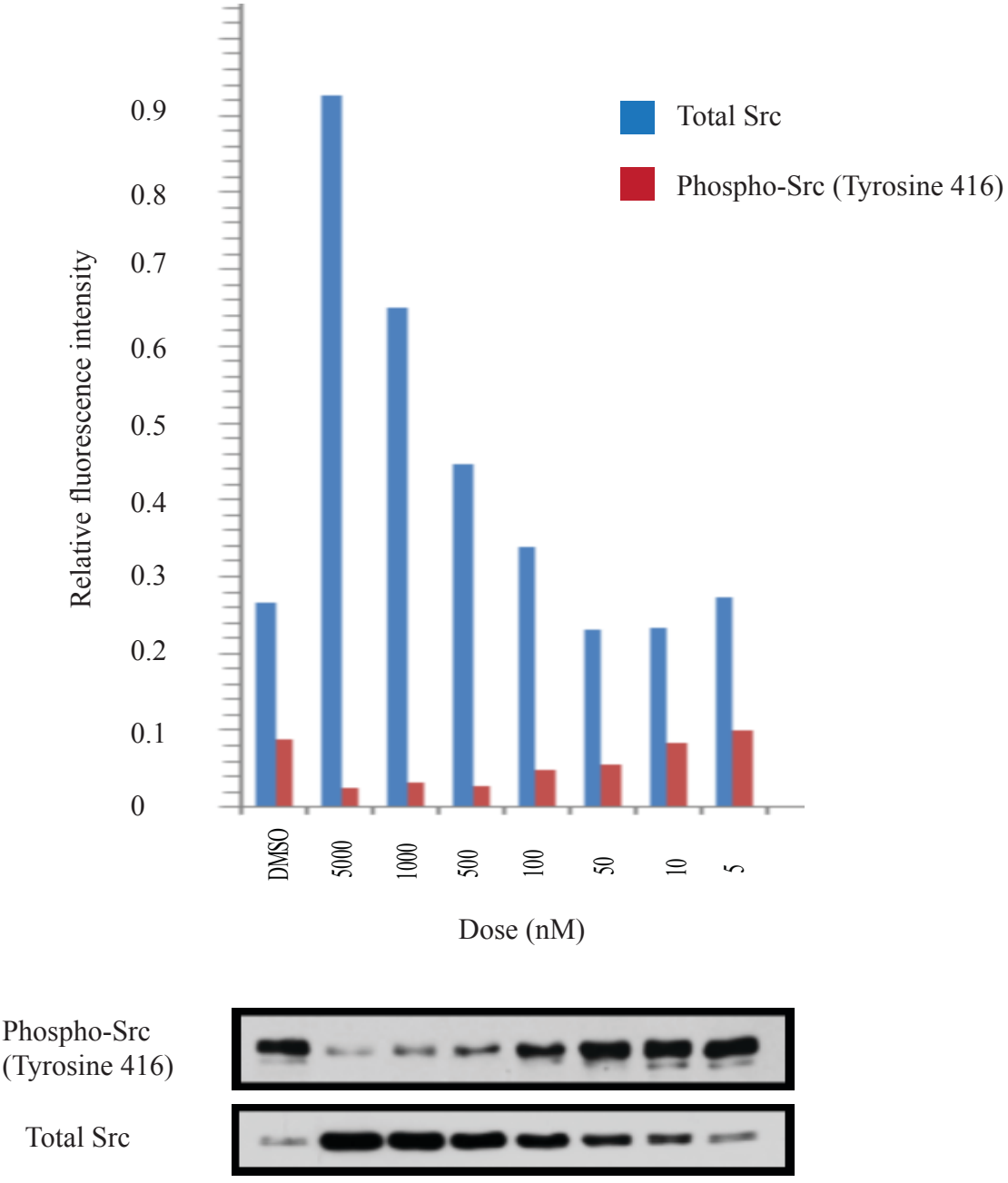

Samples were denatured with Zeptosens sample buffer and 10% 2-mercaptoethanol, and then heated to 80°C for 5 minutes. A 1:10 dilution was made in Zeptosens' CSBL spotting buffer, then a 4-fold serial dilution (75%, 50% and 25% of original sample) prepared in lysis buffer diluted 1:10 in spotting buffer to equalise the portion of lysis buffer in each dilution.

Lysates were spotted on hydrophobic dodecyl phosphate coated ZeptoMARK protein microarray chips at 50% humidity and 14°C using a non-contact piezoelectric spotter. On each chip six arrays of 380 spots, containing/covering the lysate dilutions of 64 samples as well as several reference spots consisting of fluorescence-labelled bovine serum albumin, were printed. Chips were blocked in BB1 blocking buffer for 1.5h using the ZeptoFOG blocking (ultrasonic nebulizer) station, rinsed three times with distilled water and then dried by spinning at 200g for 5 minutes. Subsequently, array chips were placed in the Zeptosens carriers and pre-incubated with assay buffer CAB1 for a few minutes. Each array was incubated with a different primary antibody, diluted in either CAB1 (BSA based) or CAB2 (milk powder based) buffer, over night at room temperature. Excess antibody was removed and arrays washed four times with CAB1, then incubated with rabbit or mouse Alexa Fluor 647-labeled antibodies diluted in CAB1 (1:500) for 2.5 h. Two further washing steps followed, before the arrays were finally scanned in CAB1 assay buffer with the ZeptoREADER. The fluorescence intensity is measured via planar wave-guide technology. The primary antibody was omitted to test the non-specific binding of the secondary antibody and this data was used to calibrate the experimental data.

2.3.6 Genetically engineered mouse model breeding and analysis

The derivation and breeding of mice genetically engineered with a cre recombinase under the control of the *Cnp* promoter, a floxed *PTEN* transgene, or a floxed *ERBB2* transgene, has already been described [205-207]. The C57BL/6xFVB strain of laboratory mice was used. The genotype of progeny of breeding mice was

determined using DNA from tail samples. Mice were bred to obtain the desired genotypes detailed in Chapter 5. These mice were then monitored on a daily basis for any clinical evidence of the development of tumours and at the first signs of distress were euthanized using a carbon dioxide chamber to ensure preservation of cervical and cranial neural structures. Tissues were dissected and fixed in 2% paraformaldehyde for 24-96 hours depending on the volume of tissue. The University Histology Service embedded fixed tissue in paraffin.

2.3.6.1 Immunohistochemistry

Sections 3µm in size were cut from paraformaldehyde-fixed paraffin-embedded tissue blocks by the University Histology Service and mounted onto Superfrost Plus slides. Slides were dewaxed in xylene for 2x 5 minutes, rehydrated successively through 100%, 80%, and 50% ethanol each for 2x 5 minutes, then placed in water. Antigen retrieval was performed by placing the slides into a pressure cooker containing pre-heated sodium citrate (pH 6.0) for 10 minutes at maximum power. Water was then added to the sodium citrate to reduce the temperature and the slides were left to cool for 20 minutes, before transferring to PBST for 2x 5 minutes. The tissue segment was outlined with an ImmEdge hydrophobic barrier pen to allow subsequent reagents to be localised to the areas of interest on the slide. Slides were then processed using the Envison System-HRP according to the manufacturer's instructions. Primary antibodies were diluted in Antibody Dilutant and slides incubated overnight at 4°C (Ki67 (1:100), PTEN (1:100), S100B (1:1600)). The next day slides were washed twice in PBST, then incubated with Envision labelled polymer for 30 minutes. After two further PBST washes slides were stained with the diaminobenzidine (DAB) chromogen for 10 minutes at room temperature before washing with water, counter-staining with Haematoxylin for 15 seconds then rinsing in Scot's Tap water for 20 seconds. Slides were subsequently dehydrated back though 50%, 80% and 100% ethanol, and xylene, each for 2 minutes, before mounting with DPX mounting medium.

Chapter 3. Enriching glioma stem-like cells from human gliomas

3. 1 Background

The invasiveness of glioma cells into normal brain limits the efficacy of surgical resection [35]. Furthermore, even with optimal adjunctive chemoradiotherapy strategies the median survival of newly diagnosed patients is only 14 months [2]. New chemotherapies are clearly needed to improve this poor prognosis. Unfortunately, many therapies that have appeared promising during in vitro and in vivo preclinical development have failed to translate effectively into the clinic [50]. This suggests that the models used previously to predict compound efficacy in the laboratory do not adequately recapitulate human disease [83]. These models have been based on the so-called multistep model of tumourigenesis where mutations occur spontaneously in differentiated cells, conferring a selective advantage on those cells and allowing them to outcompete other cells [208]. In contrast, the recently described hierarchical hypothesis suggests a different theory of tumour development where a subpopulation of cells within the tumour that have stem cell-like properties are responsible for tumour initiation [3, 75]. These glioma stem-like cells are resistant to current glioma therapies and it is therefore plausible that they are responsible for tumour recurrence [125]. Modelling these glioma stem-like cells and identifying therapies that effectively target them is a principal goal of this thesis.

In Chapter 3 I will describe the methodology that I have developed to enrich putative glioma stem-like cells from a range of human gliomas, and to expand these cells in vitro for experimentation. This provides an opportunity to better understand the process of glioma initiation and provides a platform on which assays can be developed to screen the efficacy of inhibitor compounds. I have been able to interrogate the heterogeneity of putative glioma stem-like cells across a spectrum of primary cultures derived from multiple different gliomas because of my unique access to fresh, patient-derived material. I present evidence that rather than a single

universal type of glioma stem-like cell, there are in fact two distinct types of stem-like cells that may be enriched from gliomas under stem cell growth conditions. This observation has significant implications for our understanding of glioma initiation and for development of effective treatment strategies.

3.2 Collection of human brain tumours

Biopsy specimens were taken from 31 human gliomas over the course of this project. Tissue was sampled from the tumour during debulking surgery when the cranial vault was opened and the tumour visible. The site of tumour sampling was determined by visual inspection of the tumour guided by the available patient imaging. At least 1 cm^3 of tissue was collected wherever possible, although the volume of tumour available for biopsy depended on the size of the lesion and the surgeon's operative objective. A neuropathologist made a histological diagnosis of each tumour from adjacent formalin-fixed tissue as part of the patient's routine care. A summary of the histological diagnosis and patient demographics for the 20 tumours sampled after I had optimised my primary culture technique (see below) is given in Table 3.1. Each tumour was designated by a letter(s) at the time of collection in order to maintain the anonymity of the donor. The mean age of patients at diagnosis was 51.1 years (range 27-69 years). There were tumours from 12 females and 8 males. Thirteen gliomas were Grade 4, five were Grade 3 and two were Grade 2, based on the WHO classification [1]. Seventeen gliomas were primary tumours. Three tumours were secondary gliomas that had developed from earlier lower grade lesions.

Table 3.1 Histological and demographic details of human gliomas sampled. Gliomas are listed by their designated alphabetic code. The gliomas from which primary cultures were successfully established are indicated in green. Unsuccessful cultures are highlighted in red. Sex M=Male, F=Female. Age of patient at diagnosis is given in years.

Primary culture code	Histological diagnosis	Tumour grade	Sex	Age at diagnosis
L	Secondary oligodendroglioma	3	M	27
M	GBM	4	M	28
N	Secondary GBM	4	F	43
O	Secondary GBM	4	F	50
P	GBM	4	M	69
Q	Oligodendroglioma	3	F	43
R	GBM	4	F	67
S	Oligodendroglioma	2	M	62
T	GBM	4	F	67
U	GBM	4	F	72
V	Infiltrating astrocytoma	3	F	54
W	GBM	4	M	58
X	GBM	4	M	61
Y	GBM	4	M	45
Z	GBM	4	M	57
AA	Diffuse fibrillary astrocytoma	3	F	29
BB	GBM	4	F	57
CC	Anaplastic oligodendroglioma	3	F	40
DD	Gliosarcoma	4	F	58
EE	Oligodendroglioma	2	F	35

3.3 Optimisation of glioma stem-like cell culture

I initially attempted to enrich glioma stem-like cells from fresh human glioma tissue as free-floating spheres, similar to neurospheres, in serum-free media using a method developed from an amalgamation of relevant techniques in the published literature [65-67, 97]. Under these conditions differentiated cells from the parent glioma do not form glioma-derived spheres and so can be separated out [66, 67]. However, after multiple attempts with different glioma samples to optimise this technique I was still unable to serially passage the putative glioma stem-like cells as glioma-derived spheres for more than five passages. At each passage the single cells that had previously formed a glioma-derived sphere proliferated into fewer new glioma-derived spheres. After less than 5 passages there was no further glioma-derived sphere growth. The number of viable cells in each glioma derived sphere was low (<10000 per ml), and it was not possible to count the cells in each culture and to calculate the proportion that were developing into glioma-derived spheres at each passage. The assessment that it was not possible to maintain these glioma-derived spheres for more than a few passages is therefore based on a simple visual assessment of failed growth in the cultures.

I next investigated whether I could overcome this problem by culturing glioma primary culture cells in low oxygen conditions, because neural stem cells have reduced cell death and improved survival when grown in low oxygen tension conditions (<4% oxygen) [65-67, 97, 209]. To examine the role of hypoxic growth conditions, once a single cell suspension of glioma was prepared it was immediately divided into two culture flasks. One flask was placed in an incubator containing a 3% oxygen (hypoxic) atmosphere and the other in 21% oxygen (normoxic). On visual inspection, cells in low oxygen conditions appeared to form glioma-derived spheres more rapidly than cells grown at 21% oxygen, but the proliferation of cells and sphere formation over multiple passages did not appear to increase (Table 3.2). Cells grown in hypoxia were no better able to survive multiple passages than those grown

Table 3.2 Optimising growth of glioma stem-like cells in monolayer culture. The proliferation of putative glioma stem-like cells in a series of glioma primary cultures was assessed by visual inspection in 21% (normoxic) and 3% (hypoxic) oxygen conditions. Growth was also compared between Advanced DMEM/F-12 (Ad DMEM), DMEM and Neurobasal media. A summary of this is recorded in the table: ++ excellent proliferation, + good proliferation, +/- poor proliferation, - no proliferation. The alphabetical code of the putative glioma stem-like primary culture is indicated in the left-hand column with the histology of the associated primary tumour indicated in brackets; oligo – oligodendroglioma, GBM-glioblastoma. 'Secondary' indicates that the tumour developed from a pre-existing lower grade lesion. Hypoxia and Advanced DMEM/F-12 were observed to optimise cell proliferation.

Primary Culture	Normoxia	Hypoxia	Ad DMEM	Neurobasal	DMEM
P (GBM)	+	+/-	++	+	+
Q (Oligo)	+	++	+	+/-	+
R (GBM)	-	-	-	-	-
S (Oligo)	+	++	++	+	+
T (GBM)	+	++	+	+	+
U (GBM)	+	++	++	+	+

in 21% oxygen conditions. For the reasons of low cell number, as described above, it was not possible to formally quantify whether there was a difference in growth rate between cultures grown in hypoxia and normoxia. It may be that the 3% oxygen atmosphere is still too high for optimal glioma-derived sphere culture. In this regard I note that other researchers have identified a 1% oxygen concentration as being ideal for glioma stem-like cell growth [112]. An alternative explanation is that the equilibration of cells cultured in 3% oxygen to atmospheric oxygen concentrations at the time of culture feeding and passaging may be detrimental to their survival. Unfortunately, I did not have the facilities to try to overcome these potential obstacles during this project. Primary cultures for subsequent experiments were therefore grown in a 21% oxygen atmosphere unless otherwise stated.

I explored other ways of optimising the generation and serial passage of glioma primary culture cells. For example, I speculated that the erythrocyte and cellular debris associated with the tumour tissue might interfere with proliferation of the stem-like cells. I therefore experimented with incorporating a red cell lysis step or Percoll gradient to remove the erythrocyte cells, but neither technique made a discernable difference to glioma-derived sphere growth, determined by visual inspection as described above. Of note, some of my initial cultures also failed because of fungal contamination, but I was able to solve this problem.

3.3.1 Adherent glioma stem-like cell culture

To overcome the problems that I have described with sphere-based culture I next investigated whether plating my glioma-derived spheres onto matrix-coated substrate would improve the ability to serially expand the cell populations. Adherent culture is used with embryonic stem cells to maintain them in an undifferentiated state and it has similarly been suggested that growing glioma stem-like cells in adherent culture preserves their stem-like characteristics better than in non-adherent culture [67]. To

achieve this, glioma-derived spheres were first generated from single cell suspensions of gliomas as described above. I initially tried dissociating these spheres mechanically (pipetting) or enzymatically (trypsin or Accutase) prior to plating onto substrate-coated plastic ware. This was unsuccessful. Based on visual inspection of the cultures the dissociated cells adhered to the substrate-coated plastic ware, but did not proliferate sufficiently to passage them even once. I reasoned that this was perhaps because the heterogeneous cell microenvironment within the glioma-derived sphere is important in supporting the survival and proliferation of the small proportion of constituent cells with stem-like characteristics contained within them. I therefore instead experimented with plating the glioma-derived spheres directly onto the substrate-coated plastic ware.

Prior to plating onto substrate-coated plastic ware, glioma-derived spheres were allowed to grow for 10-14 days after preparation of a single cell suspension from fresh human glioma tissue. If glioma-derived spheres did not form over this time period then I observed that the culture was not viable. This strategy also allowed time for the differentiated cells in the single cell suspension to die, because the media conditions were not selected to support their survival [65-67, 97]. I observed that glioma-derived spheres plated directly onto substrate-coated plastic ware adhered to the substrate. The constituent cells proliferated and migrated out of the spheres and across the substrate such that the primary cultures could be expanded and passaged, apparently indefinitely.

I tested 3 different substrates (gelatin, laminin and growth factor-reduced (GFR) Matrigel) to identify the optimal conditions for expansion of putative glioma stem-like cells (Table 3.3). Glioma-derived spheres did not adhere to uncoated plastic or to gelatin; in contrast, neural stem cells do adhere to gelatin [87]. Similar to previous reports, my glioma-derived spheres adhered to laminin and the constituent cells proliferated [67] (Table 3.3).

Table 3.3 Optimising the proliferation of glioma stem-like cells in adherent cell culture. The adherence and proliferation of putative glioma stem-like cells in a series of glioma primary cultures was assessed by visual inspection using a phase microscope after plating of glioma-derived spheres onto gelatin, laminin or growth factor reduced Matrigel-coated plastic ware. A summative assessment of the adherence of cells in the glioma-derived spheres to the substrate, and the subsequent proliferation of these cells, is recorded in the table: ++ adhere strongly and proliferate, + adhere and proliferate, +/- proliferate but semi-adherent, - no growth/adherence. The alphabetical code of the putative glioma stem-like primary culture is indicated in the left-hand column. The histology of the associated primary tumour is indicated in brackets; oligo – oligodendroglioma, GBM-glioblastoma. 'Secondary' indicates that the tumour developed from a pre-existing lower grade lesion. Growth factor reduced Matrigel was observed to be the optimum substrate for putative glioma stem-like cell adherence and proliferation.

Primary Culture	Gelatin	Matrigel	Laminin
L (Secondary Oligo)	-	++	+
M (GBM)	-	+	+/-
N (Secondary GBM)	-	+	+
O (Secondary GBM)	-	+/-	+/-
P (GBM)	-	++	++
Q (Oligo)	-	+/-	-
R (GBM)	-	-	-
S (Oligo)	-	+	+/-
T (GBM)	-	++	++
U (GBM)	-	++	+

However, cells proliferating on laminin were generally only poorly adherent and as they proliferated they formed semi-adherent glioma-derived spheres. My putative glioma stem-like cells also adhered to GFR Matrigel. In contrast to laminin I observed that across the majority of the glioma primary cultures tested cells adhered firmly to GFR Matrigel and proliferated (Table 3.3). The morphology of cells observed within the adherent culture on GFR Matrigel was similar to published descriptions of glioma stem-like cells, as I will discuss below [67]. I therefore decided to use GFR Matrigel for all subsequent experiments. In contrast to glioma primary culture cells I observed that traditional serum grown glioma cells lines, namely U87, U251 and GCCM, could not be expanded on GFR Matrigel, presumably because they had been selected over many years for growth on uncoated plastic.

Having improved my ability to expand and serially passage putative glioma stem-like cells with the use of an adherent culture technique on GFR Matrigel I next modified the media type and concentration of added supplements to further optimise growth conditions (Table 3.2). The starting point for the choice of media and growth factor supplementation for culture of glioma primary culture cells was based on the published glioma stem-like cell literature that is itself developed from experience of neural stem cell culture [65, 67]. A key feature of the growth media is that it is serum-free because cells grown in these conditions have genomic changes more representative of their parent tumour than cells grown in serum-supplemented media [61, 210, 211]. I compared the growth of primary culture cells from individual tumours in parallel experiments using Neurobasal, DMEM and Advanced DMEM/F-12 media (Table 3.2). Based on visual inspection of cell proliferation and survival over a small number of passages Advanced DMEM F12 was selected as the media of choice. The media was supplemented with B27® and N2® supplements, as well as growth factors EGF and basic FGF, based on the published glioma stem-like cell literature [65, 67]. The resultant media became the standard expansion media for primary culture in all subsequent experiments (Advanced DMEM/F-12 (1:1), 1%

B27 (10x), 0.5% N2 (100x), 1% Glutamax 100mM, 1% Penicillin-Streptomycin, 1% Fungizone, EGF 10ng/ml, basic FGF 10ng/ml, Heparin 5ug/ml). Subsequent experiments were performed on low passage number cultures (<10 passages), unless stated.

My protocol for derivation of glioma primary cultures is summarised in Figure 3.1. After developing and optimising this protocol glioma primary cultures were successfully expanded from 16 of the next 20 tumours that I biopsied (80%) (Table 3.4). The number of tumours sampled is too few to make statistical observations about the factors predicting successful generation of a primary culture from any individual glioma. However, there was no suggestion that age, tumour histology or grade influenced this (Table 3.4).

3.3.2 Enrichment of putative glioma stem-like cells with CD133 antigen

Having optimised enrichment and expansion of the putative glioma stem-like cells, I observed that the constituent cells in each culture were phenotypically heterogeneous (Figure 3.2). This contrasted with the clonal homogeneity of the constituent cells in traditional serum-grown glioma cell lines. This observation raised a question as to whether the primary cultures contained not just putative glioma stem-like cells, but also more differentiated cells. Since at this stage in the project I thought that a pure population of the putative glioma stem-like cells would be the most useful for interrogating the role that these cells play in gliomagenesis, I attempted to develop a technique for enriching the stem-like cells from these heterogeneous cultures.

Early descriptions of glioma stem-like cells suggested the CD133 cell surface marker could be used to distinguish them from other glioma cells, because CD133 distinguishes neural stem cells from other brain cells [3]. I assessed whether CD133 expression could be used to enrich for putative stem-like cells and whether this purified population could be expanded to allow further characterisation.

Figure 3.1 Derivation of primary cell cultures from human gliomas. Biopsies were taken from human gliomas (A) and processed to single cell suspensions as indicated by the steps in the flow chart. (B) These cells were then incubated in uncoated tissue culture flasks where they remained non-adherent and grew as glioma-derved spheres. (C) After 10 to 14 days, the glioma-derived spheres were plated onto Matrigel-coated flasks where they adhered and proliferated. Image A shows an axial section of a cranial computed tomography scan. The glioma is indicated by a red asterix. The scale bar indicates 200 microns. Further details of all the tumours from which primary cultures were derived are given in Table 3.1.

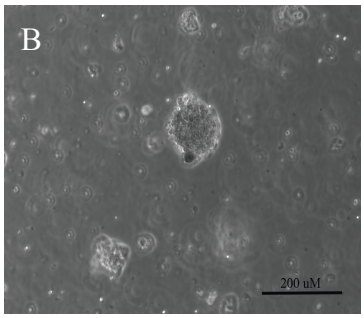

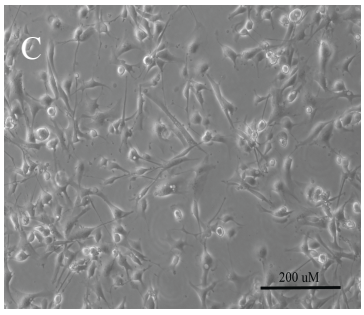

Tumour biopsies taken

Washed in PBS

Finely chopped with scalpel

Incubted in 0.8% trypsin at 37^{O}C

Digestion terminated with soybean trypsin inhibitor

DNase I added

Single cell suspension created with 70 micron filter

Filtrate centrifuged at 1300rpm for 3 minutes

Cell pellet resuspended in proliferation media and grown in suspension

10-14 days

Neurospheres selected from suspension cultures

Spheres plated onto matrigel coated flasks

Table 3.4 Histological characteristics of human gliomas collected. Tumour tissue was harvested intra-operatively, processed into a single cell suspension and grown in suspension culture for 10-14 days to allow for the growth of glioma-derived spheres. Cell suspensions from which glioma-derived spheres were *not* grown are listed in the table as '*unsuccessful.*' It was not possible to expand these cells as an adherent primary culture. Conversely, where glioma-derived spheres did form from a glioma single cell suspension, an adherent culture could be subsequently be grown and passaged apparently indefinitely. These tumours are listed as '*successful*'.

Histology	Successful	Unsuccessful
Grade II	1	1
Grade III anaplastic oligodendroglioma	4	1
Grade IV GBM (primary)	9	2
Grade IV GBM (secondary)	2	0
Total	16	4

Figure 3.2 Glioma primary culture cell phenotypes. Tissue biopsies were taken from both superficial and deep regions of glioblastoma designated by the alphabetic code BB. Primary cell cultures were grown from both the tissue biopsies using the serum-free adherent culture technique described. Image **A** and **B** are phase microscope images of the cultures derived from the superficial and deep biopsies, respectively. These images demonstrate the characteristic appearance of branched and flat phenotype cells, respectively. The inset in each image shows an enlargement of the main picture. The scale bar indicates 500 microns.

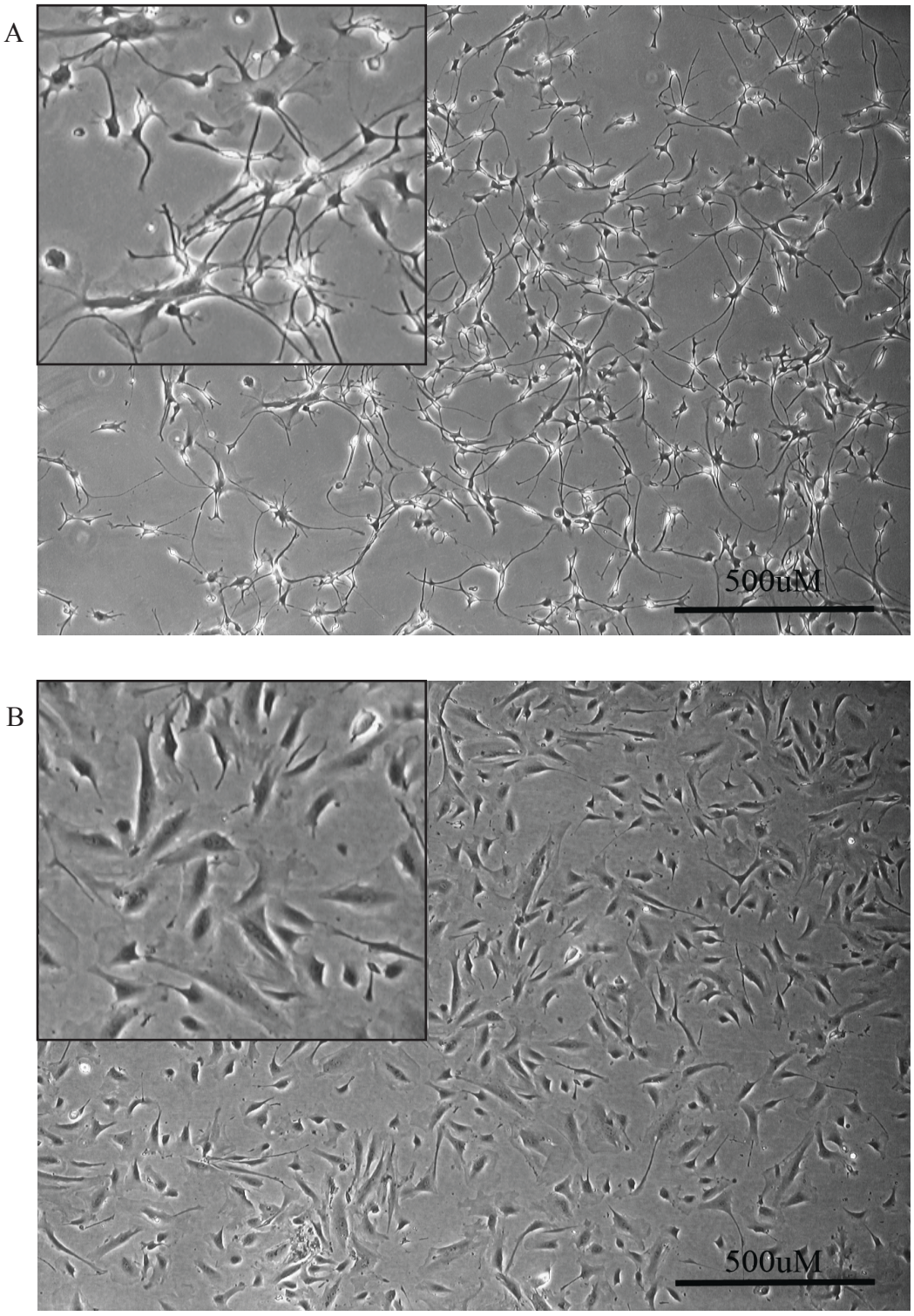

After labelling the primary culture cells with an anti-CD133 antibody I sorted them using flow cytometry into CD133 positive and negative fractions. These purified fractions were then grown separately in adherent culture, as described above. I identified that the proportion of CD133 positive cells varied between primary cultures from 2.8-39.3% (+/- 0.5%), which is similar to other published results (Table 3.5) [212]. There were no morphological differences between CD133-positive and CD133-negative cells in culture. After the purified cell populations had been grown for two passages to bulk up the cell numbers they were subjected to repeat CD133 sorting using flow cytometry. On repeat sorting, the cultures that had been enriched for CD133-negative cells remained almost entirely CD133 antigen negative (Table 3.6). In contrast, after just 38 days, cultures enriched for CD133-positive cells were only 7.6-14.4% CD133 antigen positive (Table 3.6). This suggested that CD133 antigen enrichment was not a reliable strategy for cell sorting.

In Chapter 1 I reviewed evidence that antigens other than CD133 might be used for glioma stem-like cell purification. I concluded that none had compelling evidence for their use. I therefore decided that I would perform the remainder of my investigations on the heterogeneous cell population within each unsorted glioma primary culture.

3. 4 Characterisation of putative stem-like cells

3.4.1 Glioma primary cultures contain cells with one of two distinct phenotypes

The phenotypic appearance of cells within an individual glioma primary culture is heterogeneous (Figure 3.2). However, I observed that the predominant cell morphology in each primary culture could be described as having one of two phenotypes. As I will explain, I have called these cell phenotypes '*branched*' and '*flat*' (Figure 3.2). My initial finding was that each primary culture derived from a single human glioma contained only one of these cell phenotypes.

Table 3.5 Proportion of cells in glioma primary culture expressing CD133 antigen. Cells from five glioma primary cultures were labelled with CD133 antibodies and sorted using flow cytometry. The cultures are labelled by their alphabetic designation and the histological diagnosis of each tumour is given in brackets; oligo – oligodendroglioma, GBM-glioblastoma. The proportion of positive and negative cells in each primary culture was determined from the flow cytometry results and is accurate to +/-0.5% based on analysis of an unlabelled cell population.

Primary culture	CD133 positive (%)	CD133 negative (%)
L (oligo)	3.8	96.2
M (GBM)	5.9	94.1
N (GBM)	39.3	60.7
O (GBM)	2.8	97.2
P (GBM)	3.9	96.1

Table 3.6 Maintenance of the CD133 status of enriched glioma primary cultures. Primary culture cells were first sorted using flow cytometry based on their CD133 antigen status and were then allowed to proliferate for two passages before a second round of CD133 antigen selection by flow cytometry was performed. In the table below the cultures are labelled according to their alphabetic designation. The proportion of positive and negative cells in each culture has been determined from the flow cytometry results and is accurate to +/-0.5% based on analysis of an unlabelled cell population.

Primary culture	CD133 positive (%)	CD133 negative (%)
L CD133 positive	14.4	85.6
L CD133 negative	0.9	99.1
P CD133 positive	7.6	92.4
P CD133 negative	1.4	98.6

Branched phenotype cells had a prominent nucleus with thin processes extending in two or more directions (Figure 3.2). As they proliferated, the cellular processes overlapped those from other cells. These branched phenotype cells had the same radial glia-like appearance that has been previously described for glioma stem-like cells [67]. Branched phenotype cells were able to proliferate apparently indefinitely (more than 20 passages).

Flat phenotype cells in contrast had a larger nucleus and more abundant cytoplasm. They had few if any cellular processes (Figure 3.2). As the cells proliferated they did not overlap with each other. Flat phenotype cells ceased to proliferate after 6-10 passages.

3.4.2 Different cell phenotypes can be grown from the same tumour

My initial development of a protocol for deriving glioma primary cultures was made using single biopsies from each tumour. To investigate whether or not the primary culture cell phenotypes that I had observed were specific to a given tumour, rather than just to a particular biopsy from a tumour, I sampled multiple regions across a series of tumours and derived primary cultures from each tissue sample. The tumour sampling sites were determined from pre-operative imaging. The heterogeneous and ill-defined nature of gliomas makes it difficult to define distinct regions, so I selected superficial (invading edge) and deep (usually more necrotic) areas, where possible adding in an intermediate region. All samples were processed as described previously (Figure 3.1). I sampled at least two different regions from 5 gliomas (designated AA (diffuse astrocytoma), BB (GBM), CC (Anaplastic oligodendroglioma), DD (Gliosarcoma), EE (Oligodendroglioma)), and successfully grew primary cultures from each biopsy (Table 3.7). The cell phenotype in these cultures was not entirely predictable either by tumour histology or the position from which the biopsy was taken. There was a trend towards flat phenotype cultures being

Table 3.7 Cell phenotypes of glioma primary cultures. Glioma primary cultures were derived from multiple tissue biopsies taken from five distinct tumours designated AA to EE. The histology of the parent tumour and the phenotype of the cells characterising the derived primary culture are indicated in the table.

Tumour	Histology (Grade)	Cell phenotype
AA	Diffuse fibrillary astrocytoma (3)	Flat
BB	GBM (4)	Flat/branched
CC	Anaplastic oligodendroglioma (3)	Flat
DD	Gliosarcoma (4)	Branched
EE	Oligodendroglioma (2)	Flat/branched

derived from lower grade gliomas, and branched phenotype cells from higher-grade gliomas (Table 3.7). However, there were no differences observed in the glioma-derived spheres that gave rise to primary cultures containing cells with the different cell phenotypes (Figure 3.3-3.5).

Using tissue samples taken from the tumours designated AA (diffuse astrocytoma), CC (anaplastic oligodendroglioma) and DD (gliosarcoma) I grew a total of 7 primary cultures. The constituent cell phenotype was consistent between cultures from within each tumour; intratumoural homogeneity (Figure 3.3). In contrast, I found that both branched and flat cell phenotypes could be identified in different primary cultures from each of the tumours designated BB (GBM) and EE (oligodendroglioma) (Figures 3.4 and 3.5). For example, both superficial and deep biopsies (as defined above) were taken from the tumour designated BB (GBM). The superficial biopsy culture contained a mixture of branched and flat phenotype cells, whilst the deep biopsy culture contained branched phenotype cells only. Interestingly, the matched primary cultures from the tumour designated BB grown in 3% oxygen (hypoxia) were different. The superficial culture contained only branched phenotype cells and the deep culture only flat phenotype cells. In mixed cultures I observed that the flat phenotype cells ceased to proliferate after approximately 6 passages, and the primary culture then became dominated by branched phenotype cells. From the tumour designated EE (oligodendroglioma), the primary culture derived from the superficial biopsy contained branched phenotype cells whilst the primary culture from the deep biopsy contained flat phenotype cells (Figure 3.5). Unlike the tumour designated BB there were unfortunately no cultures from the tumour designated EE grown in hypoxia to allow observation of whether or not the cell phenotype differed depending on the oxygen tension in which it was cultured. The tumours designated CC (anaplastic oligodendroglioma) and DD (gliosarcoma) had matched hypoxic and normoxic (21% oxygen) cultures for each tissue biopsy, but there were no oxygen tension-dependent differences in cell phenotype (Figures 3.3 and 3.5). It was actually not always possible to derive primary cultures from a given tumour tissue biopsy

Figure 3.3 Intratumoural homogeneity of primary culture CC cell phenotypes. Three biopsies were taken from different regions of the anaplastic oligodendroglioma designated CC, progressing from superficial to deep, as indicated by the blue dots from right to left on the axial computed tomograph scan (A). A single cell suspension was prepared from each biopsy, as previously described (Figure 3.1). (B) After 14 days, cells from each biopsy had formed glioma-derived spheres, as shown in the left-hand images. These spheres were then plated onto Matrigel-coated flasks and adherent cultures formed, as shown in the right-hand column. The cells in all three primary cultures had a 'flat' phenotype, as described in the text. The scale bar indicates 200 microns.

A

B

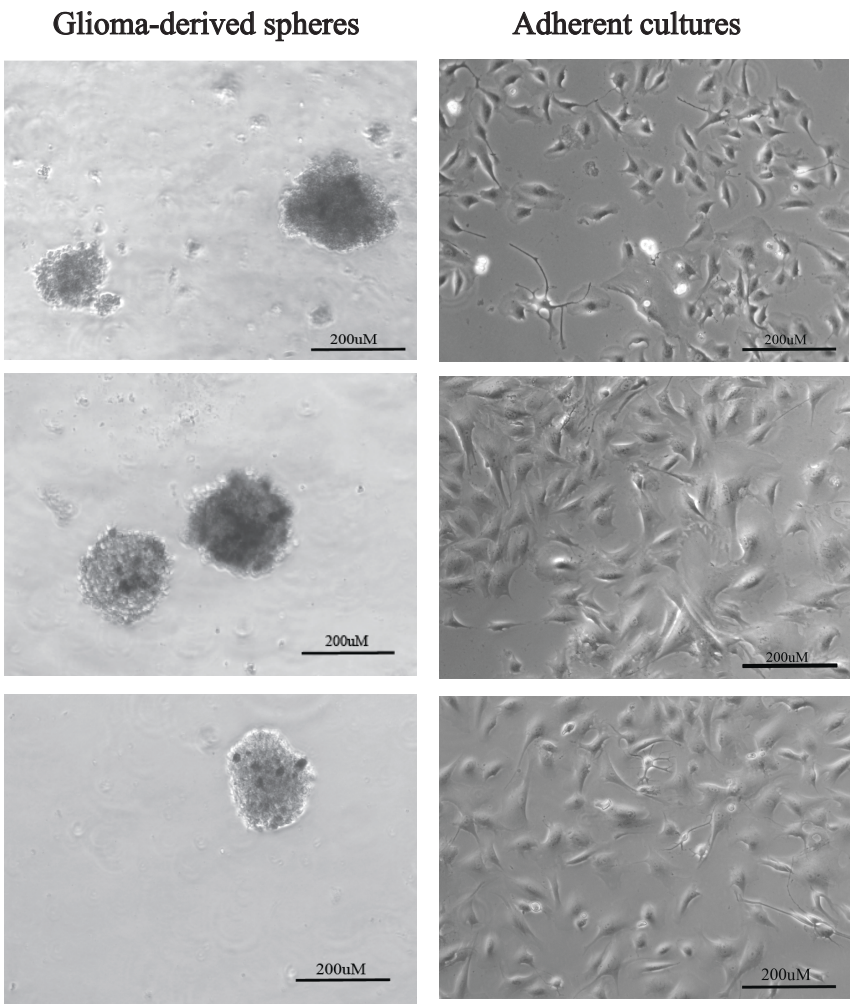

Most superficial biopsy cultured in normoxia. Flat phenotype cells

Intermediate depth biopsy cultured in normoxia. Flat phenotype cells

Deepest biopsy cultured in normoxia. Flat phenotype cells

Figure 3.4 Intratumoural heterogeneity of primary culture BB cell phenotypes. Tissue biopsies were taken from superficial and deep parts of the glioblastoma designated as tumour BB. A single cell suspension was prepared from each biopsy, as described previously. The suspension culture from each biopsy was then divided between two uncoated T25 culture flasks and incubated in either normoxic (21% oxygen) or hypoxic (3% oxygen) conditions. The left-hand column of images shows the glioma-derived spheres that had formed after 14 days. The spheres were then plated onto Matrigel-coated flasks to form adherent cultures, as shown in the right-hand column of images. The scale bar indicates 200 microns. The images illustrate that the oxygen conditions in which the primary cultures were derived appeared to influence the cell phenotype of the resultant cultures. The pimary culture derived from the deep tissue biopsy contained branched phenotype cells in normoxic conditions, but flat phenotype cells in hypoxic conditions.

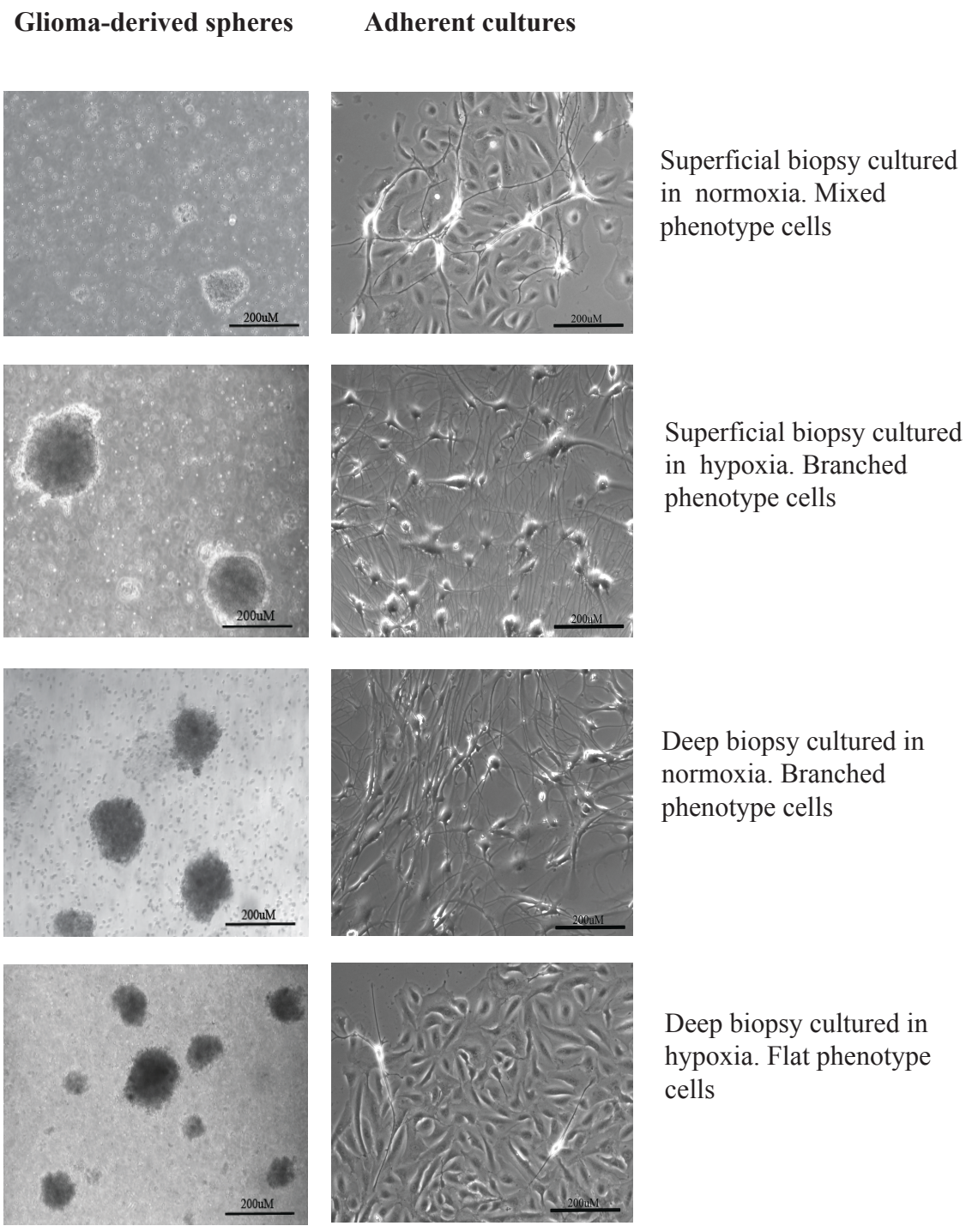

Figure 3.5 Intratumoural heterogeneity of primary culture EE cell phenotypes. Tissue biopsies were taken from superficial and deep parts of the oligodendroglioma designated as tumour EE. A single cell suspension was prepared from each biopsy, as described previously, and incubated in an uncoated T25 culture flask in normoxic (21% oxygen) conditions. The left-hand column of images shows the glioma-derived spheres that had formed after 14 days. The spheres were then plated onto Matrigel-coated flasks to form adherent cultures, as shown in the right-hand column of images. The scale bar indicates 200 microns. The images illustrate that branched phenotype cultures were derived from the superficial tumour biopsy (EE1) whilst flat phenotype cells were derived from a deeper tissue biopsy taken from the same tumour (EE2).

Superficial biopsy (EE1) cultured in normoxia. Branched phenotype cells.

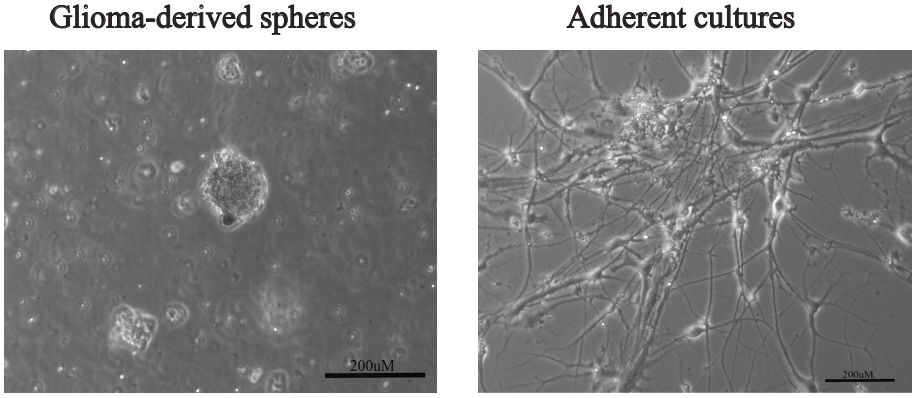

Deep biopsy (EE2) cultured in normoxia. Flat phenotype cells.

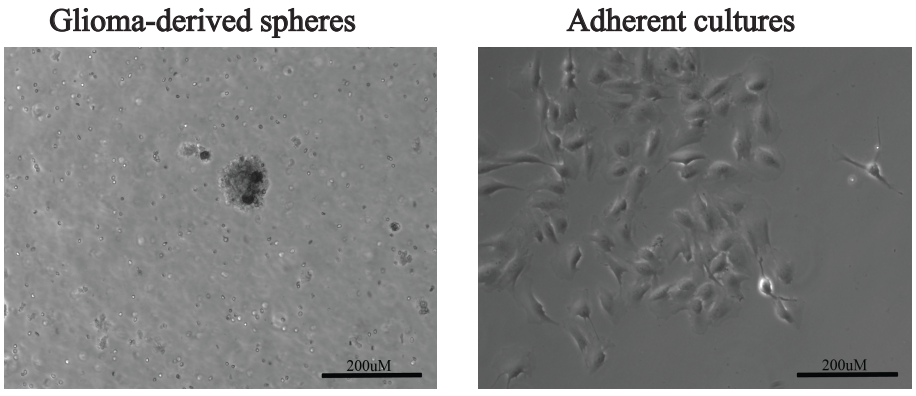

under both hypoxic and normoxic oxygen conditions. Generally speaking though, branched phenotype cell cultures grew under both oxygen conditions, but flat phenotype cell cultures grew preferentially in hypoxic conditions (Table 3.8).

3.4.3 Primary culture phenotype predicts growth and senescence characteristics

The growth characteristics of the three branched phenotype primary cultures designated DD2 (Gliosarcoma), X (GBM) and P (GBM), and the two flat phenotype primary cultures designated CC2 (anaplastic oligodendroglioma) and EE2 (oligodendroglioma) were assessed using an SRB assay. The branched phenotype cells replicated faster in adherent culture than flat phenotype cells (Figure 3.6). Branched phenotype cells also always grew indefinitely (greater than passage 20) without changing their growth rate or morphology. In contrast, flat phenotype cell growth always slowed markedly and ceased after 6-10 passages, the cells becoming larger and more irregular (Figure 3.7). In order to ascertain whether or not this change in growth characteristics resulted from senescence, I performed a senescence assay on early (passage 3) and later passage (passage 7) flat phenotype cells from the primary culture designated EE using the senescence-associated β-galactosidase (SABG) marker (Figure 3.7). There was a significant difference in the percentage of cells with SABG staining per unit area between the two passages ($p<0.0001$). This was also observed in flat phenotype cells from culture CC1 ($p=0.0005$). The branched phenotype cells did not appear to undergo growth arrest with increasing passage number and there was no change over time in the percentage of cells staining with SABG in the primary culture designated P ($p=0.63$). The proportion of cells staining with SABG in branched phenotype cells was similar to low passage flat phenotype cells.

Table 3.8 Comparison of the growth of primary cultures under normoxic (21%) and hypoxic (3%) oxygen conditions. Single cell suspensions derived from the gliomas listed were split between two culture flasks, one of which was incubated in 21% oxygen and the other in a 3% oxygen environment. A visual inspection of the cells was made using a phase microscope on a daily basis to determine whether or not the cells proliferated as a glioma-derived sphere under these conditions. After 10-14 days the glioma-derived spheres were plated into growth factor reduced Matrigel-coated plastic ware. The table provides a summary of this assessment for each primary culture. '+' indicates proliferation as a glioma-derived sphere and in adherent culture. '-' indicates failure to proliferate as a glioma-derived sphere or failure to expand in adherent culture. N/A indicates that the variable was not assessed in that primary culture. The number of primary cultures tested in both oxygen conditions is too small to draw firm conclusions about the role of hypoxia in growth of these putative stem-like cells.

Tumour	Histology (Grade)	Normoxia	Hypoxia
AA	Diffuse fibrillary astrocytoma (3)	-	+
BB	GBM (4)	+	+
CC	Anaplastic oligodendroglioma (3)	+	+
DD	Gliosarcoma (4)	+	-
EE	Oligodendroglioma (2)	+	N/A

Figure 3.6 Growth characteristics are predictable by primary culture cell phenotype. A constant number of cells from each of the 5 primary cultures designated DD2 (gliosarcoma), X (GBM), P (GBM), EE2 (oligodendroglioma) and CC2 (anaplastic oligodendroglioma), were plated into sets of 6 wells of a Matrigel-coated 96 well plate. Seven replicate plates were made. Cells on the first plate were fixed 1 hour after plating by addition of 50µl of cold 25% trichloroacetic acid. A further plate was fixed 24 hours later, and then every 24 hours subsequently until all the plates were fixed. At the conclusion of the experiment a Sulforhodamine B assay was performed on each plate. The proliferation of cells at each time point was assessed by reading the optical density of the bound dye at 540nm. These results were expressed as a ratio to the optical desnsity on day zero at each time point on the graph. The graph illustrates the growth curve of the primary cultures designated X and EE2 that were representative of the the branched and flat phenotype cultures, respectively. The branched phenotype cells proliferated more rapidly that the flat phenotype cells.

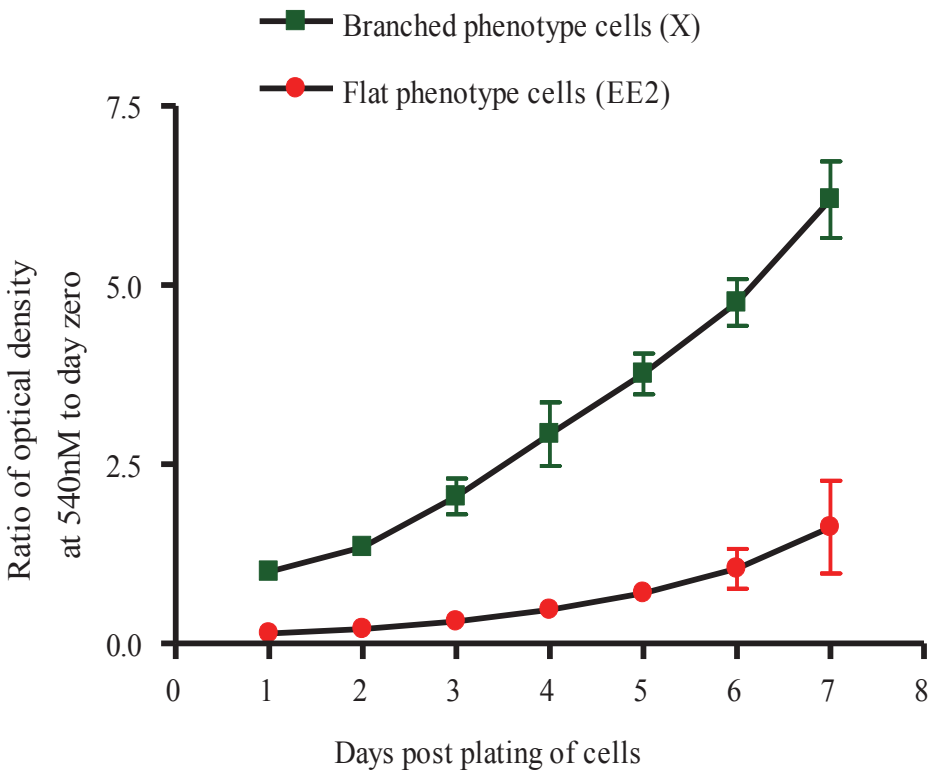

Figure 3.7 Senescence in flat phenotype primary culture cells. Primary culture cells with a flat phenotype derived from the tumours designated EE2 (oligodendroglioma) and CC2 (anaplastic oligodendroglioma) were plated at early (passage 3) and late (passage 7) passages onto Matrigel-coated coverslips. Each experiment was performed in triplicate. After incubation in standard growth conditions for 24 hours cells were fixed with paraformaldehyde and stained with a senescence-associated β-galactosidase (SABG) marker. The tumour designated EE2 is shown as representative of both primary cultures. (A) The percentage of positively-stained cells at each passage is illustrated in the box-plot. The difference in the percentage of positively-stained cells between the two cell passages examined was statistically significant (p=0.0001). (B) Brightfield images of the cells at early (passage 3) and late (passage 7) passages were taken using a phase microscope; an enlargement of each image is included in the inset. Accompanying these images is a example of the SABG marker staining at each culture passage; positively-stained cells appear blue. The scale bar indicates 200 microns.

A

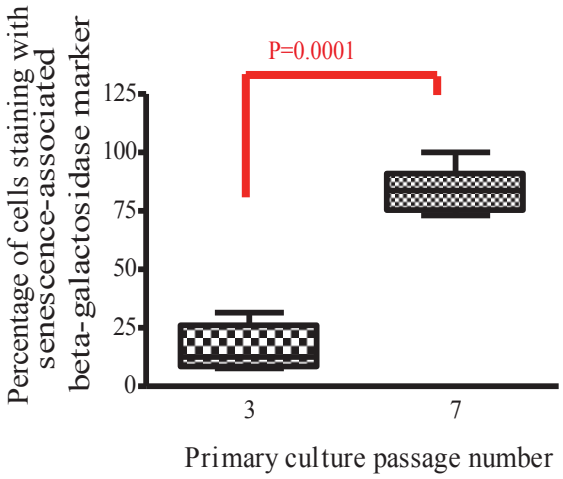

B

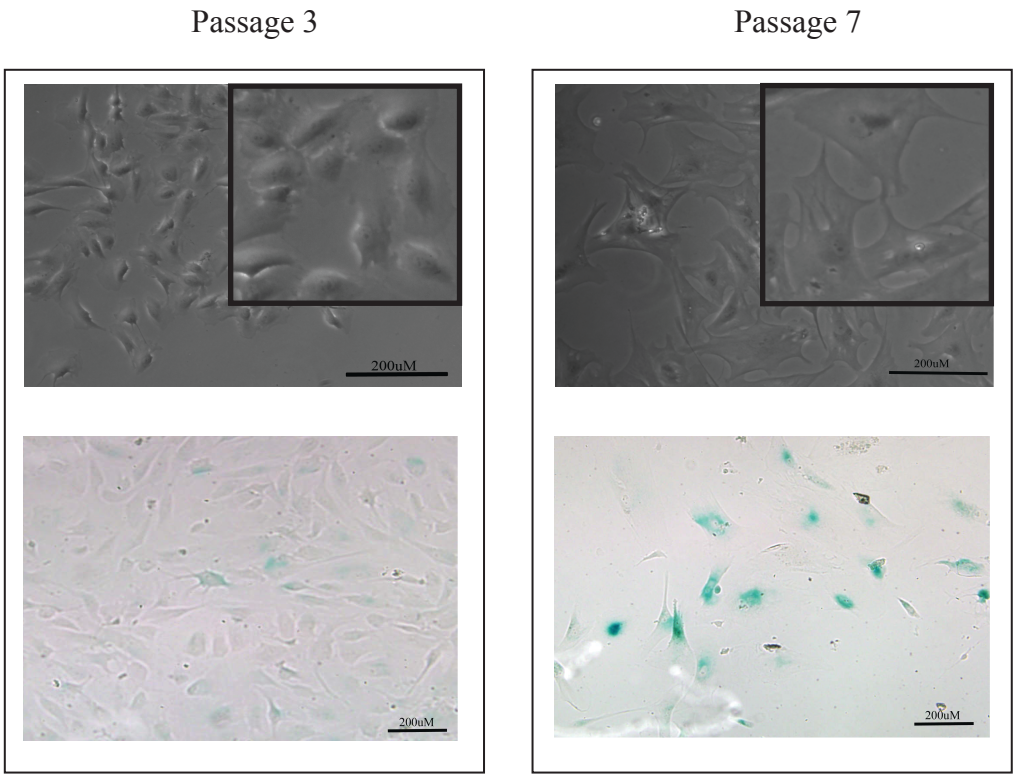

3.4.4 Flat and branched phenotype cells have different clonogenic capacities

Neural stem cells are characteristically able to undergo clonal expansion to form neurospheres [13]. Glioma stem-like cells have been proposed to have similar clonogenic capacity and are able to form glioma-derived spheres [3, 67]. To investigate the clonogenic capacity of my own glioma primary culture cells I serially diluted them until they no longer formed spheres in non-adherent culture conditions after 7 days; over a longer time period the spheres were observed to increase in size but not number. The number of spheres forming across a 96 well plate was expressed as a ratio to the number of cells per microliter originally plated. I called this ratio the *clonogenic index*, which is the minimum number of cells from which a glioma-derived sphere formed (Table 3.6). A lower clonogenic index indicates a greater clonogenic capacity, which in turn implies a more stem-like character, by analogy to neural stem cells [3, 67]. The calculation of a clonogenic index assumes that each glioma-derived sphere forms from the clonal expansion of a single cell. At high cell concentrations it was difficult to differentiate clumping of proliferating cells from clonal sphere formation. As the cell concentration decreased though, daily inspection of the cells suggested that spheres were not formed through cell clumping. Clumped cells had an irregular surface structure as would be expected from cells that had simply ‘stuck’ together, whereas spheres that had grown from clonal expansion of a single cell had a smoother, more regular surface as demonstrated in Figures 3.3 and 4.3. Moreover, clumps of cells tended to adhere to the plastic surface whereas cells in clonally expanded spheres were observed in suspension.

The clonogenic index of glioma primary culture cells varied from 17 to 1129 cells per glioma-derived sphere, although some cells were unable to form spheres at all (Table 3.9). Whilst branched phenotype cell cultures readily formed glioma-derived spheres, flat phenotype cell cultures did not (Table 3.9). The flat phenotype cells instead grew adherent to plastic ware even though, similar to the branched phenotype cells, they had originally been grown from single cell suspensions of glioma tissue as

Table 3.9 The Clonogenic Index of glioma primary culture cells. Primary culture cells were plated in uncoated 96 well plates at known dilutions. The number of glioma-derived spheres forming after one week was counted manually using a phase microscope. The clonogenic index is the minimum number of cells required to form a glioma-derived sphere. 'None' means that no glioma-derived spheres formed. Each glioma primary culture has been designated an alphabetic label to maintain donor anonymity. The histology of the tumour from which the culture was derived is indicated in brackets; Oligo – oligodendroglioma, GBM-glioblastoma. The primary cultures designated CC and EE contained flat phenotype cells, whereas those designated DD, P and X contained branched phenotype cells. These results indicate that branched phenotype cells, but not flat phenotype cells, had clonogenic capacity, suggesting that the branched phenotype cells were more stem-like than the flat phenotype cells.

Glioma primary culture	Clonogenic Index	Cell Phenotype
CC (Anaplastic Oligo)	None	Flat
DD (Gliosarcoma)	192	Branched
EE (Oligodendroglioma)	None	Flat
P (GBM)	1129	Branched
X (GBM)	17	Branched

glioma-derived spheres (Figures 3.1 and 3.4). Variation in the frequency of glioma-derived sphere formation between different glioma primary cultures has previously been reported and it was proposed that the colony forming ability of glioma stem-like cells was greatest in higher-grade tumours [61, 75]. I have demonstrated that cell phenotype was predictive of colony forming ability in my own putative glioma stem-like cells. I did not observe a clear relationship between primary culture cell phenotype and the histological grade of the tumour from which it was derived, but flat phenotype cells, and therefore poor colony forming ability, were more often associated with lower grade tumours (Table 3.7 and 3.9).

3.4.5 Stem and differentiation markers differ between cell phenotypes

I have demonstrated that flat and branched phenotype cells differed markedly in their clonogenic capacity, an indicator of the stem cell-like characteristics of glioma stem-like cells. I next compared the expression of stem cell markers and proteins associated with neural stem cell differentiation between several different primary cultures; 5 flat phenotype primary cultures (designated AA (diffuse astrocytoma), BBD (GBM), CC (anaplastic oligodendroglioma), V (infiltrating astrocytoma) and Z (GBM)) and 7 branched phenotype primary cultures (designated BBS (GBM), DD (Gliosarcoma), L (oligodendroglioma), M (GBM) P (GBM), T (GBM), X (GBM)). I did this using an immunofluorescence technique with antibodies to Nestin, GFAP, β-III tubulin and Olig 2, (Table 3.10, Figures 3.8-3.9) [65-67]. Nestin is an intermediate filament protein expressed during development in neuroepithelial precursor cells and is down regulated with differentiation [180-182]. Nestin is also expressed in glioma stem-like cells, but persists after differentiation [49][65]. Within the primary cultures that I examined Nestin was expressed in 67-100% of cells across all the cultures (Table 3.10, Figure 3.8). There was no clear pattern of variation in the percentage of positively staining cells according to cell phenotype.

Table 3.10 Expression of stem-like and differentiation markers. Glioma primary culture cells were plated for 12 hours, then fixed in 2% paraformaldehyde, permeabilised with Triton X and blocked in normal goat serum. Primary antibodies were applied for one hour at room temperature then fluorescent secondary antibodies added. Nuclei were visualised using Bisbenzimide. Images of the coverslips were taken using confocal microscopy and AxioVision software. The number of cells staining with each antibody was determined using Adobe Photoshop software and statistics were performed using Excel software. Each glioma primary culture is listed in the Table by its designated alphabetic label. The histology of the tumour from which the culture was derived is indicated; Oligo – oligodendroglioma, GBM-glioblastoma. The Flat phenotype primary cultures are designated AA, BBD and CC. The Branched phenotype primary cultures are designated BBS, DD, P and X. Mean values are indicated in the table from at least five regions imaged across three coverslips. Standard deviations are given in brackets. Both flat and branched phenotype cells express the stem cell marker Nestin. In contrast, the neuronal and glial differentiation markers BIII Tubulin and GFAP, respectively, were rarely expressed in the flat phenotype cells.

	GFAP (%)	**BIII tubulin (%)**	**Nestin (%)**	**Olig 2(%)**
AA Diffuse Astrocytoma (Flat)	0	0	87.9 (+/-6.9)	0
BBS GBM (Branched)	95.6 (+/-4.0)	66.8 (+/-13.5)	97.6 (+/-2.2)	10.33 (+/-9.63)
BBD GBM (Flat)	0.20 (+/-0.42)	0.43 (+/-0.73)	67.1 (+/-6.5)	0
CC Anaplastic Oligo (Flat)	0	0	100 (+/-0)	0
DD Gliosarcoma (Branched)	91.5 (+/-4.5)	1.6 (+/-0.9)	100 (+/-0)	0
P GBM (Branched)	7.29 (+/-4.41)	6.48 (+/-6.28)	100 (+/-0)	0
X GBM (Branched)	43.1 (+/-1.9)	23.1 (+/-19.1)	98.4 (+/-2.5)	54.0 (+/-28.0)

Figure 3.8 Expression of stem cell and differentiation markers in glioma primary culture cells. Cells from 5 flat phenotype primary cultures designated AA (Diffuse fibrillary astrocytoma), BBD (GBM), CC (anaplastic oligodendroglioma), V (infiltrating astrocytoma) and Z (GBM), and 7 branched phenotype primary cultures designated BBS (GBM), DD (gliosarcoma), L (oligodendroglioma), M (GBM), P (GBM), T (GBM), X(GBM)) proliferated for 12 hours in standard expansion media before being fixed in 2% parafomaldehyde. Cells were then permeabilised, blocked with normal goat serum and the primary antibodies (as indicated below) added. Primary antibody binding was visualised with fluorescent-labelled secondary antibodies, using a confocal microscope. Nuclei were counterstained with Bisbenzimide. The images show representative examples of staining with the indicated antibodies in flat and branched phenotype cells. The colour of the text documenting the antibodies used in each image indicates the fluorescent colour. There was no Olig 2 antibody staining in flat phenotype cells. The scale bar indicates 200 microns. At least five fields at 20x power were examined from each of three coverslips per primary culture for every antibody examined (Table 3.7). Images were analysed using AxioVision software. The images illustrate that both flat and branched phenotype cells expressed the stem cell marker Nestin, but the glilal and neuronal differentiation markers GFAP and BIII Tubulin were rarely seen in flat phenotype cells.

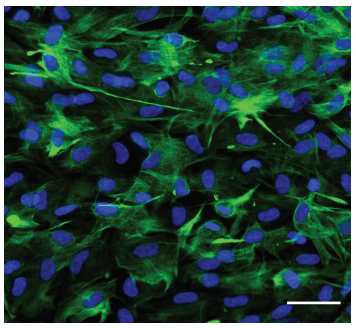

Flat phenotype cells

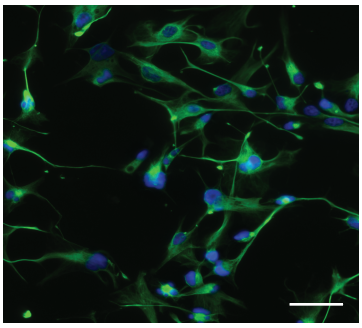

Branched phenotype cells

Nestin

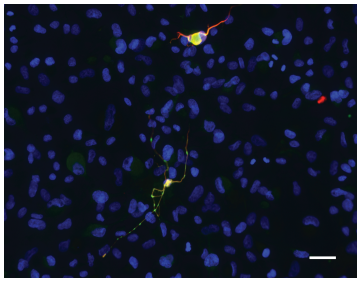

Flat phenotype cells

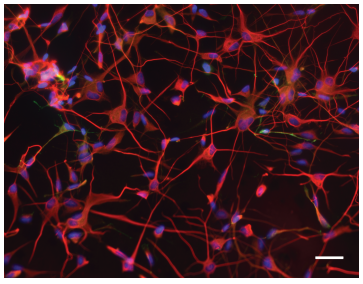

Branched phenotype cells

GFAP
BIIITubulin

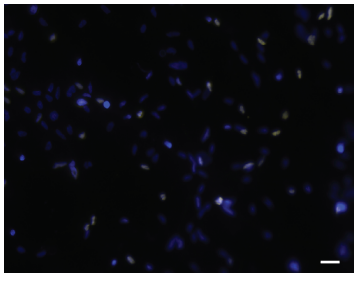

Branched phenotype

Olig 2 positive nuclei appear white

Figure 3.9 BMP-4-mediated astrocytic differentiation. Cells from the flat phenotype primary cultures AA1 (diffuse astrocytoma), BBD (GBM) and CC1 (anaplastic oligodendroglioma) were plated onto Matrigel-coated coverslips and incubated for 12 hours, washed in warm PBS, then incubated in a modified media where the mitogens EGF and FGF had been removed and the differentiation factor BMP-4 had been added. Cells were fed again with this media after 3 days. On day 5 cells were fixed in 2% paraformaldehyde, permeabilised, blocked with normal goat serum, and then incubated with anti-GFAP primary antibody. Primary antibody binding was visualised with fluorescent-labelled secondary antibodies using a confocal microscope. Nuclei were counterstained with DAPI. In the image below, nuclei are coloured blue and GFAP expression is indicated in red. The scale bar indicates 200 microns. At least five fields at 20x power were examined from each of three coverslips per primary culture for every antibody examined. Images were analysed using AxioVision software. The quantification of primary antibody staining is detailed in the text. An image from the flat phenotype primary culture designated CC1 is shown as a representative example and indicates that on exposure to serum a small proportion of cells appeared to undergo astrocytic differentiation.

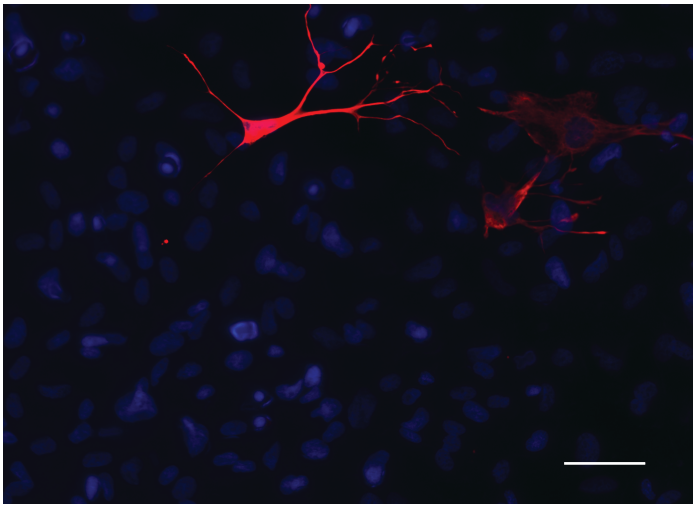

GFAP is often used as a marker of astrocytic differentiation and β-III tubulin is a neuronal marker [178, 213]. I examined the expression of GFAP and β-III tubulin in my adherent putative glioma stem-like cells (Table 3.10, Figure 3.8). I identified that in general the flat phenotype cells (for example, the primary cultures designated AA, BBD and CC) did not express either protein (Table 3.10). Only a very occasional cell in the flat phenotype culture designated BBD expressed β-III tubulin or GFAP (Table 3.10).

In contrast, more than 90% of branched phenotype glioma primary culture cells stained with antibodies to GFAP, including the culture designated BBS derived from a biopsy taken from the same tumour that the primary culture designated BBD originated from (Table 3.10). There was some variation in the expression of β-III tubulin in the branched phenotype primary cultures (Table 3.10). For example, the primary culture designated DD expressed the neuronal marker on average in 1.6% of cells (standard deviation +/-0.9%), compared to the primary culture designated BBS where 66.8% of cells were stained (standard deviation +/- 13.5%) (Table 3.10).

Expression of the transcription factor Olig2 has previously been used to identify oligodendrocyte precursor cell lineage specification in glioma stem-like cells [66, 67]. I did not identify any evidence of Olig2 expression in my flat phenotype cells (Table 3.10). In contrast, Olig2 expression was observed in 10-54% of cells in the branched phenotype cells designated BBS and X, but not in other branched phenotype cells (Table 3.10, Figure 3.8).

It has been previously described that cells in some primary cultures double-stain with antibodies to both GFAP and β-III tubulin, possibly reflecting activation of an aberrant differentiation programme in these cells [42]. I observed this same phenomenon in a proportion of the branched phenotype cultures, but not flat phenotype cultures. For example, in the glioma primary culture designated P, almost

all the cells that stained with GFAP dual-stained with β-III tubulin, and vice versa (Table 3.10).

The stem-like features of my glioma primary culture cells was further assessed by attempting to differentiate them down astrocytic, oligodendroglial or neuronal lineages. Oligodendroglial and neuronal differentiation has previously been observed in some glioma stem-like cells on removal of the mitogens EGF and bFGF [65-67]. Astrocytic differentiation can be driven by the addition of fetal calf serum (FCS), or the differentiation factor Bone Morphogenic Protein 4 (BMP-4), to the growth media [65-67]. However, when I attempted to assess the differentiation of my own putative glioma stem-like cells I observed that on removal of EGF and bFGF the cells ceased to adhere to the coverslips that they had been grown on. It was not possible to subsequently expand and passage these non-adherent cells, suggesting that they were in fact dead. Attempts to optimise the culture technique to overcome the problem of cell death were unsuccessful. Nevertheless, I did observe astrocytic differentiation after addition of BMP-4 or FCS in some of the primary cultures tested, before cell death occurred. Of particular significance was that in the flat phenotype primary cultures designated CC (anaplastic oligodendroglioma), V (astrocytoma), Y (GBM) and Z (GBM), after treatment with the differentiation factor BMP-4 or FCS for 5 days, a small proportion of cells were observed to express the astrocyte marker GFAP (Figure 3.9); for example, 1.0 % of cells in the culture designated CC1 (standard deviation 0.43%). This was despite the fact that I had observed no evidence of GFAP expression in the majority of undifferentiated flat phenotype primary culture cells (Table 3.10). In the branched phenotype primary cultures, addition of BMP-4 was also generally associated with an increase in GFAP staining. For example, in the culture designated P, the percentage of cells staining with GFAP increased after incubation with BMP-4 from 7.29% (+/-4.41%) to 22.31% (+/-7.20%), which was statistically significant ($p=0.002$).

3.5 Preservation of DNA copy number changes between cultures and tumours

I had observed that both flat and branched phenotype cultures could sometimes be derived from different tissue samples taken from the same tumour and so the question remained as to whether they were both derived from actual tumour cells, or whether one or other cell phenotype originated from a non-tumour cell. I therefore next examined DNA copy number changes present in both glioma tissue and primary culture cells. I principally used the primary cultures designated AA to EE for these experiments and the tumour type from which these primary cultures were derived is indicated in Table 3.8. If the primary culture cells were representative of the tumour tissue from which they had been derived then they would share tumour-associated DNA copy number changes with the tumour, but these changes would not be present in patient-matched somatic DNA taken from blood. It was possible though that one or other of the flat and branched phenotype cultures recapitulated a cell population that was actually tumour-associated rather than tumour-derived. I used the technique of array comparative genomic hybridisation (CGH) to analyse the copy number changes in DNA samples extracted from primary culture cells, from the tumours from which these cultures were derived, and from matched blood samples [214].

Regions of inter-individual genomic structural differences known as copy-number variation (CNV) can be detected using array CGH [215]. These changes occur in the somatic genome and so will be present in a patient's blood, their tumour and in the primary cultures derived from the tumour. I identified such regions of CNV in sets of blood, tumour and primary culture DNA from all 5 patients examined (Figure 3.10). This included both flat and branched phenotype cultures.

In contrast, DNA copy number changes present in tumour tissue but not in the patient-matched somatic genome are tumour-related changes. I identified two patterns of such DNA copy number changes and these differed between the flat and branched phenotype primary cultures (Figure 3.11).

Figure 3.10 Array CGH ideogram of DNA copy number changes. DNA copy number changes were compared between branched phenotype primary cultures grown in hypoxic conditions (3% oxygen) or normoxic conditions (21% oxygen), the tumour tissue from which the primary cultures had been derived, and blood, all taken from the patient designated DD (gliosarcoma). A portion of the array CGH ideogram for chromosome 5 is shown. The star highlights a region of copy number change present in blood, tumour tissue and primary cultures known as a common normal variant. This indicates that all the cultures and samples have been derived from the same inividual. The structural variants graph below the ideograms indicates regions in the genome that have been associated with structural variation in the normal population. This confirms that the region of copy number change indicated by the star corresponds to a region of such common variation. A similar phenomenon was observed in all the matched tumours, blood and primary cultures examined. The array CGH was performed by the Cytogenetics laboratory, NHS Lothian.

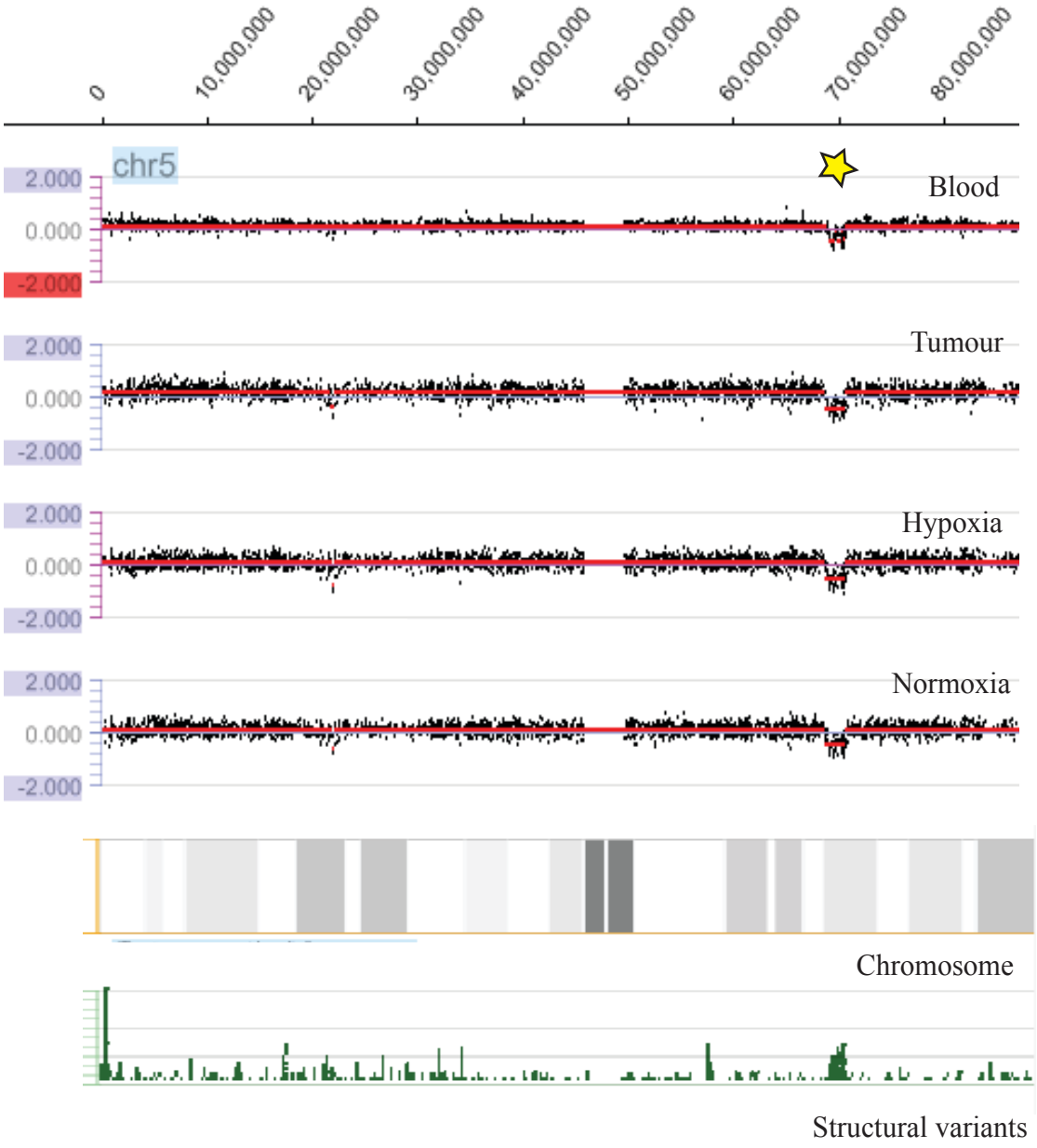

Figure 3.11 Array CGH ideogram of DNA copy number changes. DNA copy number changes were compared between branched phenotype primary cultures grown in both hypoxic conditions (3% oxygen) and normoxic conditions (21% oxygen), tumour tissue from which the primary cultures had been derived, and blood, all taken from the patient designated DD (gliosarcoma). A portion of the array CGH ideogram for chromosome 9 is shown. The star highlights a region of copy number change present in tumour tissue and primary cultures, but not in the patient's somatic genome as represented by the blood sample. This region does not correlate with an area of common structural variation. This indicates that the branched phenotype primary cultures designated DD are indeed tumour derived. A similar phenomenon was observed in all the matched branched phenotype primary cultures, blood and tumour examined. The array CGH was performed by the Cytogenetics laboratory, NHS Lothian.

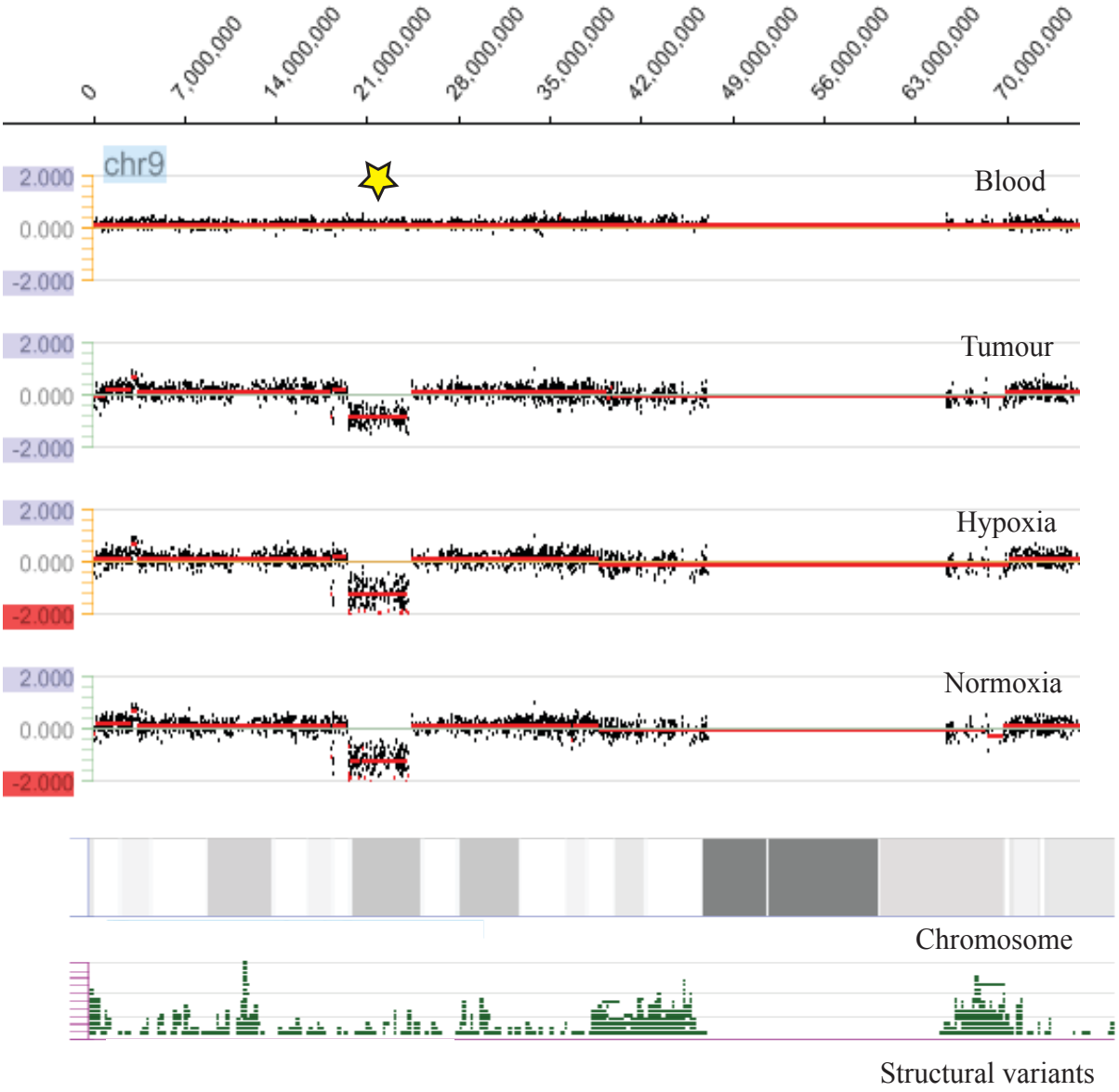

I observed that most if not all DNA copy number changes found in glioma tissue from which branched phenotype cultures were derived were also present in the branched phenotype cultures themselves, but were absent from patient-matched blood (Figure 3.11). With the array CGH technique the DNA copy number profile of a tissue sample is a composite of the profile of each constituent cell type [214]. These observations therefore suggest that branched phenotype cultures were derived from cells with a similar mutational lineage to the cells that constituted the bulk of the glioma tumour. This is consistent with the hierarchical model of glioma described earlier. This pattern of DNA copy number changes was maintained across a number of different tumours and their related branched phenotype primary cultures designated L (Oligodendroglioma), M (GBM), O (GBM), X (GBM), BB (GBM), and DD (Gliosarcoma).

Analysis of DNA from the flat phenotype cultures designated CC (Anaplastic Oligodendroglioma) and from the tumour from which they had been derived also identified some copy number changes that were present in both samples, but not in patient-matched blood (Figure 3.12). This suggests, in similarity to the branched phenotype cultures, that the flat phenotype cultures are tumour-derived. This pattern of DNA copy number changes was also observed in the flat phenotype cultures designated BB (GBM) and EE (Oligodendroglioma), and in the tumours from which they had been derived. However, only a few of the copy number changes observed in the tumours from which flat phenotype cells had been derived were actually preserved in flat phenotype cultures themselves. This contrasts with the large number of DNA copy number changes present in both branched phenotype cells and the tumours from which they had been derived. It was not possible to quantify the frequency with which copy number changes were preserved between a primary culture and the tumour from which it had been derived. This was because there were subtle variations in the description of the size and location of copy number changes

Figure 3.12 Array CGH ideogram of DNA copy number changes. DNA copy number changes were compared between flat phenotype primary cultures, the tumours from which these primary cultures had been derived, and blood, all taken from the patient designated CC (anaplastic oligodendroglioma). A portion of the array CGH ideogram for chromosome 1 is shown. The star highlights a region of copy number change present in tumour tissue and primary cultures, but not in the patient's somatic genome, as represented by the blood sample. This suggests that the flat phenotype primary cultures are tumour derived. The array CGH was performed by the Cytogenetics laboratory, NHS Lothian.

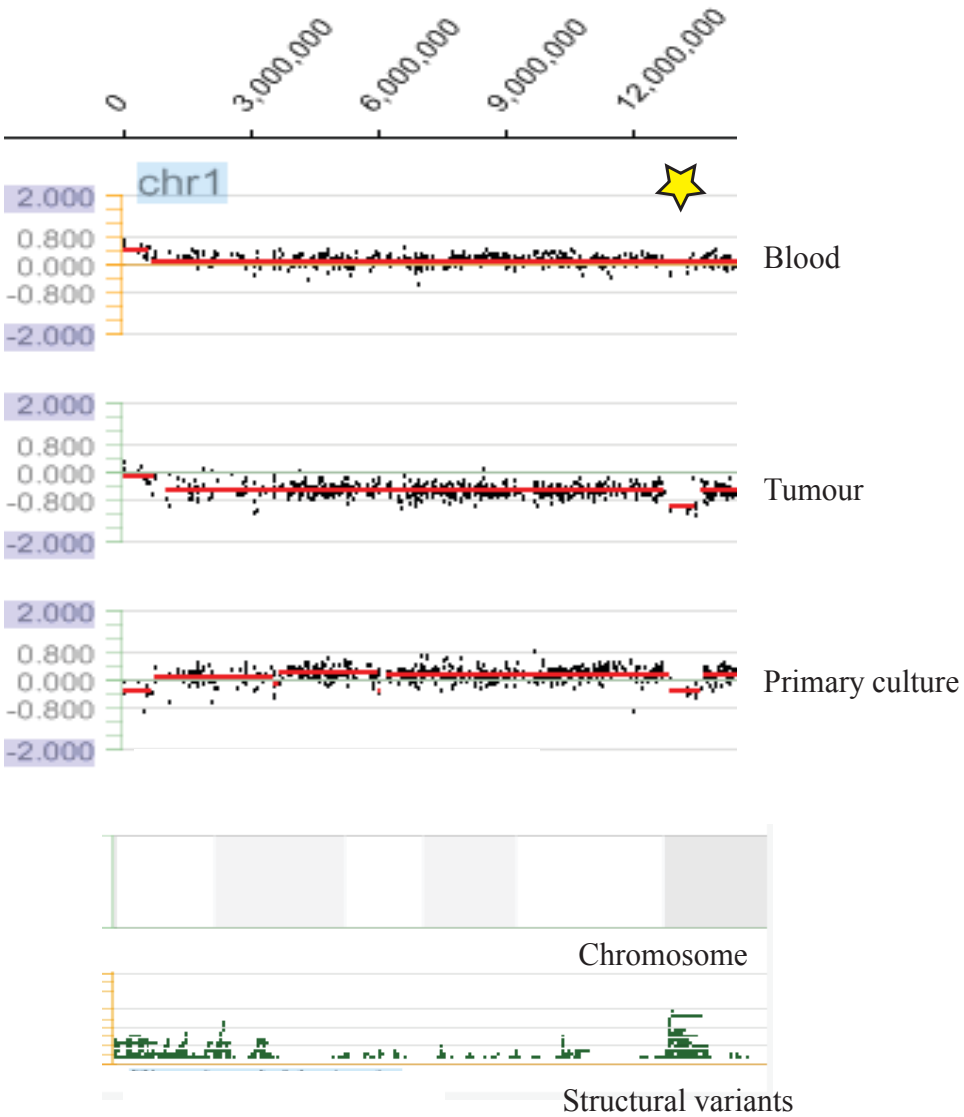

within sample sets, such that although they could readily be determined to be overlapping on manual inspection, it was not possible to automate this process to calculate the frequency of shared copy number changes across the whole data set.

The array CGH ideogram in Figure 3.12 demonstrates a region of reduced DNA copy number on chromosome 1 in the primary culture designated CC (Anaplastic oligodendroglioma) and the tumour from which this culture was derived. In the technique of array CGH the amount of copy number change present in a test sample is determined by comparison to a pooled human control [214]. It is indicated diagrammatically by the degree of deviation of a red line from the horizontal zero axis, the red line itself representing an average of the copy number change of all the individual array probes indicated by the black dots. In Figure 3.12, only a short length of DNA copy number change is consistent between the tumour and flat phenotype culture sample. There is actually a much larger segment of DNA copy number change on chromosome 1 that is present in the tumour tissue but not in the related primary culture. This observation suggests that flat phenotype cells account for only a small proportion of the cells in the tumour from which they were derived. This is consistent with the gene expression analysis I describe below (Figure 3.14 and 3.15).

3.5.1 Intra-tumoural variation in DNA copy number changes

So far in this section on array CGH analysis of DNA copy number changes I have examined the individual relationships between flat or branched phenotype cultures and the respective tumours from which these cultures were derived. However, I have previously demonstrated that primary cultures with either flat or branched phenotype cells can both be derived from different tissue biopsies taken from the same tumour (Figure 3.4 and 3.5). This presents an opportunity to examine the relationship between flat phenotype and branched phenotype cells and to ask whether both cell

phenotypes are derived from a common precursor cell, from different cells, or from each other.

I analysed the DNA copy number changes in blood, primary culture cells and tumour tissue from the patient designated EE (Oligodendroglioma) (Figures 3.13 & 3.14). The tumour biopsies designated EE1 and EE2 were taken from different regions of the same tumour. The resultant primary culture cells designated EE1 had a branched phenotype whereas the primary culture cells designated EE2 had a flat phenotype (Figure 3.5). DNA copy number analysis indicated that there were some changes consistent between the tumour tissue and primary culture samples and others that were different. For example, there was a gain of genetic material on the short arm of chromosome 10 (10p) in both tumour biopsies designated EE1 and EE2 (Figure 3.13). This abnormality was not present in the somatic genome of the matched blood sample, confirming that the change was tumour specific (Figure 3.13). As would be expected from my previously described observations, DNA from the branched phenotype culture derived from the tumour sample designated EE1 had the same gain of material on 10p as was seen in both tumour biopsies (Figure 3.13). In contrast, this 10p copy number change was not seen in DNA from the flat phenotype culture designated EE2 (Figure 3.13). DNA from the culture designated EE2 in fact lacked any of the gross copy number changes seen in either the tumour tissue or primary culture designated EE1. These observations confirm the general description of the characteristic copy number changes of flat and branched phenotype cells given previously, and reinforce the suggestion that the genetic differences between branched and flat phenotype cells are a specific feature of the cell type rather than simply reflecting the tumour from which they are derived.

Interestingly, examination of DNA copy number data from the patient designated EE also provided evidence of intra-tumoural DNA copy number change heterogeneity.

Figure 3.13 Array CGH ideogram of DNA copy number changes. DNA copy number changes were compared between a branched phenotype culture (EE1), a flat phenotype culture (EE2), the tumour biopsies from which these cultures were derived (EE1 and EE2 tumours, respectively) and blood, all originating from the patient designated EE (oligodendroglioma). A portion of the array CGH ideogram for chromosome 10 shows a region of copy number change present both in tumour samples and branched phenotype EE1 cells, but not in flat phenotype EE2 cells. The copy number change is also absent from the somatic genome, as represented by blood. This suggests that there are different types of tumour cell within this glioma, with different mutational profiles. The array CGH was performed by the Cytogenetics laboratory, NHS Lothian.

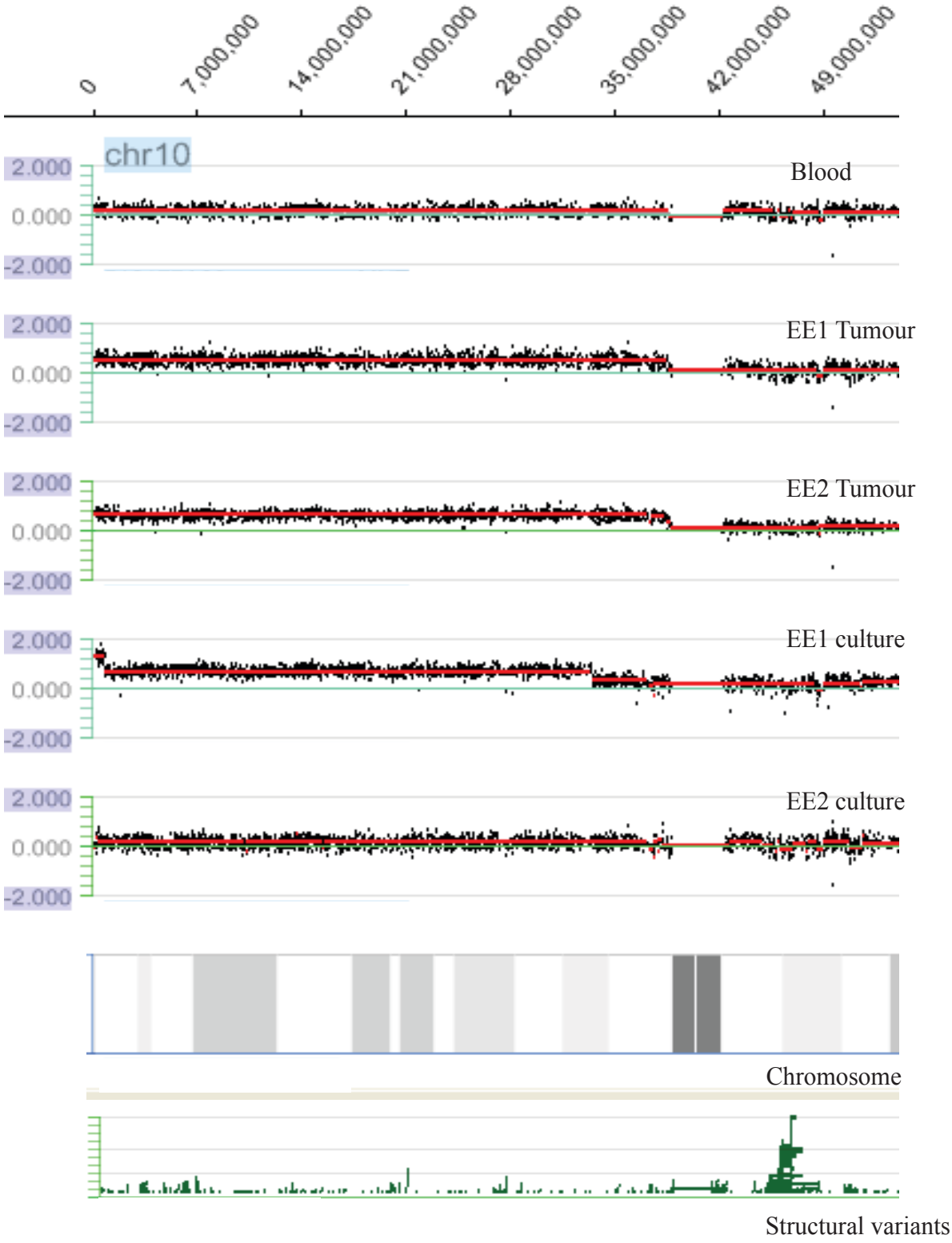

Figure 3.14 Array CGH ideogram of DNA copy number changes. DNA copy number changes were compared between the branched phenotype cell culture (EE1 culture), flat phenotype cell culture (EE2 culture), the tumours from which these cultures were derived (EE1 and EE2 tumours, respectively) and blood, all originating from the patient designated EE (oligodendroglioma). A portion of the array CGH ideogram for chromosome 8 demonstrates a region of copy number change present in the tumour genome of biopsy EE1 but not that of biopsy EE2, (as indicated by the horizontal black line), suggesting the existence of genetic heterogenetiy in the tumour itself that might contibute to the specification of cell phenotype in the primary cultures derived from each biopsy. The array CGH was performed by the Cytogenetics laboratory, NHS Lothian.

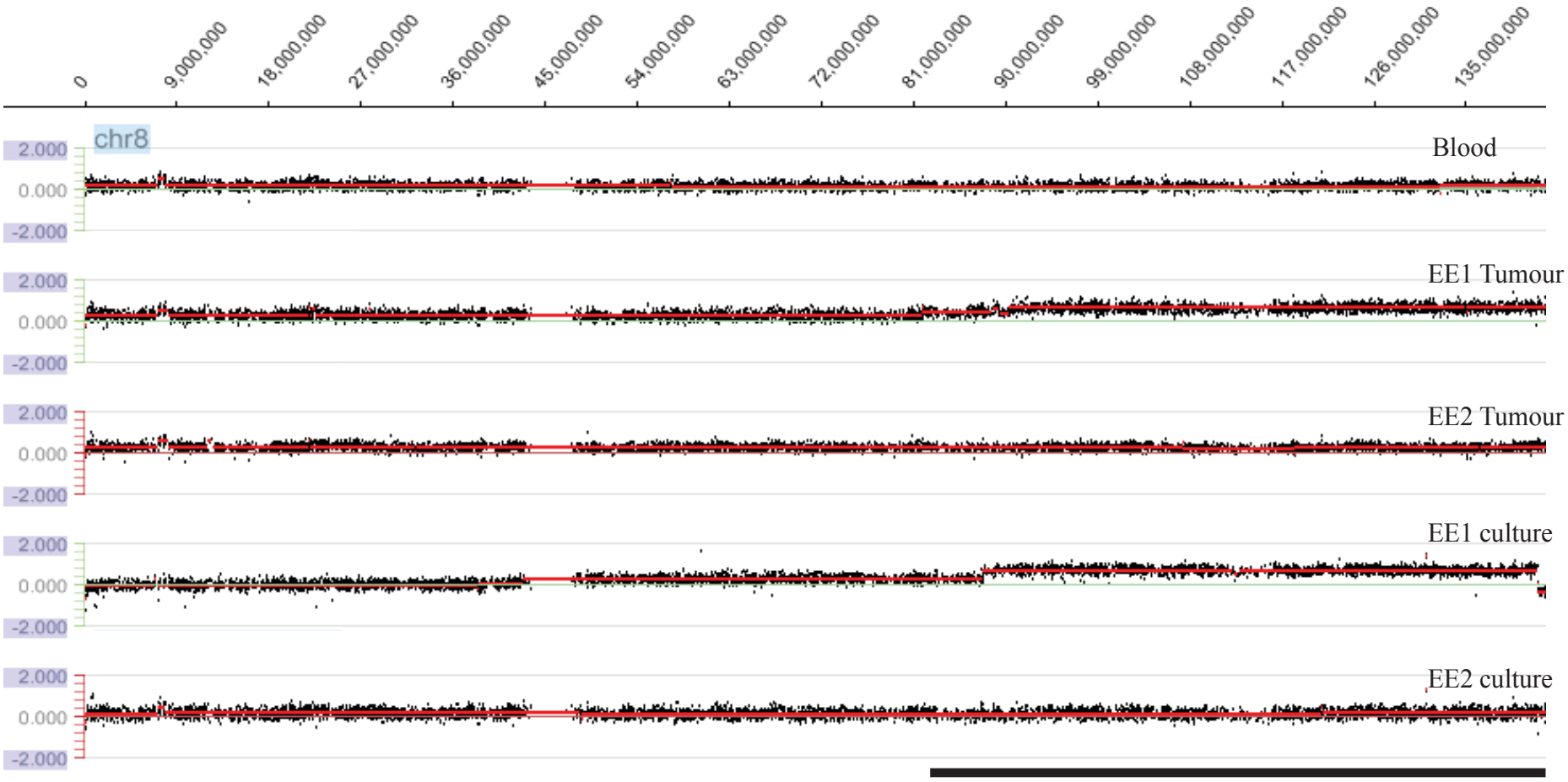

For example, I observed that there were regions of DNA copy number change that actually differed between the tumour biopsies designated EE1 and EE2 even though there were also tumour-associated copy number changes that were the same in both biopsies (Figures 3.13 and 3.14). For example, Figure 3.14 demonstrates a region of DNA copy number gain on the long arm of chromosome 8 (8q), indicated by the horizontal black line, that is present in the tumour sample designated EE1 and its associated primary culture, but not in the sample designated EE2 or the primary culture designated EE2. The copy number change that differed between tumour biopsies was absent from the matched blood sample, so was clearly tumour-associated rather than somatic (Figure 3.14). On closer inspection of the copy number data there was actually a segment of copy number change within this 8q region of interest in the tissue biopsy designated EE2, but it did not reach significance. This suggests that there were relatively few cells within the sample containing the abnormality. A similar divergence between the DNA copy number changes of EE1 and EE2 tumour samples was observed on chromosome 9 and 15. In contrast, DNA copy number changes that were similar in both tissue samples (but not in blood) were identified on chromosome 4,10,11 and 12. In fact, the majority of copy number changes were consistent between the tumours designated EE1 and EE2 suggesting that the tumour biopsy designated EE2 is not simply normal brain containing a few abnormal cells, but is in fact a region of tumour whose cells have a more primitive mutational profile than cells in the region biopsied in the tissue sample designated EE1.

3.6 Gene expression data confirms the existence of two distinct cell types

I next examined the RNA gene expression profiles of a selection of flat phenotype and branched phenotype glioma primary culture cells in order to further interrogate their stem-like characteristics (Table 3.11). I also wanted to ascertain whether the two cell phenotypes might have different biological functions.

Table 3.11 Cell phenotypes of glioma primary cultures. Glioma primary cultures were derived from multiple tissue biopsies taken from five distinct tumours designated AA to EE. The histology of the parent tumour and the phenotype of the cells characterising the derived primary culture are indicated in the table.

Tumour	Histology (Grade)	Cell phenotype
AA	Diffuse fibrillary astrocytoma (3)	Flat
BB	GBM (4)	Flat/branched
CC	Anaplastic oligodendroglioma (3)	Flat
DD	Gliosarcoma (4)	Branched
EE	Oligodendroglioma (2)	Flat/branched

Unsupervised hierarchical clustering of the gene expression datasets was performed on three sets of primary culture cells using an 'Euclidean distance approach' and 'Ward's minimum variance method' (Figure 3.15). Two principle clusters of cells were identified. These clusters matched exactly to the branched phenotype and flat phenotype groups of primary cultures that I earlier described. The 'approximately unbiased' and 'bootstrap probability' p values confirmed that the clustering was 100% accurate (Figure 3.15).

Where two primary cultures had been derived from the same tumour biopsy, but grown under different oxygen conditions, if the cell phenotype was similar then they tended to cluster together. For example, the primary cultures designated as DD (Gliosarcoma) and grown under hypoxic (3%) and normoxic (21%) oxygen conditions both had branched phenotype cells and both clustered together in this unsupervised clustering analysis of gene expression data (Figure 3.15). The gene expression profiles of cells from the primary cultures designated as DD (Gliosarcoma) also clustered with the profiles of branched phenotype cells from other cultures, such as the culture designated BBN (GBM) (Figure 3.15).

The culture designated as BBH (GBM) was derived from the same tumour biopsy as the culture designated BBN (GBM), but was grown under hypoxic (H) rather than normoxic (N) conditions. The culture designated as BBH (GBM) contained cells with a flat phenotype whereas the culture designated BBN (GBM) contained cells with a branched phenotype. The gene expression profile of cells from the culture designated BBH (GBM) did not cluster with the gene expression profile of cells from the culture designated BBN (GBM). The BBH (GBM) gene expression profile instead clustered with the profile of other cultures containing cells with a flat phenotype, such those designated CCN and CCH (Anaplastic Oligodendroglioma) (Figure 3.15). This suggests that branched phenotype cells may be fundamentally different to flat phenotype cells, a hypothesis that I will examine in more detail below.

Figure 3.15 Gene expression analysis of glioma primary cultures. RNA was prepared from glioma primary culture cells and from the tumours from which they had been derived. RNA integrity (RIN) was assessed using an Agilent 2100 Bioanalyzer (samples used had RIN score of ≥9.0). RNA was then amplified and biotinylated using an Illumina TotalPrep RNA Amplification Kit and subsequently hybridized to Illumina human HT12 version 3 Expression BeadChip by Dr Colm Nestor, IGMM. Bioinformatic analysis was performed using the statistical package R version 2.14.1. The data was normalized and hierarchical clustering performed using the Euclidian distance and the Ward algorithms. RNA samples are annotated in the Figure by their two letter designation indicating the tumour sample they relate to, e.g DD, and a suffix letter indicating that the RNA was prepared directly from tumour tissue (T), or that the source primary culture cells had been incubated in normoxic (N) (21% oxygen), or hypoxic (H) (3% oxygen) conditions. The phenotype of the cells in each primary culture is indicated beneath the Figure as 'branched' or 'flat;' sample CCT was derived directly from a tumour and so no cell phnotype is given. The numbers in red and green indicate the percentage accuracy of this clustering process confirmed by calculation of the approximately unbiased (au) and bootstrap probability (bp) p values, respectively. The values on the edge of each cluster in grey typeface are the p-values themselves (%). BB (GBM), CC (anaplastic oligodendroglioma), DD (gliosarcoma). The hierarchical clustering based on gene expression profiles grouped together the primary cultures in the same two groups as cell phenotype, indicating that these two groups likely had molecular differences.

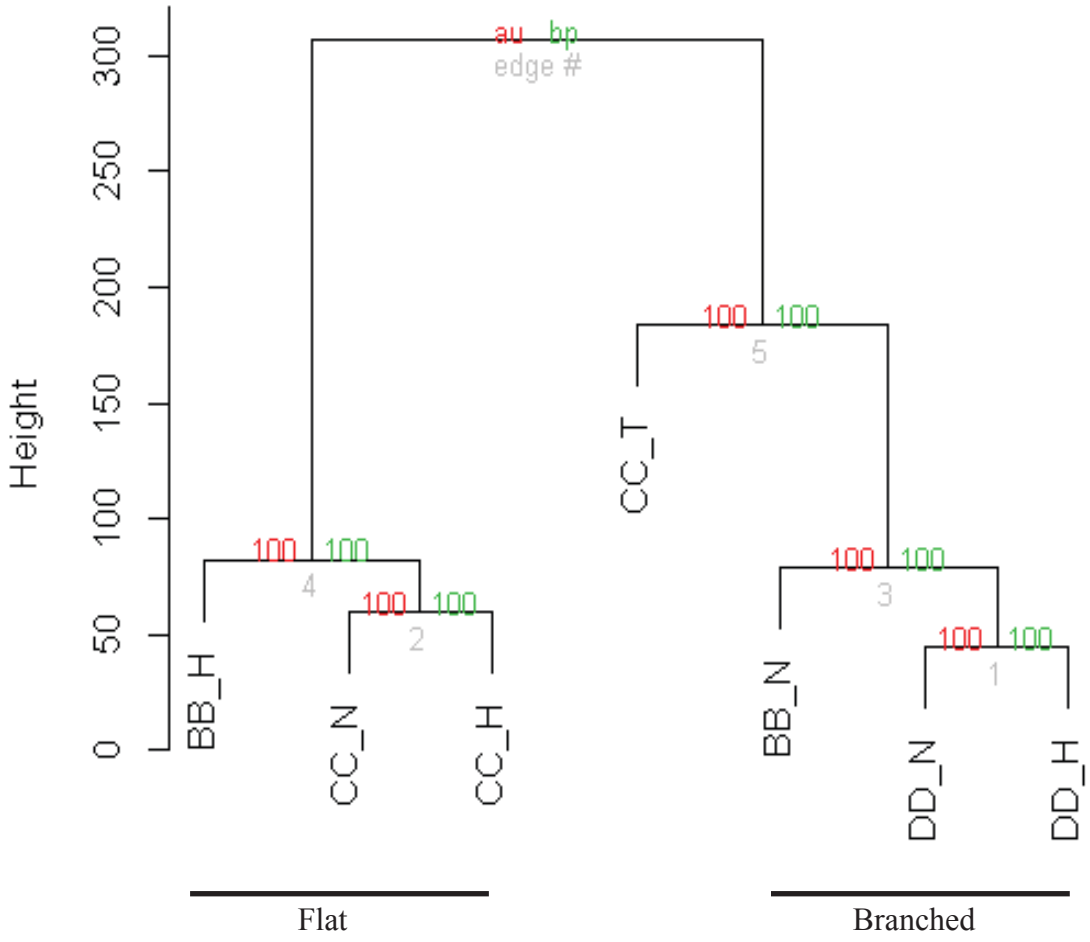

Interestingly, the gene expression profile of tumour tissue from the glioma designated CC (Anaplastic Oligodendroglioma), from which primary cultures CCN and CCH were derived, clustered closer to the profile of primary cultures with branched phenotype cells than to that of the flat phenotype cells in CCN and CCH. Further analysis is needed to establish whether this observation is replicated in other primary cultures and to understand its significance, but it might be interpreted as suggesting that the flat phenotype cells account for only a small proportion of cells in the tumours from which these cultures have been derived; I made drew a similar conclusion from the array CGH analysis described above. These tumour biopsies may instead predominantly contain cells with a branched cell phenotype.

The unsupervised clustering experiment confirmed the existence of two distinct putative stem-like cell types in my glioma primary cultures. I therefore next sought to identify the genes whose expression was most different between these groups with the aim of discerning whether they had distinct biological functions. The fold change difference in the expression of genes between the groups was determined using the R statistics package. The significance of the differences was calculated using both a student t-test corrected for multiple testing and a Wilcoxon signed-rank test; a sample of genes whose expression was most different between the branched and flat phenotype primary cultures is listed in Table 3.12 to illustrate the degree of fold change difference and the statistical significance of these differences. I next selected the 100 genes with most increased expression in each cluster and used the *DAVID* functional annotation tool (David.sbcc.ncifcrf.gov) to ascertain whether these two groups of genes were associated with different functions. The DAVID (database for annotation, visualization and integrated discovery) knowledgebase provides functional interpretation of genes by extrapolation from information available in existing publications [216, 217]. I identified that one of the gene sets was associated with a glial/neural-like profile and the other with a mesenchymal-like profile (Table 3.13). On the basis of morphology alone, I suggested that the flat phenotype cells had

Table 3.12 Comparison of gene expression data by cell phenotype. Gene expression data was compared between samples in the two groups identified by unsupervised clustering. Genes were ranked based on the fold change differences between the two groups. Representative examples from these two groups, branched and flat phenotype cultures, are given in the table, as indicated. The values given indicate a gene expression level relative to a standard control. The ten genes each with the highest and lowest fold changes represent the most up-regulated and down-regulated genes between the two clusters, respectively, and are listed in the table. Samples are listed by their designated alphabetic code and a suffix letter indicating whether RNA was prepared directly from cells incubated in normoxic (21% oxygen) (N), or hypoxic (3% oxygen) (H) conditions. The notation 'E' indicates that the number is raised to the power 10. For example, 8.23E-06 means 8.23 multiplied by 10 to the power minus 6.

	CC_H	BB_H	BB_N	DD_N	T-test p value	Fold change
	Flat Phenotype		Branched phenotype			
FABP7	5.78	5.48	12.9	13.4	8.23E-06	2.05E+02
GFAP	4.91	5.11	13.1	12.7	2.16E-05	1.92E+02
C1orf61	5.07	5.5	12.2	12.9	9.73E-05	1.75E+02
PMP2	5.30	5.20	12.8	12.3	9.98E-05	1.74E+02
PTPRZ1	5.25	5.35	11.7	12.5	9.56E-04	1.32E+02
SCRG1	5.27	5.32	10.7	12.5	4.70E-03	1.03E+02
GPM6B	5.23	5.25	12.3	11.7	6.16E-04	1.00E+02
SOX8	5.82	5.88	12.3	12.2	4.40E-04	9.70E+01
VGF	6.07	5.60	11.0	12.6	6.15E-03	8.80E+01
CYBA	10.7	11.2	5.69	5.16	5.01E-05	1.96E-02
COL1A2	11.7	12.4	7.03	5.87	6.27E-04	1.82E-02
IL8	10.4	12.2	5.46	5.81	6.24E-03	1.71E-02
TAGLN	11.9	12.6	7.47	5.40	6.33E-03	1.59E-02
GREM1	10.8	12.0	5.06	5.21	3.44E-03	1.42E-02
IER3	11.6	12.6	5.62	5.96	7.58E-04	1.30E-02
CLDN11	12.4	12.9	6.30	5.90	1.63E-05	1.14E-02
BGN	12.8	12.5	6.55	5.50	7.70E-04	7.88E-03
SRGN	12.1	12.8	5.09	5.09	6.59E-04	6.44E-03
ACTG2	12.5	13.2	6.72	4.93	2.69E-03	5.52E-03

Table 3.13 Gene expression profiles correspond to different functional annotations. A list was prepared of the top 100 genes, as defined by the highest fold-change, in each of the two clusters of primary cell cultures identified by unsupervised clustering of gene expression data. This list was submitted to the online functional annotation tool DAVID. DAVID uses multiple sources of functional annotation to group functionally related genes in a list and rank these functions within a given gene set with an *enrichment score*. The higher the enrichment score, the greater the number of genes in the dataset that have a role in that function; enrichment scores greater than 1.3 are significant [216]. Benjamini is one of the methods of statistical correction used by DAVID to avoid overestimating the significance of a result that comes from multiple comparisons. The smaller the number, the more reliable the result is. This analysis indicates that one set of primary cultures had a glial-like function and the other had a mesenchymal-like function.

A

Cluster	Enrichment score	Function	Benjamini
1	5.7	Developmental protein	9.6 E-06
		Neurogenesis	4.1 E-06
		Differentiation	7.1 E-04
2	5.05	Cell adhesion	1.2 E-04
3	3.5	Extracellular region	9.8 E-05
4	3.15	Neuron differentiation	3.4 E-07
5	2.81	Signalling	1.0 E-05
6	2.68	Glial cell differentiation	8.0 E -05

B

Cluster	Enrichment score	Function	Benjamini
1	6.45	Extracellular region part	3.4 E-13
2	4.07	Extracellular matrix	2.1 E-08
3	3.54	Cell adhesion	1.8 E-01
4	3.41	ECM-receptor interaction	2.2 E -02
5	3.36	Circulatory system process	1.4 E-03
6	2.56	Extracellular matrix	6.9 E-05

a mesenchymal-like gene expression profile and that the branched phenotype cells had a neural/glial-like expression profile.

3.6.1 RNA species confirm cell phenotype characteristics

It is not possible from examination of the gene expression data alone to determine which gene list corresponds to each of the two primary culture cell phenotypes. I therefore performed reverse transcription polymerase chain reactions (RT-PCR), using specific primers (Table 2.2), on cDNA libraries prepared using standardised amounts of RNA from seven flat phenotype and branched phenotype glioma primary cultures, as well as from the tumours from which these cultures were derived: AA (diffuse Astrocytoma), BB (GBM), CC (Anaplastic Oligodendroglioma), DD (Gliosarcoma), EE (Oligodendroglioma), X (GBM), P (GBM). Embryonic stem cells were used as a comparator for the stem-like cells (Figures 3.16 and 3.17).

GFAP is a marker of both differentiated astrocytes and progenitor cells, whilst Olig2 is a transcription factor important in determining neural progenitor cell fate [13, 218]. *GFAP* and *Olig2* were both in the top 20 expressed genes of my glial/neural-like cluster based on the unsupervised clustering of gene expression profiles of glioma primary culture cells (Table 3.12). Using a RT-PCR approach I identified that *GFAP* and *Olig2* genes were expressed in branched phenotype cells but not flat phenotype cells (Figures 3.16 and 3.17). This indicates that branched phenotype cultures, but not flat phenotype cultures, have a stem-like glial-like gene expression profile as determined by the functional annotation study described previously (Table 3.13). The expression of the glial-specific marker *S100B* in branched phenotype cell cultures, but not in flat phenotype cultures, further supports this (Figure 3.16). *GFAP* gene expression was also observed using RT-PCR in tumours from which the branched phenotype cultures were derived (Figures 3.16 and 3.17).

Figure 3.16 Measurement of RNA species to assess glial-like and mesenchymal-like characteristics. RNA was prepared from nine glioma primary cultures and from the tumours from which those primary cultures had been derived. One microgram of RNA from each sample was reverse transcribed and then reverse transcription polymerase chain reactions were performed on the cDNA using Taq 2x Master Mix and primers (Table 2.2). GFAP, Olig 2 and S100B are markers of glial progenitor-like function. Nestin is a progenitor marker. Actin is a cytoskeletal protein and its expression pattern was used as a loading control. PCR products were separated on a 1.6% agarose gel and visualised with ethidium bromide. A primary culture and tissue sample labelled with the same abbreviation, e.g AA1, come from the same source tumour. Samples designated BBD and BBS were taken from deep and superficial parts of the same tumour, respectively. The key above the sample labels indicates whether the constituent cells in primary culture have a flat, branched or mixed phenotype. Normal brain tissue and embryonic stem cells (EB) were used as controls for differentiated and stem cell expression profiles, respectively. The primer was ommitted in the negative control. The histology of each tumour is detailed in in Table 3.1. The images demonstrate that the branched phenotype cells had glial-like characteristics, implying that the flat phenotype cells had mesenchyaml-like features, according to the functional analysis of the gene expression data previously described.

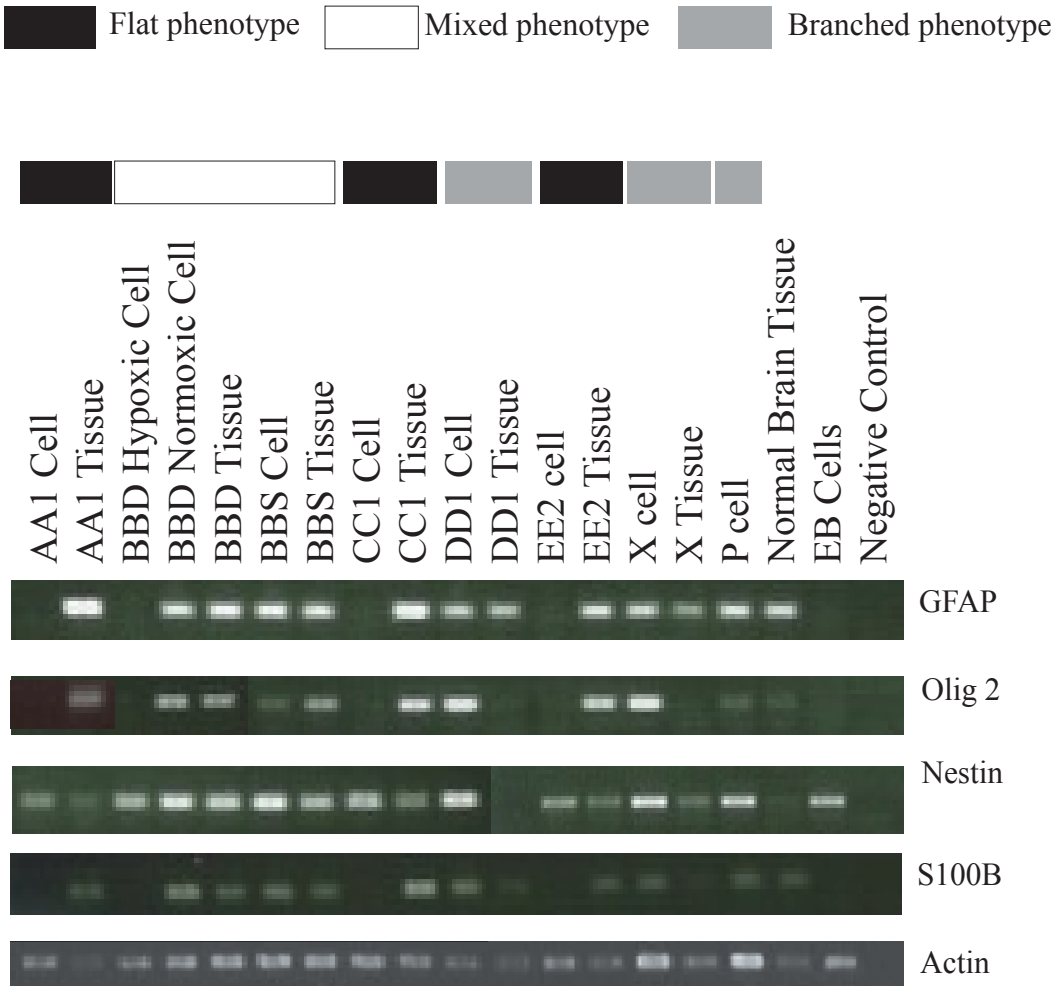

Figure 3.17 Densitometric analysis of RT-PCR products. After the PCR products were separated on a 1.6% agarose gel and visualised with ethidium bromide, images of the bands were captured in ultraviolet light. The bands were then analysed in Image J. For each experiment, actin was used as the control and the density of bands relating to expression of other genes of interest was determined as a ratio to actin. A minimum of 2 repeats was performed for each experiment and the standard deviation of the results determined. This is expressed in the Figure on each bar. The labels for each primary culture cell sample or tumour sample are derived from the abbreviation used to anonymise the samples. A primary culture and tissue sample labelled with the same abbreviation, e.g AA1, come from the same source tumour. Samples designated BBD and BBS were taken from deep and superficial parts of the same tumour, respectively. The key above the sample labels indicates whether the constituent cells in primary culture have a flat, branched or mixed phenotype. Normal brain tissue and embryonic stem cells (EB) were used as controls for differentiated and stem cell expression profiles, respectively. The primer was ommitted in the negative control. The histology of the tumours from which each primary culture was derived are listed in Table 3.1. The results indicate that the stem cell marker Nestin was present in both flat and branched primary cultures, suggesting that they both had stem-like characteristics. In contrast, the glial markers GFAP and Olig 2 were only expressed in the branched phenotype primary cultures, suggesting that these cells had glial-like function; the flat phenotype cells were therefore determined to have a mesenchymal-like function. Interestingly, the presence of Olig2 expression in tumours from which the flat phenotype cultures were derived, but not in tumours from which the branched phenotype cultures were derived, suggests that the flat phenotype cultures may have come from tumours with a more oligodendroglial lineage.

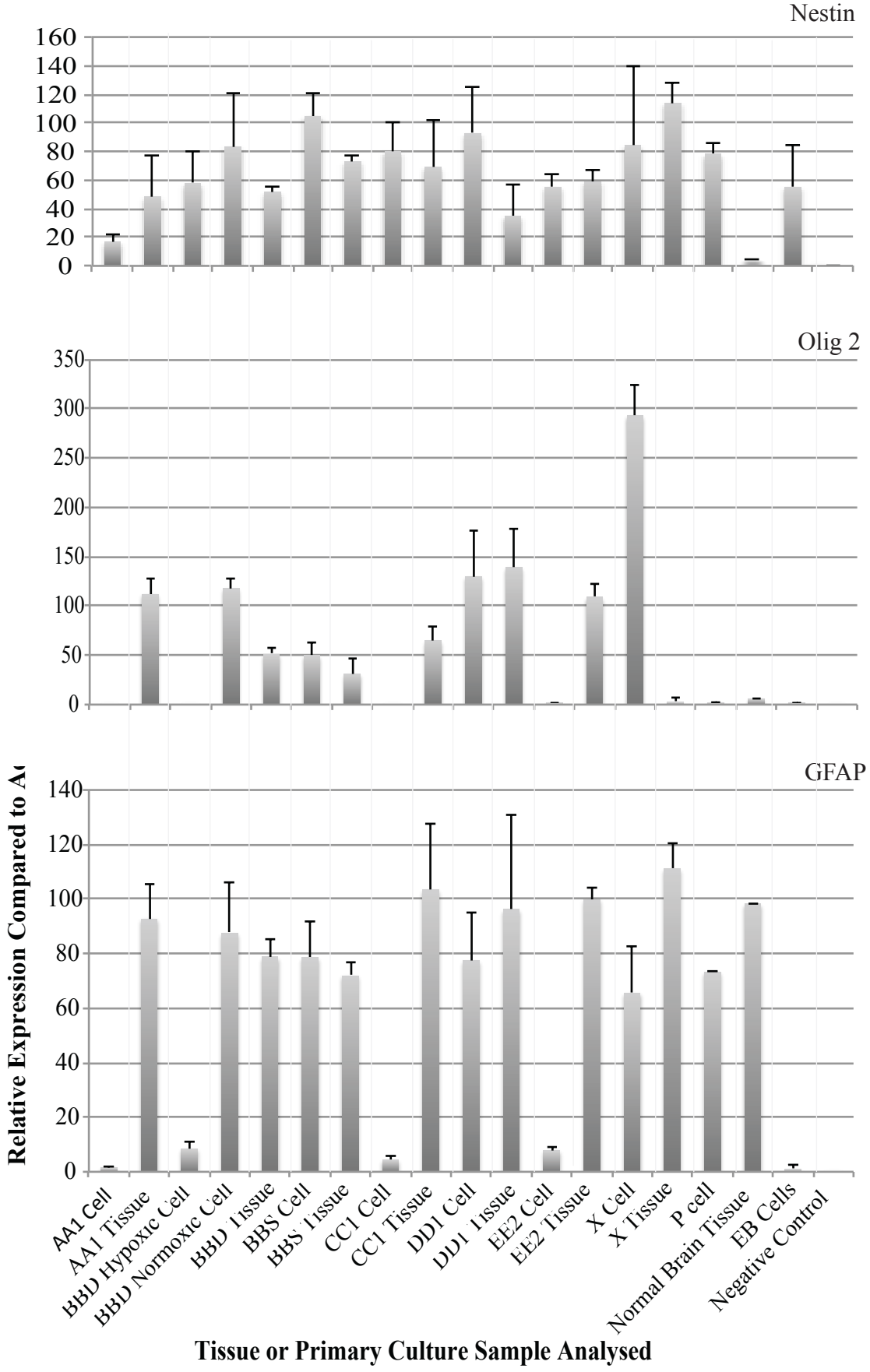
Nestin
160
140
120
100
80
60
40
20
0
Olig 2
350
300
250
200
150
100
50
0
GFAP
140
120
100
80
60
40
20
0
Relative Expression Compared to A
AA1 Cell
AA1 Tissue
BBD Hypoxic Cell
BBD Normoxic Cell
BBD Tissue
BBS Cell
BBS Tissue
CC1 Cell
CC1 Tissue
DD1 Cell
DD1 Tissue
EE2 Cell
EE2 Tissue
X Cell
X Tissue
P cell
Normal Brain Tissue
EB Cells
Negative Control
Tissue or Primary Culture Sample Analysed

In contrast, although *Olig2* expression was found in branched phenotype cultures it was generally not observed in the tumours from which these cultures had been derived (Figure 3.16). Since *Olig2* has a neural progenitor role, its increased expression in branched phenotype cultures in comparison to the parent tumours of these cultures could be interpreted as indicating that the cultures have been enriched for cells with stem-like characteristics [218]. In contrast, since *GFAP* is a marker of both differentiated astrocytes and progenitor cells it is perhaps not surprising that its expression is similar in both branched phenotype cell cultures and their parent tumours. This is because it is possible that in the tumour tissue *GFAP* antibodies stain differentiated cells, whereas in the primary culture the antibodies stain cells with stem-like characteristics.

Although neither *GFAP* nor *Olig2* expression was observed in flat phenotype primary cultures, both genes were expressed in the tumour tissue from which these cultures had been derived (Figure 3.16). This is consistent with the observation made in relation to the unsupervised clustering experiments that flat phenotype cells may not have been the dominant cell population in the tumours from which they were derived (Figure 3.15). Furthermore, the presence of *Olig2* gene expression in tumours from which the flat phenotype cultures were derived, but not in tumours from which the branched phenotype cultures were derived, suggests that the flat phenotype cultures may have come from tumours with a more oligodendroglial lineage (Figure 3.16). Gliomas with oligodendroglial features are often lower-grade tumours or secondary glioblastomas consistent with the observation that both these tumour types are often associated with flat phenotype cultures (Table 3.11). Branched phenotype cultures may in contrast have been derived from tumours with a more astrocytic lineage. The tumour designated as BB is a possible exception to this rule. Histologically this tumour was a GBM, but although some of the primary cultures derived from this tumour had a branched phenotype, the tumour itself expressed *Olig2*. This is contrary to the general observation I described previously in tumours from which other branched phenotype cultures were derived. It may

therefore be that the tumour designated as BB originated as a lower grade oligodendroglial tumour and subsequently underwent conversion to a higher-grade lesion.

Consistent with the mesenchymal-like functional annotation of the flat phenotype cells, the unsupervised clustering experiment described previously demonstrated that the Fibronectin gene, *FN1*, was the 156th most differentially expressed gene, based on fold change-differences, between the flat and branched phenotype cultures. This difference in expression was statistically significant (p=0.02). Fibronectin is a glycoprotein that mediates cell interactions with the extracellular matrix and whose expression is associated with cells of a mesenchymal phenotype [219].

Nestin is a neural stem cell marker that has also been identified in glioma stem-like cells [75, 180]. Using RT-PCR I identified *Nestin* gene expression in both branched and flat phenotype cultures and their respective parent tumours, similar to my findings in the immunofluorescence experiments described previously (Table 3.10, Figures 3.8). Within the limitations of non-quantitative PCR, expression of *Nestin* generally appeared to be greater in branched phenotype cells than in the tumours from which these cultures were derived (Figures 3.16 and 3.17). Since Nestin is a stem cell marker, this further supports the suggestion that the branched phenotype cultures are enriched for stem-like cells in comparison to the tumours from which they were derived.

3.6.2 Gene expression profiles correlate with prognostic classification

Glioma tissue DNA expression profiles have been previously sub-classified by Phillips and colleagues using unsupervised clustering into mesenchymal, proliferative and proneural types [177]. These subclasses have prognostic correlates, the most significant of which is that the mesenchymal profile is associated with the worst prognosis [177]. In addition, gliomas that recur after treatment tend to shift

their molecular profile toward the mesenchymal phenotype [177]. I wanted to establish whether the glial-like (branched phenotype cells) and mesenchymal-like (flat phenotype cells) gene expression clusters that I had identified might be similar to the subclasses in Phillips' study, and therefore perhaps have similar biological relevance. I examined whether there was a correlation between the genes characteristic of my own two subgroups and those in the subgroups in Phillips' study (Tables 3.14 and 3.15) [177]. Of note, in my own subgroup analysis I did not identify a correlate of the proliferative subgroup described in Phillips' study. This may be because of the small number of samples that I subjected to unsupervised clustering. However, it has also been recently suggested that the proneural and mesenchymal groups are actually the most important [220].

Approximately 8% of genes (26 of 340) occurred in both the gene expression profiles of my glial-like branched phenotype cell cultures and Phillips' proneural subgroup [177]. There was also a 7.6% (13 of 170) concordance between the genes expressed in my flat phenotype, mesenchymal-like cells and the genes in Phillips' mesenchymal subgroup. The actual correlation may be higher because there were some gene name incompatibilities between the data sets. Neither my glial-like nor mesenchymal-like gene sets overlapped with Phillips' proliferative subgroup. I also assessed the overlap in gene expression between my flat phenotype cells and Phillips proneural group, and between my branched phenotype cells and Phillip's mesenchymal group. Only 1 of 300 genes overlapped in these two comparisons. This suggests that my branched phenotype and flat phenotype cultures are correlates of the proneural and mesenchymal glioma subtypes, respectively, as described by Phillips. This further supports the functional annotation I described above suggesting that the branched phenotype and flat phenotype primary cultures had glial-like and mesenchymal-like gene expression profiles, respectively, because this is a similar functional annotation to that made by Phillips (Table 3.9, Figure 3.10) [177].

Table 3.14 A comparison of gene expression profile classifications. The genes characteristic of mesenchymal, proneural and proliferative subgroups of glioma from the study by Phillips and colleagues were compared with the gene expression profiles of my own glial-like and mesenchymal-like primary culture subgroups [177]. Using the R statistics package the number of times a gene occurred in the two gene sets under comparison was determined and expressed as a percentage of the total number of genes tested in that analysis. The table lists the number of genes overlapping in each comparison. The percentage of the total number of genes analysed that this represents appears in brackets. A more detailed breakdown of the genes that overlap in each comparison appears in Table 3.15. The results indicate that my glial-like and mesenchymal-like primary culture cells share gene expression profiles with the similarly named tumour classification by Phillips and colleagues.

Genes sets under comparison	**Overlap**
Proneural and Glial-like	27 (7.9%)
Mesenchymal and Mesenchymal-like	13 (7.6%)
Proliferative and Glial-like or Proliferative and Mesenchymal-like	0 (0%)
Proneural and Mesenchymal-like or Mesenchymal and Glial-like	1 (0.3%)

Table 3.15 A further comparison of gene expression profile classifications. The genes characteristic of mesenchymal (Mes), proneural (PN) and proliferative (Prolif) subgroups from Phillips' study were compared with the gene expression profiles of my own glial-like (GL) and mesenchymal-like (ML) subgroups [177]. Using the R statistics package the number of times a gene occurred in both datasets under comparison was determined (Table 3.14). Examples of the genes overlapping in each of these comparisons are listed in the table below. The gene datasets under comparison are referenced as 'Brennan' or 'Phillips' according to the abbreviations listed above.

Brennan ML	**Brennan GL**	**Brennan ML**	**Brennan GL**	**Brennan ML**	**Brennan GL**	**Phillips PN**
Phillips Mes	**Phillips PN**	**Philips Prolif**	**Philips Prolif**	**Phillips PN**	**Phillips Mes**	**Phillips Mes**
ACTN1	SOX8	None	None	NTN4	None	None
PAPPA	TTYH1					
MVP	OLIG2					
ITGA5	ASCL1					
RRAS	DLL3					
ACTA2	BCAN					
ANPEP	OLIG1					
MYL9	FXYD6					
PLAU	APOE					
SLC16A3	DLL1					
TAGLN	GRIA2					
	SCG3					
	SHD					
	GAD1					
	C19orf4					

However, whether the differences in functional annotation of my putative glioma stem-like cells reflect different cellular functions in vivo, or clinical outcomes, remains to be established. I will begin to address these questions in Chapter 4.

3.7 Assessment of primary culture tumourigenic potential

Through analysis of gene expression data and DNA copy number changes I have begun to assess the relationship of flat and branched phenotype cultures to the in vivo tumour environment sampled in glioma tissue biopsies. To further interrogate the biological relevance of the primary culture cells that I derived from human gliomas I next assessed whether they were able to form tumours in an in vivo xenotransplantation model.

Using CD 1 nude mice I first assessed the ability of 300,000 branched phenotype cells from the primary culture designated X (GBM) to form tumours subcutaneously (Figure 3.18). Cells were injected in one flank in each of two mice. The injection site was measured twice a week for two months, but no significant growth was observed over this time (Figure 3.18). At the end of the experiment the residual subcutaneous lump was excised and examined histologically (Figure 3.18). The tumour cells identified within the excised tissue predominantly localised in small spherical clumps within the subcutaneous tissue. Histologically, these collections of cells were surrounded by an infiltrate that appeared inflammatory, suggesting granuloma formation. Unfortunately, the excised lumps were too small to allow serial sectioning and Immunohistochemical analysis of the cellular constituents. Nevertheless, the implication was that the residual immune function of the mice might have been sufficient to prevent tumour growth.

I reasoned that grafting the primary culture cells orthotopically rather than heterotopically might be more successful. One hundred thousand cells from each of

Figure 3.18 A xenotransplantation assay of glioma stem-like cell tumourgenicity. (A) CD 1 nude mice were injected subcutaneously with 300,000 cells from the culture designated 'X' (GBM). The subcutaneous lump was measured in two planes twice a week to calculate volume, which is plotted against time. The graph, which is representative of the two mice in which the experiment was performed, illustrates that the cells failed to proliferate. After two months, mice were sacrificed. The remnant of the lump was excised and fixed in 2% paraformaldehyde. (B) Tissue sections were stained with haematoxylin and eosin; the scale bar indicates 100 microns. The representative images illustrate nests of cells in the subcutaneous tissue (left panel) and an infiltrate that appears inflammatory (right panel) suggesting that the residual immune system in the CD1 nude mice was sufficient to prevent proliferation of the putative stem-like cells. In a second set of experiments, 100,000 of my putative glioma stem-like cells from 4 different primary cultures (X (GBM), P (GBM), DD1 (Gliosarcoma) and CC1 (Anaplastic oligodendroglioma)) were each injected stereotactically into the striatum of four CD 1 nude mice by Dr Lesley Gilmour, Beatson Institute, Glasgow. (C) The mice were anaesthetised and subjected to cranial magnetic resonance imaging at 13 and 20 weeks post xenotransplantation to assess for tumour growth. The representative coronal cranial MRI image at 20 weeks illustrates no evidence of tumour formation, but persistence of the injection track and evidence of dural thickening at the site of injection.

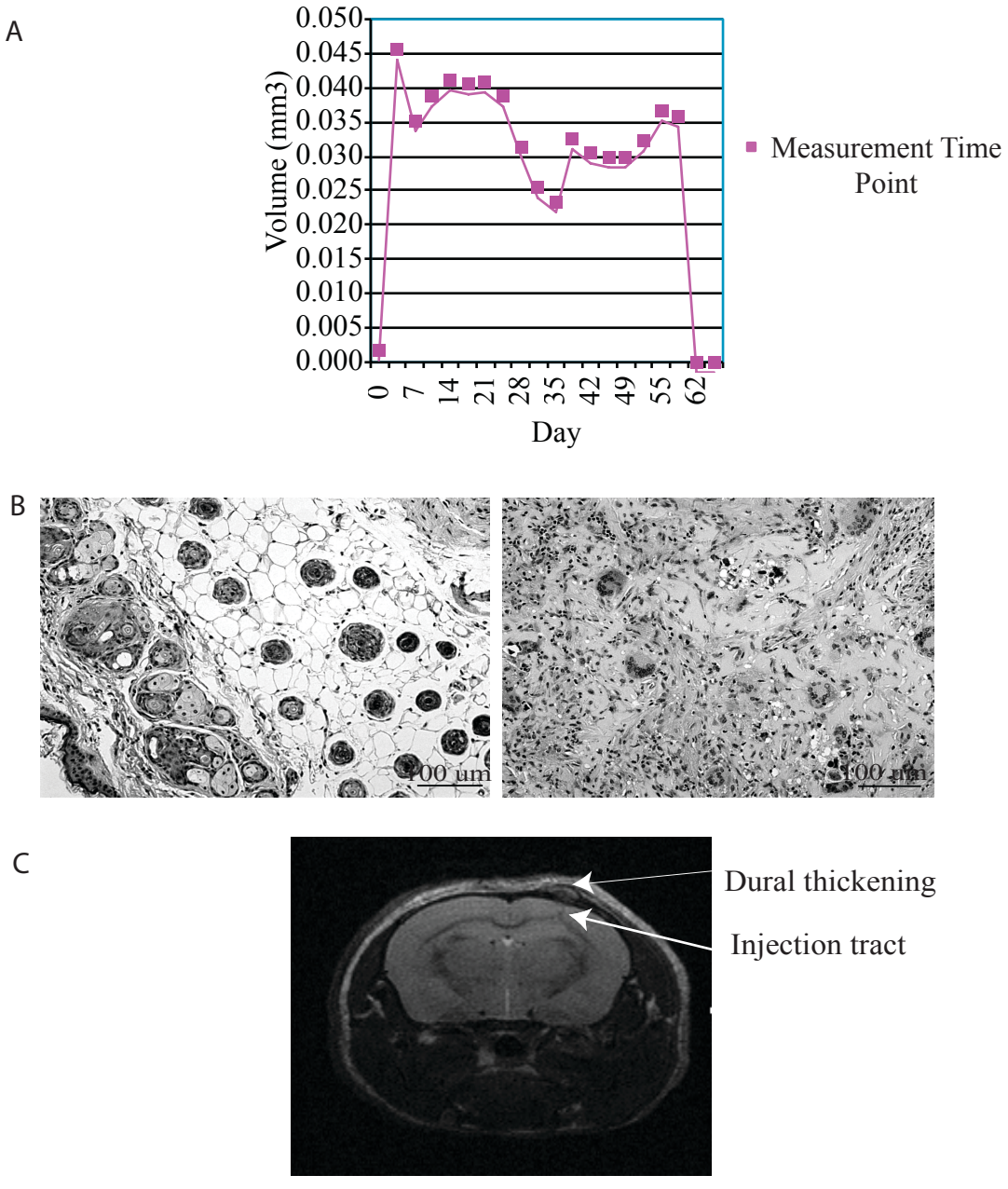

four different glioma primary cultures designated X (GBM), P (GBM), DD1 (Gliosarcoma) and CC1 (Anaplastic oligodendroglioma) were therefore injected orthotopically into the striatum of CD 1 nude mice using a stereotactic rig, in collaboration with the Beatson Institute, Glasgow. Four replicate mice were injected for each primary culture tested. The brains of each mouse were imaged with MRI, using gadolinium contrast, at 13 and 20 weeks post injection. Unfortunately, there was no evidence of tumour growth at either time point in any of the animals imaged. Twenty weeks post-transplantation all mice were sacrificed.

An illustrative coronal image from a mouse 20 weeks post-injection of cells illustrates that the injection tract was still visible (Figure 3.18). There was evidence of a small dural thickening at the proximal part of the tract, but no tumour was visible. An attempt was made post-mortem to harvest the dura located superficial to the site of primary culture cell injection. However, because of the small size of the lesions it was not possible to identify them macroscopically. It is possible that this thickening represented retrograde migration of the implanted cells, explaining the lack of intracerebral tumour growth. Alternatively, the thickening may simply have been a consequence of repair of the dural puncture wound at the site of the striatal injection. At post mortem animal brains were subjected to serial sectioning and histological analysis by a veterinary neuropathologist, but no evidence of tumour growth was found. Unfortunately, I did not have the time to repeat these xenotransplantation experiments in more immune supressed NOD-SCID mice. As I will discuss, the immune status of the mice may have an impact on the growth of transplanted tumour cells.

3.8 Discussion

Glioma stem-like cells are proposed to be a subpopulation of cells within glioma responsible for tumour initiation and for recurrence after treatment, because they are

resistant to current therapies [75, 125]. I grew glioma-derived primary cultures from single cell suspensions of patient-derived tumours. The aim of the work presented in this Chapter was to develop a reliable protocol for the enrichment and expansion of putative glioma stem-like cells from human gliomas. My success rate at deriving primary cultures from a tumour sample was better than the approximately 50% rate previously reported [65-67]. My unique access as a neurosurgeon to fresh patient tissue allowed me to collect a substantial number of tumour samples in order to optimise my technique and to achieve this.

3.8.1 Glioma primary cultures

I initially attempted to enrich glioma stem-like cells from fresh human glioma tissue using a method developed from an amalgamation of relevant techniques in the published literature [65-67, 97]. These techniques were themselves derived from experience of culturing neural stem cells, to which glioma stem-like cells are thought to have similarities. Central to this method is that serum-free culture media is supplemented with bFGF and EGF in order to maintain the glioma-derived cells in a stem-like state [66, 67]. Under these conditions differentiated cells from the parent glioma do not form glioma-derived spheres and so can be separated out [66, 67]. With this strategy I was able to generate glioma-derived spheres from human glioma tissue, similar to neurospheres that can be grown from neural stem cells under similar conditions. However, I was not able to grow these cells for more than a few passages and in fact other groups have reported similar difficulties to my own in trying to serially passage glioma-derived spheres in serum-free culture conditions [65-67, 97].

The expectation that glioma stem-like cells should be passaged as glioma-derived spheres arises from the analogy that is made between glioma stem-like cells and neural stem cells [65-67, 97]. However, much of the neural stem cell literature is actually derived from observations in mice and so one reason for the difficulty passaging glioma stem-like cells as spheres may simply be that although the cells are

neural stem cell-like, human neural stem cells actually expand more slowly in vitro than their mouse counterparts [65-67, 97]. An alternative explanation is that unlike true neural stem cells the majority of cells in the glioma primary cultures are actually short-lived progenitor cells [67]. Even a small proportion of more lineage-restricted cells in glioma-derived spheres might impair their replicative capacity in vitro [99]. Spontaneous differentiation and apoptosis of cells in glioma-derived spheres could also limit the ability to passage them [65-67, 97].

To overcome the limitations of suspension culture observed with my putative glioma stem-like cells I tried a strategy of propagating the cells in adherent culture. Such an approach to expanding putative glioma stem-like cells is actually now favoured in the literature, probably because it has been suggested that glioma primary culture cells grown in adherent culture maintain their stem-like status better than those grown in suspension culture as glioma-derived spheres [65, 67]. At the time I developed this protocol though, the concept of adherent culture of glioma stem-like cells ran counter to the prevailing view that non-adherent growth as glioma-derived spheres was the method of choice [65-67, 221].

I identified that a growth factor-reduced Matrigel substrate was optimal for culture of glioma-derived stem-like cells. Other researchers have favoured a laminin substrate for this purpose and indeed laminin is a key component of Matrigel [65, 67]. My own observation was that cells grown on a laminin substrate proliferated as semi-adherent glioma-derived spheres, in contrast to Matrigel where the cells grew as an adherent monolayer. It is possible that there is a concentration of laminin at which my cells would also have grown as an adherent layer and this would be an area for future study; in my experiments I used the concentration of laminin described in the literature, but this could be optimised for my own putative stem-like cells [65, 67]. The use of a laminin substrate might also be a useful strategy to overcome the difficulty that I had differentiating my glioma-derived cells. During my differentiation experiments on Matrigel-coated coverslips the cells became non-

adherent when EGF and bFGF growth factors were removed from the culture media. In contrast, those who have reported successful differentiation of glioma stem-like cells in the literature have generally performed these experiments on laminin-coated slides, principally because this is how neural stem cells are differentiated [65, 67].

Based on the morphological appearance of the putative glioma stem-like cells that I was able to grow in adherent culture I identified two distinct cell phenotypes that I refer to as branched phenotype and flat phenotype cultures. This contrasts with the majority of the existing glioma stem-like cell literature that has described only one type of glioma stem-like cell, which has a radial glial-like phenotype [65-67]. My experimental observations suggested that the branched phenotype cells were most similar to this previously described radial glial-like cell phenotype and so could be called putative glioma stem-like cells [65-67]. I will discuss the characteristics and possible aetiology of the flat phenotype cells below. The flat phenotype cultures were most often derived from lower-grade or secondary gliomas, whereas branched phenotype cultures were generally related to glioblastomas. Lower-grade gliomas have dysregulation of different molecular pathways compared to their higher-grade counterparts and this may therefore indicate that the tumour-initiating cell is different in different grades of glioma, consistent with the observation of the two different primary culture cell phenotypes [15, 19, 21, 222].

Having developed a technique for the reliable culture of glioma stem-like cells from human glioma tissue, I began to characterise the stem like features of the cells. For example, single glioma stem-like cells are reported to be able to form colonies in suspension and this characteristic is referred to as clonogenicity [65, 67]. On removal of the Matrigel substrate from culture flasks, cells from many of the primary cultures were observed to re-form glioma-derived spheres. By plating the cells at increasing dilutions in 96 well plates I was able to confirm by serial microscopic observation that these cells grew into glioma-derived spheres clonally and not through cell clumping. However, not all the cultures were observed to behave in the same way.

Although all the primary cultures had been derived as glioma-derived spheres that were then plated onto Matrigel-coated substrate, cultures that contained the flat phenotype cells did not form non-adherent glioma-derived spheres once the substrate was removed. Based on what is known of neurosphere formation in neural stem cells, this suggests that these cultures did not contain cells with neural stem-like characteristics [3, 66, 88]. Cells without stem-like or progenitor-like features have more restricted self-renewal capacity and lineage potential, and so tend to adhere to the plastic of the culture dish, differentiate and cease to proliferate [3, 66, 67]. Variation in the frequency of glioma-derived sphere formation between different glioma primary cultures has in fact previously been reported and it was proposed that the colony forming ability of glioma stem-like cells was greatest in higher-grade tumours [61, 75]. In this Chapter I have demonstrated that cell phenotype was predictive of colony forming ability in my own putative glioma stem-like cells. Although, I did not observe a clear relationship between primary culture cell phenotype and the histological grade of the tumour from which it was derived, flat phenotype cells, and therefore poor colony forming ability, were more often associated with lower grade tumours, consistent with the studies referred to above [61, 75]. The relationship between tumour histology and cell phenotype is an important area for future study and will depend particularly on my ability to derive putative glioma stem-like cells from low-grade gliomas. Low-grade tumours are less often managed surgically than high-grade tumours, making them less available to culture.

It is important to note that the formation of glioma-derived spheres does not itself actually prove the existence of stem-like cells, because transiently amplifying precursors are known to also produce neurospheres [66]. Even within neural stem cell-derived neurospheres originating from normal brain tissue, only approximately 1% of cells is actually stem cells with the ability to self-renew and generate all neural lineages [85, 89]. I therefore needed a strategy to further characterise the stem-like features of the cells within the primary cultures that I had derived.

To begin to address this question I asked whether it was possible to further enrich the stem-like cells from within the heterogeneous primary cultures that I had observed. I adopted a strategy well described in the glioma stem-like cell literature of using expression of the marker CD133 to define the target stem-like cell population [3]. I observed that when my heterogeneous primary cell culture populations were separated into two fractions based on expression or absence of expression of CD133, the cells in the positive fraction rapidly became less pure for CD133 expression over just two passages. The CD133 negative population remained CD133 negative. I would postulate that had the original CD133-positive cell population been cultured for a longer period, then the proportion of CD133-positive cells in the 'CD133 positive culture' may have actually dropped even lower, to a level similar to the proportion observed in the first round of cell sorting. This observation could be interpreted as suggesting that CD133-positive cells are more stem-like than CD133-negative cells and are able to asymmetrically divide into CD133-negative and CD133-positive cells [99]. In contrast, CD133-negative cells appear unable to generate CD133-positive cells as they proliferate. An alternative explanation is that there is a technical element to these observations. For example, the CD133 antigen might be subject to degradation or loss during cell passage or flow cytometry. A more thorough examination of this question would be a valuable topic for future research. Interestingly though, it has now been demonstrated that both the CD133 positive and CD133 negative fractions of cells are tumourigenic in a xenotransplantation model, so separating cells by their CD133 expression may no longer be desirable [106]. For the purposes of my own study it was clear that if a population of CD133 positive cells could not be maintained in their CD133 positive state over several passages then it was going to be difficult to utilise these cells for further experiments. I therefore made the decision not to sort the cells for CD133 expression. In Chapter 1 I reviewed the evidence for employing antigens other than CD133 in glioma stem-like cell purification, but concluded that none had compelling evidence for their use. I therefore decided that I would perform the remainder of my investigations on the heterogeneous cell population within each unsorted glioma

primary culture. This transpires to have been a valuable decision because it probably allowed me to avoid screening out the flat phenotype cells from the primary cultures, as I will discuss below.

Other strategies that have been used to distinguish between stem-like and transit amplifying-like cells in glioma-derived spheres or primary cultures are self-renewal capacity, multipotency and tumourigenicity in vivo [58, 60][65-67]. I therefore next assessed my own primary culture cells using these same criteria.

In terms of self-renewal, I demonstrated that although the branched phenotype radial glial-like cells appeared to proliferate indefinitely, the flat phenotype cells underwent senescence after less than 10 passages and stopped proliferating. Combined with evidence reviewed above that the same flat phenotype cells failed to demonstrate clonogenicity in a substrate-free culture, this suggests that either these cells are not neural stem-like or that the culture conditions were not optimised for their growth. As I will discuss below, these cells transpired to have a mesenchymal-like gene expression profile and it is certainly the case that the culture conditions were not optimised for proliferation of mesenchymal-like stem-like cells. Optimisation of the culture conditions to attempt to facilitate the indefinite proliferation of the flat phenotype cells is therefore a key area for future research, and this would probably begin with reference to the culture technique for mesenchymal stem cells [223].

3.8.1.1 Multipotency

Multipotency describes the ability of stem-like cells to be differentiated down multiple lineages. Since neural stem cells can be differentiated into neurons, astrocytes or oligodendrocytes, the same ability has been sought in glioma stem-like cells [65, 67]. Conversely, prior to differentiation, glioma stem-like cells should be characterised by expression of stem cell markers, such as Nestin, an intermediate filament protein that is expressed during development in neuroepithelial precursor

cells and radial glial cells and that is downregulated with differentiation, but re-expressed by reactive astrocytes [90, 91, 180-182].

Pollard and colleagues in their original paper on the derivation of glioma stem-like cells in adherent culture observed that when these cells were maintained in culture conditions containing the growth factors bFGF and EGF they did not express markers of either neuronal or oligodendroglial differentiation [66, 67]; Pollard does not give any details of the expression of the astrocytic marker GFAP by cells in this undifferentiated state [66, 67]. In contrast, Al-Mayhani and colleagues, who also described a protocol for culturing stem-like cells from glioma, demonstrated that the oligodendroglial markers NG2 and Olig2 were both present in cultures before withdrawal of growth factors and actually reduced on removal of the mitogens [65]. A third group, Galli and colleagues, observed that both GFAP (21-60%) and β-III tubulin (5.5-21%) staining was observed in their glioma-derived stem-like cells on removal of growth factors [42]. Galli also observed that some cells double-stained with both GFAP and β-III tubulin, which they conclude reflected activation of an aberrant differentiation programme [42]; I observed this same phenomenon in a proportion of my branched phenotype cultures, but not the flat phenotype cultures.

These often conflicting acounts of stem-like and differentiation marker expression in glioma stem-like cells reported in the literature suggests that the actual stem-like status of glioma stem-like cells is not yet fully understood [65-67]. Indeed, I also observed heterogeneity in the expression of stem-like markers in general between my different primary cell cultures. Importantly though, expression of some stem-like markers, such as Nestin, was observed in both my flat and branched phenotype cells, suporting the proposition that both are putative glioma stem-like cells, although it has also been suggested that the regulation of *Nestin* expression in glioma-derived cells may be dysfunctional and therefore not actually representative of a stem-cell like function [65-67].

It may be the case that the actual stem-like phenotype of glioma stem-like cells varies according to the pathology of the tumour from which the cells are derived, reflecting differences in the biological behaviour of these tumours. This is an important topic area for study, because it may have implications for treatment strategies. By expanding primary cultures from a spectrum of human gliomas I have positioned myself well to be able to conduct this work.

Although there were some similarities in stem-like marker expression between my primary culture flat and branched phenotype cells, there were nevertheless also some differences. This was the case even where the flat and branched phenotype cells were both derived from the same individual glioma tumour. This therefore suggests that the different cell phenotypes might be functionally different or might even be related to different cell lineages. This does not however exclude them both having stem-like features or having a shared lineage from a more primitive stem-like cell, as I discuss below. The hypothesis that flat and branched phenotype cells may have different functional characteristics was subsequently supported by the gene expression data that I have presented and I will discuss the implications of this in more detail below.

In order to further interrogate the multipotency of my putative glioma stem-like cells I attempted to differentiate them into neuronal, astrocytic and oligodendroglial lineages. Unfortunately, I observed that in the absence of EGF and bFGF growth factors the cells died before the effects of differentiation could be fully assessed. Contrasting my technique for the differentiation of putative glioma stem-like cells with that of the published literature at the time, the principal difference is that my cells were grown on Matrigel rather than laminin [65-67]. Conversely, my cells only partially adhered to plasticware coated with laminin. A key future experiment would therefore be to optimse the concentration of laminin substrate on which my cells were plated such that they remain adherent and I can then attempt to differentiate them as has been previously been described [65-67].

I nevertheless was able to observe in most branched phenotype cultures examined that in response to BMP-4 or serum the cells took on an astrocytic rather than radial-glilal appearance, and expression of GFAP increased. This is consistent with reports that the majority of so-called glioma stem-like cells are actually quite lineage restricted to astrocytic differentiation and only rarely do cells in any individual culture express markers of neuronal or oligodendroglial differentiation [65-67]. Flat phenotype cells did not appear to undergo neural cell lineage differentiation. I will discuss below that these cells actually have a mesenchymal-like rather than glial-like gene expression profile and so the experiment that needs to be done is to attempt to differentiate these cells down mesenchymal lineage. This is a key piece of future work. Interestingly though, whilst the flat phenotype cells themselves did not appear to undergo any neural stem cell-like differentiation, the addition of differentiation media to these primary cultures was associated with the rare appearance of cells lying on the surface of the flat phenotype cells that expressed glial or neuronal markers. Since it was not possible to interrogate this observation in detail, for the reasons of cell death that I described above, I have not been able to establish whether these cells were derived from flat phenotype cells themselves or whether their origin was from a different cell type that had been co-cultured with the flat phenotype cells. I did attempt to co-culture the flat phenotype cells with primary human neurons to ask whether there was any glial-neuronal interaction that would give insight into the role of these flat phenotype cells. Unfortunately though, the inevtiable technical difficulties inherent in such an experiment were not overcome in the single trial of this experiment that I was able to perform. This would nevertheless be an interesting assay to optimise and explore in further detail in the future.

Although my immmunofluorescence data has not permited me to make a systematic analysis of the multi-lineage potential of my putative glioma stem-like cells and to conclusively describe the stem cell characteristics of these primary culture cells, I did demonstrate an increased expression of key stem cell genes in the gene expression

analayis that I subsequently performed, as I will discuss below. This supports the designation of my primary culture cells as putative stem-like cells.

3.8.1.2 Tumourgenicity

I next assayed the stem-like characteristics of my putative glioma primary culture cells by their ability to form tumours in an in vivo xenotransplantation model [65-67]. Cells were first injected subcutaneously into CD 1 nude mice. Over the time course of the experiment there was no evidence of tumour growth in the mice tested. The limited histological analysis that was possible, because of the small size of the tissue samples, suggested that there was an inflammatory infiltrate around the implanted cells. This granuloma formation may therefore have restricted development of a tumour.

In collaboration with researchers at the Beatson Institute in Glasgow I next injected putative glioma stem-like cells into the striatum of CD 1 nude mice. The rationale for this experiment was that the mouse brain microenvironment would be more conducive to glioma formation than subcutaneous tissue. Mice were followed up over twenty weeks with serial imaging, but no evidence of tumour formation was observed. All the mice were then sacrificed and their brains subjected to serial sectioning for histological analysis by a veterinary neuropathologist, but again, no evidence of tumour growth was found. It is possible that tumours may have been missed with this sectioning technique, because some studies have reported that tumour growth in glioma stem-like cell xenotransplantation models can be as little as 2.7mm even after 20 weeks [224]. It is also possible that the implanted primary culture cells simply needed longer to develop into a macroscopic tumour; for example, one group has shown that tumours in a similar model were only apparent after 18 months [176]. However, other groups have observed tumour formation in glioma-stem like cell xenotransplantation models within 20 weeks [65, 67].

The failure of my own in vivo experiments may indicate that the mice were not sufficiently immune compromised to prevent an immune reaction to the implanted cells. In fact, most of the glioma xenotransplantation experiments described previously have used more profoundly immunosuppressed mice than the CD 1 nude mice used in this experiment, including NOD-SCID mice, SCID/bg mice and NMRI nu/nu mice [65, 67]. Unfortunately, I did not have the time to repeat these xenotransplantation experiments in NOD-SCID mice, but this would be an important experiment for future study. However, the failure of my primary culture cells to grow in an in vivo xenotransplantation model does not necessarily undermine their putative glioma stem-like cell characteristics. As I will discuss below, the primary cultures retained genetic features of the tumours from which they were derived, supporting their use as a biologically relevant model.

3.8.2 Gene expression profiling of putative glioma stem-like cells

The flat phenotype cells that I have identified in some glioma primary cultures have not previously been described in the majority of the glioma stem-like cell literature [65-67]. Both the branched and flat phenotype cells were enriched from human tumours in media known to support growth of neural stem cells rather than differentiated, post-mitotic cells. I have detailed how the branched phenotype cells are very similar to the radial glial-like glioma stem-like cells described in the existing literature [65, 67]. However, it was possible that the flat phenotype cells may actually have been derived from non-tumour cells. I therefore performed DNA copy number analysis to ascertain the relationship between the primary culture cells, the tumour samples from which they had been derived and matched patient blood.

This copy number analysis demonstrated that the genome of the flat phenotype cells did contain a few tumour-specific changes not present in the patient's somatic genome, suggesting that the cells were derived from a tumour cell. This nevertheless contrasted with the observation that most if not all DNA copy number changes found

in the glioma tissue from which branched phenotype cultures were derived were also present in the branched phenotype cultures themselves. This suggested that branched phenotype cells, but not flat phenotype cells, were derived from cells with a similar mutational lineage to the cells that constituted the bulk of the glioma tumour, consistent with the hierarchical model of glioma described earlier [214]. Importantly, where flat and branched phenotype primary culture cells were derived from the same glioma I observed that they each had different DNA copy number change profiles, indicating that they were distinct cell types.

The observation that the flat phenotype cell genomes contained fewer tumour-associated mutations than the tumours from which they had been derived indicated that there was at least one other cell type within these tumours that was responsible for the observed DNA copy number profile of the tumour itself. Where both branched and flat phenotype cell primary cultures were derived from the same primary tumour then this 'second' cell type was plausibly the branched phenotype cell. However, sometimes only flat phenotype cells were derived from multiple biopsies taken from the same glioma. This may indicate that the flat phenotype cells can produce more differentiated progeny that accumulate additional mutations, but that are not enriched in culture conditions that support stem-like cells. One way to begin to address this question in future would be to better trace the lineage relationship of the flat phenotype cells to the other cells in the tumours from which they were derived. Since the flat phenotype cells only contained a few DNA copy number changes on array CGH analysis, it would be useful to adopt an approach that interrogated the genome in more detail to ascertain whether there are smaller mutations, not evident as copy number changes, that are present in the flat phenotype cells and the tumour from which they have been derived. One strategy to achieve this would be to use a more probe rich array CGH chip that would be able to detect smaller copy number changes. Another approach would be to use a single-nucleotide polymorphism technique where DNA sequence variation at a single nucleotide can be compared between samples [225]. This genetic analysis might help identify a cell

surface antigen on the flat phenotype cells that would then permit similar cells to be enriched from within the tumour tissue itself with a FACS technique to help determine the cellular origin of the flat phenotype cells themselves.

In trying to interrogate the lineage relationship of the flat phenotype cells in order to understand their role in glioma development, it was interesting to observe that the gene expression profile of tumour tissue from the glioma designated CC (Anaplastic oligodendroglioma) clustered closer to the profile of primary cultures with branched phenotype cells than to that of the flat phenotype cells in primary cultures CCN and CCH that were derived from tumour CC itself. Further analysis is needed to establish whether this observation is replicated in other primary cultures and to understand its significance, but it might confirm, as I suggested above, that the flat phenotype cells account for only a small proportion of cells in the tumours from which these cultures have been derived. If this is the case then I need in future to understand why only flat phenotype cells grow with my primary culture technique from some tumours in which there must be other tumour-derived cell types; the stem-like characteristics of the flat phenotype cells may explain this. However, if the dominant cell type in these tumours was actually a branched phenotype-like cell, why did these not grow in the primary cultures? Since the flat phenotype cells tended to come from low-grade tumours and it is known that low-grade tumours generally have different genetic mutations when compared to high-grade tumours, this may be one possible explanation worthy of investigation [140]. An alternative explanation, as I have already suggested, is that flat phenotype cells are precursors of the less stem-like cells that form the tumour bulk.

An insight into whether or not there was such a lineage relationship between flat and branched phenotype cells came from analysis of the DNA copy number changes common to both EE1 and EE2 tissue samples and to the branched (EE1) and flat (EE2) phenotype primary cultures derived from these different biopsies of the oligodendroglioma designated EE. The tumour-associated mutations observed in

both these primary cultures suggested that there may be a lineage relationship between these two cell populations and it is possible that these two cell phenotypes represent clones from different phases in the tumour's evolution [67]; I made no observations during my in vitro work to suggest that flat phenotype cells could actually be driven to develop into branched phenotype cells, or vice versa.

Interestingly, however, although the two tissue samples from the tumour designated EE shared some non-somatic DNA copy number changes, there was also some intra-tumoural copy number heterogeneity. These genetic differences may be responsible for determining the different primary culture cell phenotypes observed. Regions of intra-tumoural genetic heterogeneity have recently been described in relation to tyrosine kinase gene expression in glioma [25, 226]. However, the relationship that I have observed between tumour tissue heterogeneity and primary culture heterogeneity has not been previously described. It requires further investigation, not least to examine whether similar findings can be replicated in other sets of tumour samples and associated primary cultures. I will discuss possible cellular aetiologies of the flat and branched phenotype cells below.

3.8.3 Gene expression and functional annotation of putative stem-like cells

The evidence that I have presented led me to the conclusion that rather than there existing a single universal type of glioma stem-like cell, there are in fact two distinct types of stem-like cell that may be enriched from gliomas under neural stem cell-like growth conditions. These distinct cell types may have different biological functions and cellular origins. If this were the case then it would have significant implications for our understanding of glioma initiation and therefore also for the development of effective treatment strategies; I discuss this in Chapter 4 when I describe the utilisation of these primary cultures for an in vitro model to assess the efficacy of potential inhibitor compounds. To understand the functional roles of the flat and branched phenotype cells I next explored their gene expression profiles.

Unsupervised clustering of gene expression profiles from several different primary cultures identified two different groups that were each characterised by either flat or branched phenotype cells. This therefore supported all the other data that I have presented indicating that flat and branched phenotype cells were different from each other and not just variations of a single cell type. Functional annotation of the gene expression profiles of the two primary culture cell phenotypes, supported by subsequent confirmation of gene expression with Real Time PCR, indicated that the flat phenotype cells had a mesenchymal-like profile whilst the branched phenotype cells had a glial-like profile. I demonstrated that the gene expression profiles of my in vitro primary cultures correlated with the work of Phillips and colleagues who described subtypes of glioma tumour tissue that have implications for treatment efficacy and prognosis [177]. Further work is needed to establish whether these same clinical correlates can be made with my in vitro samples. In particular, I need to examine whether the mesenchymal-like flat phenotype cells are derived from tumours or tumour regions with a mesenchymal-like profile. The single assessment of this that I have made so far indicates that this may not be the case. When I compared the gene expression profile of the primary culture designated CC1 with that of the anaplastic oligodendroglioma tissue from which it was derived, I observed that the CC1 flat phenotype, mesenchymal-like, primary culture was actually derived from a tumour with a predominantly branched phenotype-like, glial-like expression profile. This suggests that I may not find a similar correlation as Phillips between clinical outcome data and in vitro cell phenotype. Interestingly though, Phillips' study relied on single biopsies taken from each tumour, but it has been clearly demonstrated that such biopsies may not be representative of the tumour as a whole [25, 177, 226]; the evidence from my own primary culture analyses suggesting that primary cultures derived from different regions of the same tumour can have different cell phenotypes, which in turn may have differing functions, supports the existence of intra-tumoural heterogeneity.

3.8.4 The role of flat phenotype cells in glioma cell biology

Although the majority of glioma stem-like cells described in the existing literature are similar to my branched phenotype cells, heterogeneity in the phenotype, growth rates and major histocompatibility complex class II proteins profile of glioma stem-like cells has been reported [66, 98, 227]. Nevertheless, the heterogeneity that has been reported has not in general included primary culture cells similar to the flat phenotype cells that I have described. There are actually a number of reasons why primary culture cells akin to my flat phenotype cells may not have been described previously. For example, it may be that flat phenotype cells have been disregarded because of their mesenchymal-like appearance. Also, my identification of flat phenotype cells was facilitated by access to multiple primary cultures derived from different tissue samples taken from the same glioma. Most non-neurosurgeons would have more limited access to glioma tissue, especially to the low-grade tumours from which I observed flat phenotype cells were most often derived. Another explanation is that flat phenotype cells may have previously been inadvertently removed from glioma primary cultures. This is because previous studies have often employed cell sorting techniques, for example using the CD133 antigen, in an attempt to enrich their primary cultures for glioma stem-like cells [97]. I observed that the CD133 gene *Prominin 1* was expressed in branched phenotype but not flat phenotype cells ($p=0.035$), so flow cytometric sorting of cultures would have discarded the flat phenotype cell population.

My analysis of the glioma stem cell literature has nevertheless identified two studies that describe cells with similar characteristics to my flat phenotype cells [227, 228]. Functional annotation of the gene expression profile of my flat phenotype cells suggested they were mesenchymal-like and in fact the two studies that I will review also refer to cells that are mesenchymal-like.

In the first study, primary cultures were derived from human gliomas using a glioma-derived sphere-based technique [227]. Two distinct cell types were identified in these cultures, one with a 'neural developmental' expression profile and the other with a 'restricted' stem-like phenotype associated with mesenchymal features [227]. Interestingly, in contrast to my own observations, this study found no consistent differences in the proliferation rates of the two cell types in vitro; I observed that the flat phenotype cells proliferated more slowly than the branched phenotype cells and were not immortal. However, in similarity to my flat phenotype cells, these mesenchymal-like cells were less clonogenic than the 'neural developmental' cells and also less tumourigenic and infiltrative in a NMRI-*nu*/*nu* mice model [227].

In the second study, published in 2012, primary cultures were derived from sets of two tissue samples taken from each glioma assessed [228]. Cultures derived from biopsies taken from the tumour centre were described as spindle shaped glioma stem-like cells, similar to my branched phenotype cells. In contrast, cultures derived from biopsies taken from the tumour periphery were said to be characteristic of cancer-associated fibroblasts, because of their mesenchymal-like appearance; in my own experiments I did not observe a relationship between tumour biopsy position and the resultant primary culture cell phenotype, principally because the tumours themselves are heterogeneous in shape. The mesenchymal-like cells described in this study could only be maintained below ten passages in vitro, they had a normal DNA copy number change profile and did not form tumours in vivo, all of which characteristics are similar to my flat phenotype cells [228]. Unfortunately, these investigators did not compare the primary culture DNA copy number profile to that of the tumour from which the primary culture was derived, so may have overlooked the small frequency short copy number changes that I have described in my flat phenotype cells [228].

There are certainly similarities between the flat phenotypes cells that I have described and the mesenchymal-like cells described in both these studies [227, 228].

Interestingly, one of the studies suggests that the mesenchymal-like cells may be a glioma stem-like cell variant whilst the other concludes that they are cancer associated fibroblast-like cells [227, 228]. I will therefore now discuss the possible origins of my own flat phenotype cells.

3.8.5 Probing the origin of flat phenotype primary culture cells

The evidence that I have presented in this Chapter suggests that flat phenotype cells are tumour-derived, have a mesenchymal-like gene expression profile and stem-like properties. I have already discussed that glioma stem-like cells similar to these have only twice been reported in the literature [227, 228]. However, actual mesenchymal differentiation of glioma stem-like cells has in fact previously been described in an in vivo xenotransplantation model [222, 227, 228]]. In that study, the microenvironment into which the radial glial-like glioma stem-like cells were transplanted was thought to be important in determining the mesenchymal-like phenotype. This has parallels to my own preliminary observation that low tissue culture oxygen tension may select for flat rather than branched phenotype cells from glioma tissue.

Mesenchymal differentiation also occurs in human gliomas themselves, albeit in a rare type called a gliosarcoma that is defined by its mesenchymal characteristics [1]. I actually derived four primary cultures from one set of gliosarcoma tumour biopsies. Interestingly, all these primary cultures were characterised by branched phenotype rather than flat phenotype cells. This is perhaps not surprising, because it is consistent with my observation that high-grade gliomas, such as gliosarcoma, were generally characterised by branched phenotype cells in primary culture. Furthermore, as I described above, in vivo it is branched phenotype-like putative stem-like cells that are able to undergo mesenchymal differentiation [222, 227, 228]. This data suggests that it is unlikely that flat phenotype cells are simply derived from a subset of gliomas with mesenchymal differentiation.

Aside from studies in glioma, mesenchymal marker expression has also been observed in normal glial cultures [229-231]. Explanations for this have included mesenchymal drift of cells from their glial origin, overgrowth of mesenchymal cells from tumour vasculature or leptomeninges, or the presence of mesenchymal stem cells from the blood [229-231]. In one study of explanted non-transformed human astrocytes, although the dominant cell type was a radial glial-like cell there were also a smaller proportion (<10%) of pyramidal cells [232]. These pyramidal cells had abundant cytoplasm and large central nuclei, similar to the appearance of my flat phenotype cells [232]. Importantly, these pyramidal cells were morphologically distinct from flat, spindle shaped fibroblast cells and did not stain with antibodies to Fibronectin [232].

The explanted human astrocyte cultures in the study described stained with antibodies to both Vimentin and GFAP [232]. Other investigators have observed that GFAP-negative/Vimentin-positive glial progenitors can differentiate into such Vimentin-positive/GFAP-positive cells [233, 234]; GFAP is normally considered the dominant intermediate filament in astrocytes whilst Vimentin is generally a mesenchymal cell marker [232]. My flat phenotype cells were GFAP-negative/Vimentin-positive (based on gene expression profiling) and so share features with these astrocyte progenitors. However, whilst in the explanted human astrocyte culture the dominant radial glial-like cells were observed to evolve into polygonal shaped cells over just a few days, I did not observe any evidence that my branched phenotype cells could convert into flat phenotype cells [230]. In any case, it seems unlikely that there would be a direct lineage relationship between flat and branched phenotype cells based on the DNA copy number change data I discussed above; if there were to be a lineage relationship between flat and branched phenotype cells then the relative DNA copy number changes that I observed in each would suggest that it is the flat phenotype cell, rather than the branched phenotype cell, that is the precursor.

A different study has described a Nestin-positive GFAP-negative population of mitotically active cells with fibroblast-like features in the adult human brain, similar to the characteristics of my own flat phenotype glioma stem-like cells [231]. However, rather than having stem-like characteristics, these cells were thought to have been derived from perivascular fibroblasts resident in the brain. This was despite the fact that the cells had actually been enriched using culture conditions optimised for neural stem cell growth and that on removal of mitogens some early neuronal differentiation was observed [231]. Since the cells could not be reliably differentiated into astrocytic, mature neuronal and oligodendroglial lineages the authors in this particular study concluded that the cells were unrelated to neural progenitor cells [231]. However, the limited differentiating capacity of some in vitro glioma stem-like cells has been previously described [65-67]. In these studies this was interpreted as dysfunctional differentiation of a stem-like cell caused by tumour associated genomic changes rather than evidence that the primary culture cells are not stem-like [65-67].

The Nestin-positive GFAP-negative cells were nevertheless subjected to a gene expression analysis in order to interrogate the origin of the putative fibroblast-like cells [231]. The investigators determined that they had been derived from perivascular fibroblasts in the brain, because they expressed high levels of PDGFRβ and αSMA [231]. These observations therefore support the study I described earlier that described cancer-associated fibroblasts in glioma primary cultures [228, 231].

Cancer–associated fibroblasts are thought to play an active role in tumour proliferation, malignant transformation and invasion, so it is plausible that they have a similar role in glioma [228, 235]. For example, when glioma associated stromal cells were injected together with U87 serum-derived glioma cell lines into an immune deficient mouse model there was an increased tumour volume compared to injection of U87 cells alone, or U87 cells injected with normal stromal cells [235].

Interestingly, genes that are indicative of cancer-associated fibroblasts such as PDGFRβ (p=0.007), alpha smooth muscle actin (αSMA) (p=0.00023) and ACTA2 (p=0.00023), were expressed at higher levels in my flat phenotype cells compared to the branched phenotype cells; the p values are indicated in the brackets [228]. In contrast, the expression of genes specific to other fibroblasts, or to smooth muscle cells, was not significantly different between the flat and branched cell phenotypes: MYH11 (p=0.3), Desmin (p=0.3), NRGN (p=0.8), RAB20 (p=0.6) and CDH6 (p=0.03) [228]. These observations would support a hypothesis that the flat phenotype cells in my primary cultures are cancer-associated fibroblasts derived from constituent perivascular fibroblasts. It is therefore interesting that vascular niches in glioblastomas have been described as sites of enrichment of glioma stem-like cells [112, 120]. It is possible then that in gliomas flat phenotype cells localise with branched phenotype cells in these niches. This is an important topic for future study and could be approached with an analysis of histological tissue sections to observe the co-localisation of relevant proteins using a immunostaining technique.

The tumour promoting phenotype of cancer-associated fibroblasts has been proposed to result from genetic mutations in the cells from which they are derived [228]. This would be consistent with my observation that flat phenotype cells have a small number of DNA copy number changes that distinguish them from the patient's somatic genome [228]. Nevertheless, the cell of origin of the flat phenotype cells remains uncertain. Indeed, my observation that some tumour-associated DNA copy number changes were shared between both flat and branched phenotype cultures derived from a single glioma suggests that the flat phenotype cells have a lineage shared with the tumour cell of origin, rather than with a distinct cell precursor to a cancer associated-fibroblast-like cell. The experiments that I described above to interrogate the lineage relationship between flat phenotype cells and the tumour from which they were derived will be useful to explore this further. It may be that both the tumour stem-like cell and the cancer associated fibroblast-like cell in fact have a shared precursor cell, explaining the stem-like features of the flat phenotype cells.

Another possibility to explore for the origin of the flat phenotype cells is the possibility that they arise from differentiated glial cells through epithelial to mesenchymal transition (EMT) [228]. EMT is associated with a loss of differentiated characteristics and acquisition of mesenchymal features such as motility, invasiveness and a heightened resistance to apoptosis. It is an important process in development and unsurprisingly has also been implicated cancer progression [236].

3.9 Summary

I developed a technique for the derivation of putative glioma stem-like cells from human gliomas. I identified two distinct stem-like cell types, a 'branched' phenotype, radial glial-like cell and a 'flat' phenotype, mesenchymal-like cell with stem-like features. Further interrogation of the aetiology of the flat phenotype cells is required. They may have a lineage shared with branched phenotype cells, or alternatively may have a non-glial or non-stem cell origin. Throughout this Chapter I detailed some of the principal experiments necessary to further interrogate these stem-like cells. A key goal is to be able to predict, or even determine, whether a glioma-derived sphere from a single cell suspension of a patient-derived tumour will form a culture containing branched or flat phenotype cells. Separately, the media conditions of the flat phenotype cells need to be optimised for growth of mesenchymal-like cells and the ability of these cells to differentiate into mesenchymal lineages should be assessed to ascertain their 'stemness'.

Even if the flat phenotype cells transpire to be tumour-associated rather than tumour-derived, as seems a possibility from my observations, they may still have an important role in the pathogenesis of glioma, not least because a mesenchymal-like rather than glial-like gene expression profile in glioma tissue has been associated with worse outcomes for patients [177]. By modelling the intra- and inter-tumoural heterogeneity I have observed in gliomas, I have the potential to develop in vitro

assays of compound inhibition that may be more predictive than current models of the likely efficacy of drugs in the clinic, as I will discuss in Chapter 4.

Chapter 4. Using glioma stem-like cells from patients to develop high throughput assays to screen for novel inhibitors

4. 1 Background

Currently, the optimal treatment of glioma consists of maximal surgical resection, adjuvant radiotherapy with concomitant chemotherapy using the DNA alkylating agent Temozolomide (TMZ), followed by TMZ alone [2]. With this regimen the average life expectancy from diagnosis is 14.6 months [2]. Complete surgical resection of a glioma is not possible, because of the invasiveness of glioma cells amongst normal brain tissue, so adjuvant therapies are important [237]. TMZ is the current chemotherapeutic agent of choice and works by methylating DNA, usually at a guanine residue, triggering cell death [46]. Unfortunately, many patients are resistant to TMZ-induced methylation because of elevated expression of the repair protein O-6-methylguanine-DNA methyltransferase (MGMT) in their tumours, or a defect in a mismatch repair pathway [45, 238]. In other patients the MGMT promoter is methylated, preventing synthesis of the MGMT enzyme and making the tumour more susceptible to TMZ [29]. About 45% of gliomas have MGMT promoter methylation and these patients have a favourable prognosis [29]. However, this means that for the majority of patients with glioma, there is no effective chemotherapy.

Despite promising preclinical research, no new chemotherapy agents for glioma have made a significant impact in the clinic since the introduction of TMZ [50]. This may be because the preclinical models of glioma on which novel agents are screened do not accurately recapitulate human disease. These models were based on the traditional multistep theory of glioma development that implicates a differentiated glial cell as the cell of tumour origin. The emergence of the glioma stem cell hypothesis therefore offers an opportunity to develop new in vitro assays of these

cells thought to be responsible for resistance to chemotherapeutic agents, as well as glioma initiation [3, 100, 128]. These models might improve the predictive value of preclinical compound screening.

A significant challenge for compound screening in glioma stem-like cells is the need to expand and maintain the cells in their undifferentiated stem-like state at scale [129]. In this Chapter I will present the strategy by which I achieved this with my own unique resource of putative glioma stem-like cells derived from a spectrum of glioma types and grades, as described in Chapter 3. In Chapter 1 I described the technique of high content phenotypic analysis and I employed this for the development of my in vitro assays to enable a dose rage of different inhibitors to be screened across multiple glioma primary cultures, simultaneously.

It was essential that the assays of compound efficacy were themselves biologically relevant to glioma. For example, simply assaying changes in cell number or proliferation in response to a compound does not inform whether the mechanism underlying the observation is cell cycle arrest or cell death [134]. This is important, because a compound that exclusively represses cell cycle progression without initiation of tumour cell death (referred to as a cytostatic agent) leaves cancer cells in a state of readiness to re-enter the cell cycle when the drug-level subsides [134]. In patients this could result in tumour recurrence. I therefore present data from a panel of biologically relevant assays that distinguish cytotoxic from cytostatic effects in response to inhibitor compounds.

In Chapter 3 I described the identification of two different types of glioma-derived stem-like cell in vitro, one with glial-like characteristics that I refer to as branched phenotype cells and the other with mesenchymal-like characteristics that I have called flat phenotype cells. These different cell phenotypes may need to be targeted separately with compound inhibitors in order to successfully eradicate a tumour. In

this Chapter I therefore examine the drug sensitivities and cellular responses of these cell phenotypes in different glioma primary cultures.

It is the invasion of glioma cells into normal brain that limits the efficacy of surgical resection, contributing to tumour recurrence [237]. These invading cells are also thought to undergo transient cell cycle arrest and so may evade the toxic effects of chemotherapeutic agents [239]. The identification of compounds that can limit glioma cell invasion would have the potential to effectively downgrade glioma into a localised disease susceptible to surgical excision and localised radiotherapy. This requires in vivo tumour invasion to be modelled in vitro. I therefore describe the development of an in vitro assay of the invasive ability of putative glioma stem-like cells, which to my knowledge has not previously been documented. I present a preliminary screen of potential inhibitors against putative glioma stem-like cell invasion. I also compare the invasive potential of branched and flat phenotype primary cultures cells.

Compound screening assays were performed on monolayer primary culture cells, rather than glioma-derived spheres, because the former are more readily adapted to reproducible and high throughput screening [129, 240]. The majority of the experiments that I describe in this Chapter were, as a minimum, performed on the same group of 2 flat phenotype and 3 branched phenotype primary cultures. However, because of the difficulty of culturing these primary culture cells and the need to maintain them at low passage number to best preserve their genomic integrity, cells were not always available in sufficient quantities for each assay. I therefore indicate the primary cultures utilised in each assay. The primary cultures used illustratively in each Figure also vary, but in each case are representative of the assay results across all the cultures tested.

To increase the likelihood that the compounds I tested in vitro would be able to translate effectively into the clinic I chose to screen inhibitors predominantly targeted

against a single signalling pathway known to be important in glioma cell biology. This contrasts with the current chemotherapy of choice in the clinic for glioma, TMZ, which has a non-specific cytotoxic action through DNA damage mechanisms [2, 45]. The selection of a signalling pathway against which to screen inhibitor compounds was informed by an analysis of genes that were both commonly mutated in glioma and that are known to have a cell-signalling role.

The principal signalling pathway targeted by the inhibitor compounds that I screened in this series of experiments was the PI3 kinase pathway. This pathway is particularly relevant to glioma cell biology, as I discussed in Chapter 1. PTEN, a negative regulator of the pathway, is mutated in 70% of tumours, resulting in increased PI3 kinase pathway activity [127, 148]. Activation of this pathway correlates with poor prognosis for patients diagnosed with glioma [241]. Interestingly, this same pathway regulates self-renewal, proliferation, and survival of the neural stem cell, to which glioma stem-like cells are proposed to have some similarities [140, 151].

4.2 PTEN gene mutation is associated with higher-grade gliomas

Before examining the efficacy of PI3 kinase pathway inhibitors against my primary culture cells I assessed the status of the PTEN gene in the tumours from which these cultures had been derived. In Chapter 3 I described the analysis of DNA copy number changes in tumour tissue and related primary cultures using an array CGH technique (Figures 3.10 to 3.16). I examined this same data set for evidence of loss of genetic material in the region of the PTEN gene on chromosome 10q23.3 between base pairs 89,623,194 and 89,728,531 [127]. I observed no evidence of DNA copy number changes in this region in one grade 2 tumour and four grade 3 tumours, but did identify relevant changes in four of six grade 4 tumours (Table 4.1, Figure 4.1). Grade 4 is the highest grade of glioma. This is consistent with reports that PTEN

Table 4.1 The incidence of PTEN mutation in glioma tissue. DNA was extracted from the same tumour tissue from which the primary cultures had been derived. The DNA was examined for copy number changes using an array CGH approach. The region of the genome incorporating the PTEN gene was analysed to assess whether it was subject to DNA copy number loss or gain. Samples are listed in the table by their alphabetic designation and the histological diagnosis and grade of each tumour is indicated; GBM – glioblastoma.

Primary Culture Code	Histological Diagnosis	Tumour Grade	Presence of copy number change in region of PTEN gene
L	Secondary anaplastic oligodendroglioma	3	No
M	GBM	4	Yes
O	Secondary GBM	4	No
V	Astrocytoma	3	No
X	GBM	4	Yes
Y	GBM	4	No
AA	Astrocytoma	3	No
BB	GBM	4	Yes
CC	Anaplastic oligodendroglioma	3	No
DD	Gliosarcoma	4	Yes
EE	Oligodendroglioma	2	No

Figure 4.1 PI3 kinase pathway activation. (A) DNA was prepared from 11 tumour tissue biopsies. Evidence of genomic loss in the region of the PTEN gene was sought using array CGH; hybridisation was performed by the Cytogenetics Unit, NHS Lothian. A summary of the results is given in the text. The ideogram below demonstrates a representative example of DNA copy number gains (above 0) and losses (below 0) on chromosome 10 in the glioblastoma designated 'X' and the anaplastic astrocytoma designated 'CC.' The primary cultures derived from tumours X and CC had branched and flat phenotype cells, respectively. The yellow bar indicates the region in which the PTEN gene is found, demonstrating a loss of DNA in the region of the PTEN gene in sample X, but not in sample CC. (B) Cells from the branched phenotype primary cultures designated DD2 (gliosarcoma), P (GBM) and X, and the flat phenotype culture designated EE2 (oligodendroglioma), were subjected to the PI3 kinase inhibitor PIK75 across a range of concentrations for 30 minutes. Cells were washed, snap frozen, then lysates were prepared in RIPA buffer. A bicinchoninic acid (BCA) protein assay was performed and 20 micrograms of each sample were denatured in sample buffer, then resolved on a 10% gel at 180V, 230mA, 30W for 70 minutes. Proteins were transferred to a nitrocellulose membrane at 100V 400mA 50W for 70 minutes. Membranes were blocked, probed with the primary antibodies indicated at a 1:1000 dilution, then incubated in HRP-conjugated secondary antibodies (1:5000). Visualisation was by enhanced chemiluminescence. The representative western blots below are from the branched phenotype culture designated DD2. They demonstrate that increasing concentrations of PIK75 are associated with reduced phospho-Akt (Serine 473), but constant total Akt levels. This indicates that the PI3 kinase pathway is activated in these primary cultures.

A

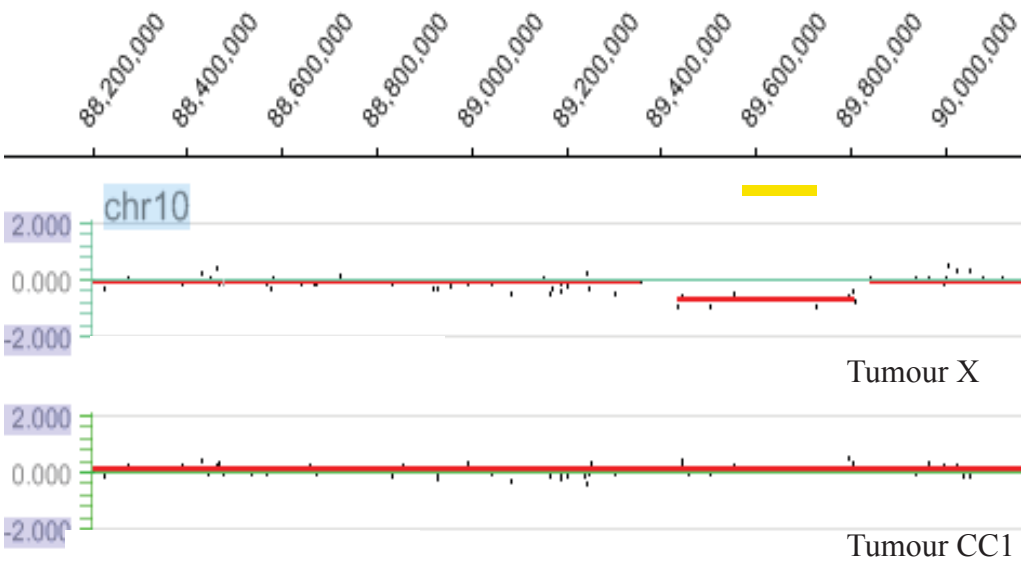

B

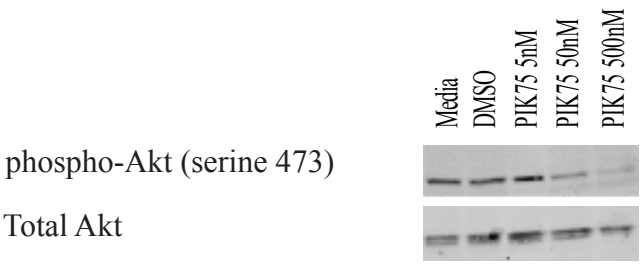

mutations and activation of the PI3 kinase pathway are more common in primary higher grade gliomas than lower grade tumours or secondary GBMs [241, 242].

There are some limitations to using only an analysis of DNA copy number change to identify PTEN mutations. For example, very few probes on the array CGH chip that I used covered the 110-kilobase region of interest. Only genomic gains or losses several hundred kilobase pairs in size in this region would actually have been detected (Figure 4.1). Shorter genomic gains or losses, or even single point mutations, would not have been detected, but could still have disrupted the PTEN gene. Furthermore, PTEN methylation has been reported in lower grade tumours to result in PI3 kinase activation in the absence of PTEN mutations [243]. The PI3 kinase pathway can also be activated in gliomas by mechanisms other than PTEN loss, such as expression of the EGFRvIII mutant, or mutations in the p110α subunit of PI3 kinase [159, 241]. Therefore, rather than focusing solely on identifying PTEN mutations, I used a western blotting technique to assess the overall activation state of members of the PI3 kinase pathway, of which PTEN is a negative regulator. I prepared lysates from the branched primary cultures designated DD2 (Gliosarcoma), X (GBM) and P (GBM), and from the flat primary culture designated CC2 (Anaplastic oligodendroglioma), that had been subjected to treatment for 30 minutes with the PI3 kinase inhibitor PIK75 at 0nM, 5nM, 50nM and 500nM concentrations. Total levels of Akt were assayed along with its phosphorylated species, phospho-Akt (serine 473). Increased levels of phosphorylation indicate protein activation [241]. The protein species in Figure 4.1 illustrate a reduction in Akt phosphorylation with increasing compound dose in the primary culture designated DD2 (Gliosarcoma) [241]; this phenomenon is further demonstrated in the primary cultures designated P (GBM) and CC2 (Anaplastic oligodendroglioma) in section 4.9 and Figure 4.13. This indicates that the PI3 kinase pathway is activated in these primary cultures. I will examine the PI3 kinase inhibitor PIK75 and PI3 kinase pathway activation in more detail in Section 4.9, where I confirm that there is evidence of activation of this

pathway in both flat and branched phenotype cells. This supports the rationale from the literature for targeting this pathway with compound inhibitors.

4.3 PI3 kinase pathway inhibitors have a heterogeneous effect on primary cultures

I proceeded to screen my glioma primary cultures with a panel of inhibitors targeted against the PI3 kinase pathway. The primary cultures against which inhibitor efficacy was examined included both those with flat and branched phenotype cells, as detailed in Table 4.2. I first determined the optimal number of cells from each culture that needed to be plated in a 96 well format to give log phase growth after 48 hours, the time of compound dosing. Using a sulphorhodamine (SRB) total protein assay I then screened a panel of 13 glioma primary cultures across an eight-point half-log dose response range with a selection of inhibitors to the PI3 kinase pathway (Table 2.3). In this experiment total protein was used as a proxy measurement of cell growth. Where there was a reduction in total protein with increasing inhibitor concentration, the values at each dose were plotted and the absolute half-maximal effective concentration (GIC50) of the inhibitor determined. The GIC50 is calculated from the dose response curve as the concentration of compound required to slow cell growth by 50% in comparison to a vehicle-treated control [244]. The GIC50 values for eight of the primary cultures tested are detailed in Table 4.3 and Figure 4.2. The primary cultures are indicated in the table by their alphabetic designation. The primary culture designated ‘L’ was derived from an anaplastic oligodendroglioma whilst the remainder were derived from glioblastomas.

The manufacturer of the PI3 kinase inhibitors screened provided information on the 50% inhibitory concentration (IC50) for each compound (www.symansis.com). The IC50 was usually within the nanomolar range and was determined from on target activity, not from cell growth inhibition.

Table 4.2 Cell phenotype of glioma primary cultures. Cells from each of the glioma primary cultures grown in serum-free conditions were observed to establish whether the constituent cell phenotype was 'branched' or 'flat' in adherent culture, as described in Chapter 3. The primary cultures are listed according to their alphabetic designation below, along with an indication as to whether the constituent cell phenotype was branched or flat. The histology of the tumour from which each primary culture was derived is detailed in Table 4.1.

Primary culture	Dominant cell phenotype
L	Branched
M	Branched
N	Branched
O	Branched
P	Branched
U	Branched
X	Branched
ZH	Flat
BB	Branched/Flat
CC	Flat
DD	Branched
EE	Branched/Flat

Table 4.3 Efficacy of PI3 kinase pathway inhibitors on primary culture growth. A panel of glioma primary cultures (designated 'L', 'M' etc. as detailed in Table 4.2) were plated onto Matrigel-coated 96 well plates and allowed to proliferate for 48 hours. The cells were then treated with inhibitor compounds across an eight-point half-log dose response range. After 48 hours the cells were fixed in 25% trichloroacetic acid and a SRB assay of total protein was performed. The table details the inhibitors used and the IC50 provided by the manufacturer for each compound. The absolute half-maximal effective concentration (GIC50) is indicated in the body of the table and was determined from analysis of at least three repeats of compound treatment of primary cultures at each inhibitor concentration. Results highlighted in green indicate a GIC50 in the nanomolar range and/or within a magnitude of 10 of the IC50. Results highlighted in red indicate effective inhibitory concentrations that fell outwith this range, which was interpreted as off-target cytotoxicity. Panels marked 'nil' indicate that there was no observable change in total protein content in response to increasing compound concentration. For compound PI103 the three IC 50 values apply to DNA-PK, P110α and mTORC, respectively. The 'E' notation used in the table indicates the preceding number is raised to the power 10. For example, 'E-07' indicates that the preceding number is raised by 10 to the minus 7.

Inhibitor	PIK75	TGX221	PIK294	AS252424
IC 50	8.00E-09	9.00E-09	1.00E-08	3.00E-08
Target	P110α	P110β	P110γ	P110δ
L	6.04E-08	nil	9.16E-07	1.44E-07
M	2.47E-08	nil	nil	1.19E-07
N	4.70E-08	8.45E-07	nil	6.35E-06
O	7.07E-08	nil	nil	nil
P	5.84E-08	nil	nil	nil
U	2.58E-08	nil	nil	nil
X	4.12E-08	nil	nil	nil
ZH	9.99E-09	nil	nil	3.68E-06

IC 50	LY294002	PI103	Rapamycin	KU63794
	5.00E-07	2.00E-08 8.00E-09 2.00E-07	1.00E-08	1.00E-08
Target	PI3 kinase	PI3 kinase, DNA PK	mTOR	mTOR
L	9.21E-06	8.64E-06	nil	5.18-07
M	1.19E-05	Nil	nil	7.75E-07
N	1.73E-05	7.26E-06	nil	3.24E-06
O	2.66E-02	Nil	8.39E-04	6.67E-07
P	nil	5.42E-06	nil	nil
U	3.22E-02	1.97E-02	nil	21.8E-07
X	nil	4.46E-02	nil	nil
ZH	5.54E-06	1.35E-08	8.82E-07	4.98E-06

Figure 4.2 Graphs illustrating the efficacy of PI3 kinase pathway inhibitors on primary culture growth. A panel of glioma primary cultures designated 'L' (oligodendroglioma), 'P' (GBM) and ZH (GBM) illustrate the results summarised in Table 4.3. The primary cultures designated L and P were branched phenotype cultures whereas the primary culture designated ZH was a flat phenotype culture. Each experiment was performed in at least triplicate. The cells were treated with inhibitor compounds across an eight-point half-log dose response range. After 48 hours the cells were fixed in 25% trichloroacetic acid and a SRB assay of total protein was performed. Data was analysed within the GraphPad Prism software. At each dose point the total protein was determined as a percentage of a vehicle (DMSO)-treated control. The data in Table 4.3 detailed the absolute half-maximal effective concentration, (GIC50), of compounds that was calculated from each dose response curve as the concentration of compound required to slow cell growth by 50% in comparison to a vehicle-treated control. The graphs are derived from non-linear regression analysis of the results at each inhibitor dose concentration. The box plot at each data point illustrates the standard error of the mean. Where possible, a sigmoidal dose response curve was fitted to the data. The percentage inhibition of growth compared to the vehicle-treated control is presented against the log to the base 10 of the inhibitor concentration. The actual dose range varied slightly for each compound, according to the recommendations of the manufacturer (Symansis, New Zealand). This variation is illustrated in the graphs. The graphs illustrate that the only compound with an effective dose response within range of its target IC50 against all the primary culture cells tested was PIK75. Some graphs, such as those for the compound TGX221, do not contain a curve fitted to the data points. This illustrates that there was no dose-dependent compound inhibition in these cells. Graphs such as those for PI-103 inhibition in the primary cultures designated as L and P illustrate that there was a dose-dependent compound inhibition at higher inhibitor concentrations, suggestive of an off-target effect; in these experiments the GIC50 recorded in Table 4.3 is an estimation for illustrative purposes made by the GraphPad Prism software. Only in PIK75 was a dose-dependent inhibition of cell growth observed across all the primary cultures examined.

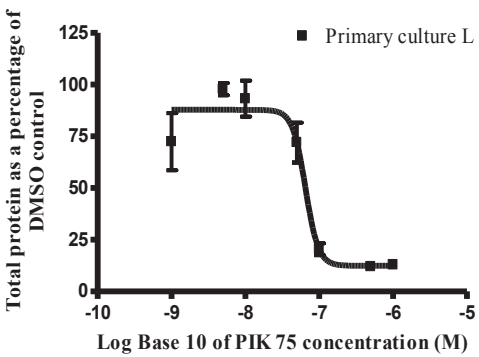
Total protein as a percentage of DMSO control
Primary culture L
Log Base 10 of PIK 75 concentration (M)

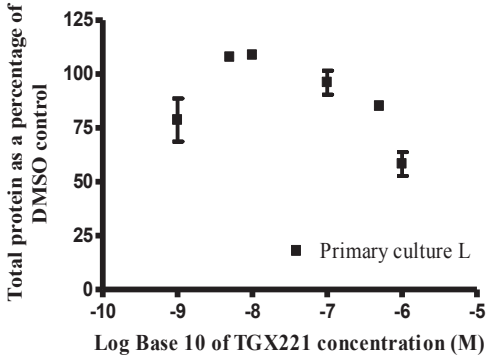
Total protein as a percentage of DMSO control
Primary culture L
Log Base 10 of TGX221 concentration (M)

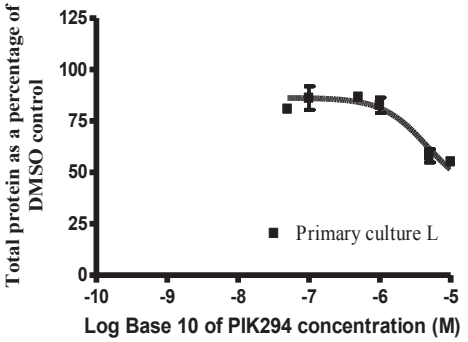
Total protein as a percentage of DMSO control
Primary culture L
Log Base 10 of PIK294 concentration (M)

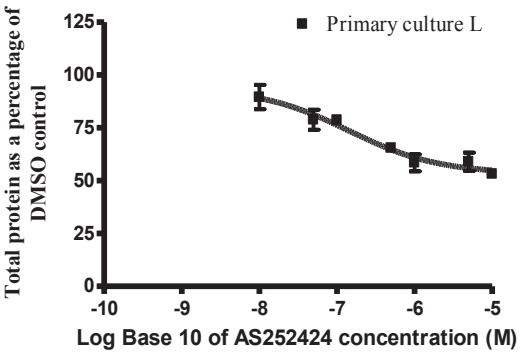
Total protein as a percentage of DMSO control
Primary culture L
Log Base 10 of AS252424 concentration (M)

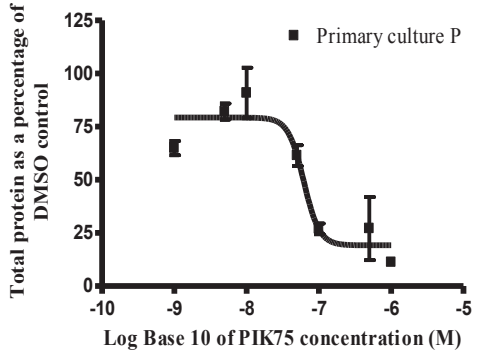
Total protein as a percentage of DMSO control
Primary culture P
Log Base 10 of PIK75 concentration (M)

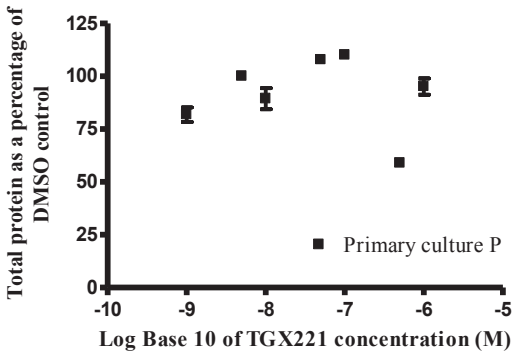
Total protein as a percentage of DMSO control
Primary culture P
Log Base 10 of TGX221 concentration (M)

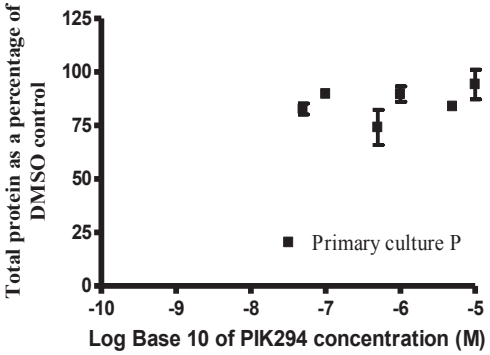
Total protein as a percentage of DMSO control
Primary culture P
Log Base 10 of PIK294 concentration (M)

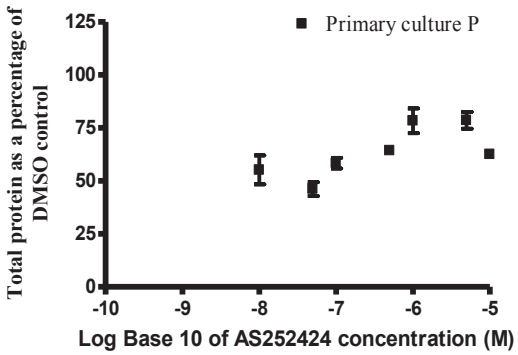
Total protein as a percentage of DMSO control
Primary culture P
Log Base 10 of AS252424 concentration (M)

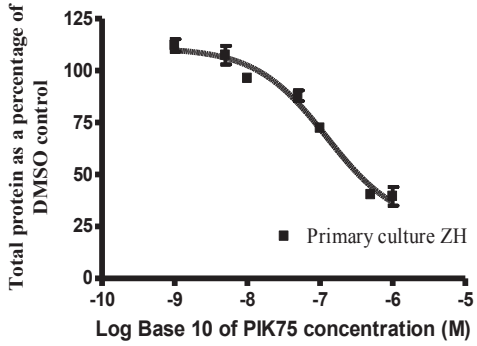
Total protein as a percentage of DMSO control
Primary culture ZH
Log Base 10 of PIK75 concentration (M)

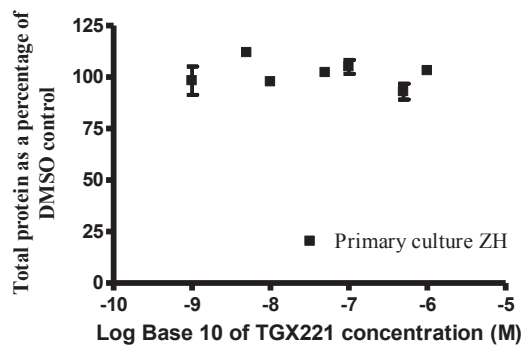
Total protein as a percentage of DMSO control
Primary culture ZH
Log Base 10 of TGX221 concentration (M)

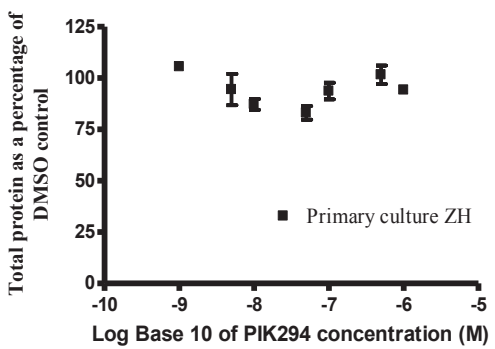
Total protein as a percentage of DMSO control
Primary culture ZH
Log Base 10 of PIK294 concentration (M)

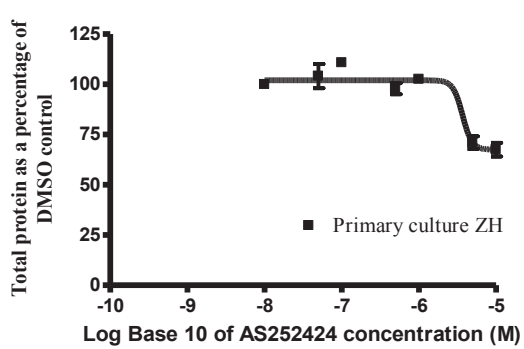
Total protein as a percentage of DMSO control
Primary culture ZH
Log Base 10 of AS252424 concentration (M)

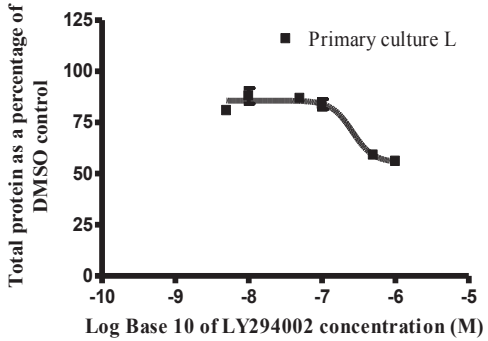
Total protein as a percentage of DMSO control
Primary culture L
Log Base 10 of LY294002 concentration (M)

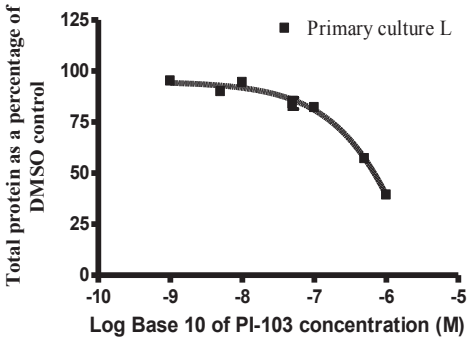
Total protein as a percentage of DMSO control
Primary culture L
Log Base 10 of PI-103 concentration (M)

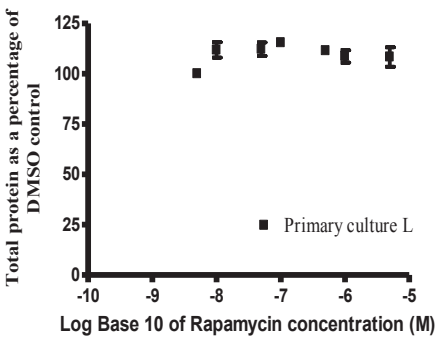
Total protein as a percentage of DMSO control
Primary culture L
Log Base 10 of Rapamycin concentration (M)

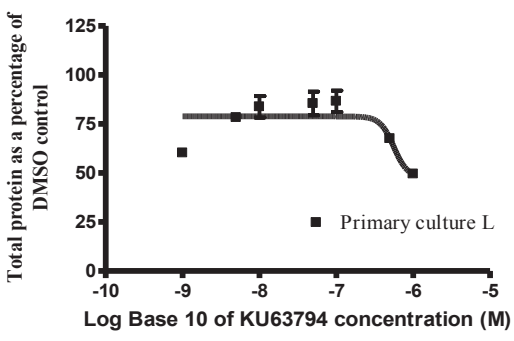
Total protein as a percentage of DMSO control
Primary culture L
Log Base 10 of KU63794 concentration (M)

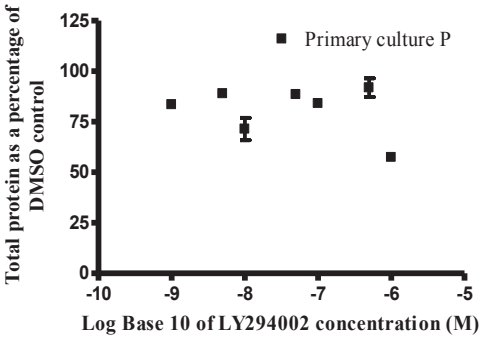
Total protein as a percentage of DMSO control
Primary culture P
Log Base 10 of LY294002 concentration (M)

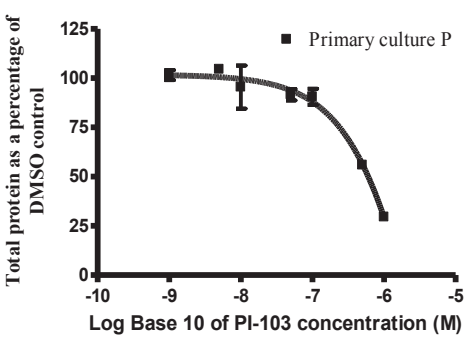
Total protein as a percentage of DMSO control
Primary culture P
Log Base 10 of PI-103 concentration (M)

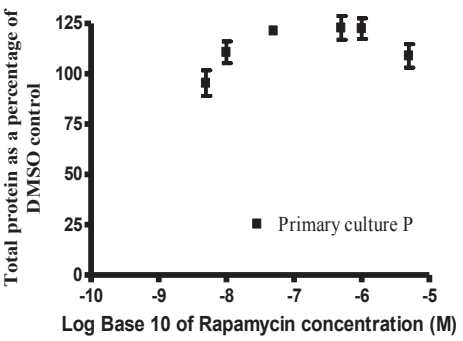
Total protein as a percentage of DMSO control
Primary culture P
Log Base 10 of Rapamycin concentration (M)

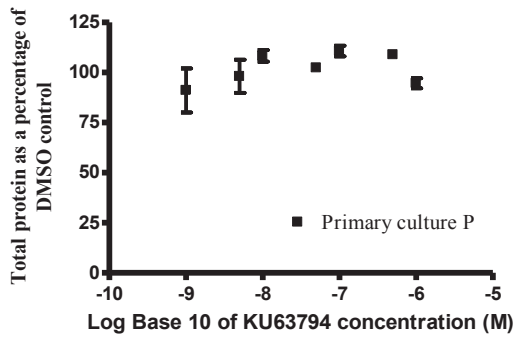
Total protein as a percentage of DMSO control
Primary culture P
Log Base 10 of KU63794 concentration (M)

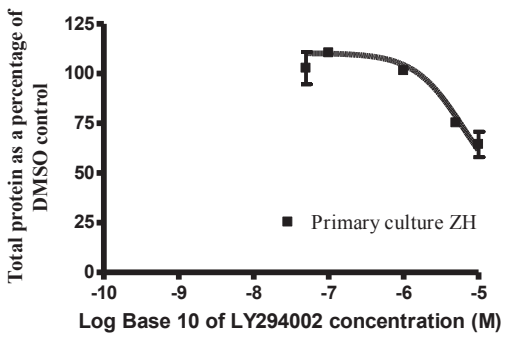
Total protein as a percentage of DMSO control
Primary culture ZH
Log Base 10 of LY294002 concentration (M)

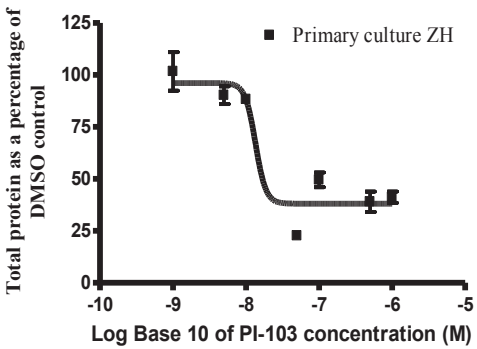
Total protein as a percentage of DMSO control
Primary culture ZH
Log Base 10 of PI-103 concentration (M)

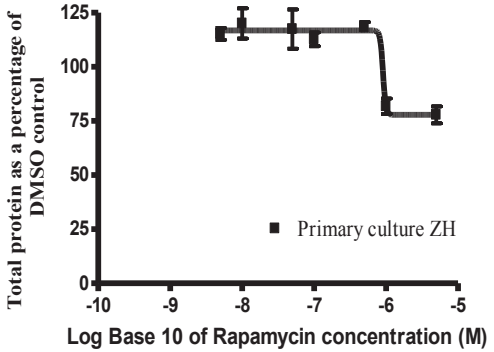
Total protein as a percentage of DMSO control
Primary culture ZH
Log Base 10 of Rapamycin concentration (M)

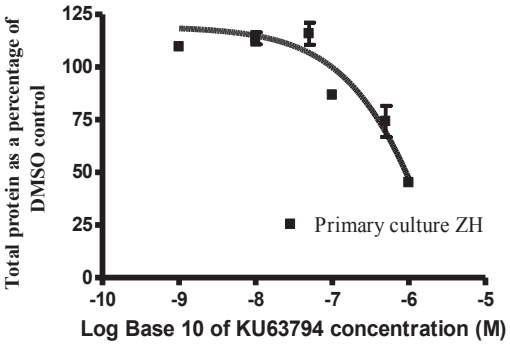
Total protein as a percentage of DMSO control
Primary culture ZH
Log Base 10 of KU63794 concentration (M)

Where the GIC50 from my experiments was at least equal to the IC50, or within a magnitude of 10 of this value, the interpretation was made that the observed effect was attributable to on target inhibitor activity. Effective inhibitors are highlighted in the table in green (Table 4.3). Some inhibitors were not effective at all in certain primary cultures; these are indicated by 'nil' in the table. Where compounds inhibited cell growth only at inhibitor concentrations greater than the IC50 this was interpreted as a possible off-target effect; these are indicated in red. Off target effects often have unpredictable biological consequences that can be manifest clinically as toxicities and so I did not pursue analysis of these compounds [137].

The most significant result from this analysis was that the inhibitor PIK75 was the only compound efficacious in the nanomolar range across the whole panel of primary cultures tested (Table 4.3). PIK75 is an inhibitor of the class IA PI3 kinase catalytic subunit p100α [160]. There are 3 variants of the p110 catalytic subunit, (α, β and δ), and inhibitors against the other subunits were ineffective against the glioma primary cultures (Table 4.3). Moreover, the non-specific PI3 kinase inhibitor LY294002 was not generally effective at inhibiting cell growth (Table 4.3). The fact that PIK75, but not LY294002, inhibits glioma primary culture growth may suggest a role for the isoform specificity of PIK75. LY294002 inhibits all the p110 catalytic subunits and also has cellular targets other than PI3 kinase, such as casein kinase 2 and DNA-dependant protein kinase [245, 246]. An alternative explanation for the efficacy of PIK75 is that it has off-target activity, as I will discuss below. Both branched and flat phenotype cells were inhibited by PIK75 in the nanomolar range and there was no difference in the GIC50 inhibitory concentrations between the two groups (Table 4.3).

Only a small number of glioma primary cultures had their growth inhibited by any of the other compounds tested. It was therefore not possible to draw firm conclusions as to whether there was any variation in susceptibility to inhibitors between the flat and branched phenotype cells. Of the other PI3 kinase pathway inhibitors screened, the

mTOR inhibitor Rapamycin was effective in 1 of 8 primary cultures, whilst the mTOR inhibitor KU63794 inhibited growth in 5 of 8 cultures (Table 4.3). This difference in efficacy may reflect the actual mechanism of action of each drug. Rapamycin binds the cytosolic binding protein FKBP12 and the complex directly binds mTOR Complex 1 (mTORC1) but not mTORC2 [247]. In contrast, compound KU63795 inhibits both mTORC1 and mTORC2 by targeting the mTOR kinase domain itself [248]. I also screened a panel of inhibitors targeting signalling pathways other than the PI3 kinase pathway that are implicated in glioma cell biology, as listed in Table 2.3. One of the compounds tested, the aurora kinase B inhibitor Barasertib, did have a marginal effect at inhibitor concentrations above 3μM, but only in branched phenotype cells (Figure 4.10); this data is discussed below in Section 4.8. I therefore included this compound in some of the mechanistic assays that I will describe subsequently (Figures 4.11 and 4.12).

4.4 Glioma primary cultures and established glioma cell lines respond differently to PIK75

Despite the availability of in vitro primary cultures that model the cancer stem cell hypothesis of glioma initiation, compound screening continues to be performed predominantly on established, serum-grown glioma cell lines [249]. I therefore examined whether PIK75 was effective against three serum-grown glioma cell lines known as U87, U251 and GCCM (Table 4.4). I discovered that, despite the efficacy of PIK75 in the nanomolar range against glioma primary culture cells, it was only effective against established serum-grown glioma cell lines in the micromolar range (Figure 4.3). The difference in GIC50 between the established serum-grown glioma cells lines and my patient-derived glioma primary culture cells was significant ($p=0.007$). Compounds effective only at micromolar concentrations are normally considered to be acting through off-target effects [250].

Table 4.4 PIK75 has poor efficacy against established glioma cell lines. The effect of the PI3 kinase catalytic subunit p110α-specific inhibitor PIK75 on established serum-grown glioma cell lines known as GCCM, U87 and U251 was assessed using a SRB assay of total protein content. After proliferating for 48 hours each cell line was treated for a further 48 hours with PIK75 across an eight point half-log dose schedule ranging from nanomolar to micromolar inhibitor concentrations. Cells were then fixed in 25% trichloroacetic acid and the assay performed. The absolute half-maximal effective dose (GIC50) was calculated from a dose response curve based on analysis of at least three repeats of compound treatment of cultures at each inhibitor concentration tested (Figure 4.3). The GIC50 is indicated in the table for each of the cell lines. The 'E' notation used in the table indicates the preceding number is raised to the power 10. For example, 'E-06' indicates that the preceding number is raised by 10 to the minus 6.

Glioma cell line	GIC50
GCCM	1.93E-06
U87	2.62E-05
U251	3.04E-06

Figure 4.3 Comparison of the effect of PIK75 on established glioma cell lines and novel primary culture cells. Cells from the established serum-grown glioma cell lines designated U87, U251 and GCCM, and from the glioma primary cultures designated DD1 (gliosarcoma), X (GBM) and P (GBM), were plated and allowed to proliferate for 48 hours on Matrigel-coated 96 well plates before treatment with the PI3 kinase inhibitor PIK75 at a range of doses on a half-log scale. After 48 hours the cells were fixed in 25% trichloroacetic acid before analysis of total protein content using a SRB assay. The total protein content at each inhibitor dose was normalised to a control treated with DMSO, the solvent in which PIK75 was solubilised. Each experiment was repeated at least 3 times. A non-linear regression analysis was performed to obtain a sigmoidal dose-response curve using the GraphPad Prism software version 4.00. The graph illustrates the results for U87 and X as representative of established serum-grown glioma cell lines and glioma stem-like primary cultures, respectively. The error bars indicate the average of triplicate repeats at each dose point. The results demonstrate that whilst PIK75 has a dose dependent effect on putative glioma stem-like cells within the nanomolar range, established serum-grown glioma cell lines only respond at micromolar concentrations, suggestive of an off-target effect.

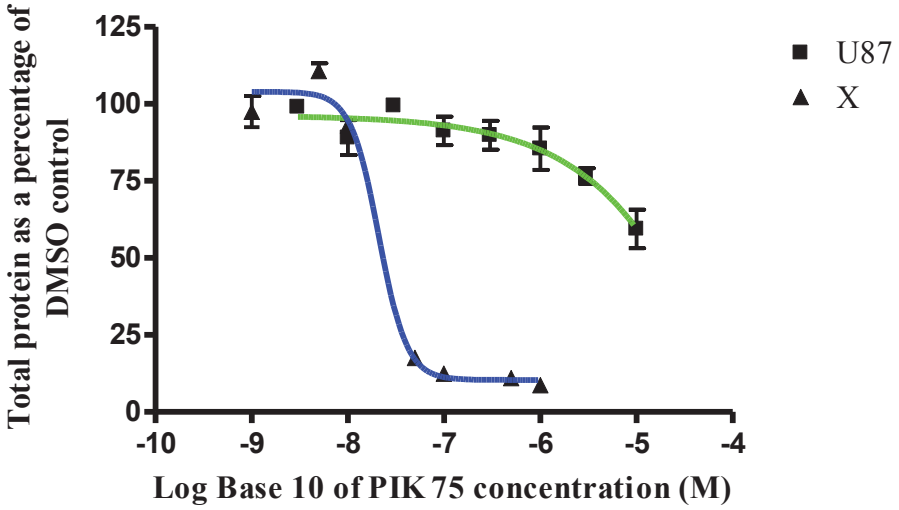

4.5 Neurosphere inhibitor assays

I have so far described the development of an adherent rather then sphere-based culture technique for screening inhibitor compounds. This was because of the difficulty both passaging glioma-derived spheres and also assaying inhibitor efficacy in three dimensions [129, 251]. However, I observed that when the Matrigel substrate was removed from adherent branched phenotype primary cultures, the cells became non-adherent and grew as spheres, indistinguishable from the glioma-derived spheres from which primary cultures were first derived. I therefore used this sphere-based model to assess the effect of PIK75 on 3-dimensional cell growth. Previously adherent primary culture cells from the tumour designated X (GBM) were plated in matrix-free non-adherent culture as single cells for 48 hours, during which time they proliferated as glioma-derived spheres. These spheres were then treated with PIK75 at concentrations on the same eight-point half-log dose range as for the adherent culture experiments (Figure 4.3). Forty-eight hours later the spheres were visually inspected with brightfield microscopy for dose-dependent differences in size and number (Figure 4.4). The selected images in Figure 4.4 demonstrate that increasing PIK75 concentration reduced the size and number of glioma-derived spheres. This is likely because of cell death, but this would require confirmation with a cell viability assay. As a comparison, spheres were also treated with the aurora kinase B inhibitor, Barasertib. Barasertib reduced cell growth in adherent culture at micromolar concentrations, as I discuss below. Barasertib had no observable impact on the size or number of glioma-derived spheres in this current assay.

4.6 Inter-tumoural variation in inhibitor-induced cell death

The preliminary screen of inhibitor compounds in adherent, patient-derived glioma primary cultures that I have described was performed using an SRB assay of total

Figure 4.4 Clonogenic drug assay. Glioma primary culture cells derived from the tumour designated X (GBM) were plated in suspension culture in a 96 well plate at 1 cell per microlitre. After growing as glioma-derived spheres for 48 hours the cells were treated with either the PI3 kinase inhibitor PIK75 or the Aurora kinase B inhibitor Barasertib at doses on a half-log range. After 48 hours the cells were visually inspected to assess the impact of increasing inhibitor concentration on sphere growth. The panels from left to right illustrate the appearance of the glioma-derived spheres at increasing inhibitor concentrations. PIK75, but not Barasertib, inhibited sphere formation at increasing concentrations. Media and DMSO controls are shown for comparison. The scale bar indicates 200 microns in length.

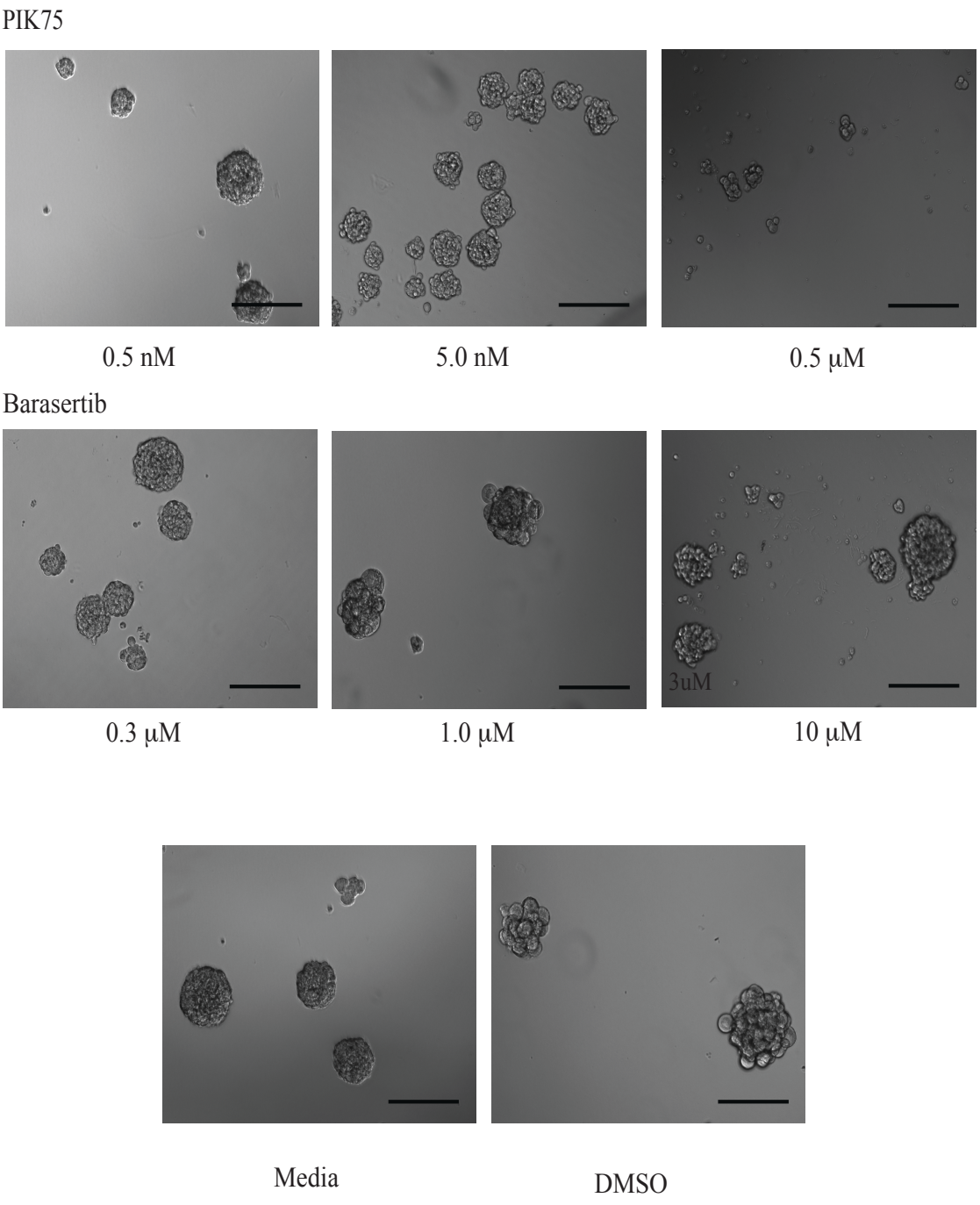

protein. This assay was a proxy for changes in cell number that resulted from reduced cell proliferation or increased cell death. However, the SRB assay itself does not provide information about the actual mechanism by which the total protein is being reduced. I therefore next developed a method for assaying the cell cycle and apoptosis-inducing effects of compounds on glioma primary culture cells using high content imaging assays [137].

The NucView caspase-3 substrate is cleaved by the caspase enzyme essential for apoptosis and so detects apoptotic cell death [252]. This releases a fluorogenic dye that migrates to the nucleus and fluoresces on complexing with DNA. I used this NucView substrate to assay the amount of apoptotic cell death in 5 of my glioma primary cultures over an eight-point half-log dose range of PIK75. The total number of nuclei at each dose point was also assessed, so that the proportion of non-apoptotic cells could be determined.

In Figure 4.5 the primary cultures designated CC2 (Anaplastic oligodendroglioma) and X (GBM) are shown as representative of the 2 flat phenotype and 3 branched phenotype cultures, respectively, that I assayed. The five primary cultures examined were DD1 (gliosarcoma), P (GBM) and X (GBM) (branched phenotype), and CC2 (anaplastic oligodendroglioma) and EE2 (oligodendroglioma) (flat phenotype). Each experiment involved three replicates of each compound treatment and this was repeated at least twice for every primary culture examined. The statistical significance of changes in the proportions of apoptotic cells or nuclei at each dose point was determined by ANOVA tests (Figure 4.5).

Interestingly, I observed a significant PIK75 concentration-dependent decrease in the total number of nuclei in all the branched phenotype primary cultures examined, but not in any of the flat phenotype cultures ($p<0.001$) (Figure 4.5). In contrast, all the flat phenotype cells, but none of the branched phenotype cells, demonstrated significantly increased numbers of apoptotic cells ($p<0.001$) (Figure 4.5). I plotted

the change in the total number of nuclei (for branched phenotype cells) or apoptotic cells (for flat phenotype cells) across the dose range tested, as for a dose response curve. From this I observed that the concentration of PIK75 that resulted in an absolute 50% inhibition of the maximal inhibitory effect (GIC50), as determined by reduction in nuclei number or increase in apoptotic cells, was similar to the GIC50 values calculated from the SRB assays (Tables 4.3 and 4.5).

It is intriguing that although PIK75 is observed to have a similar dose-dependent effect on both flat phenotype and branched phenotype cells using a SRB assay, the mechanism of this effect differs between the two different primary culture cell phenotypes. Whilst the flat phenotype cells undergo dose-dependent apoptosis, the mechanism of the dose-dependent reduction in total nuclei number in the branched phenotype cells is not clear. However, not all cell death is apoptotic, so in order to detect whether there was evidence of dose-dependent non-apoptotic cell death in the branched phenotype cultures I next performed an assay using the nuclear marker Sytox green (Figure 4.6). Sytox green does not enter live cells and its accumulation in dead cells is not dependant on enzyme-induced activation [253]. It is therefore a non-specific marker of all dead cells, not just apoptotic cells.

Branched phenotype primary cultures were treated with PIK75 across an eight-point half-log dose range as before. Each experiment was performed on at least three separate replicate plates, each plate containing three replicate wells. The total number of nuclei, and of Sytox green-positive nuclei, were plotted at each dose point, as illustrated in Figure 4.6. These charts have a similar profile to those in Figure 4.5; there is a dose-dependent reduction in total nuclei number, but no evidence of dose-dependent non-apoptotic cell death. This suggests that in branched phenotype primary cultures the PIK75 dose-dependant reduction in nuclei number does not result from increased cell death. It is therefore possible that cell cycle arrest is involved, which I investigated next.

Figure 4.5 An assay of PIK75-induced apoptosis. Putative glioma stem-like cells proliferated for 48 hours before treatment with the PI3 kinase p110α catalytic subunit-specific inhibitor PIK75 for 48 hours across a half-log dose range, as indicated below. The cells were then stained, first with the Nucview 488 caspase detection reagent to detect apoptosis and then with Hoechst nuclear dye to visualise the total number of nuclei present. Automated image capture and analysis was performed with the Olympus ScanR microscope and software. The primary cultures designated CC2 (anaplastic oligodendroglioma) and X (GBM) are shown as representative examples of the 2 flat phenotype and 3 branched phenotype primary cutures, respectively, that were assayed in this experiment. Each experiment involved three replicates of each compound treatment and this was repeated at least twice for every primary culture examined. The columns represent the mean total number of nuclei, normalised to a DMSO-treated control, from three independent experiments. The error bars represent the standard error of the mean. The red sections (with negative error bars) are the portion of Nucview positive, apoptotic cells. The portion of Nucview negative cells is shown in blue. Asterisks indicate a significant decrease in nuclei number and crosses indicate a significant increase of the percentage of apoptotic cells, compared to the DMSO-treated control. Significance was determined by ANOVA tests. */+, $p < 0.05$; **/++, $p < 0.01$; ***/+++, $p < 0.001$. Media (untreated), staurosporin (STS) and Taxol, were used as controls. The graphs illustrate that PIK75 has a dose dependent effect on both flat and branched phenotype cells. This results from apoptosis in the flat phenotype cells, but not in the branched phenotype cells.

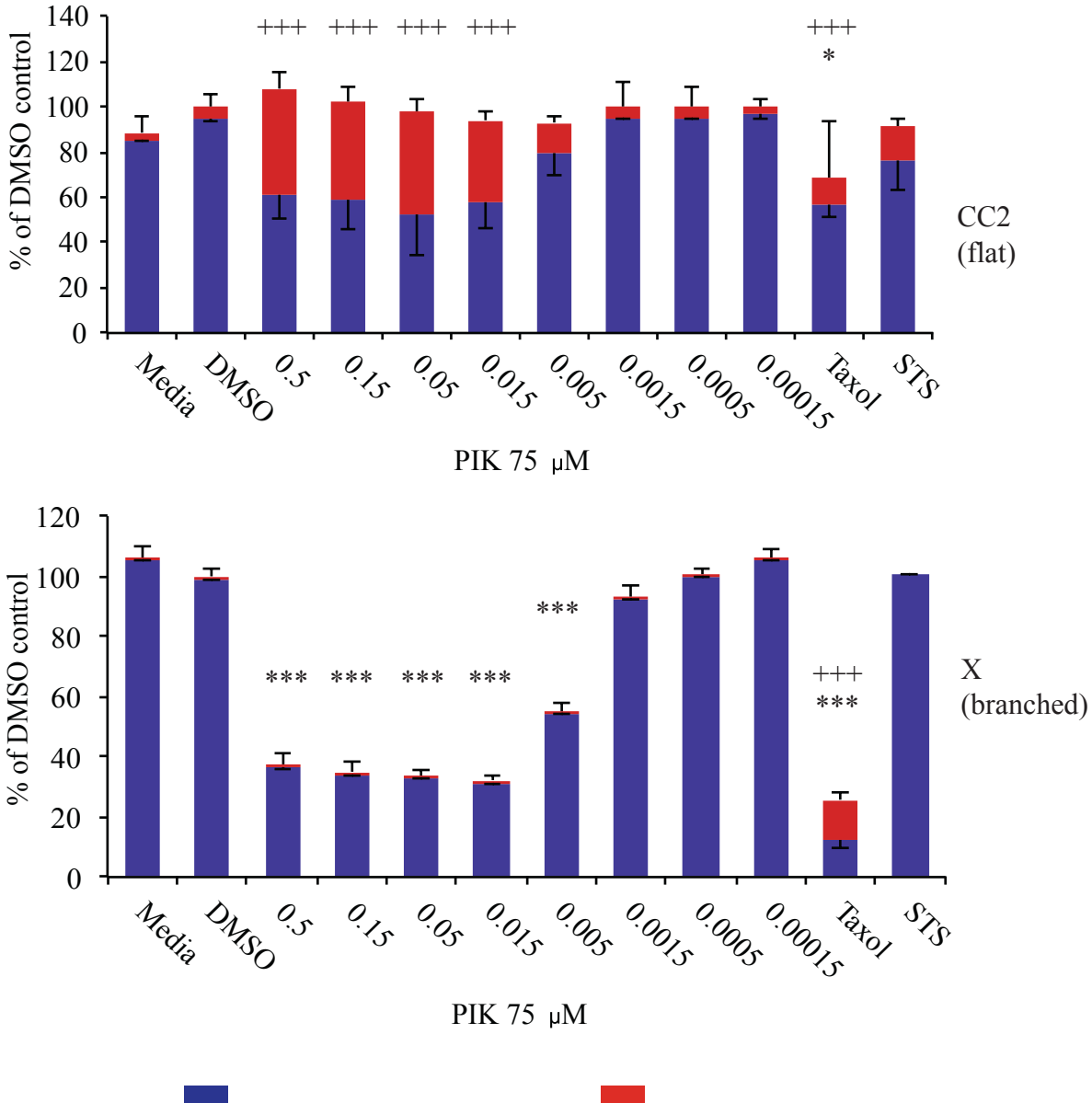

Table 4.5 The half-maximal effective concentration of PIK75. Glioma primary culture cells were plated for 48 and then treated with PIK75 for a further 48 hours. Nuclei were stained with Hoechst dye and apoptotic cells were stained with NucView substrate. The total number of nuclei (for branched phenotype cells) or apoptotic nuclei (for flat phenotype cells) at each treatment dose was plotted to obtain a dose response curve, similar to Figure 4.3. The concentration of PIK75 required to give the absolute 50% inhibition of the maximal inhibitory effect (GIC50) was then determined, using the GraphPad Prism software. Primary cultures are listed in the table according to their alphanumeric designation. The 'E' notation used in the table indicates the preceding number is raised to the power 10. For example, 'E-09' indicates that the preceding number is raised by 10 to the minus 9. The results indicate that the GIC50 are similar to the results obtained from the SRB experiments described earlier.

Primary culture	GIC50
DD1 (gliosarcoma)	2.26E-09
X (GBM)	4.66E-09
CC2 (anaplastic oligodendroglioma)	1.04E-08
EE2 (oligodendroglioma)	1.51E-08

Figure 4.6 An assay of PIK75-induced cell death. The branched phenotype glioma primary cultures designated DD1 (gliosarcoma) and X (GBM) were plated for 48 hours and then treated with PIK75 across a half-log dose range for a further 48 hours (as indicated below). Cells were then incubated with the Sytox green nuclear stain that is impermeable to live cells. This allows the total number of dead cells to be counted. Each experiment was performed on at least three separate replicate plates, each plate containing three replicate wells. The total number of nuclei was determined using Hoechst nuclear dye. Automated image capture and analysis was performed with the Olympus ScanR microscope and software. In the graphs, nuclei stained with Sytox Green appear in green and unstained nuclei are indicated in blue. The columns represent the mean total number of nuclei, normalised to a DMSO-treated control, from the three independent experiments. The error bars represent the standard error of the mean. Media (untreated), staurosporin (STS) and Taxol, were used as controls. The graphs illustrate that the dose-dependent decrease in branched phenotype cell number in response to PIK75 is not caused by non-apoptotic cell death.

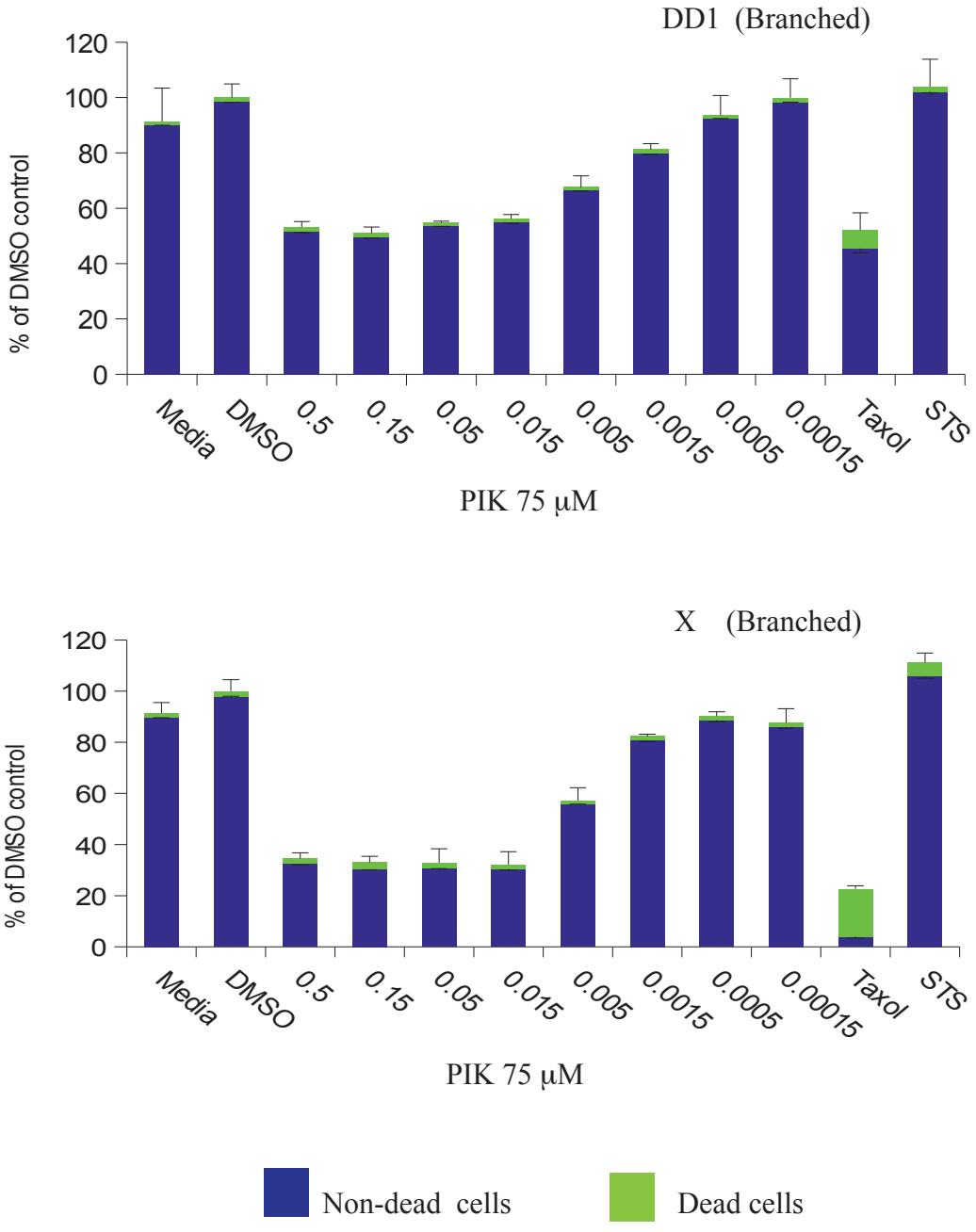

4.7 PIK75 induces G2/M arrest in branched phenotype cells

I examined whether cell cycle arrest of PIK75-treated branched phenotype primary culture cells explained the observed dose-dependent reduction in nuclei number in the absence of increased cell death (Figure 4.7). Primary culture cells were treated with PIK75 across an eight-point half log dose range as before. After 48 hours cells were fixed and the nuclei stained with Hoechst dye. Hoechst 33342 binds to AT-rich regions in DNA and internalisation into cells is accomplished by the ABC-transporter [254]. The DNA content of each cell was therefore determined from the intensity of the Hoechst stain in each nucleus, and this information was used to establish the cell cycle status (G1, S and G2/M) of each cell using Olympus Scan^R software. PIK75 was observed to induce a subtle but not statistically significant dose-dependent G2 arrest in the two branched phenotype primary culture cells examined, designated DD1 (Gliosarcoma) and X (GBM) (Figure 4.7). This was also seen in the flat phenotype primary cultures designated CC2 (Anaplastic oligodendroglioma) and EE2 (Oligodendroglioma) (Figure 4.7).

Cells from the 3 branched phenotype primary cultures designated X (GBM), P (GBM) and DD1 (Gliosarcoma) were next probed with antibodies to the cell cycle marker phosphohistone H3 (pHH3). Antibody binding was visualised with secondary fluorescent antibodies. There was a marked PIK75 dose-dependant reduction in pHH3 at high inhibitor concentrations in all three primary cultures (Figure 4.8). This was statistically significant as determined by ANOVA tests. Histone H3 is specifically phosphorylated during mitosis to give pHH3, and dephosphorylated on exit from mitosis [255]. This suggests that branched phenotype cells treated with PIK75 arrest in late G2 or early prophase, prior to the onset of mitosis.

Figure 4.7 Cell cycle effects of PIK75. Glioma primary cultures were plated for 48 hours and then treated for a further 48 hours with PIK75 across a half-log dose range, as indicated below. Cells were fixed with 4% Paraformaldehyde and the distribution of cells in G1/S and G2/M phase was determined based on nuclear DNA content after staining with Hoescht nuclear stain. Automated image capture and analysis was performed with the Olympus ScanR microscope and software. The graphs show the mean of three replicates from each of three independent experiments. The error bars represent the standard error of the mean. Asterisks indicate a significant change in the proportion of cells in the respective cell cycle phase compared to a DMSO-treated control. Significance was determined by ANOVA tests. */+, $p < 0.05$; **/++, $p < 0.01$; ***/+++, $p < 0.001$. Media (untreated), staurosporin (STS) and Taxol, were used as controls. The primary cultures DD1 (gliosarcoma) and EE2 (oligodendroglioma) are shown as representative examples of branched phenotype and flat phenotype cultures, respectively. The graphs illustrate that PIK75 induces a subtle but not statistically significant dose-dependent G2 arrest in the branched phenotype primary culture cells designated DD1. A similar G2 arrest in the flat phenotype primary culture designated EE2 did reach statistical significance at higher inhibitor concentrations.

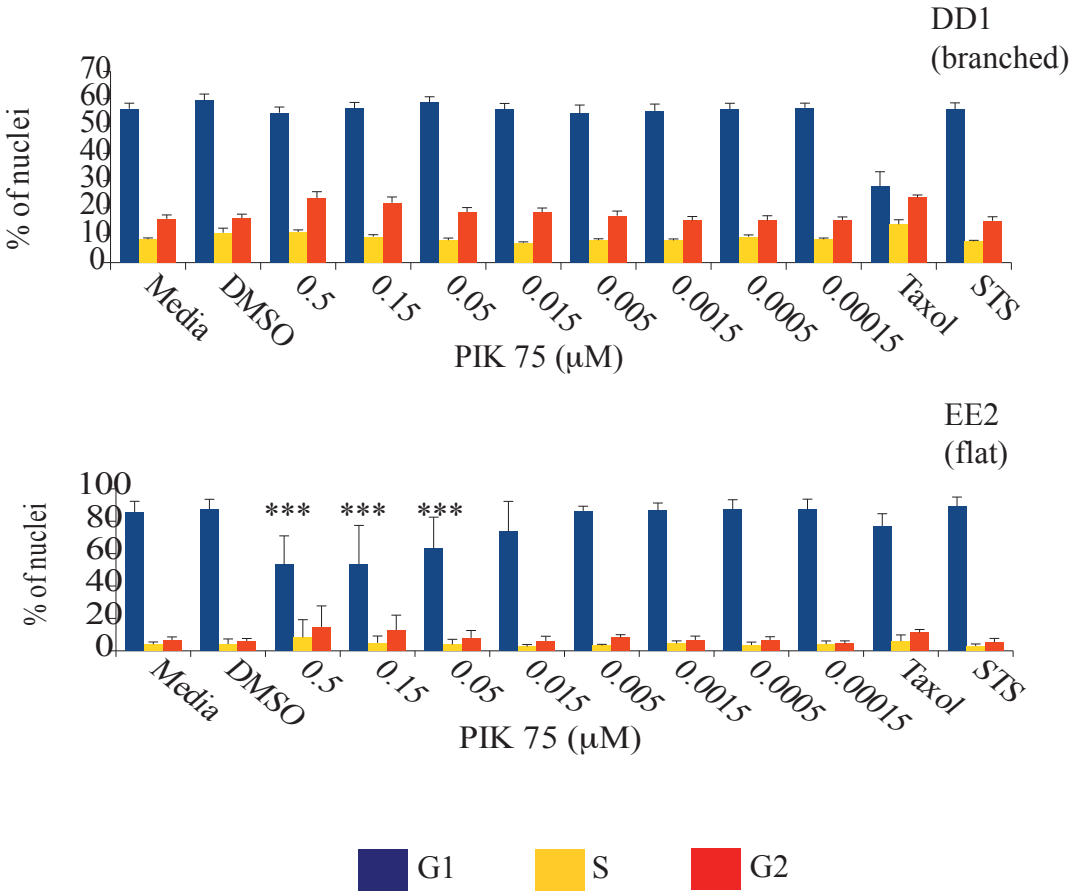

Figure 4.8 Analysis of PIK75-induced cell cycle arrest. Cells from the branched phenotype glioma primary cultures DD1 (gliosarcoma), P (GBM) and X (GBM) proliferated for 48 hours before treatment with PIK75 for a further 48 hours. Cells were then fixed with 4% Paraformaldehyde, incubated with a blocking buffer to prevent non-specific antibody binding, then stained with a rabbit anti-phospho Histone H3 (pHH3) antibody (1:1000) for 1 hour. Secondary fluorescent-labelled antibodies were used for visualisation of primary antibody binding. The total number of nuclei was determined by staining with a Hoechst nuclear stain. Automated image capture and analysis was performed with the Olympus ScanR microscope and software. The graphs show the mean percentage of nuclei staining with antibodies to pHH3. Each experiment contained three replicates and was performed twice. The error bars indicate the standard deviation. Asterisks indicate the statistical significance of PIK75-induced changes on cell cycle compared to a DMSO-treated control, as determined by ANOVA tests. *, $p < 0.05$; **, $p < 0.01$; ***, $p > 0.001$. There was a marked PIK75 dose-dependant reduction in pHH3 at high inhibitor concentrations, suggesting that branched phenotype cells treated with PIK75 arrest in late G2 or early prophase, prior to the onset of mitosis.

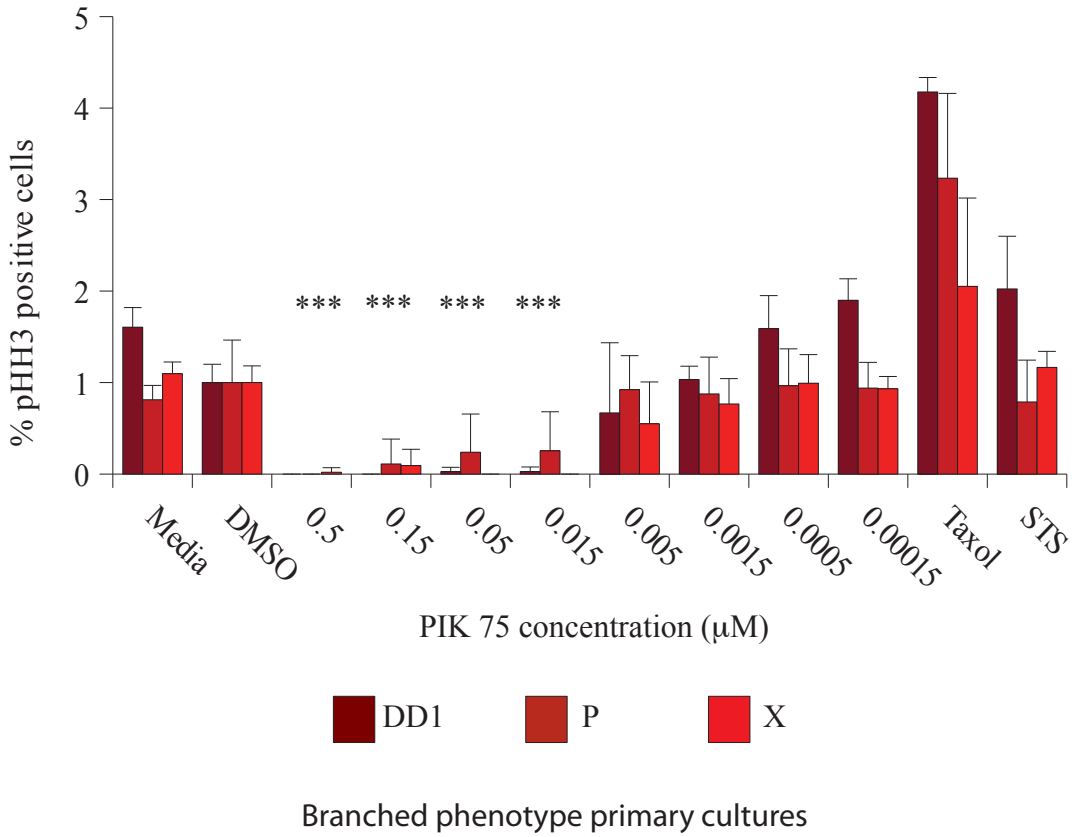

4.8 Analysis of the cell death response to inhibitors KU63794 and Barasertib

I next assayed the apoptotic response of glioma primary cultures to the compounds KU63794 and Barasertib. I described above that the efficacy of these inhibitors varied between different glioma primary cultures when assessed with an SRB assay (Table 4.2). For example, the mTOR inhibitor KU63794 was observed to have a dose-dependant effect on five of eight of the branched phenotype primary cultures examined (Table 4.3). No response in flat phenotype cells was observed (Table 4.3). I therefore wanted to ascertain whether the cell death and cell cycle assays might be more sensitive to dose-dependant compound efficacy than the total protein assay alone. This is important to know if potentially effective therapies are not to be inadvertently overlooked at the in vitro screening stage.

I observed no significant dose-dependant change in the number of apoptotic cells in either the branched or flat phenotype primary cultures treated with the KU63794 inhibitor (Figure 4.9). However, in the primary cultures in which a dose-dependant reduction in total-protein was previously observed with the SRB assay, such as that designated DD1 (Gliosarcoma), a significant dose-dependent reduction in total nuclei number was seen, supporting the SRB data (Table 4.3). These experiments suggest that the action of the KU63794 inhibitor against my putative glioma stem-like cells is not mediated through induction of apoptosis.

I described previously that the aurora kinase B inhibitor Barasertib had a dose-dependant effect on glioma primary cultures in a SRB assay of total protein, but only at micromolar concentrations (Figure 4.10). Consistent with this, there was no dose-dependent reduction of cells in the flat phenotype primary cultures designated CC2 (Anaplastic oligodendroglioma) or EE2 (Oligodendroglioma), within the dose range examined (Figure 4.11). However, the apoptosis assay did demonstrate a significant dose-dependant reduction in total cell nuclei in branched phenotype cultures (DD1)

Figure 4.9 The dose-dependant effect of the mTOR inhibitor KU63794 on glioma primary cultures. Primary culture cells were treated with the mTOR inhibitor KU63794 for 48 hours across a half-log dose range, as indicated below. Cultures were stained with the Nucview 488 caspase detection reagent to identify apoptotic cells and the Hoechst nuclear dye to visualise the total number of nuclei. The primary cultures designated CC2 (anaplastic oligodendroglioma) and X (GBM) are shown as representative examples of flat phenotype and branched phenotype primary cutures, respectively. The columns represent the mean total number of nuclei, normalised to a DMSO-treated control, from three independent experiments. The error bars represent the standard error of the mean. The red sections (with negative error bars) are the portion of Nucview positive, apoptotic cells. The portion of Nucview negative cells is shown in blue. Asterisks indicate a statistically significant decrease in nuclei number. Crosses indicate a statistically significant increase in the percentage of apoptotic cells compared to the DMSO-treated control. Significance was determined by ANOVA tests. */+, $p < 0.05$; **/++, $p < 0.01$; ***/+++, $p < 0.001$. Media (untreated), staurosporin (STS) and Taxol were used as controls. I observed no significant dose-dependant change in the number of apoptotic cells in either branched or flat phenotype cells.

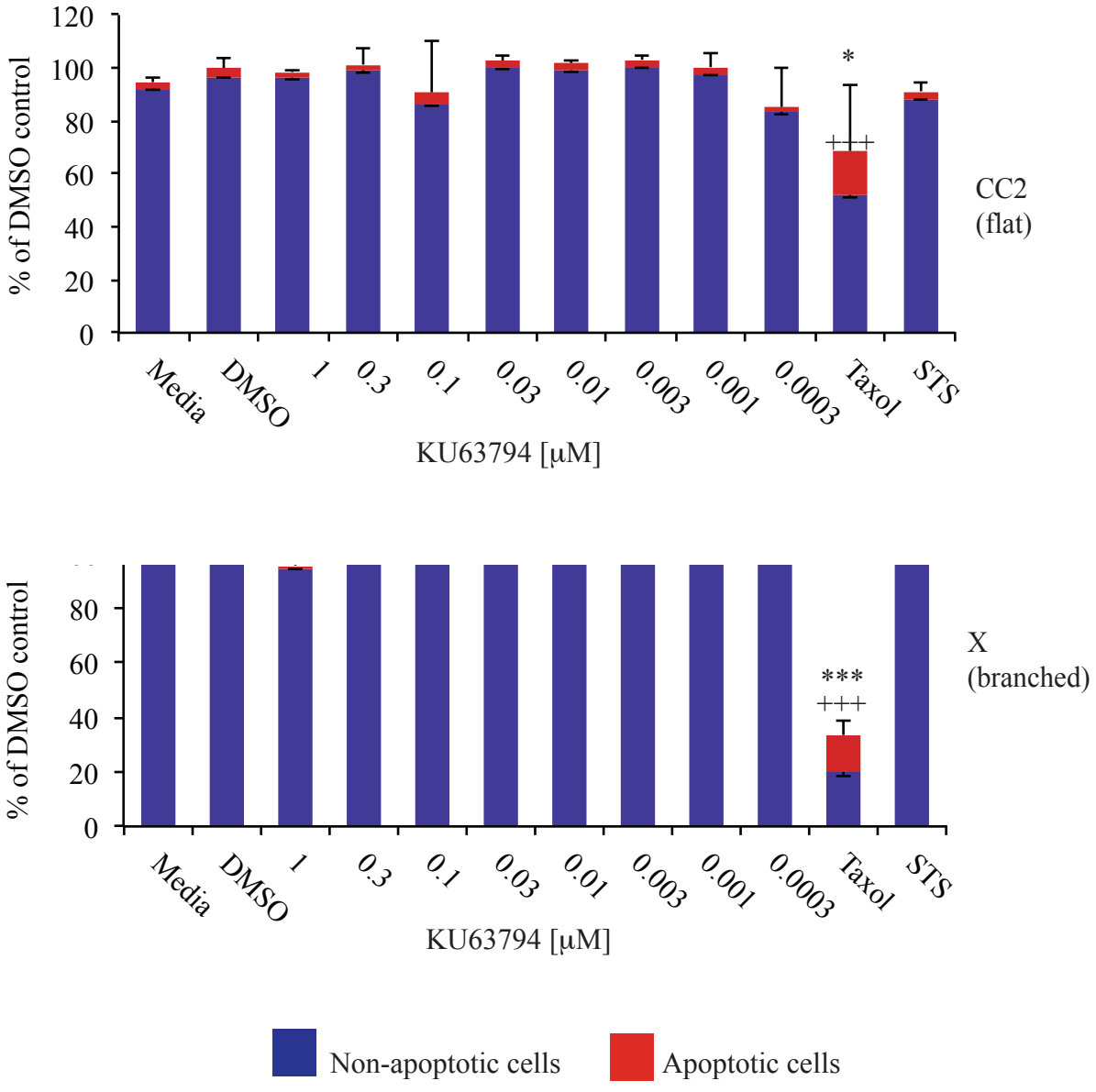

Figure 4.10 Efficacy of the Aurora kinase inhibitor Barasertib on glioma primary cultures. Branched phenotype cells from the primary cultures designated DD1 (gliosarcoma), X (GBM) and P (GBM) were plated for 48 hours and then treated for a further 48 hours with the Aurora kinase B inhibitor Barasertib across a half-log dose range, as indicated. Cells were then fixed with 25% trichloroacetic acid and the total protein assayed with a SRB assay. The percentage change in total protein compared to a DMSO-treated control is plotted against inhibitor concentration in the graph. Each experiment contained three repeats at each inhibitor concentration. Each experiment was performed at least twice. A sigmoidal dose-response curve was fitted to the points using the GraphPad Prism software version 4.00. The results demonstrate that this compound had a marginal effect at inhibitor concentrations above 3μM in branched phenotype primary culture cells.

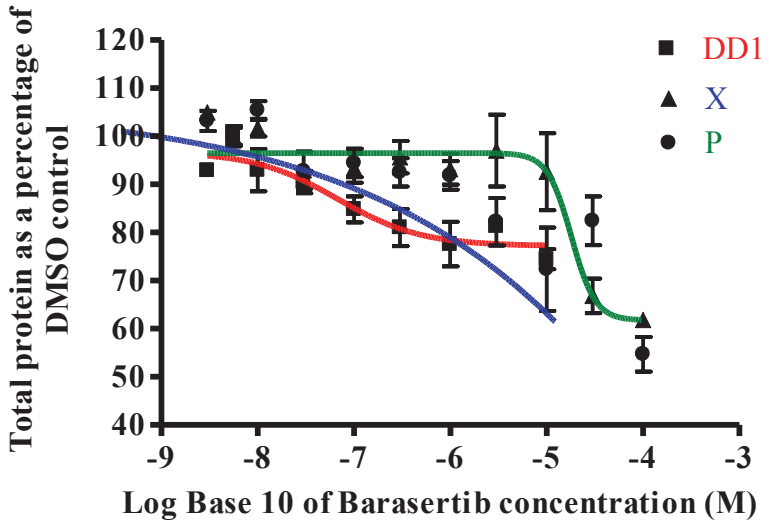

Figure 4.11 The dose-dependent effect of Barasertib on glioma primary cultures. Cells were plated for 48 hours and then treated for a further 48 hours with the Aurora kinase inhibitor Barasertib across a half-log dose range (as indicated below). Cells were stained with the NucView 488 caspase detection reagent to identify apoptotic nuclei. The total number of nuclei was determined using a Hoechst nuclear stain. Automated image capture and image analysis was performed with the Olympus ScanR microscope and software. The primary cultures designated DD1 (Gliosarcoma) and CC2 (anaplastic oligodendroglioma) are shown as representative examples of branched and flat phenotype cells, respectively. The columns of the graph represent the mean total number of nuclei, normalised to a DMSO-treated control, from three independent experiments. The error bars represent the standard error of the mean. The red sections (with negative error bars) are the portion of Nucview positive apoptotic cells. The portion of Nucview negative cells is shown in blue. Asterisks indicate a significant decrease in nuclei number. Crosses indicate a significant increase in the percentage of apoptotic cells, compared to the DMSO-treated control. Significance was determined by ANOVA tests. */+, $p < 0.05$; **/++, $p < 0.01$; ***/+++, $p < 0.001$. Media (untreated), staurosporin (STS) and Taxol were used as controls. The results illustrate that Barasertib had a dose dependent effect on branched phenotype cells only, but this was not mediated through increased apoptosis.

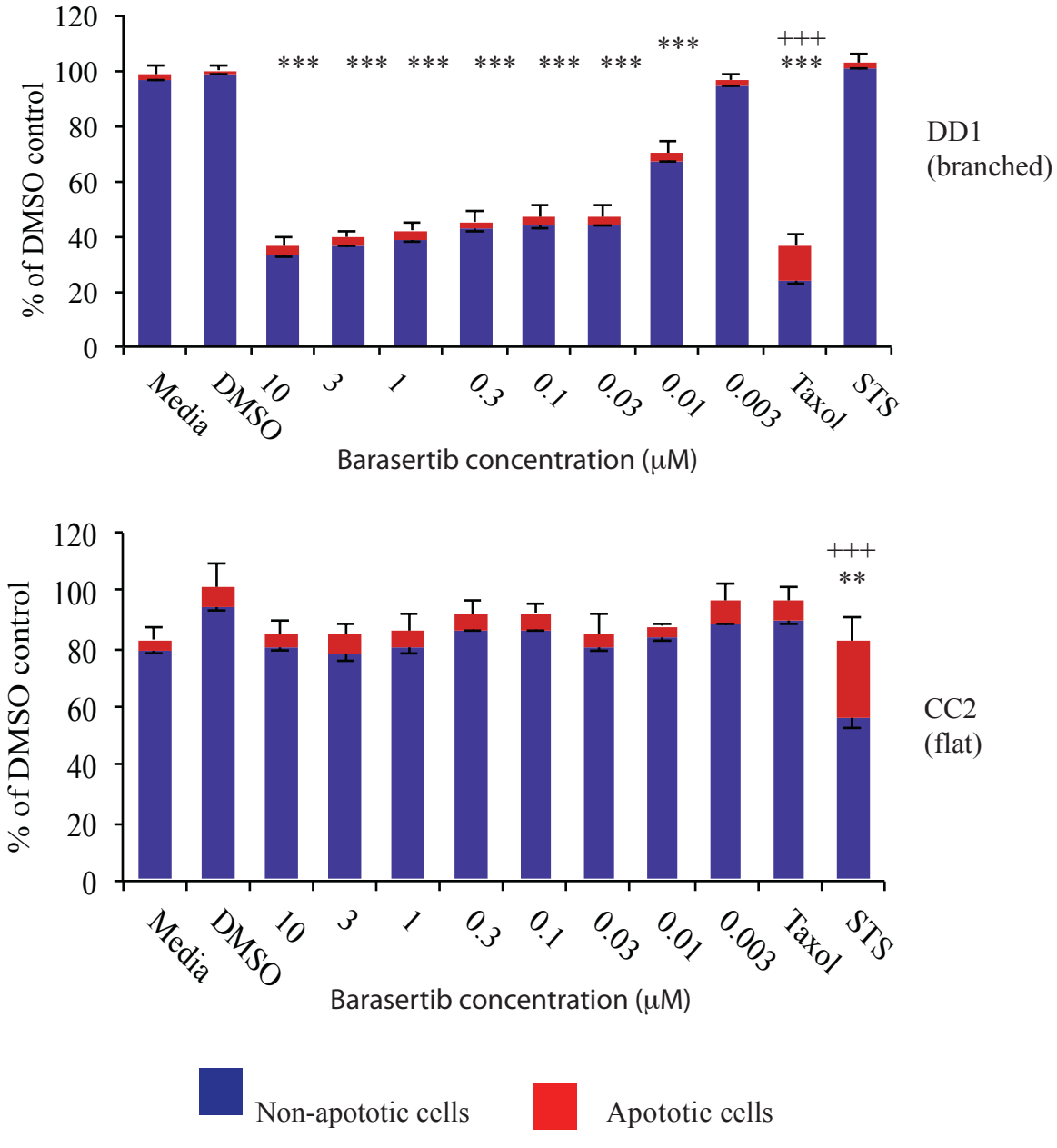

(Gliosarcoma), P (GBM) and X (GBM), although there was no significant change in the number of apoptotic cells (Figure 4.11). The absolute half-maximal effective concentration (GIC50) of the inhibitor Barasertib was calculated by plotting the dose-dependent reduction in cell number as for a dose response curve using GraphPad Prism software as described above. The GIC50 was calculated at $1.2x10^{-8}$ Molar.

The observation of a dose-dependant reduction in cell nuclei number in branched phenotype cultures in the absence of evidence of a concomitant increase in apoptosis is perhaps expected. This is because the Aurora kinases control transit of cells through G2 to cytokinesis, so inhibitors prevent mitosis and cause G2 arrest [256]. To test this hypothesis, I performed a cell cycle analysis of Barasertib-treated primary glioma cultures (Figure 4.12). As suspected, this identified that Barasertib induced a dose-dependant G2 cell cycle arrest in the branched phenotype but not flat phenotype cultures (Figure 4.12). The cell cycle arrest was observed as an increase in the number of cells in G2 and a decrease in the number of cells in G1 (Figure 4.12). The total protein content of a cell arrested in G2 immediately prior to mitosis will be greater than at other points in the cell cycle. This increased amount of protein may compensate for a reduction in total cell number caused by the inhibitor-induced cell cycle arrest (Figures 4.11 and 4.12). This perhaps explains why the SRB assay did not detect a significant dose-dependant reduction in total protein in the branched phenotype cells in response to Barasertib, despite the dose-dependent cell cycle arrest.

Aurora kinases act by directly phosphorylating Histone H3, a protein that is specifically phosphorylated during mitosis and dephosphorylated on exit from mitosis [255]. I therefore next assayed levels of pHH3 in Barasertib-treated branched phenotype primary cultures (Figure 4.13). As expected, I observed a dose-dependent reduction of pHH3 (Figure 4.13). This was statistically significant as determined by ANOVA tests, supporting the hypothesis that the compound is acting on glioma

Figure 4.12 Cell cycle effects of Barasertib. After 48 hours proliferation cells were treated for a further 48 hours with the Aurora kinase inhibitor Barasertib across a half-log dose range, as indicated below. Cells were fixed with 4% Paraformaldehyde. The distribution of cells in G1/S and G2/M phase was determined from the nuclear DNA content of each cell after staining with Hoechst nuclear stain. Automated image capture and analysis was performed with the Olympus ScanR microscope and software. The primary cultures designated DD1 (gliosarcoma) and EE2 (oligodendroglioma) are shown as illustrative examples of branched and flat phenotype cells, respectively. Each experiment included three replicates at each inhibitor concentration. Each experiment was performed three times. The error bars represent the standard error of the mean. Asterisks indicate a significant change in the proportion of cells in the respective cell cycle phase compared to a DMSO-treated control. Statistical significance was determined by ANOVA tests. */+, $p < 0.05$; **/++, $p < 0.01$; ***/+++, $p < 0.001$. Media (untreated), staurosporin (STS) and Taxol were used as controls. The graphs illustrate that the dose-dependent effect of Barasertib on branched phenotype cells was mediated through G2/M cell cycle arrest, as would be predicted from the known mechanism of action of the Aurora kinase inhibitors.

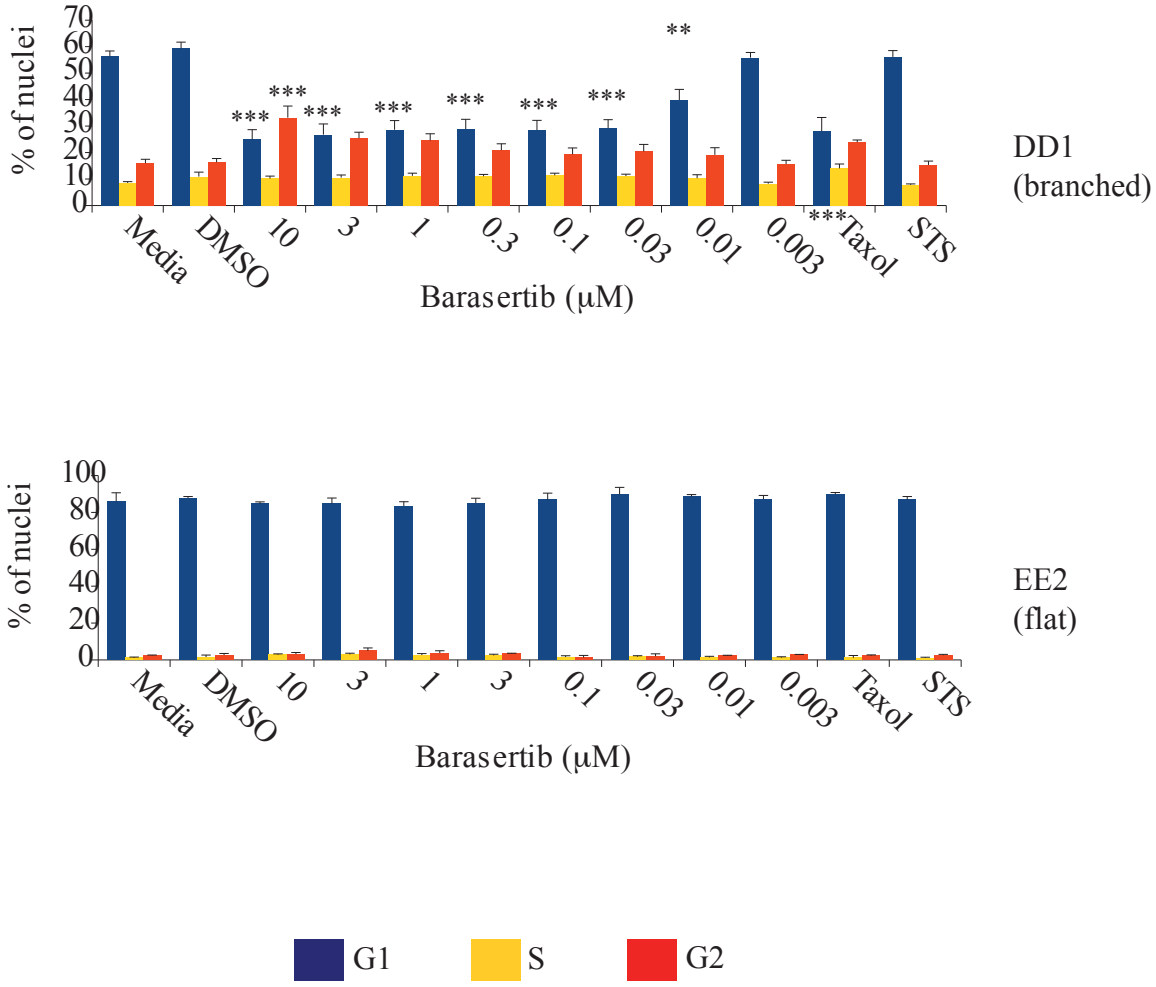

Figure 4.13 Analysis of Barasertib-indued cell cycle arrest. After proliferating for 48 hours, glioma primary culture cells were treated with the Aurora kinase inhibitor Barasertib for a further 48 hours across a half-log dose range, as indicated below. Cells were fixed with 4% Paraformaldehyde, incubated in a blocking buffer, then stained with a rabbit anti-phospho Histone H3 (HH3) antibody (1:1000) for 1 hour. Secondary fluorescent-labelled antibodies were used for visualisation of primary antibody binding. The total number of nuclei was determined by staining with Hoechst nuclear stain. The graph shows the percentage number of nuclei staining with antibodies to pHH3 at each inhibitor concentration. The branched phenotype primary cultures designated DD1 (gliosarcoma), P (GBM) and X (GBM) are shown as representative examples. Each experiment contained three replicates and was performed at least twice. The error bars indicate the standard deviation. Asterisks indicate significant changes at a given inhibitor concentration compared to a DMSO-treated control, as determined by ANOVA tests. *, $p < 0.05$; **, $p < 0.01$; ***, $p > 0.001$. The graph illustrates a dose dependent reduction in phospho-histone H3 in all the primary cultures. This is consistent with the expected mechanism of action of the aurora kinase inhibitor Barasertib, causing cell cycle arrest prior to entry into mitosis.

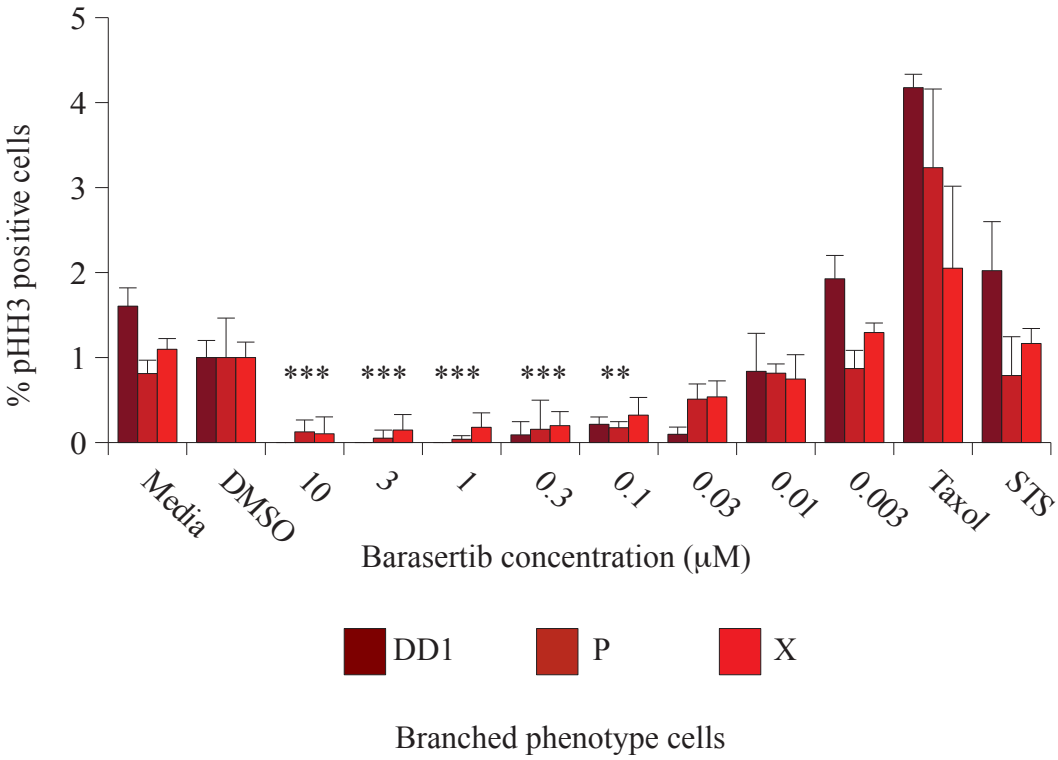

primary culture cells through induction of cell cycle arrest, although an alternative explanation is that the inhibitor changes the length of the cell cycle phases rather than actually inducing cell cycle arrest. Levels of pHH3 were not examined in flat phenotype primary cultures because Barasertib did not have a dose-dependent effect on the cell cycle in these cells (Figure 4.11).

4.9 Assessing the specificity of PIK 75 inhibitory action on the PI3 Kinase pathway

I have previously described the dose-dependent effect of the inhibitor PIK75 on both branched and flat phenotype glioma primary cultures (Table 4.1, Figure 4.3). I have interrogated the effector mechanism of this inhibitor (Figures 4.5-4.7). It is important to also examine whether the action of PIK75 on these primary culture cells is specifically mediated through its PI3 kinase p110α catalytic subunit target, or instead via off-target actions; off target actions are likely to manifest as toxicity in the clinic. To address this question I performed a reverse phase protein microarray (RPPA) that permits measurement of protein expression levels in a large number of biological samples simultaneously and quantitatively [203]. By examining changes in expression of a protein in response to increasing inhibitor concentrations it is possible to ascertain whether the inhibitor is acting via its predicted mechanism of action [203]. In Chapter 2 I described the rationale for using a RPPA approach to assaying proteins rather than western blotting. RPPA has also been validated as equivalent to western blotting [204].

I examined the PIK75 dose-dependant change in phosphorylation of the PI3 kinase pathway protein Akt at its serine 473 residue in the branched phenotype primary cultures designated DD1 (Gliosarcoma) and P (GBM), and in the flat phenotype primary culture designated CC2 (Anaplastic oligodendroglioma). Phosphorylation of Akt is mediated by upstream PI3 kinase activity and is a feature of pathway

activation [241]. Inhibition of the p110α catalytic subunit of PI3 kinase activity should reduce Akt phosphorylation (Figure 1.6). As predicted, I observed that increasing PIK75 inhibitor concentration was associated with decreasing levels of Akt phosphorylation in both branched and flat phenotype primary culture cells (Figure 4.14). In contrast, levels of total Akt remained unchanged across the inhibitor dose range examined, indicating that the observed change in the levels of phosphorylated Akt was a true reflection of altered Akt activation (Figure 4.14). In contrast, there was no dose-dependent change in levels of the p110α protein, confirming that PIK75 is inhibiting only the function of p110α and not its synthesis.

In a screen of proteins in other key cancer survival pathways, including the Mitogen Activated Protein Kinase pathway, I did not observe any PIK75 dose-dependent changes. Interestingly, interrogation of mTOR and S6 ribosomal protein expression downstream of Akt suggested that there was some heterogeneity between primary cultures in the response to PIK75 inhibition. For example, in the branched phenotype primary culture designated P (GBM) there was a decrease in levels of the mTOR protein with increasing PIK75 concentration, but this was not seen in the flat phenotype primary culture designated CC2 (Anaplastic oligodendroglioma) (Figure 4.15). This is an important area for further interrogation in future RPPA studies, because the changes that occur in signalling pathways in response to inhibitor compounds have implications for therapy resistance. These changes therefore need to be understood to guide development of effective combinatorial therapies.

4.10 Developing an assay of glioma stem-like cell invasion

Glioma cells that invade into the normal brain surrounding a tumour limit the adequacy of surgical resection and contribute to tumour recurrence [33, 237]. Eliminating these invading cells might effectively downgrade a tumour into a more focal mass that could be dealt with by local treatments such as surgery. The

Figure 4.14 PIK75 inhibits Akt phosphorylation. Cells were plated for 48 hours, then treated with PIK75 for 30 minutes across the dose range indicated below. Lysates were prepared from these samples and spotted onto coated ZeptoMark protein microarray chips across a dilution series. The chips were then blocked before primary antibody incubation overnight at a 1:1000 dilution. The chips were washed, incubated with a fluorecent-labelled secondary antibody at a 1:500 dilution, then the fluorescent intensity was measured by planar wave-guide technology. The primary cultures designated P (GBM) and CC2 (anaplastic oligodendroglioma) are shown as illustrative examples of branched and flat phenotype cells, respectively. The columns represent the mean of triplicate repeats, each repeat representing a series of serial dilutions of each lysate. The error bars indicate the mean of the standard deviation of each repeat. Controls were performed by omitting the primary antibody and were used to calibrate the test antibodies. The graphs illustrate a dose-dependent reduction in phospho-Akt (serine 473), but not total Akt, suggesting that PIK75 is acting through its PI3 kinase target.

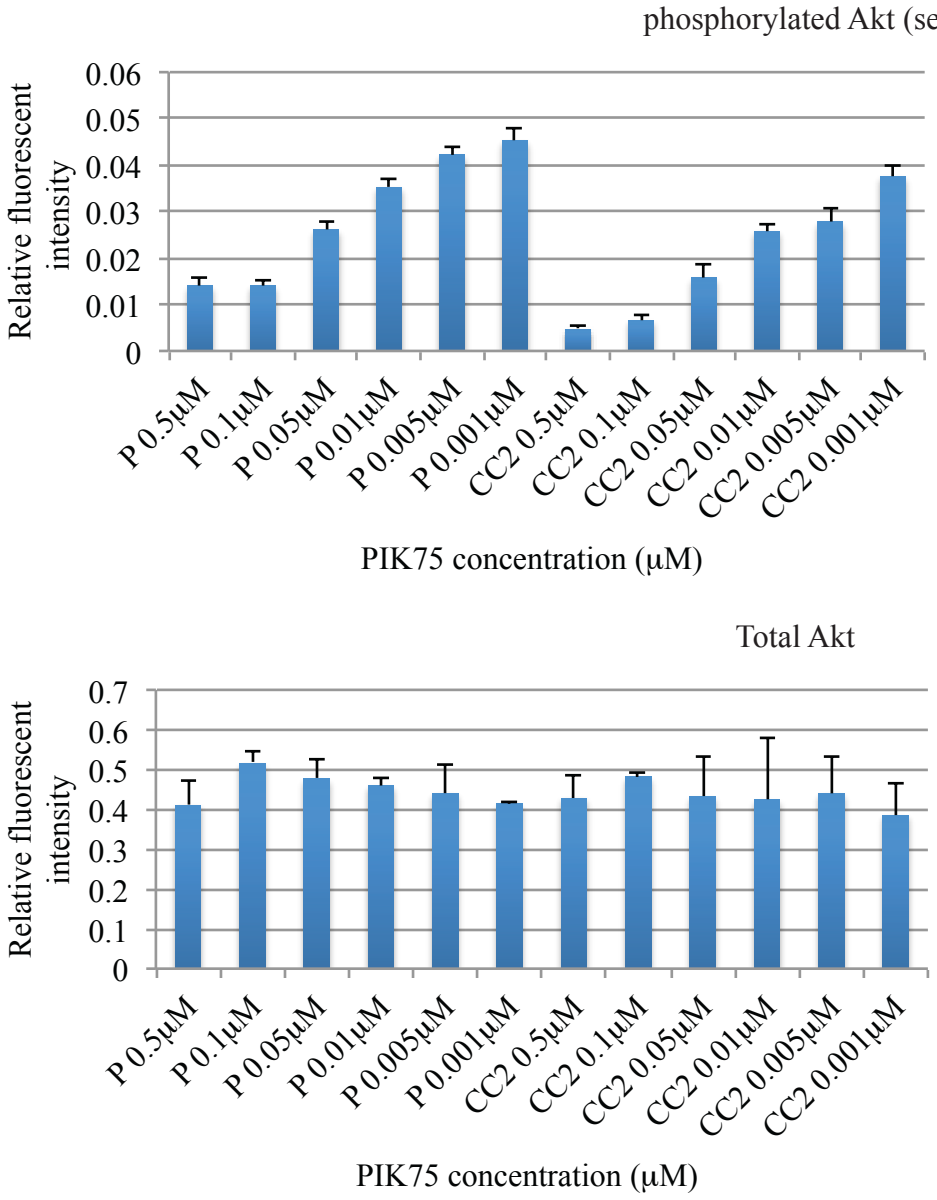

Figure 4.15 Heterogeneity between primary cultures of PIK 75-induced mTOR activation. Cells were plated for 48 hours, then treated for 30 minutes with the PIK75 inhibitor across the dose range indicated. Lysates prepared from each sample were spotted onto coated ZeptoMark protein microarray chips across a dilution series. Chips were blocked to prevent non-specific binding and then incubated with an antibody to the protein mTOR (1:1000) overnight. After washing, the chips were incubated with a fluorecent-labelled secondary antibody (1:500). The fluorescent intensity was measured by planar wave-guide technology. The primary cultures designated P (GBM) and CC2 (anaplastic oligodendroglioma) are illustrated as examples of branched and flat phenotype cultures, respectively. The columns represent the mean of triplicate repeats, each repeat representing a series of serial dilutions of each lysate. The error bars indicate the mean of the standard deviation of each repeat. Controls were performed by omitting the primary antibody and these results used to calibrate the test antibodies. The graphs illustrate heterogeneity amongst the primary cultures in their mTOR response to the inhibitor PIK75. Cells in the primary culture designated P have a dose-dependent reduction in mTOR protein levels, but this is not seen in the culture designated CC2. Signalling pathway changes in response to compound inhibition have important implications for treatment resistance and need to be understood to guide development of effective combinatorial therapies.

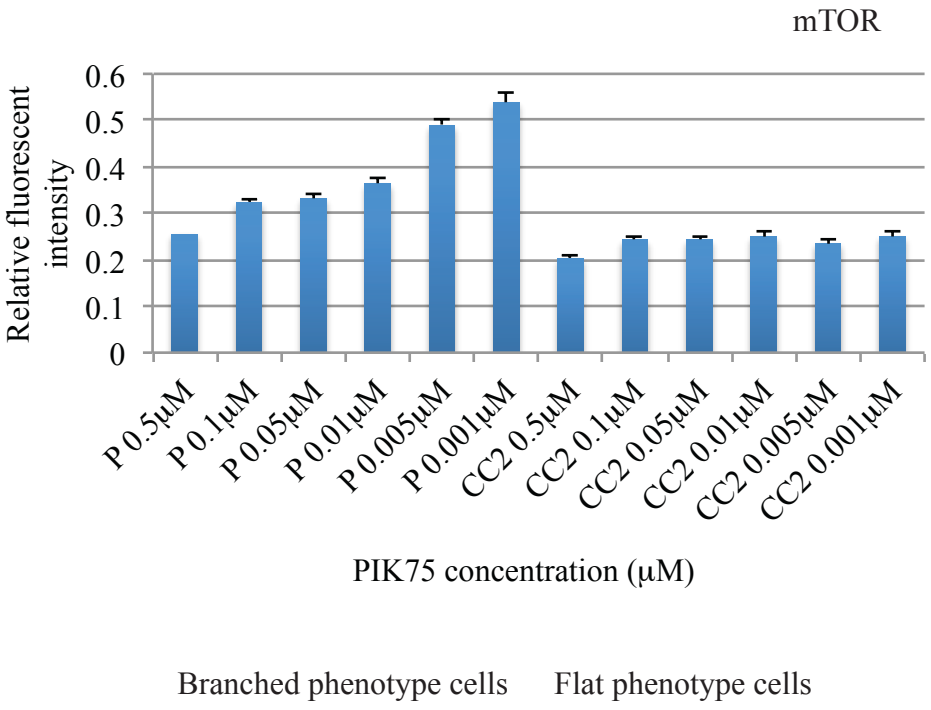

identification of new anti-invasive compounds is therefore a priority for glioma research. This requires in vitro assays of cell invasion to screen compounds. However, despite the emergence of the glioma stem cell hypothesis, in vitro assays of glioma invasion continue to utilise established serum-grown glioma cell lines rather than glioma stem-like cells [257]. To my knowledge, no in vitro assay of glioma stem-like cell invasion has been described. I therefore developed an assay of putative glioma stem-like cell invasion based on the previously described inverse invasion assay [258]. I used this model to screen potential inhibitors of cell invasion and also to compare the invasive abilities of branched and flat phenotype cells. The invasion of cells upwards though a matrix plug placed in a Transwell filter was examined over a five-day time course. Confocal microscopy was used to acquire a Z-stack of images through the plug at 15 micron intervals from the chamber filter onto which the cells had been plated. The maximum distance of invasion was the furthest distance that any single cell was detected from the filter. At least four measurements were made in each matrix plug with at least two replicate experiments.

The standard matrix substrate used in inverse invasion assays is Matrigel [258]. However, I observed little cell invasion with a Matrigel plug, presumably because my primary cultures were selected to adhere to Matrigel. I instead utilised a type I collagen matrix (Purecol™) and observed that cell invasion through the plug did occur (Figure 4.16). This collagen matrix plug was chosen because its structure is thought to best recapitulate the brain environment in vivo through which glioma cells invade [259]. However, even with the type I collagen plug only a small proportion of the cells plated appeared to actually cross the chamber filter and invade. The branched phenotype primary culture cells that did not invade proliferated on the chamber filter and formed non-adherent or semi-adherent glioma-derived spheres (Figure 4.16). The formation of glioma-derived spheres on the chamber filter was not observed with flat phenotype cultures, consistent with the clonogenic assay data I described previously (Table 3.6). The flat phenotype cells adhered to the chamber filter and invaded into the type I collagen plug (Figure 4.16).

Figure 4.16 Assays of glioma primary culture cell invasion. Glioma primary culture cells were plated onto the filter of an inverted Transwell chamber containing a plug of type 1 collagen. After 5 days the Transwell chambers were incubated with 4μM Calcein to stain live cells. An Olympus FV1000 confocal microscope was used to take a Z-stack of images through the collagen plug from the level of the filter at 15 micron intervals using a 20x objective. (A) and (B) Montages of Z stack images made using Image J software to illustrate invasion of branched phenotype and flat phenotype primary culture cells, respectively. Branched phenotype cells that did not invade formed glioma-derived spheres on the Transwell filter, but this was not observed with the flat phenotype cells. (C) Image J software was used to calculate the maximum distance of cell invasion under standard media conditions (Media) or with the addition of 1nM Hepatocyte Growth Factor (HGF). The box plots in the graph represent measurements of the maximum distance invaded by any single cell made from at least 4 Z-stacks in at least three replicate chambers. The cell phenotype of each primary culture is indicated; flat or branched. The graph illustrates that the addition of HGF to the standard culture media improved the invasion of cells in the primary culture designated EE2.

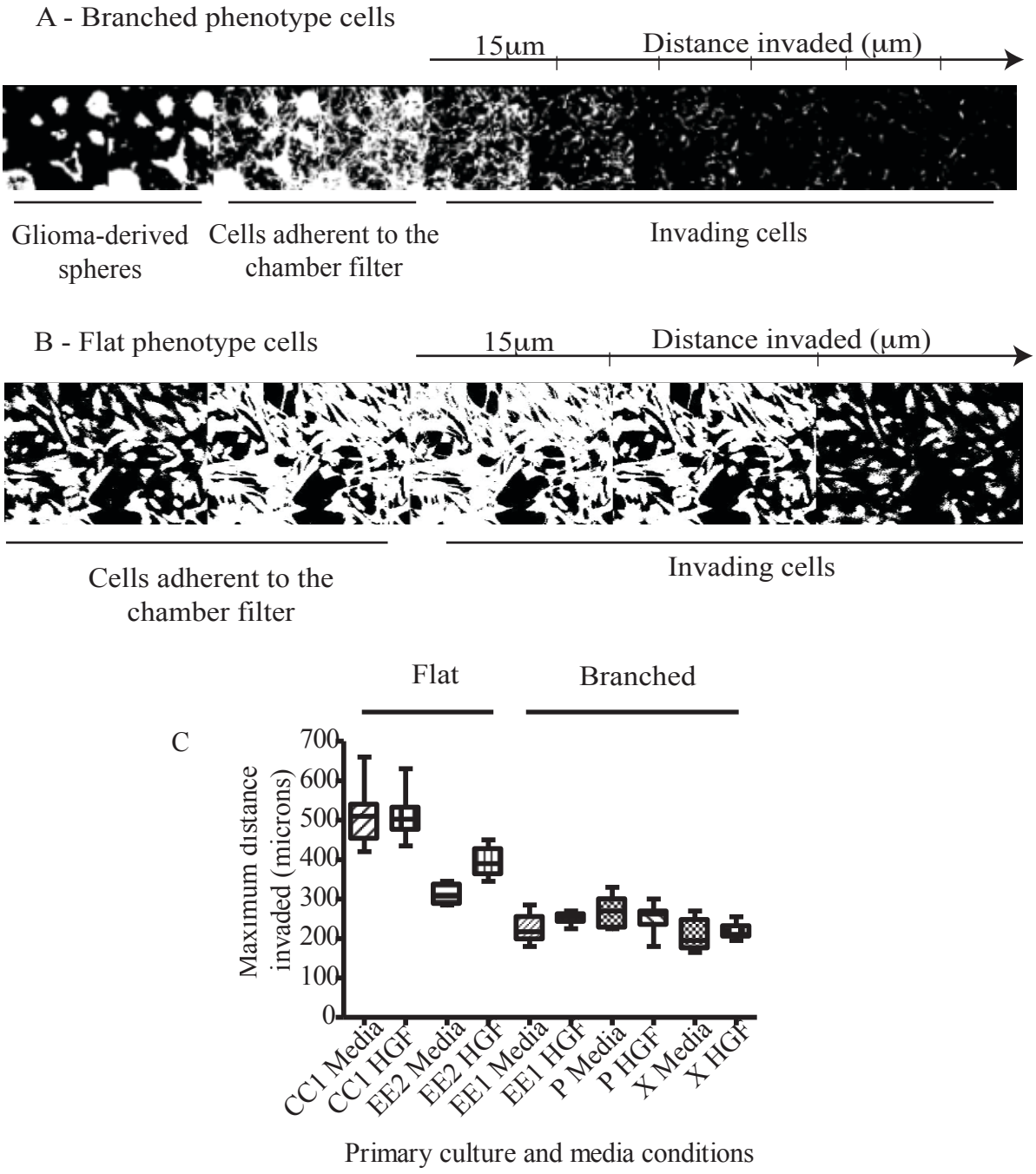

In an attempt to decrease the formation of glioma-derived spheres from branched phenotype cells plated onto the chamber filter, with the anticipation that this would improve the proportion of cells invading into the type I collagen plug, I tried coating the chamber filter with a thin layer of Matrigel before adding primary culture cells. Unfortunately, as I had observed with the use of an actual Matrigel plug, cells adhered to the Matrigel and proliferated, but did not invade.

I next attempted to increase the proportion of cells that invaded into the type I collagen matrix, and to increase the distance that these cells invaded, by manipulating the basic primary culture media conditions. I was particularly interested in the potential of different growth factor combinations to stimulate cell invasion. For example, it is known that Hepatocyte Growth Factor (HGF) levels within glioma tissue rise with increasing tumour grade [260]. HGF also promotes the in vitro migration of established serum-grown glioma cell lines on type IV collagen, laminin and Fibronectin substrates [260]. Basic FGF, in addition to HGF, is released from gliomas and both these growth factors are thought to have a role in glioma cell invasion [261]. Basic FGF was one of the two major growth factors already included in my standard growth media, along with EGF (Section 3.3.1).

I performed a number of experiments where the concentration of HGF and bFGF was varied, either together or in parallel, to assess the effect on in vitro cell invasion. In 4 of the 5 primary cultures examined, (CC1 (Anaplastic Oligodendroglioma), DD1 (Gliosarcoma), P (GBM) and X (GBM)), I did not observe any significant increase in the invasion of putative glioma stem-like cells in response to changing the HGF concentration, (over the range 0.1 nM to 100 nM), when compared to standard media conditions (Figure 4.16). However, there was a slight increase in the distance cells from the primary culture designated EE2 (Oligodendroglioma) invaded in response to addition of 1 nM HGF ($p=0.023$) (Figure 4.16). This increase in invasion was not associated with a statistically significant change in the total area of invading cells, suggesting that the increased distance invaded was not simply the consequence of an

increased number of cells invading (p=0.097). As HGF appeared to enhance invasion of cells from at least one of the primary cultures examined and since HGF had been shown in previous studies to influence the invasion of established serum-grown glioma cell lines, I decided to continue to supplement the standard primary culture media with HGF at a concentration of 1nM for all further experiments [260]. The 1nM HGF concentration was chosen because it is reported to be physiological [260].

I next examined the effect of bFGF on cell invasion over a range of concentrations from 6.3nM to 12.5μm, both alone and in combination with HGF. I observed no effect of bFGF concentration on the maximum distance of cell invasion in the primary cultures designated (CC1 (Anaplastic Oligodendroglioma), DD1 (Gliosarcoma), EE2 (Oligodendroglioma), P (GBM) or X (GBM)) (Figure 4.17). There was also no difference in the total area of invading cells. In my standard primary culture media bFGF is included to maintain cells in a state of dedifferentiation [61, 196]. Therefore, in order to ascertain whether differentiation of the primary culture cells would improve invasion, I next added 10% fetal bovine serum (FBS) to the culture media; FBS is often used to differentiate glioma stem-like cells [67]. Unfortunately, after addition of FBS the primary culture cells simply adhered to the chamber filter and in fact invaded less well than cells not treated with serum (Figure 4.17).

4.10.1 Development of a drop-off assay for enriching the invasive fraction of cells

The reason why only a small proportion of the cells plated onto each chamber filter actually invaded into the type I collagen plug may be because the invading cells have different characteristics to the cells that do not invade. I therefore developed a technique to purify and expand the invasive population of cells with a view to characterising the two different cell populations in more detail.

Figure 4.17 Optimising conditions for in vitro invasion of glioma primary culture cells. Cells plated onto the filter of a Transwell chamber containing a type I collagen plug were allowed to invade for 5 days. Cells were then stained with 4μM Calcein to visualise nuclei and a Z-stack of images was prepared using confocal microscopy. From these images the maximum distance invaded by any single cell from the chamber filter was calculated using Image J software. (A) The media in which the adherent cells were incubated was manipulated with respect to the concentration of its consistuent growth factors, as indicated in the graph. The primary culture designated P (GBM) is illustrated as an example of branched phenotype cells. Each column indicates the mean maximum distance invaded by any single cell under the specified growth factor conditions from four measurements made in each of at least two chamber replicates. The error bars indicate the standerd error of the mean. The graph illustrates that manipulating the media FGF concentration does not impact on cell invasion. This was the case in both branched and flat phenotype cells. (B) A similar experiment was performed where the standard culture media was supplemented with 10% fetal bovine serum. The Z-stack of images of invading cells has been formed into a montage using Image J software to illustrate cell invasion under these conditions. The addition of serum did not improve the invasion of cells into the collagen matrix plug.

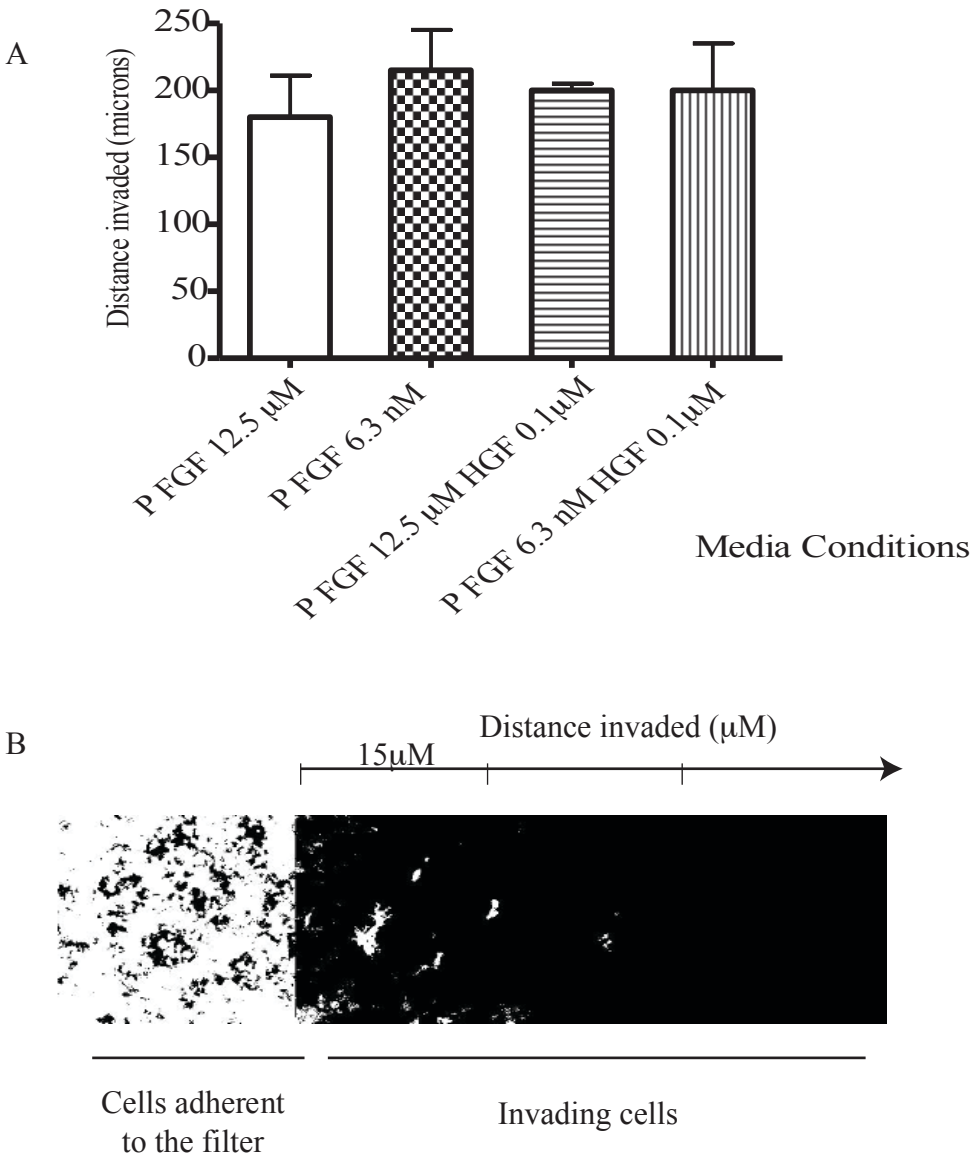

To establish this model, instead of plating cells on the underside of the chamber filter and allowing them to invade upwards through a type I collagen plug, cells were plated directly onto the top of the plug in an inverted Transwell chamber (Figure 4.18). A smaller type I collagen plug was used than in my standard invasion assay with the aim that cells would transit the whole length of the matrix plug; 40µl of type I collagen was used compared to the standard 100µl. The well in which each chamber sat was coated with growth factor-reduced Matrigel, the intention being that cells crossing the filter would 'drop off', adhere to the Matrigel, and then proliferate. For this assay cells were incubated in the same HGF-supplemented media as described previously.

As predicted, cells invaded through the type I collagen plug. Five to seven days after plating cells onto the collagen plug, single cells from branched phenotype primary cultures could be identified with brightfield microscopy on the Matrigel-coated well. These cells then proliferated and appeared phenotypically similar to the branched phenotype primary culture cells. Glioma-derived spheres were also visible on top of the type I collagen plug from cells that had proliferated instead of invading. I was therefore able to collect both an invasive and non-invasive group of branched phenotype primary culture cells. In contrast, flat phenotype cells did not migrate out of the type I collagen plug and proliferate on the Matrigel-coated well, even after several weeks.

4.10.2 Flat-type cells invade further than branched-type cells in vitro

Using the standard invasion assay that I have described, the maximum distance of cell invasion into a type I collagen plug was compared between 5 glioma primary cultures. I observed that there was a difference in the invasive ability of the flat phenotype cells in cultures designated CC2 (Anaplastic oligodendroglioma) and EE2 (Oligodendroglioma) when compared to the branched phenotype cells in cultures designated DD1 (Gliosarcoma), P (GBM) and X (GBM) (Table 4.6, Figure 4.19).

Figure 4.18 Development of a drop-off assay of glioma stem-like cell invasion. In the conventional inverse invasion assay (top image) glioma primary culture cells are plated onto a filter beneath a collagen plug and incubated for five days before imaging. Cells are expected to invade upwards through the plug. In contrast, in the drop-off assay (lower image), glioma primary culture cells were plated directly onto the collagen plug. The cells were again incubated in standard media. Cells migrated downwards through the plug and 'dropped' onto the growth factor reduced Matrigel-coated well.

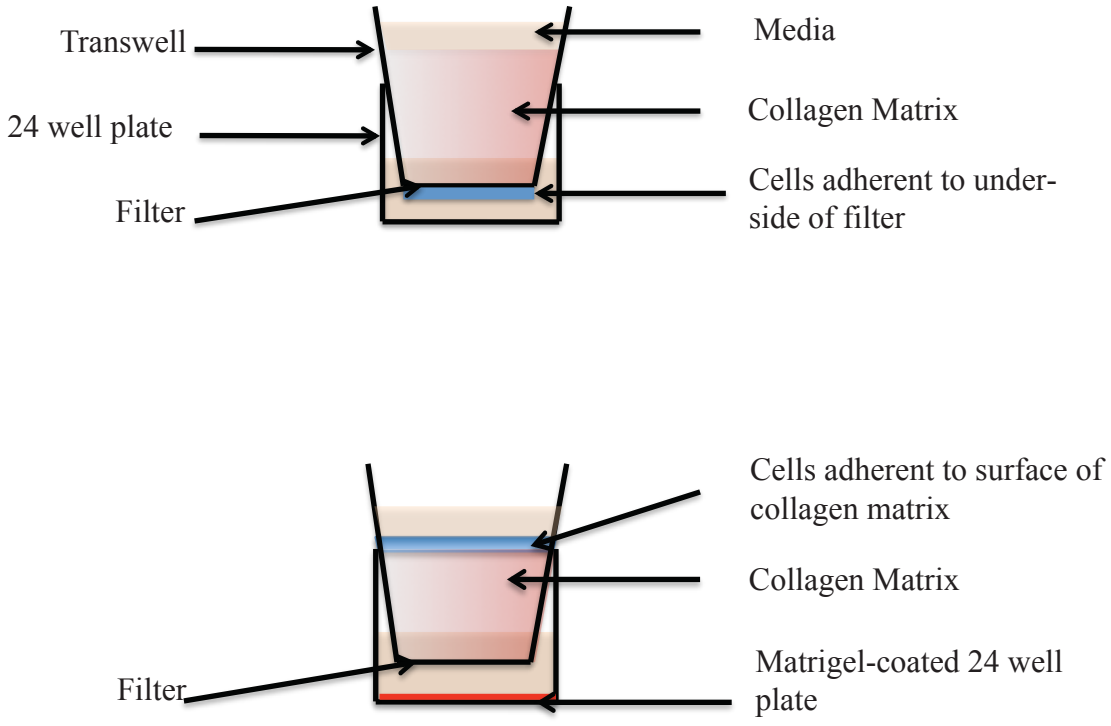

Figure 4.19 Comparison of the in vitro invasion of flat and branched phenotype cells. Flat or branched primary culture cells were plated onto the filter of a Transwell chamber containing a type I collagen plug. After 5 days, the maximum distance of invasion of any single cell from the filter was determined by taking a Z-stack of images through the type I collagen plug using confocal microscopy. A minimum of four measurements were made in each chamber, from at least two replicates for each primary cultures. (A) The graph compares the distance invaded by the flat phenotype cultures designated CC1 (anaplastic oligodendroglioma) and EE2 (oligodendroglioma) with the distance invaded by the branched phenotype cultures designated DD1 (gliosarcoma), P (GBM) and X (GBM). (B) The graph compares the distance invaded by the flat phenotype culture designated EE2 and the branched phenotype culture designated EE1, both of which were derived from the tumour designated EE (oligodendroglioma). Statistical significance was calculated using a Student's t-Test. The results indicate that on average the flat phenotype cells invaded further than the branched phenotype cells and that this difference is statistically significant ($p<0.0001$). This difference is phenotype-related and not related to a specific tumour type.

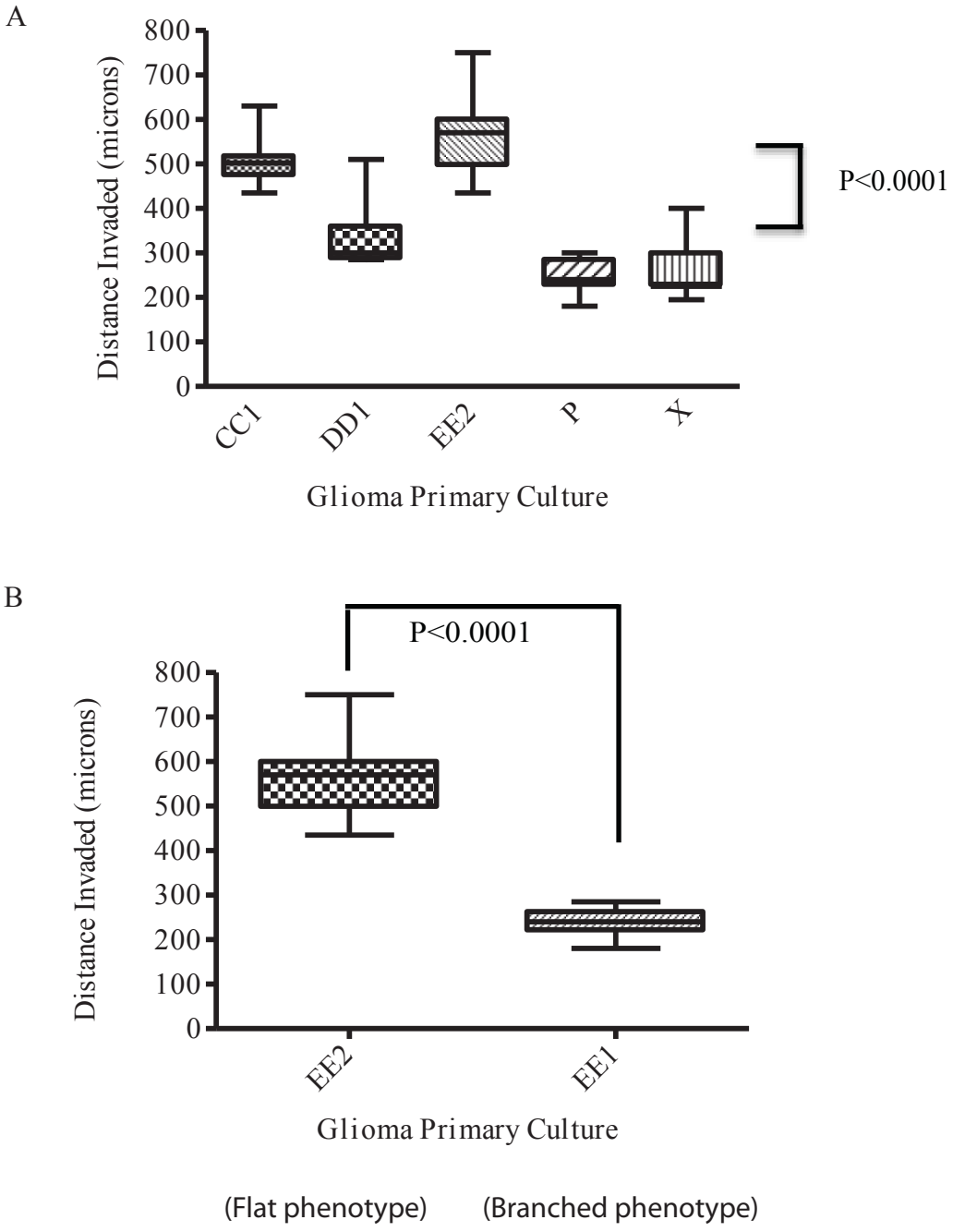

Table 4.6 Glioma primary culture cell invasion. Glioma primary culture cells were plated onto the filter of an inverted Transwell chamber containing a type I collagen plug. After 5 days a Z-stack of images was taken through the collagen plug using a confocal microscope to ascertain the maximum distance that any single cell had invaded. The average maximum distance invaded by a single cell is listed below for each glioma primary culture according to its designated alphanumeric code. Each measurement was performed at least four times in each chamber and at least two chambers were analysed per culture. The standard deviation of the measurements is given in brackets. GBM – glioblastoma. The results indicate that on average the flat phenotype cells invaded further than the branched phenotype cells and this difference was statistically significant <0.0001.

Primary culture	Cell Phenotype	Glioma Histology	Average Maximum Distance Invaded (microns)
CC1	Flat	Anaplastic oligodendroglioma	478.6 (81.7)
DD1	Branched	Gliosarcoma	273.8 (134.2)
EE1	Branched	Oligodendroglioma	293.1 (91.0)
EE2	Flat	Oligodendroglioma	540.8 (77.2)
P	Branched	GBM	279.0 (44.2)
X	Branched	GBM	287.8 (63.0)

The statistical significance of this difference, calculated using Student's t-Test, was <0.0001. Examination of the invasion of branched (EE1) and flat (EE2) phenotype cells derived from different tissue biopsies taken from the same tumour designated EE (Anaplastic oligodendroglioma) confirmed that the difference in invasion was phenotype-related and not tumour-related (Table 4.6, Figure 4.19). The average distance invaded by cells into the collagen matrix was 293.1 microns for the primary culture designated EE1 and 540.8 microns for the primary culture designated EE2 (Table 4.6). This phenotype-related difference in cell invasion was statistically significant (P<0.0001).

4.10.3 The inverse invasion assay can be used to screen inhibitor compounds

I next examined whether the primary culture inverse invasion assay could be used to screen compounds that might inhibit cell invasion. To test the ability of the assay to detect changes in invasion in response to compound inhibition I selected two c-Met inhibitors (PF 04217903 and BMS 777607) that are already in use in early clinical studies, although not for glioma [262]. They inhibit the enzymatic activity of the c-Met receptor tyrosine kinase [262]. The c-Met receptor binds HGF, which has been implicated in glioma cell invasion [260, 261]. I first determined the effect of the inhibitors on proliferation of cells in a group of five glioma primary cultures across an eight-point half log dose range using a SRB total protein assay (Figure 4.20); each experiment was performed in triplicate wells. This was to identify inhibitor concentrations at which cell proliferation was impaired so that any anti-proliferative effects of the compound could be distinguished from anti-invasive effects subsequently observed. In the SRB assay, compound BMS 777607 inhibited cell proliferation only at high inhibitor concentrations (above 0.3μm) (Figure 4.20). PF 04217903 had no effect on cell proliferation in any of the primary cultures across the dose-range examined, except for the primary culture designated CC1 (Anaplastic oligodendroglioma) whose proliferation was inhibited only at micromolar concentrations.

Figure 4.20 Growth inhibitory effect of c-Met inhibitors. Cells from 5 primary cultures were plated for 48 hours before treatment for a further 48 hours with the c-Met inhibitor BMS 777607 across a half-log dose range, as indicated below. The primary cultures designated X (GBM) and EE2 (oligodendroglioma) are shown as representative of branched and flat phenotype cells, respectively. Cells were then fixed with 25% trichloroacetic acid and the total protein measured in a SRB assay. Each experiment was performed in triplicate wells. The error bars indicate the standard error of the mean. A non linear regression analysis of the data was made and a sigmoidal dose-reponse curve plotted using GraphPad Prism software. The graph illustrates a dose-dependent inhibition of proliferation of both branched and flat phenotype cells at a concentration greater than 0.3μM. The stars indicate the inhibitor concentrations chosen for the invasion assay experiments described subsequently.

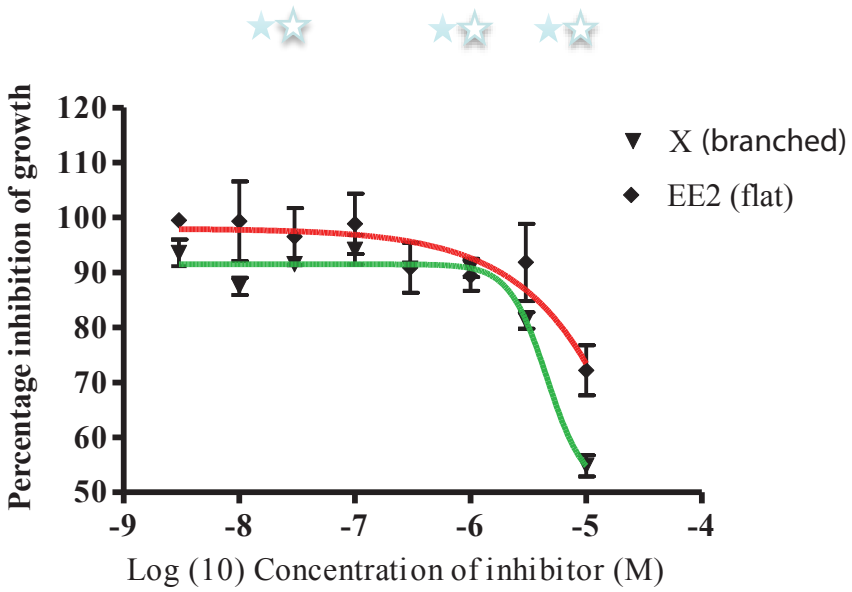

I next assessed the effect of the same inhibitors on invasion of glioma primary culture cells using my modified inverse invasion assay (Section 4.9). A range of three inhibitor concentrations of BMS 777707 was chosen for these experiments from the SRB assay data to include doses that both did and did not reduce total protein levels (Figure 4.20). The range of PF 04217903 concentrations used were simply selected from across the breadth of doses used in the SRB assay. The maximum invasion of cells at each inhibitor concentration was compared with the invasion of cells incubated in media supplemented only with DMSO, the vehicle in which the inhibitor compounds were solubilised. A minimum of four measurements of the maximum invasion of any single cell was made in each chamber, and at least two replicate chambers examined for each inhibitor dose point. Statistical tests of the significance of any inhibitor-induced reduction in cell invasion compared to DMSO were performed using Student's t-Test (Table 4.7, Figure 4.21).

The inhibitory effect of compound BMS 777607 only reached statistical significance at a concentration of 10μM, except in the primary culture designated CC2 (anaplastic oligodendroglioma) where inhibition of invasion was also significant at 1μM (Table 4.7). However, I had observed a reduction in cell proliferation with compound BMS 777607 at a concentration of 10μM in the SRB assay (Figure 4.20). The apparent anti-invasive effect of BMS 777607 at 10μM might therefore be all or in part a result of impaired cell proliferation or increased cell death. To examine these possibilities I determined the total area of cells invading through the chamber filter at each inhibitor concentration with Image J software (Figure 4.22). I reasoned that if the total area of invading cells at each inhibitor concentration was constant, then the reduction in invasion was probably not primarily a result of a reduction in the numbers of invading cells, but actually resulted from an anti-invasive action of the compound. In fact, I observed that there was no statistically significant difference in the total area of invading flat or branched phenotype cells incubated in media supplemented with 10μM BMS 777607 compared to cells incubated in media containing lower concentrations of the inhibitor compound ($p=0.08$) (Figure 4.22).

Table 4.7 C-Met inhibition of glioma primary culture cell invasion. Glioma primary culture cells were plated onto the filter of an inverted Transwell chamber containing a type I collagen plug. The chambers were incubated for five days in media supplemented with either the compound BMS 777607 or PF 04217903, at the concentrations indicated. After five days invading cells were stained with 4μM Calcein and a Z-stack of images taken at 15μm intervals through the collagen plug using confocal microscopy. The maximum distance of invasion into the type I collagen of any single primary culture cell was determined for each media condition and compared to a control chamber incubated in media supplemented only with DMSO, the vehicle in which the inhibitor compounds were solubilised. Four measurements were made from each Transwell and individual treatments were repeated a minimum of two times. The statistical significance of the differences in invasion was determined for each comparison using a Student's t-Test. These are listed in the Table. p values less than 0.05 are highlighted in bold. CC1 – anaplastic oligodendroglioma, DD1 – gliosarcoma, EE2 – oligodendroglioma, P – GBM, X – GBM.

BMS 777607	Phenotype	0.3μM	1μM	10μM
CC1	Flat	0.89	**0.026**	**0.041**
DD1	Branched	0.38	0.23	**0.034**
EE2	Flat	0.90	0.89	**0. 049**
P	Branched	0.49	0.13	**0.023**
X	Branched	0.21	0.094	**0.0059**

PF 04217903	Phenotype	0.003μM	0.03μM	0.3μM
CC1	Flat	0.37	0.60	**0.034**
DD1	Branched	0.22	0.52	0.32
EE2	Flat	0.44	0.42	0.79
P	Branched	0.21	0.24	0.61
X	Branched	**0.013**	0.61	0.31

Figure 4.21 Inhibition of in vitro invasion of primary culture cells by c-Met inhibitors. Cells from 5 primary cultures were plated onto a Transwell chamber containing a collagen plug and were incubated in media supplemented with either inhibitor BMS 777607 (BMS) or PF 04217903 (PF) at the concentrations indicated. After 5 days cells were stained with 4μM Calcein fluorescent dye and a Z-stack of images made using confocal microscopy. The maximum distance of invading cells was determined from four different measurements in each chamber, with at least two replicates at each inhibitor concentration. The box plots illustrate the results for the primary cultures designated CC1 (anaplastic oligodendroglioma) and DD1 (gliosarcoma), representing flat and branched phenotype cultures, respectively. Statistical significance was determined using a Student's t-Test. The inhibitory effect of the compounds on invasion reached statistical significance ($p<0.05$) in all the primary cultures treated with BMS 777607 and in the primary cultures designated CC1 treated with PF 04217903 (Table 4.7).

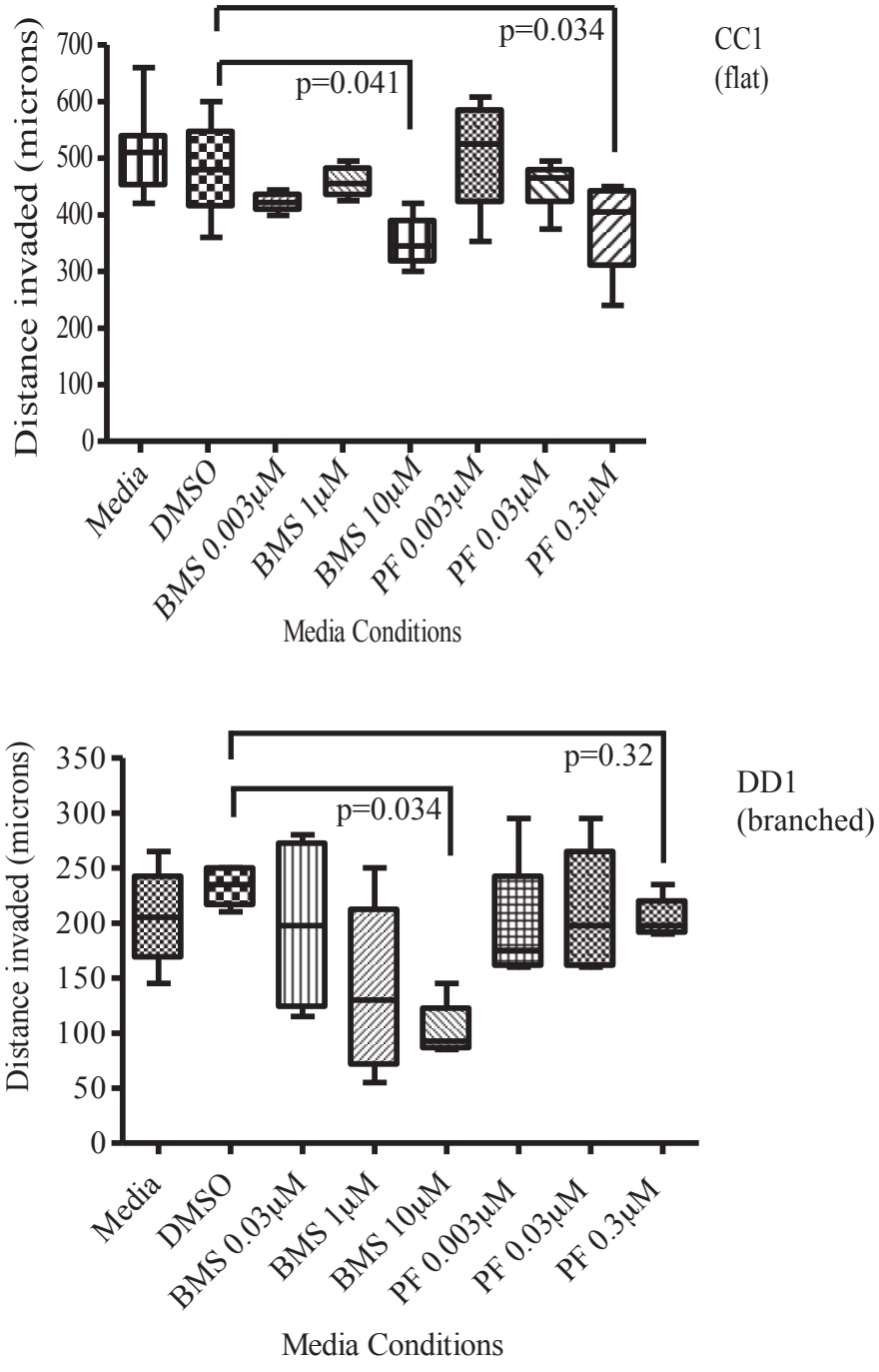

Figure 4.22 The effect of compund BMS 777607 on in vitro cell invasion. Glioma primary culture cells were plated onto the filter of an inverted Transwell chamber containing a collagen plug. The media in which the chambers were incubated was supplemented with the c-Met inhibitor compound BMS 777607 at the concentrations indicated below. After five days cells invading into the collagen plug were stained with 4μM Calcein fluorescent dye and a Z-stack of images prepared at 15μm intervals through the plug using confocal microscopy. The total area of invading cells in each chamber was calculated using Image J software and is measured in pixels. The box plots indicate the range of data from at least four Z-stacks of images made in each chamber, with at least two treatment replicates at each dose concentration. The primary cultures designated CC1 (anaplastic oligodendroglioma) and X (GBM) are shown to illustrate the 5 flat and branched phenotype cultures examined, respectively (Table 4.7). The graphs illustrate that there was no significant reduction in the total area of invading cells with increased inhibitor concentration ($p>0.05$).

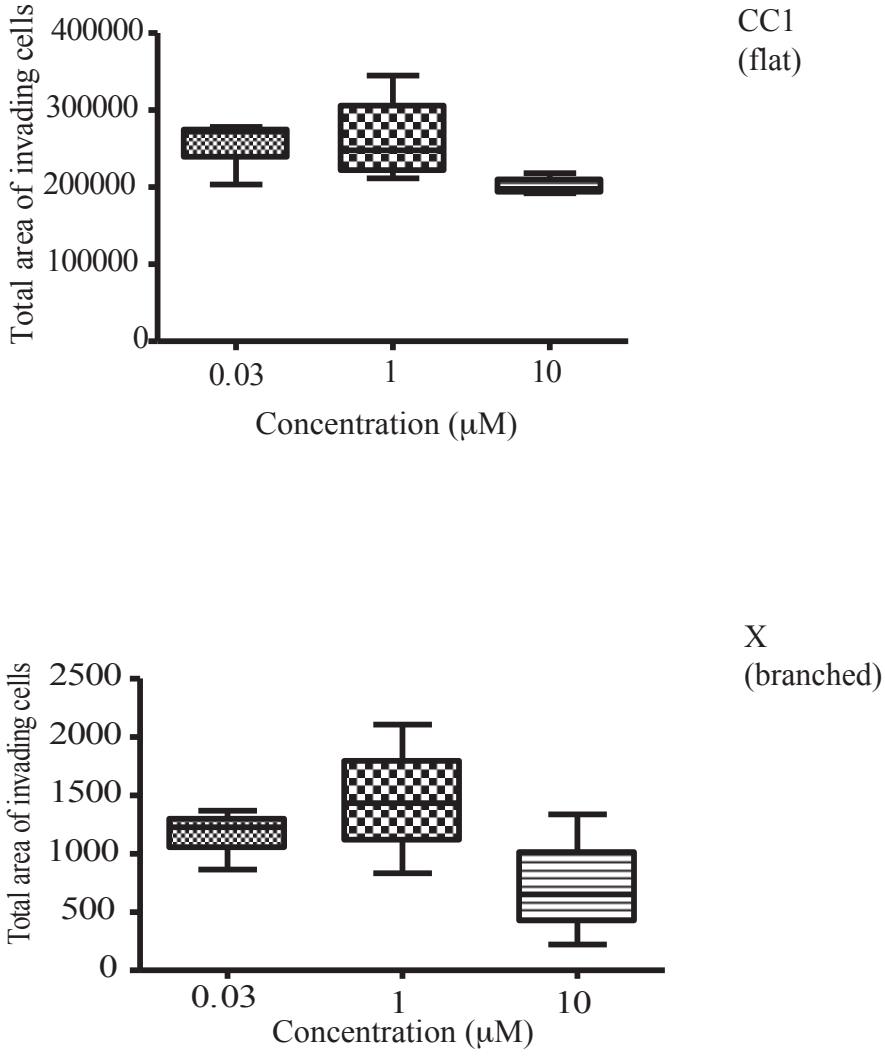

This suggests that the compound may indeed have an anti-invasive action. In contrast to BMS 777607, compound PF 02417903 had no statistically significant dose-dependent effect on invasion of primary culture cells over the dose range examined (Table 4.7). The only exception was the culture designated CC1 where statistically significant inhibition of invasion was observed at an inhibitor concentration of 0.3μM ($p=0.034$) (Table 4.7).

4.11 Discussion

The aim of the experiments presented in this Chapter was to develop high throughput assays that could be used to screen potential inhibitors of glioma stem-like cells. This is necessary, because the failure of many compounds that appeared promising in previous pre-clinical studies to subsequently demonstrate clinical efficacy in the treatment of glioma suggests that the in vitro models on which pre-clinical compound screening was performed failed to adequately recapitulate human disease [50]. The emergence of the hypothesis that implicates a stem-like cell in glioma initiation therefore presents an opportunity to revisit the design of pre-clinical glioma models [3]. Further impetus for renewed glioma drug discovery is provided by my observation that inhibitors effective against glioma stem-like cells in vitro can be ineffective against established serum-grown glioma cell lines used in previous pre-clinical compound screening assays, indicating that potentially effective compounds might have been overlooked in the past.

Utilising the putative glioma stem-like cells that I described in Chapter 3 I developed a series of in vitro assays to screen inhibitors for their ability to reduce cell number as well as cell invasion. By designing these assays to be compatible with high throughput techniques I have demonstrated that it is possible to interrogate the mechanisms of inhibitor action at multiple dose points across several primary cultures, simultaneously, rapidly and efficiently. The assays were also designed to be

biological relevant. For example, they distinguish between inhibitor actions mediated through cell death and those mediated through cell cycle arrest. This is important, because cells that are arrested, but not dead, can re-enter the cell cycle and contribute to tumour recurrence once the inhibitor is removed [134].

4.11.1 The inhibitory effect of PIK75

Amongst the PI3 kinase pathway inhibitors that I examined, PIK75 was the only compound that had an inhibitory effect on cell number, as determined by a SRB protein assay, across all the primary cultures examined. PIK75 is a selective inhibitor of the p110α subunit of PI3 kinase [160]. PI3 kinase is itself a heterodimer of p110 and p85 [263]. The p110α subunit is particularly interesting because its gene, *PIK3CA*, is mutated in a number of cancers and activating missense mutations have been reported in gliomas [159, 264]. None of the other p110 isoform specific inhibitors that I screened consistently attenuated growth of my putative glioma stem-like cells. Interestingly, PIK 75 had a dose-dependent effect on established serum-grown glioma cells only at micromolar concentrations. Efficacy at such doses is normally considered to be evidence of off-target effects [250]. The difference in GIC50 between the established serum-grown glioma cells lines and my patient-derived glioma primary culture cells was significant ($p=0.007$). This highlights that glioma primary culture-based assays can identify compounds that would have been overlooked by previous in vitro screens. However, whether in the longer-term glioma primary culture assays better predict the likely clinical efficacy of compounds remains to be determined.

Treatment of glioma-derived spheres with PIK75 resulted in reduced sphere size at increasing inhibitor concentration. This may not be surprising if the adherent cell culture assay results are taken as evidence of inhibitor-induced reduction in cell growth or increase in cell death, as I will discuss below. However, since the growth of glioma-derived spheres is itself an assay of the clonogenicity of the cells, a

measure of their stemness, then this suggests that PIK75 may be acting against the stem-like cells in these primary cultures [65, 67]. To interrogate this observation further it would have been useful to be able to chart the change in size, number and growth rate of glioma-derived spheres more precisely than is possible with daily visual inspection. I experimented with several automated image analysis systems to try to objectively quantify changes in the size and number of glioma-derived spheres in response to drug treatment. However, I was unable to identify a system that achieved this reliably or reproducibly. It appeared to be difficult for the software examined to differentiate small glioma-derived spheres from non-adherent clumps of cells or adherent colonies of cells; this was however possible with visual inspection though, as I described in Chapter 3. Another problem with attempting to develop a sphere-based assay of inhibitor efficacy is that it was not possible to assess the actual number or viability of the constituent cells in each glioma-derived sphere in real time. More sophisticated analysis algorithms associated with whole-well imaging may be able to overcome at least some of these problems, but I did not have time to explore this further during this project.

The remainder of my experiments were performed on adherent cell cultures. Both branched and flat phenotype cells were inhibited by PIK75 in the nanomolar range and there was no difference in the GIC50 inhibitory concentrations between the two groups. Only a few of the glioma primary cultures examined had their growth inhibited by any of the other compounds tested, so it was not possible to draw any conclusions as to whether there was variation in susceptibility to inhibitors between the flat and branched phenotype cells. Nevertheless, variation in the efficacy of mTOR inhibitors between glioma primary cultures illustrates the heterogeneity in pathway signalling amongst cultures derived from histologically similar tumours. This supports the rationale for screening compounds across multiple primary cultures, because this heterogeneity might not have been apparent if only a smaller number of cultures were examined. A goal of future studies would be to identify biomarkers that predict this heterogeneity in therapy response to guide patient-

specific drug selection in the clinic. Such biomarkers might include genetic or protein markers specific for the different cell phenotypes, as I discussed in Chapter 3. Differences in response to inhibitor compounds between flat and branched phenotype cultures, even from the same tumour, would not be surprising, because I demonstrated in Chapter 3 that they have contrasting DNA copy number change profiles that suggests variations in signalling pathways. Additional sets of primary cultures that contain flat or branched phenotype cells, derived from single tumours, will be required in the future to further interrogate differences in susceptibility to inhibitors between the two cell types.

4.11.2 Interrogating the inhibitory effect of PIK75

Whilst the SRB assay failed to demonstrate any difference in the dose dependant efficacy of PIK 75 in flat phenotype cells compared to branched phenotype cells, I did observe that the effector mechanism of PIK75 differed between these cell types. I examined the cell cycle and apoptosis-inducing effects of compounds on glioma primary culture cells using high content imaging assays where cellular phenotypic changes in response to an inhibitor treatment were detected through automated image analysis [137]. Flat phenotype cells underwent apoptosis in response to an increasing concentration of PIK75, whereas branched phenotype cells entered cell cycle arrest, but did not die. This is significant, because there is a clinical relevance to differentiating the group of patients that might respond to drug treatment with tumour cell death from patients whose tumour cells undergo tumour cell cycle arrest; arrested cells would have the potential to re-enter the cell cycle and cause tumour recurrence [249, 250]. The cell cycle status (G1, S and G2/M) of each cell was assessed from its DNA content that was determined from the intensity of Hoechst stain in each nucleus of each cell using Olympus Scan^R software. Hoechst 33342 was chosen for these cell cycle experiments rather than the DNA dye propidium iodide (PI), because PI cannot cross intact cell membranes requiring that cells must first be fixed and permeabilised [265]. In contrast, Hoechst can be used in live cells,

allowing temporal changes to be assessed on repeated analyses, along with the simultaneous assessment of apoptosis. This would not be possible using propidium iodide with a FACS technique.

Since the cell phenotype of my putative glioma stem-like cells appeared to relate to the effector mechanism of PIK75, it would be useful to be able to predict which gliomas would behave with either cell cycle arrest or apoptosis without having to actually enrich glioma stem-like cells from every patient, because this is time consuming and expensive. Future research might therefore focus on identifying biomarkers, such as gene expression profiles, that could predict the likely primary culture cell phenotype that would be derived from an individual's glioma. Also important to the potential clinical application of PIK75 is an assessment of whether it has on-target activity in gliomas. Off-target activity of drugs is associated with side effects in the clinic, limiting their use. I therefore demonstrated using a RPPA approach that PIK75 selectively targets the PI3 kinase pathway, suggesting that it has an on-target effect [160].

It is interesting that the combined p110α/mTOR inhibitor, PI-103, did not inhibit the majority of glioma primary culture cells tested, even though it has been demonstrated in other studies to inhibit glioma cell proliferation in vitro and in vivo, albeit using established serum-grown glioma cell lines [161]. If PI-103 and PIK75 both target p110α then PI-103 might be predicted to have the same dose-dependant inhibitory effect on proliferation of putative glioma stem-like cells as PIK75. It may therefore be the case that a combination of mTOR and p110α inhibition mediated by PI-103 somehow reduces the benefit of p110α inhibition alone. However, in contradiction of this suggestion, the RPPA data demonstrated a PIK75 dose-dependant increase in mTOR protein in some of the glioma primary cultures, so the mTOR effect of PI-103 should be beneficial (Figure 4.15). The observation that the mTOR inhibitor KU63794 had an inhibitory effect on some glioma primary cultures further supports this suggestion. Future studies examining signalling pathway changes in my putative

glioma stem-like cells in response to PI-103 are therefore needed in order to understand the apparent lack of efficacy on this compound.

One explanation for the lack of similar in vitro efficacy of PI-103 and PIK75 is that, in spite of the available RPPA data, PIK75 may actually not be acting through its p110α target. In fact, PIK75 has previously been demonstrated to have an off-target effect [266]. An in vitro study of breast cancer cell lines identified that whilst PIK75 initially had an on-target inhibitory action on cell proliferation, after 48 hours of treatment one of the cell lines examined recovered its S6 ribosomal protein phosphorylation whilst its proliferation remained inhibited [266]. This was interpreted as suggesting that the observed decrease in cell number actually resulted from action on targets other than PI3 kinase [266]. This argument was further supported in the same study by evidence that in some breast cancer cell lines PIK75 triggered apoptosis without any PI3 kinase pathway changes.

These observations all related to the effects of administration of PIK75 over 48 hours. In contrast, although my SRB, cell death and cell cycle assays were all analysed after 48 hours of treatment with PIK75, the RPPA experiments that I have described were performed on cells treated with PIK75 for only 30 minutes. It is therefore plausible that the outcome of the assays performed over 48 hours reflected off-target action of PIK75 that was not identified on the RPPA because the primary culture cells in the latter experiment were not exposed to PIK75 for long enough. It would be crucial in future to repeat the RPPA on primary culture cells exposed to PIK75 at multiple different time points, particularly 48 hours.

Aside from this breast cell line study, PIK75 has been reported to have cytotoxic activity in recent ovarian and breast cancer experiments and has also been proposed to have a beneficial role in an experimental model of inflammation [267-269]. None of these studies reported evidence of off-target effects of PIK75. Nevertheless, it is in part because of concern that off-target effects of PIK75 observed in vitro could

manifest clinically as dose-dependant cytotoxicity that PIK75 is yet to progress to clinical studies for the treatment of cancer [266]. However, even if the beneficial effect of PIK75 is mediated through an off-target effect, it could still be of clinical utility and so a more detailed understanding of its mechanism of action is required. One approach is to perform more extensive signalling pathway modelling using the RPPA technique that I have described. This is also a valuable tool for identifying inhibitor-induced activation of redundant signalling pathways in response to single agent therapy that could contribute to tumour recurrence [135]. If activation of signalling pathways can be predicted then these redundant pathways can be targeted with combinations of inhibitors. Significantly, the assays that I have described in this Chapter allow dose ranges of multiple compounds to be tested simultaneously and in combination on each primary culture.

There are three other strategies that I could also employ in future experiments to probe the mechanism of action of PIK75. Firstly, instead of focusing on p110α as a target, I could take a compound-centric approach to explore the off-target activity that might be responsible for PIK75 efficacy. Utilising information on the molecular structure of PIK75 I would perform a 'chemical similarity search' to determine whether molecules with a similar chemical structure to PIK75 elicit the same response [270]. I can then use this information to compare the target selectivity of these compounds and uncover a common mechanism of action with PIK75 that may not involve p110α. A second strategy is to probe PIK75 off-target activity with a small interfering RNA library screening approach to find a sequence that induces the same effect as PIK75 [271]. A third and related approach is to use cell microarray technology where a high-density array of expression vectors encoding thousands of plasma proteins is used to transfect cells [272]. This produces cell microarrays that can be used to determine the target of a drug molecule [272]. If it is found that PIK75 acts through off-target mechanisms then once the signalling pathways that are actually responsible for its in vitro utility are delineated, it may be possible to identify other compounds that directly target these pathways. The mechanisms of

action of these inhibitors can then be tested in much the same way as I have outlined in this Chapter. This strategy might identify a compound that had an on-target action as effective at inhibiting putative glioma stem-like cells as the off-target action of PIK75, but without the other off-target actions of PIK75 that might manifest clinically as toxicities.

If PIK75, or a related compound, is to progress to early clinical assessment of its efficacy, then it will also be crucial to establish that it can cross the blood brain barrier (BBB). As I discussed in Chapter 1, the blood brain barrier restricts the movement of most inhibitor compounds between the blood and the brain. It is not known whether PIK75 can cross the BBB, but its poor solubility suggests that this might not be the case [267]. In any future studies to optimise the transport of PIK75 across the BBB it will be necessary to first establish how well PIK75 actually crosses the BBB in an in vivo model. An important strategy in drug development to overcome the restrictions of the BBB is to utilise native cell transport mechanism in the brain to facilitate the uptake of drugs. With this in mind, the recent development of a PIK75 nanosuspension that targets PIK75 uptake to folate receptors is encouraging [267]. These experiments were performed using an in vitro model of ovarian cancer and demonstrated a 5-10 fold increased accumulation of PIK75 in the tumour cells, with an associated increase in cytotoxicity. Folate receptors are expressed on the blood brain barrier and on primary brain tumours themselves, so this same nanosuspension may be a useful strategy for facilitating the movement of PIK75 across the BBB [273]. Other strategies to promote the uptake of PIK75, or indeed any other compound, across the BBB include the focal disruption of the BBB using ultrasound or osmotherapy [274].

4.11.3 The glioma stem-like cell invasion assay

The invasion of glioma cells into normal brain is a key determinant of patient prognosis because it limits surgical resection [237]. To begin to tackle this problem I

have described a modified inverse invasion assay for screening potential inhibitors of my putative glioma stem-like cells in vitro. To my knowledge, an in vitro assay optimised for the assessment of putative glioma stem-like cell invasion has not previously been described; the in vitro assays of glioma cell invasion described in the existing literature utilise established serum-grown glioma cell lines [275]. These assays generally analyse changes in the number of cells on the assay chamber filter surface rather than the proportion of cells actually invading into a matrix plug [275]. The assumption is made that the difference between the cells plated on the filter and the number remaining on the filter at a given time point indicates the proportion of invading cells [275]. However, the observations that I have made in this Chapter suggest that this would not be an adequate approach for the assessment of glioma stem-like cell invasion, because these cells proliferate on the chamber filter and form glioma-derived spheres. As I discussed in Chapter 1, it is difficult to accurately quantify the number of cells in such glioma-derived spheres.

The observation that only a small proportion of the putative glioma stem-like cells in any individual primary culture appeared able to invade into a type I collagen plug underlines the fact that there is still much to be understood about the mechanism of invasion of these cells. The 'drop-off' invasion assay that I have described separated an invasive and non-invasive cell population from branched glioma primary cultures. I would like to characterise these two cell populations further in the future to examine the multifactorial processes that have been proposed to be important in glioma cell invasion and that might differentiate the invading cells from the non-invading fraction [276]. This might identify future targets for inhibitor compounds.

In contrast to branched phenotype cells, although flat phenotype cells invaded through the type I collagen plug they could not subsequently migrate out of the plug and proliferate on the Matrigel-coated well in the 'drop-off' assay, even after several weeks. The inability of flat phenotype cells to grow as non-adherent glioma-derived spheres as described Chapter 3 probably explains this observation. Of particular

interest for future study will be to understand the biological significance of the observation that flat phenotype putative glioma stem-like cells invade further in vitro over a defined time period than the branched phenotype cells. I described in Chapter 3 that the flat phenotype cells had a mesenchymal-like gene expression profile and that a mesenchymal gene expression profile in glioma tumours had already been associated with a poor prognosis [177]. It is possible that this poor prognosis could be because of increased glioma cell invasion. Targeting these flat phenotype mesenchymal-like cells may therefore be a key strategy in my stated aim to try to downgrade glioma to a more focal disease amenable to effective localised surgical and radiotherapy treatment. Since PIK75 effectively inhibited flat phenotype cells in adherent culture it will be particularly important to assess whether this compound can also inhibit the invasion of flat phenotype cells in vitro. A preliminary attempt to address this question was limited by the fact that the drug concentrations I assayed using my in vitro invasion model caused marked cell death such that very few cells actually invaded into the matrix plug. This study could be repeated at lower concentrations of PIK75 that do not trigger cell death.

The inhibitor-induced reductions in cell invasion that I observed with c-Met inhibitors require further validation using a greater number of glioma primary cultures. Nevertheless, I have demonstrated that the modified inverse invasion assay I described for use with putative glioma stem-like cells is sufficiently sensitive to detect statistically significant differences in cell invasion in response to inhibitor compounds. It can also differentiate these effects from compound-mediated reduction in cell survival or proliferation. This suggests that the in vitro strategy that I have described for screening potential anti-invasive compounds is valid. A next step would be to scale up this system for high throughput screening of a greater number of inhibitors across a larger dose range, for example by using the Oris™ Invasion Assay system from Platypus. Effective inhibitors could then be interrogated using in vivo models.

4.12 Summary

The work presented in this Chapter builds on the hypothesis that compounds selected in preclinical in vitro screening using models based on the cancer stem cell model are more likely to be effective in the clinic than drugs that were successful in previous preclinical screening approaches using established serum-based glioma cell lines. It still requires to be demonstrated that this assertion is true. Since I began the work in this thesis other investigators have begun to use glioma stem-like cell models to screen for compound efficacy, but it is still too early for these studies to have translated into clinical benefit [129, 130, 277].

I have shown that high throughput screening of glioma stem-like cells in biologically relevant assays is possible and is also desirable because it allows the efficient comparison of multiple glioma primary cultures that represent the heterogeneity of human disease. Screening large numbers of inhibitor compounds across a broad spectrum of cultures is a useful way to align inhibitor efficacy with inter-tumoural features with a view to predicting patient responsiveness. This is necessary, because despite the remarkable efficacy of PIK75 in vitro, the phenotypic and molecular heterogeneity observed between different primary cultures and gliomas makes it unlikely that a single inhibitor compound will be identified that can effectively treat all gliomas in the clinic. Instead, effective treatment may require the targeting of multiple facets of glioma stem-like cell biology, such as proliferation and invasion. More work is needed to understand what role PIK75 might have in such strategies and also to elucidate its mechanism of action before it can be considered for the clinic. A screen of compound inhibitors targeting other pathways important in glioma cell biology, such as the Mitogen Activated Kinase Pathway, will also be undertaken in a future study. Such compounds would likely be required for effective combinatorial therapies.

Chapter 5. A novel mouse model of malignant peripheral nerve sheath tumour

5. 1 Background

In Chapter 3 I described the development and characterisation of an in vitro model of glioma based on the so-called cancer stem cell hypothesis. In Chapter 4 I developed a series of compound screening assays using these putative glioma stem-like cells. The expectation was that modelling glioma cell biology in this way recapitulated human disease better than established serum-grown glioma cell lines. Inhibitor compounds selected through screening using glioma stem-like cells will hopefully be more likely to translate effectively into the clinic than drugs selected with serum-grown glioma cell line-based assays. The next stage in the process of drug discovery after in vitro compound screening is to subject the inhibitors to in vivo testing of their efficacy. I therefore sought to develop an in vivo model of glioma based on the hierarchical development of tumours predicted by the cancer stem cell hypothesis. This would be a tool for in vivo compound screening, but also allows interrogation of the glioma stem-like cell's role in tumour initiation, as I will discuss.

In Chapter 1 I discussed the two principal types of in vivo glioma models in current usage, namely xenotransplantation models and genetically engineered mouse models (GEMMs) [278]. In a xenotransplantation model cell lines, glioma-derived spheres, or dissociated tumour tissue, are injected either orthotopically or heterotopically into immune compromised mice [278]. The absence of an intact immune system means that these mice lack a key component of the human tumour microenvironment and this is an important reason why they have failed to accurately predict the efficacy of inhibitor compounds subsequently translated into the clinic [278]. In contrast to xenotransplantation models, in GEMMs of glioma mutant genes are expressed in specific cell lineages leading to the spontaneous development of tumours in the context of an intact immune system. This is therefore the model system that I chose to work with [83, 279]. There are nevertheless some drawbacks to GEMMs. For

example, multiple cells within each mouse contain the mutant alleles, in contrast to the single tumour-initiating cell implicated in human glioma formation. Furthermore, therapeutic studies can be difficult to perform in GEMMs because the precise timing of tumour initiation and development is less easy to control, and therefore less predictable, than in xenotransplantation models [278].

A new GEMM model was needed because existing GEMMs of glioma have variable tumour penetrance and histology [83, 279]. This is possibly because mutant gene expression has often been targeted to cells that express Nestin and GFAP proteins; I discussed in Chapter 1 that Nestin and GFAP may not specifically define the glioma-initiating cell [83]. Therefore, based on the hierarchical model of gliomagenesis that implicates a cell with stem-like or progenitor-like characteristics in the initiation and maintenance of gliomas, I instead proposed to target mutant genes to the multi-potent oligodendrocyte precursor cell (OPC) that has been implicated in glioma initiation, as I discussed in Chapter 1. For example, a GEMM of low-grade glioma has previously been described where PDGF-B overexpression was targeted to the OPC [185]. I directed expression of floxed transgenes to the OPC using a cre recombinase under the control of the OPC-specific 2',3'-Cyclic-nucleotide 3'-phosphodiesterase (*Cnp*) promoter (Figure 5.1). By targeting expression of transgenes other than *PDGFB* to the OPC I aimed to produce a model with a higher penetrance of glioma formation; in the PDGF-B model the incidence of gliomas was only 33% [185]. Helpfully, mice with a *Cnp* promoter-driven cre recombinase were readily available for me to utilise in this study [202]. I therefore used this strategy for directing transgene expression. The transcriptional regulation of the native *Cnp* was used to direct Cre recombinase-mediated expression of floxed transgenes; *Lox* sequences are placed flanking either side of the gene of interest, which is then said to be ‘floxed’ [172]. The Cre recombinase removes the *Lox* sequences, resulting in gene expression.

Figure 5.1 Genotype predicts survival in GEMM of peripheral nerve sheath tumours. (A) Schematic representation of the GEMM. The GEMM was generated from the breeding of pre-existing mice. A cre recombinase (Cre) under the control of the 2',3'-Cyclic-nucleotide 3'-phosphodiesterase (*Cnp*) promoter was used to drive the expression of mutant *PTEN* and *ERBB2* transgenes that were both floxed, as indicated by 'loxP' in the diagram. This localised the expression of *PTEN* and *ERBB2* to cells expressing the myelin-associated protein Cnp. (B) Mice were monitored on a daily basis for any clinical evidence of the development of tumours or general illness. At the first signs of distress they were euthanized using a carbon dioxide chamber to ensure preservation of cervical and cranial neural structures. The Kaplan Meier curve shows the age at death of each mouse in the study; the number of mice in each geneotype group is listed in Table 5.1. Each line represents a different genotype combination. The statistical significance of differences in average survival between mice in each geneotype group was calculated using Student's t-Test. Wt - wild type, Het - heterozygous, Hom - homozygous.

A

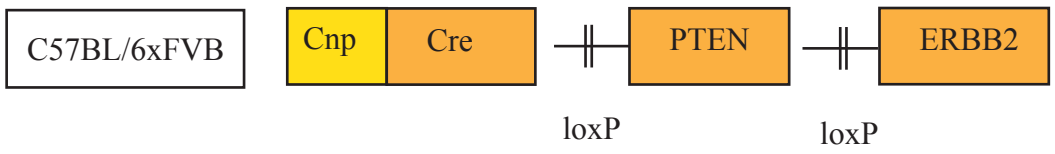

B

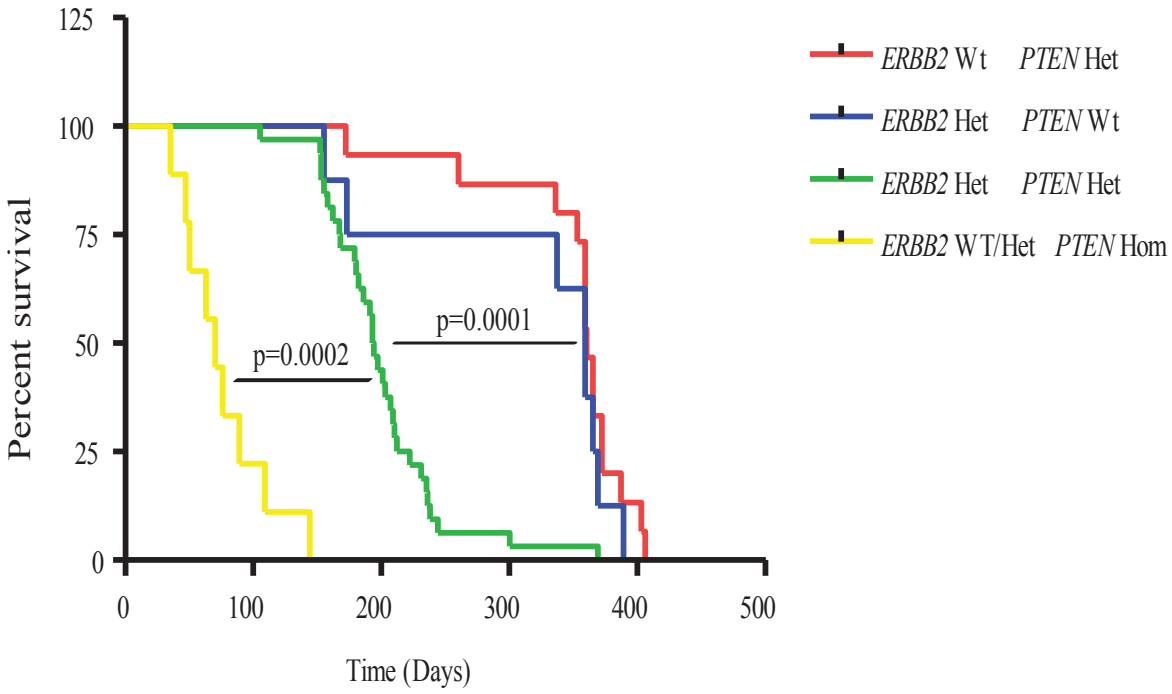

I selected transgenes known to be important both in gliomas and in regulation of neural stem cell self-renewal, proliferation, and survival, because glioma stem-like cells are thought to have similarities to neural stem cells, as I discussed previously. I examined the central role of the *PTEN* gene in both glioma cell biology and neural stem cell biology in Chapter 1. The same rationale supported the use of a mutant *PTEN* transgene in my novel GEMM. I used a *PTEN* allele floxed across exons 4 and 5, because exon 5 encodes the phosphatase domain of PTEN and this exon is one of the most commonly mutated in human gliomas [207]. However, previous GEMM have shown that *PTEN* loss alone is insufficient to drive gliomagenesis, although its co-deletion does decrease the latency to tumour appearance and increases tumour aggressiveness [83, 280]. My novel GEMM therefore required a second transgene.

The choice of a second transgene was in part guided by a GEMM previously developed in our laboratory where the mice unexpectedly developed intracranial tumours (Sansom et. al., unpublished data). This GEMM incorporated a Cre recombinase under the control of a beta-lactoglobulin (*Blg*) promoter that was designed to target transgene expression to lactating cells within the mammary gland [281]. The *Blg* promoter is not expressed in the brain and so the appearance of poorly differentiated intracranial masses was unexpected [281]. The transgenes in this GEMM were a floxed *PTEN* gene, similar to that described above, and a floxed *ERBB2* transgene designed to overexpress ERBB2 [282]. The first exon of the endogenous *ERBB2* gene had been replaced with a floxed activated *ERBB2* cDNA so that activated *ERBB2* was expressed under the control of its endogenous promoter [282]. ERBB2 is a tyrosine kinase receptor and a member of the EGFR family [283, 284]. The ERBB2 protein functions as a heterodimer with ERBB3 and signals through both the MAPK and PI3 kinase pathways [285]. In the normal brain ERBB2 influences the emergence of oligodendrocytes from multipotent precursors [286]. Animal knockout studies have demonstrated that *ERBB2* down-regulation leads to transformation of multipotent radial glia into astrocytes, and its reintroduction reverses this transformation [287]. Interestingly, *ERBB2* has also been implicated in

the development of a proportion of human gliomas in a genome-wide association study [27]. Based on these observations, I proposed that overexpression of *ERBB2* in addition to *PTEN* loss would precipitate glioma formation when targeted to the OPC as a putative glioma-initiating cell in my GEMM.

Mice were therefore bred that included all the genotype combinations predicted by my GEMM. All mice were subjected to a full gross pathological examination at the time of euthanasia. This took place either on development of clinical symptoms or at the end point of the study, which was when mice were one year of age. Abnormal tissue was subjected to detailed histological examination.

Unexpectedly, these genetically engineered mice did not develop tumours that histologically resembled gliomas. However, mice heterozygous for both the mutant *PTEN* and *ERBB2* transgenes instead succumbed to peripheral nerve sheath tumours (PNSTs). PNSTs are the murine equivalent of human malignant peripheral nerve sheath tumours (MPNSTs) [288]. I will therefore present a preliminary analysis of these GEMM tumours and discuss the relevance of this new model to our understanding of MPNSTs and to glioma biology. I will also discuss ways to refine the model with the goal of achieving the objective of a glioma GEMM in the future.

5.2 GEMM genotype significantly predicted survival

A total of 63 mice were bred that included all transgene combinations (Table 5.1). PNST were observed in mice heterozygous for both mutant *PTEN* and *ERBB2*, but not in mice with only one mutant transgene (*PTEN* or *ERBB2*) or mice homozygous for the mutant *PTEN* allele. The age at death of all mice was plotted on a Kaplan Meier curve and it was observed that the mice could be categorized into three groups according to survival (Figure 5.1). The mice that developed PNSTs are in Group 3. There was a statistically significant difference in the survival of mice between

Table 5.1 Number of mice studied according to genotype. The genotype of the progeny of breeding mice was determined using DNA from tail samples. WT - wild type for the gene of interest, Het - heterozygous for the gene of interest, Hom - homozygous for the gene of interest.

Genotype	Number of mice bred
ERBB2 Het *PTEN* Het	31
ERBB2 Het *PTEN* Hom	3
ERBB2 WT *PTEN* Hom	7
ERBB2 WT *PTEN* Het	14
ERBB2 Het *PTEN* WT	8

Group 1 and Group 3 (p=0.0001) and between those in Group 3 and Group 2 (p= 0.0002), as calculated by a Student's t-test (Table 5.2). I will discuss each of these groups in turn.

Group 1: Mice with only one of the two transgenes.
Group 2: Mice homozygous for *PTEN* loss.
Group 3: Mice heterozygous for *PTEN* loss with *ERBB2* overexpression.

5.3 Mice with only one mutant allele did not develop clinical abnormalities

Mice heterozygous for only either the mutant *PTEN* allele or the mutant *ERBB2* allele did not develop any significant clinical abnormality before they were culled at the one-year study end point. These mice were subjected to a thorough autopsy and no macroscopic nervous system or major organ pathology was evident. A small number of mice in this group required to be euthanized prior to 1 year of age because of injuries sustained from their cage mates, or because they developed progressive evidence of poor self-care suggesting that they were unwell; no specific cause of the mice being unwell was ascertained on clinical or gross pathological examination. The mice may have been unwell because of a pathology related to their genotype, but the low frequency of the clinical phenotype amongst the mice and the observation that a similar clinical picture was occasionally reported in wild-type mice suggested that it was less unlikely that these deaths were significant. There were no differences in clinical signs, or statistically significant differences in survival, of mice heterozygous for the *PTEN* transgene alone compared to those heterozygous for the *ERBB2* transgene alone (mean survival 348.5 days versus 313.3 days, respectively, p=0.28) (Table 5.2). However, the survival of both these groups of mice was significantly longer than that of the mice that were heterozygous for both transgenes and developed clinically evident PNST (mean survival 75.9 days versus 313.3 days, p=0.0001). The lack of significant clinical sequelae in mice containing

Table 5.2 Survival of mice by genotype. Mice were monitored on a daily basis for any clinical evidence of the development of tumours and at the first signs of distress were euthanized using a carbon dioxide chamber to ensure preservation of cervical and cranial neural structures. The mean survival of mice in each genotype group is indicated in the table. The range and standard deviation are given in brackets. WT - wild type for the gene of interest, Het - heterozygous for the gene of interest, Hom - homozygous for the gene of interest.

Genotype	**Survival in Days (range) (standard deviation)**
ERBB2 Het *PTEN* Het	199.5 (105-369) (47.8)
ERBB2 Het/WT *PTEN* Hom	75.9 (35-144) (34.1)
ERBB2 WT *PTEN* Het	348.5 (172-406) (59.2)
ERBB2 Het *PTEN* WT	313.3 (155-389) (93.3)

only one mutant allele suggests that the coexistence of both *PTEN* and *ERBB2* transgenes had a cooperative effect in driving PNST formation.

5.4 Mice homozygous for the mutant PTEN allele developed hypermyelination

Mice homozygous for the mutant *PTEN* allele (*PTEN*$^{-/-}$), with or without the mutant *ERBB2* allele, survived on average 76 days (range 34-144 days) (Table 5.2). Approximately 5-7 days prior to death they developed a clinical syndrome characterised by tremor, ruffled hair, poor feeding and general debilitation. They subsequently required to be euthanized. These mice were subjected to a full autopsy to establish the cause of death. The principle abnormality identified was generalized peripheral nerve enlargement (Figure 5.2). For example, in Figure 5.2 the trigeminal nerve observed in a *PTEN*$^{-/-}$ mouse at autopsy is much larger than a trigeminal nerve in a mouse heterozygous for only the mutant *ERBB2* allele along with a wild type *PTEN* gene. In the *PTEN*$^{-/-}$ mice even pericardial nerves that cannot normally be delineated were easily observed, emphasising the extent of the generalised peripheral nerve enlargement (Figure 5.2). Histological examination demonstrated that within the enlarged trigeminal nerves there was evidence of malignant transformation manifest as cells from within the nerve invading into the surrounding tissue (Figure 5.2). However, there was no macroscopic evidence of tumours. Immunohistochemical examination of the enlarged pericardial nerves for the proliferation marker Ki67 demonstrated a high proliferative index 10.6% (standard deviation 2.9%). Direct comparison of cardiac nerves between *PTEN*$^{-/-}$ and wild type mice was not possible because pericardial nerves are not visible histologically in wild type mice.

Since I began this study, my collaborators have independently made a more detailed analysis of these *PTEN*$^{-/-}$ mice [205]. In that study mice succumbed to a similar clinical syndrome to one that I have described. The authors identified that this related

Figure 5.2 Characterisation of mice homozygous for the mutant PTEN allele. Mice homozygous for the floxed mutant PTEN allele, with or without the floxed ERBB2 transgene, expressed under the control of a Cnp promoter-driven cre recombinase, were observed until they showed signs of clinical distress. They were then euthanised in a carbon dioxide chamber. Selected tissues were fixed with 2% Paraformaldehyde. (A) Dissection of the cranial fossa floor demonstrated diffuse enlargement of the trigeminal nerves (top, arrowhead) when compared to a wild type mouse (below). (B, C) H&E-stained sections demonstrating the trigeminal nerve (TN) in wild-type (B) and homozygous (C) mice. (C) The enlarged trigeminal nerve demonstrates malignant transformation and invasion into surrounding tissue (arrowhead). (D,E) H&E-stained sections of the heart from wild-type (D) and homozygous (E) mice demonstrating enlarged pericardial nerves in the latter (arrowhead); the comparable nerves cannot be visualised in the wild-type mice.

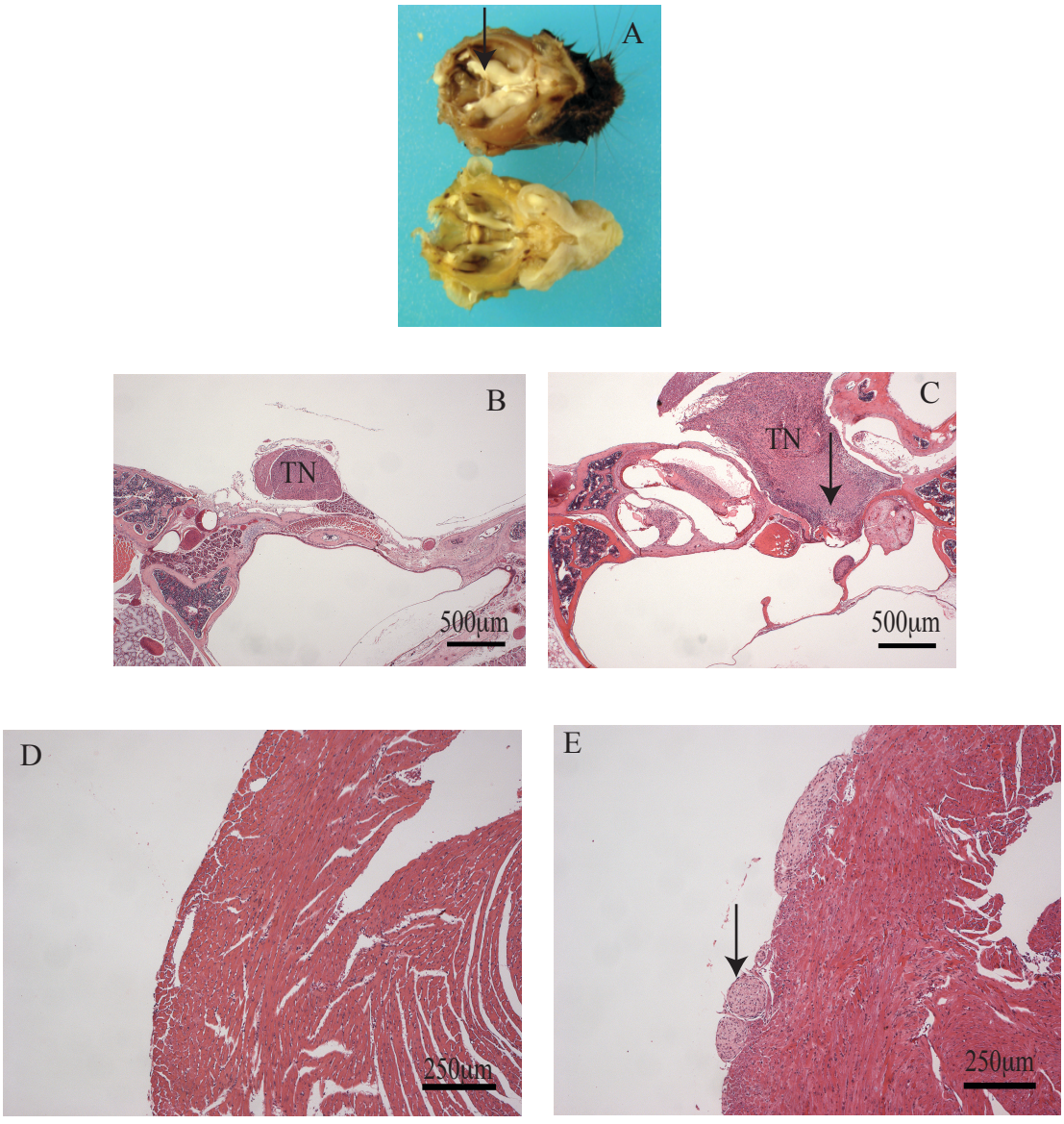

to hypermyelination of both central and peripheral nervous systems [205]. I did not investigate the phenotype or molecular biology of these mice any further.

5.5 Mice heterozygous for both transgenes develop peripheral nerve sheath tumours

Mice heterozygous for both *PTEN* and *ERBB2* mutant alleles ($PTEN^{+/-}ERBB2^{+/-}$) developed tumours that were clinically apparent at age 200 days on average (range 105-369 days, standard deviation 47.8 days) (Table 5.2). Tumours were observed in all 31 mice examined with this genotype. The most common clinical presentations were chemosis secondary to proptosis of the orbital contents, or the appearance of a rapidly growing swelling on the dorsal surface of a hind leg causing paresis. Once evident, these clinical symptoms progressed rapidly and the mice were euthanized within 1-2 weeks. An autopsy was performed on all animals and the lesion dissected to identify any related anatomical structures. Chemosis resulted from lesions in the middle cranial fossa that arose from a cranial nerve, most often the trigeminal nerve. Hind leg lesions arose from the sciatic nerve. The tumours at both sites were similar macroscopically, consisting of a firm, encapsulated growth that on careful dissection was always found to be in direct continuity with a single peripheral nerve.

The cut surface of the tumour was white, similar in appearance to the associated myelinated nerves. Formalin-fixed paraffin-embedded tumour tissue was sectioned and subjected to histological examination. Staining of tissue sections from a number of $PTEN^{+/-}ERBB2^{+/-}$ tumours with the proliferation marker Ki 67 demonstrated that the tumours were highly proliferative (Figure 5.3). Five to 13% of nuclei were positive for Ki67. This compares to less than 1 per cent in unaffected nerves, and typically 1-5% in human and mouse gliomas [185, 289].

Figure 5.3 Heterozygote mice developed peripheral nerve sheath tumours. Mice heterozygous for both the mutant *PTEN* and *ERBB2* alleles were euthanised when they devloped clinical symptoms of tumour growth. (A) Sections of Paraformaldehyde-fixed and paraffin-embedded tumour tissue were stained with primary antibodies to the proliferation marker Ki67. Antibody binding was visualised with HRP-conjugated secondary antibodies and a DAB chromogen. The number of Ki67 positive cells was counted as a proportion of the total number of nuclei in a unit area. The mean percentage calculated from several regions of each tumour are presented graphically for the four tumours examined. The error bars indicate the standard error of the mean. The results for each tumour are represented by their alphanumeric mouse indentifier and indicate the high proliferative rate of each tumour. (B) Haematoxylin and eosin staining of tumour tissue sections demonstrated that the tumour ,'T,' was characterised by tightly packed cells invading into the surrounding brain. 'Br.' (C-D) Sections of tissue at the junction between tumour and its parent nerve were stained with Luxol Fast Blue stain for myelin. The arrowheads indicate myelination in the parent nerve (C) and the tumour (D), demonstrating that the tumour is not myelin producing, but has developed within the pre-existing nerve. The composition of the tumour is examined in Figure 5.4. The scale bars indicate 100 microns.

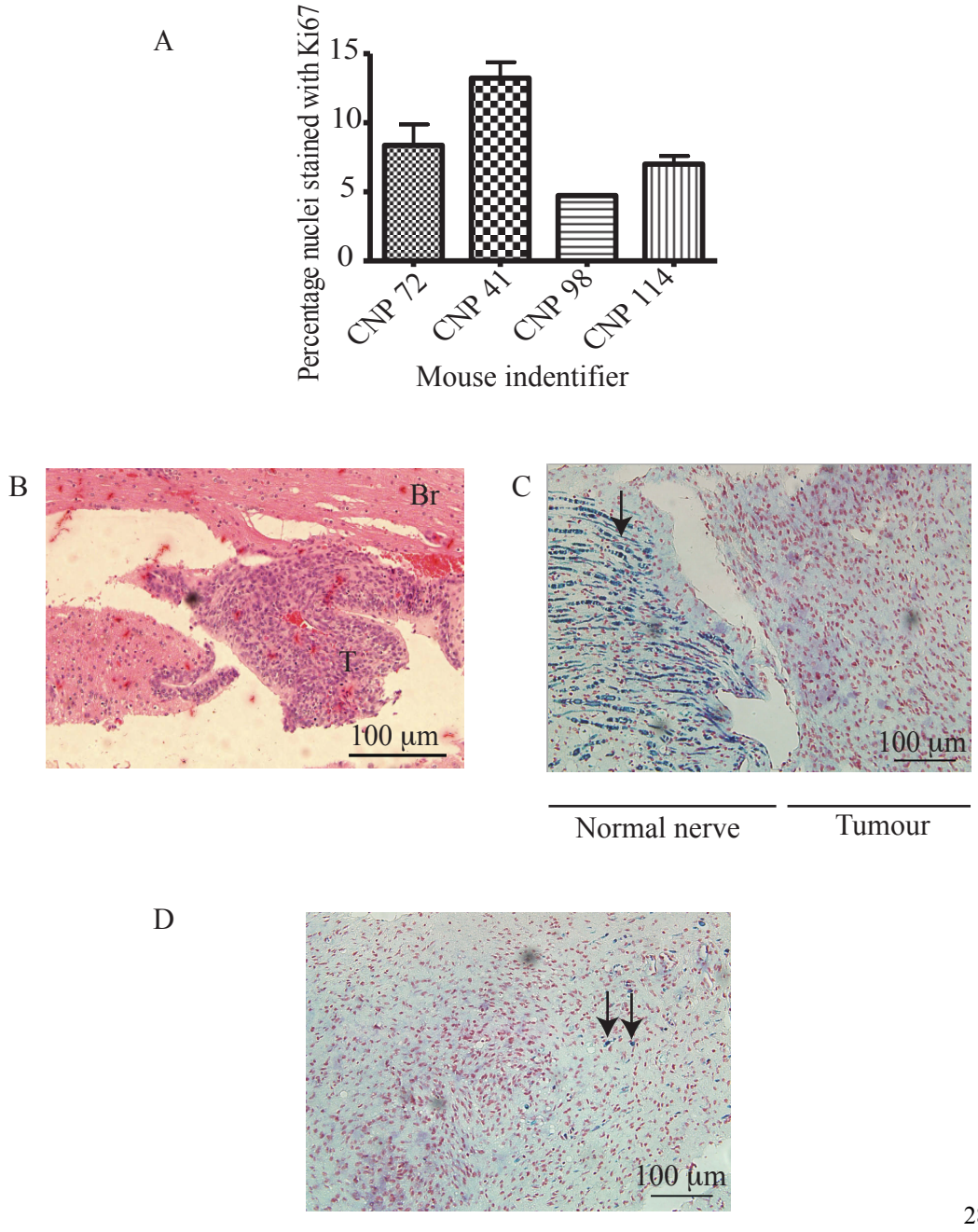

Histologically, the tumours themselves were observed to be located within the structure of the nerve itself and to be poorly differentiated lesions with tightly packed cells and large nuclei, contrasting the normal spindle shaped nuclei of the peripheral nerve (Figure 5.3). A Luxol fast blue stain for myelin demonstrated that although the normal nerve architecture was rich in myelin, the tumour itself was not (Figure 5.3). Within the bulk of the tumour there were a small number of cells positive for Luxol fast blue stain suggesting that the tumour had engulfed normal myelinated cells. This supported the hypothesis that the tumour had grown within a normal nerve (Figure 5.3).

Masson's trichrome connective tissue stain identified that the non-cellular component of the tumour was collagen (Figure 5.4). Amongst the collagen component of the tumour were whorls of densely packed cells (Figure 5.4). At the centre of each whorl was often a single cell with a white halo (Figure 5.4). This halo appearance was interpreted as evidence of lipid that had been lost in the fixation process, suggesting that at the centre of these cellular collections there was a differentiated Schwann cell surrounding an axon (Figure 5.4). In the context of the histological findings this indicates that the tumour probably had a Schwann cell rather than neuronal origin. To confirm this, tissue sections were examined with a silver stain that indicates neuronal axons (Figure 5.4). This demonstrated that there were axons within the parent nerve, but not within the tumour, supporting the assertion that this is not a neuronal tumour (Figure 5.4).

5.6 Peripheral nerve sheath tumours are similar to human malignant peripheral nerve sheath tumours

The gross pathological and histological analysis that I have presented suggests that the highly proliferative tumours that developed in *PTEN*$^{+/-}$*ERBB2*$^{+/-}$ mice arose from Schwann cells in peripheral nerves (Figure 5.1-5.4). Peripheral nerve sheath tumours

Figure 5.4 Heterozygote mice developed peripheral nerve sheath tumours. Mice heterozygous for both the mutant *PTEN* and *ERBB2* alleles were euthanised when they developed clinical evidence of tumours. Paraformaldehyde-fixed and paraffin-embedded tissue was sectioned. (A,B) Sections of tissue at the junction between tumour and its parent nerve were stained with Massons's Trichome stain for collagen. The double arrowhead indicates interstitial collagen (A) which forms the bulk of the tumour. The single arrowhead (B) indicates a pericellular halo suggestive of a myelinated axon around which the tumour has formed, consistent with a Schwann cell origin for the tumour (B). (C) Additional sections were stained with silver to visualise axons. The double arrow head indicates neuronal axons. The line drawn across the section indicates the junction of the tumour and its parent nerve. This image also demonstrates that the tumour has not formed from a proliferation of axons.

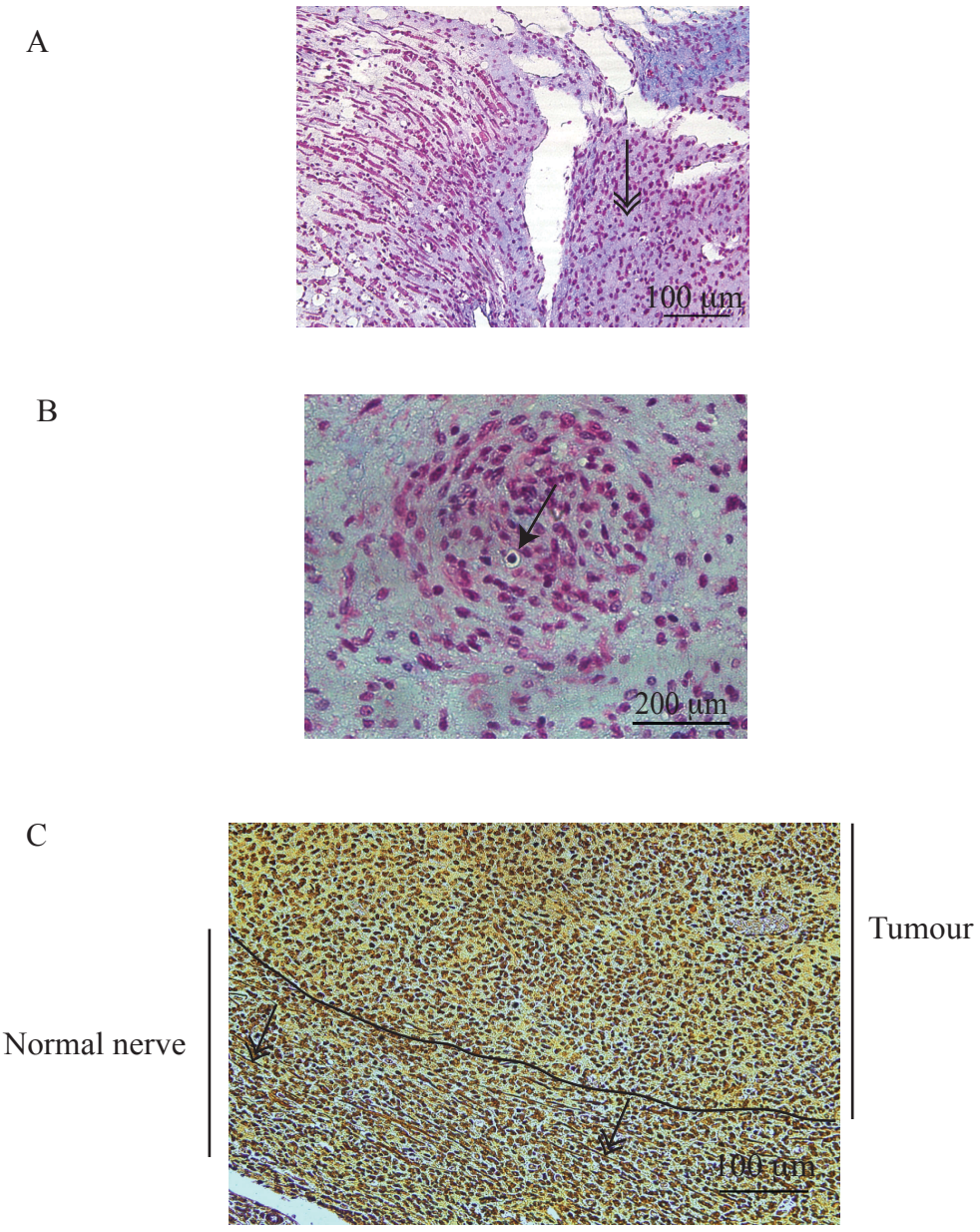

in mice are equivalent to human MPNSTs [288]. MPNSTs usually demonstrate positive staining with antibodies to the protein S100B and I did in fact observe expression of this protein in these murine tumours, supporting the diagnosis of PNSTs (Figure 5.5) [288]. A preliminary analysis has suggested that the regions of tumour that stained with antibodies to S100B corresponded to areas of decreased PTEN protein expression (Figure 5.5). This may suggest that loss of *PTEN* heterozygosity in these mice is important for tumour development or malignant progression. This hypothesis will require further analysis in future studies.

5.7 Discussion

GEMMs are a valuable way to investigate the role of defined genes in a cell-specific expression on tumour development, incorporating the important role of the microenvironment, tumour heterogeneity and immune reaction [83]. I designed a novel GEMM to interrogate the putative role of the OPC as the tumour-initiating cell in gliomas. I also intended that an in vivo model of glioma with high tumour penetrance, and that recapitulated human disease, would be a valuable resource for the screening of inhibitor compounds identified through in vitro screening. In my GEMM model, *PTEN* and *ERBB2* transgenes were expressed specifically in myelinating cells using a *Cnp* promoter-driven Cre recombinase. Unexpectedly, no evidence of gliomas was observed in these mice. Instead, mice heterozygous for the two mutant transgenes developed high- grade PNSTs similar to human MPNSTs.

MPNSTs in humans are aggressive soft tissue tumours thought to arise from the neuroectoderm [290]. There is an incidence of 1 per 100,000 in the general population and MPNSTs account for 3-10% of soft tissue sarcomas [290, 291]. Patients with the inherited neurocutaneous syndrome Neurofibromatosis type 1 (NF1) have an increased incidence of MPNST with a lifetime risk of 4.6%, compared to 0.001% in the unaffected population [292]. NF1 is associated with a germline

Figure 5.5 GEMM tumours are homologous to human peripheral nerve sheath tumours. Mice heterozygous for both the *PTEN* and *ERBB2* mutant alleles were observed until they developed clinical evidence of tumours. Mice were then euthanised in a carbon dioxide chamber. Tissue was fixed with 2% paraformaldehyde and embedded in paraffin. Sections of tumour tissue were incubated with primary antibodies to the PTEN protein (1:100) (top image) or S100β protein (1:1600) (lower image) overnight in a cold room. Antibody binding was visualised with HRP-conjugated secondary antibodies and a DAB chromogen (brown). Nuclei were counterstained with eosin (purple). The matched images illustrate that regions of low PTEN protein expression (top image) also demonstrate increased S100β expression (lower image). Since S100β is characterisitc of PNSTs this observation suggests that loss of PTEN heterozygosity may be necessary for tumour development or progression. The scale bar indicates 100 microns.

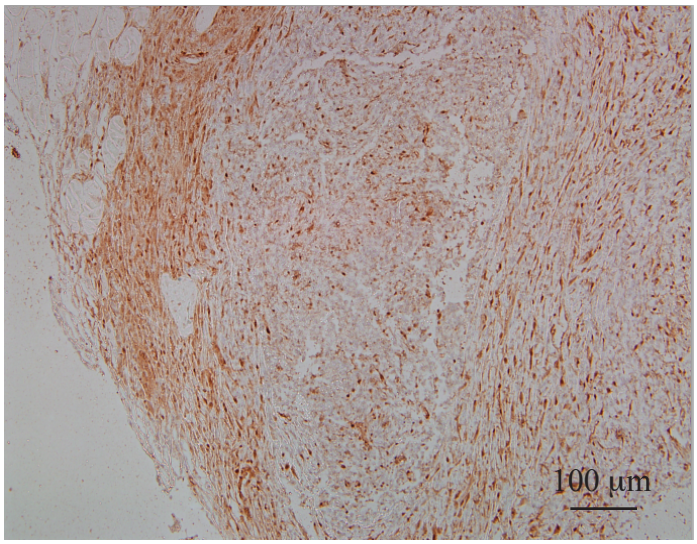

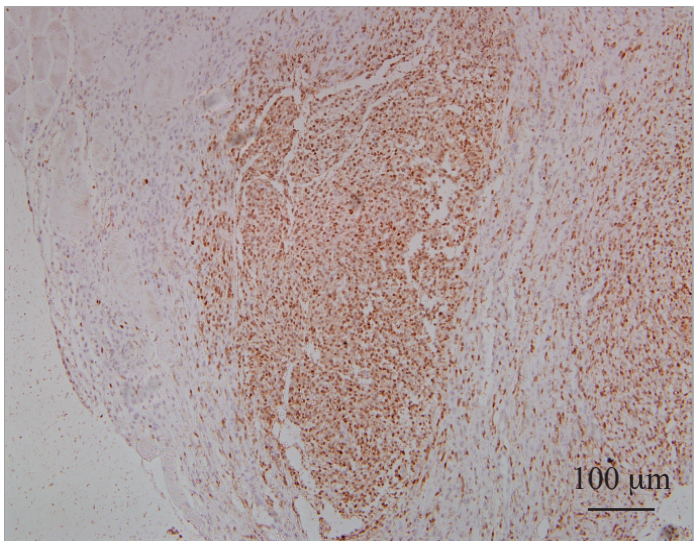

mutation in one *Nf1* allele on the long arm of chromosome 17 (17q11.2) that occurs with an incidence of 1:3500 and is associated with myriad clinical manifestations, including nerve sheath tumours [293].

MPNSTs are thought to develop from hyperplastic lesions known as plexiform neurofibromas [294]. Consequently, distinguishing MPNST from other soft-tissue sarcomas usually requires identification of a nerve associated with the tumour, or the demonstration of the premalignant neurofibroma contiguous with the malignant lesion [294]. The tumours in my GEMM did in fact arise from peripheral or cranial nerves. Furthermore, I have presented preliminary evidence that suggests the more malignant lesions developed in areas of pre-existing hyperplasia. This is a key area for future research to understand the molecular events that characterise the transition from hyperplastic to malignant lesions. I have collected samples of both tissues and so this study could be accomplished, for example, with an array CGH screen looking for copy number changes that differ between the two samples sets and then targeting these areas of difference to identify the specific genes affected. Any 'hits' could then be validated by interrogation of in human tissue samples.

The anatomical association of normal nerve sheaths with MPNSTs has implicated the Schwann cell, or its precursor cell, as the cell of origin in this tumour [295]. Immunoreactivity for S100B protein in more than 50% of human MPNSTs supports this hypothesis, as does the observation in NF1 patients that biallelic *Nf1* mutations are found in Schwann cells [255, [296]. Nevertheless, there are other investigators who have implicated a perineurial cell or nerve sheath fibroblast as the cell of tumour origin [295, 297]. My GEMM supports the hypothesis that the Schwann cell is in fact the tumour cell of origin for PNSTs, for the reasons that I will now explore.

Expression of transgenes in my GEMM was restricted to *Cnp*-expressing cells. I had intended that this would target tumour initiation to the central nervous system OPC, because *Cnp* gene products have been demonstrated to be expressed in cells of the

oligodendrocyte lineage, and to persist in mature oligodendrocytes [202, 298]. However, what I observed was that tumours developed in relation to either peripheral nerves or cranial nerves, both of which are known to be myelinated by Schwann cells rather than oligodendrocytes; the optic nerve, the second cranial nerve, is an exception to this rule, because it is myelinated by OPCs, but I did not observe any tumours related to this nerve.

Interestingly, there have been reports that OPCs can undergo Schwann cell-like differentiation, for example at the site of experimental spinal cord injury, so it is possible that a similar phenomenon was responsible for PNST development in my GEMM [299]. It could also be postulated that the unexpected development of PNSTs in my GEMM resulted from *Cnp* expression in a non-glial cell that is also the PNST cell of origin. For example, the *Cnp* gene product has been identified in cells such as lymphocytes and platelets [300, 301]. However, the existing literature indicates that the *Cnp* gene product is principally a myelin-associated protein and this protein is actually present in peripheral nervous system Schwann cells, as well as central nervous system OPCs [202, 298] [300, 301]. It is therefore most likely that the tumour cell of origin in my GEMM is actually the Schwann cell.

5.7.1 A novel GEMM of malignant peripheral nerve sheath tumour

Examination of the MPNST literature provides evidence that the development of PNSTs in my GEMM is not actually entirely unexpected. For example, *PTEN* loss in both human MPNSTs and in vivo models of PNSTs is associated with malignant progression of the underlying lesion [302]. Consistent with this, I observed variations in PTEN immunostaining within my GEMM tumours that suggested *PTEN* loss of heterozygosity might be associated with tumour progression. The second transgene in my GEMM, *ERBB2*, is also implicated in MPNST biology. Polymorphisms have been identified in human tumours in the tyrosine kinase-encoding domain of *ERBB2* that actually increase gene expression [302, 303]. Furthermore, *ERBB2* gene

expression is greater in MPNST than more benign neurofibromas [302, 303]. Interestingly, ERBB2 has a role in the differentiation, survival and proliferation of normal Schwann cells during development [303]. It is therefore plausible that in my GEMM *ERBB2* overexpression in the developing mouse may promote Schwann cell hyperplasia, subsequent to which *PTEN* loss of heterozygosity drives malignant transformation. This is an important area for future research in order to characterise the molecular pathways responsible for tumourigenesis in my GEMM. For example, using an in vitro model of wild type human Schwann cells the effects of *ERBB2* overexpression and PTEN loss could be sequentially interrogated. In support of this hypothesis, Keng and colleagues recently reported a GEMM where a desert hedgehog regulatory element was used to drive cre recombinase-mediated *PTEN* inactivation, alongside *EGFR* overexpression under the control of a *Cnp* promoter [296]. They concluded, as I have proposed, that *PTEN* cooperates with *EGFR* in the genetic evolution from benign to malignant PNSTs.

5.7.2 A failed GEMM of glioma

The failure to observe evidence of glioma formation in my GEMM was unexpected given the rationale for the development of the model that I detailed in the Background to this Chapter. It may be that gliomagenesis simply takes longer than PNST development in these mice, so that the gliomas did not have time to form before the mice were euthanised; I may have actually overlooked microscopic foci of intracranial glioma growth in the absence of clinical evidence of a central nervous system tumours. Nevertheless, there are also possible genetic and molecular explanations for why glioma development did not occur.

One of the rationales that I discussed in Chapter 1 for incorporating the *Cnp* promoter-driven cre recombinase in my GEMM was that a RCAS/tv-a model of low-grade oligodendroglioma that included the *Cnp* promoter had previously been described [185]. In that model, PDGF targeted to *Cnp*-expressing cells precipitated

glioma formation [185]. Interestingly though, when K-Ras or Akt oncogenes were targeted to *Cnp*-expressing cells instead of PDGF, tumour formation was not initiated [185]. This is surprising, because loss of the tumour supressing effect of PTEN, which is common in glioma, results in increased Akt phosphorylation and therefore its activation (Figure 1.5) [304]. The failure of PI3 kinase pathway activation in this RCAS/tv-a model to precipitate glioma formation may relate to the reasons why gliomas did not develop in my own GEMM. It remains to be understood exactly why PI3 kinase pathway activation does not precipitate glioma formation and this is an important topic for future study. After all, the use of *Akt* as an oncogene has been demonstrated to precipitate glioma formation in other GEMMs of glioma [83]. For example, in a RCAS/tv-a model using *Nestin* or *GFAP* promoters along with *K-Ras* and *Akt* oncogenes, mice develop gliomas [305]. The *Akt* oncogene clearly has the capacity to contribute to the initiation of glioma formation, but perhaps the experience from my own GEMM and the RCAS/tv-a model I have described suggest that this ability is cell type-specific. An important topic for future study will be to compare signalling pathway activation between wild type, $PTEN^{+/-}$ and $PTEN^{-/-}$ mice in my own GEMM to ascertain the precise role that PI3 kinase pathway activation has in tumour formation. As I discuss below, other signalling pathways recognised as important in MPNST formation may in fact be deranged. Genetic profiling of the tumour and non-tumour tissue from my GEMM to characterise the mutations that drive tumour progression will support this pathway analysis.

The combination of transgenes in GEMM also appears to be important in determining the type of tumours that form. For example, mutant *PTEN* alleles have been observed to contribute to glioma formation when targeted to *Nestin*- or *GFAP*-expressing cells, either alone or in association with other some mutant alleles [83]. However, when *PTEN* expression using a *GFAP* promoter-driven cre recombinase was combined specifically with homozygous loss of *Nf1*, PNST rather than glioma developed [306]. This is despite the fact that *Nf1* is mutated in a proportion of human gliomas and that astrocytomas develop when *Nf1* homozygous loss is expressed

using a GFAP promoter-driven cre recombinase in combination with a germline p53 mutation [20, 83]. These findings further underline the fact that the key cell signalling pathways and cell of origin of gliomas and MPNSTs are not yet fully understood.

If similar approaches to the cell-specific targeting of transgene expression can result in the formation of different tumours then it may be that there are actually differences in the promoters used between apparently similar models. For example, the *Cnp* gene has two separate promoters that have different temporal expression patterns during development [185, 202]. This in turn could influence the timing of expression of floxed transgenes, which may therefore impact on tumour initiation and development. In support of this hypothesis, a comparison of GEMMs in which PNST formation occurred using Schwann cell-specific promoters identified that the timing of transgene expression influenced the grade of the lesions that formed, as well as the tumour type [307]. This therefore suggests that it might in fact be possible in future to generate a GEMM of gliomas using a similar design to the GEMM that I have described, but with a promoter to drive cre recombinase to an earlier or later developmental time point than is achieved with *Cnp* promoter expression. One possibility would be to use the promoter for the oligodendrocyte-specific proteolipid protein (PLP). A Tamoxifen-inducible PLP driven Cre recombinase already exists and the inducible element of this model would afford the opportunity to assess whether differences in the temporal expression of transgenes drives the initiation of gliomas rather than PNSTs, or vice versa [307]. PLP is a major component of central nervous system myelin, but its expression begins later than Cnp [308, 309].

There is a further change that I could make to the design of my GEMM to attempt to generate gliomas using the OPC as the tumour-initiating cell. Since the *Cnp* promoter has been successfully employed in a previous glioma model and the *PTEN* transgene has also been demonstrated to be important in glioma GEMMs, the weakest part of my model is possibly the *ERBB2* transgene [83, 185]. Based on existing glioma

GEMMs, a possible choice of transgene for a future novel GEMM would be *K-Ras* [83].

5.7.3 Developing novel approaches to management of MPNSTs

The most effective treatment of MPNST is total surgical resection, but the invasiveness and anatomical location of these tumours limits the success of this approach such that recurrence occurs on average just 13.3 months after surgery [292]. Adjuvant radiotherapy and chemotherapy lack significant efficacy [3]. Metastasis further limits the 5-year survival rate for MPNSTs to 21% for those with NF1 and 42% for those without NF1 [3]. In patients with NF1 who have multiple neurofibromas there are no clinical or pathological means of identifying or predicting which will progress to MPNST, limiting the potential value of preventative surgery [292]. There is therefore a need to identify novel chemotherapeutic targets in order to develop more effective treatment regimens. The novel GEMM that I have generated could assist in identification of such compounds. In particular, it is one of only a handful of MPNST models that do not depend on the deletion of the *Nf1* gene [310]. This is interesting, because loss of the remaining *Nf1* allele is not always observed even in NF1-associated MPNST [311]. My GEMM therefore offers an opportunity to explore the role of alternative signalling pathways in MPNST tumourigenesis that may in turn identify novel targets for drug therapies.

My GEMM has other advantages when compared to existing MPNST models. For example, in my GEMM the tumours occur with 100% penetrance, making it useful for interrogation of therapy effectiveness without the additional cost and delay of a poorly penetrant model. Additionally, in many GEMMs other than my own, the PNSTs that develop occur multi-focally in young mice [310]. Multi-focal disease is actually rare in humans (<1%), so these models may not satisfactorily recapitulate human disease [292]. The sciatic nerve and trigeminal nerve are two of the

commonest sites in humans to be affected by MPNSTs and were also the commonest sites of PNST formation in my model [292].

These observations indicate that there is a strong rationale for informing the process of drug discovery and validating the efficacy of inhibitor compounds using my GEMM. In particular, it will be of interest to investigate the possible clinical utility of drugs targeting the ERBB2 receptor. This receptor has been implicated by my GEMM, and that of Keng and colleagues, as important in MPNST development [296]. Inhibitors targeting this receptor, such as Erlotinib and Trastuzumab, are already in clinical use in the management of breast cancer, so might be rapidly incorporated into management strategies for MPNSTs, if they are effective [312]. In fact, Trastuzumab has already been shown to reduce proliferation of MPNST cells in vitro by 20-30% [261].

5.8 Summary

A GEMM where mutant PTEN and ERBB2 alleles were targeted to cells expressing the *Cnp* protein unexpectedly generated mice with MPNSTs rather than gliomas. Further work is therefore needed to validate my hypothesis that the OPC is the glioma-initiating cell and I have outlined some of the steps that this would involve. The precise design of any future GEMM should be informed by further study of my in vitro glioma stem-like cells to probe the cell of tumour origin and the mutant genes key to tumour initiation. However, the development of a novel GEMM should not delay the process of drug discovery and so there may be a case for utilising existing glioma GEMMs to validate the efficacy of compounds such as PIK75 that were successful in my in vitro inhibitor compound screen.

Whilst the failure to generate a GEMM of glioma was disappointing, my novel model of MPNST is a valuable resource for interrogating the pathogenesis of this deadly disease and for developing novel therapeutic strategies in the future.

Chapter 6. Concluding remarks and future perspectives

The work in this thesis represents an investigation into the application of the cancer stem cell hypothesis of gliomagenesis to the development of preclinical inhibitor compound screening assays. The aim was to identify potential drugs that target this subpopulation of cells implicated in glioma initiation and therapy resistance [3, 125]. In recent years many compounds tested on traditional serum-grown glioma cell lines that appeared efficacious in preclinical studies have failed to be successful in patients. It is therefore hypothesised that inhibitor compounds selected with models based on the glioma stem-like cell are more likely to translate into the clinic effectively, although this is yet to be proven [130]. In this final section I will summarise my findings and the key experiments for future study, which I have already detailed throughout the thesis.

The poor prognosis for patients diagnosed with glioma reflects the lack of efficacy of available therapies. This in turn suggests that previous in vitro models for compound screening failed to adequately recapitulate human disease. I have therefore detailed a technique for the enrichment of putative glioma stem-like cells from human tumours and examined how these in vitro models could be developed into biologically relevant assays for high throughput screening of inhibitor compounds.

A unique aspect to this development of primary cultures is that my access to fresh, patient-derived tissue facilitated multiple samples to be taken from a spectrum of glioma types and grades; this is important, because the vast majority of the published literature has focused on only high-grade gliomas, usually glioblastomas [3, 65, 67, 227]. As a result, I have demonstrated some inter-tumoural and intra-tumoural heterogeneity at the molecular and genetic level that has not previously been described. Examination of this heterogeneity permits interrogation of tumour pathogenesis. Key amongst my observations is that in contrast to the majority of the existing literature describing a single glioma stem-like cell I identified two distinct

cell types in glioma with stem-like characteristics. The glial-like branched phenotype cells had similarities to the radial glial-like cells described as glioma stem-like cells in the literature [65-67]. In addition, I described a distinct, mesenchymal-like, flat phenotype cell. The flat phenotype cells were tumour-derived and invaded in vitro, but their aetiology is uncertain and the detailed characterisation of these cells is the principal area on which I would focus future study. It is important to ascertain the origin of these mesenchymal-like cells and whether they perhaps have a non-glial or non-stem cell-like origin. In support of their classification as stem-like cells, they were derived in growth conditions that support neural stem cell growth, and expressed some markers of the stem cell state. However, they had less neural stem cell-like behaviour than the branched phenotype cells. One explanation for this is that they are actually mesenchymal stem cell-like cells. It will therefore be crucial in future to attempt to differentiate the flat phenotype cells into mesenchymal lineages to ascertain their multi-potency. There are established protocols for assessing mesenchymal stem cell differentiation that I can adapt to my own primary cultures [222, 223].

If the mesenchymal-like cells cannot be differentiated, then this does not detract from their potential importance in gliomagenesis. This is because these cells invaded into type I collagen in a modified inverse invasion assay, supporting the assertion that they are tumour cells and not simply bystander cells [239]. Since the invasion of glioma cells into normal brain is a barrier to effective surgery and therefore survival, the mesenchymal-like cells offer a novel target against which therapies might be directed; assays of compound inhibition of glioma cell invasion are currently performed using established serum-grown glioma cells, or rarely with radial-glial like stem-like glioma cells [239]. The goal is to limit glioma cell invasion in vivo, effectively downgrading the tumour aggressiveness into a localised disease that is amenable to focal therapies such as surgery and radiotherapy.

I presented data in this thesis demonstrating that the flat phenotype cells have a less mutated genetic profile than the branched phenotype cells, indicating that these cells are not directly related to one another. If the mesenchymal-like cells are derived from a precursor cell shared with radial glial-like glioma stem-like cells then this cell remains to be identified. I did not culture both cell phenotypes from all of the gliomas that I took multiple samples from. This may reflect the efficacy of my culture technique, tissue sampling heterogeneity, or may perhaps indicate that there is more than one cellular mechanism of glioma development. If the branched and flat phenotype cells do not have a lineage relationship, the flat phenotype cells may instead have a role in assisting invasion of the radial glial-like glioma cells, at least in some gliomas, akin to a cancer-associated fibroblast. In contrast to many other solid cancers, the potential role of cancer-associated fibroblasts in gliomas has received very little attention [235, 313]. Nevertheless, the observation that glioma stem-like cells reside in a perivascular niche, similar to cancer associated fibroblasts in other tumours, potentially implicates these same cells in glioma cells biology [120]. This is therefore a key area for future research.

If flat and branched phenotype cells do have a cooperative role in the tumour microenvironment than I will need to examine their interactions together. This will require co-culture of the cells, which in turn depends on my ability to define the optimal growth conditions for both. This may be difficult if the flat phenotype cells prefer growth conditions similar to those optimised for mesenchymal stem cells rather than neural stem cells. Co-localisation studies with a immunohistochemistry technique will ascertain whether or not these two cell phenotypes do in fact reside in the same niche. In some of the tumours that I examined I observed that flat and branched phenotype cells were actually derived from tumour regions that themselves had different DNA copy number change profiles. Whether or not these regions also have variations in gene expression profiles that perhaps explain the differences in the phenotype of the cells in the primary cultures derived from them remains to be demonstrated. Interestingly, analysis of the expression of protein kinases across

glioma tissue samples has suggested that there is such genetic heterogeneity, although the implications of this for tumour development are not clear [25, 26]. This heterogeneity may actually result in different regional microenvironments that support the existence or activity of flat phenotype rather than branched phenotype cells, or vice versa. The observation in my own experiments that hypoxic tissue culture conditions appeared to be predictive of flat phenotype cultures may support such a hypothesis, and requires further analysis. However, hypoxia has also been implicated in the proliferation and survival of glioma stem-like cells, so other environmental factors may be important instead [112, 120].

Another reason why the flat phenotype cells may have an important role in our understanding of gliomagenesis is because a similar mesenchymal-like gene expression profile in glioma tissue has been associated with worse outcomes for patients [177]. In fact, the gene expression profiles of both the flat and branched phenotype primary culture cells correlated with different categories of the subtype classification of glioma tumour tissue that has been proposed by Verhaak and colleagues [27]. Further work on gliomas derived from genetically engineered mice also correlated with this classification [174]. However, to my knowledge there has been no demonstration of a correlation between the gene expression profile of primary culture cells and these tissue subtypes. This is therefore an important topic for future research as it could help define the relevance of the mesenchymal-like cells that I have described to the wider published literature. Further interrogation of these primary culture cells will require the generation of multiple primary cultures from different tissue biopsies taken from individual gliomas. I am therefore uniquely placed as a neurosurgeon to carry out this work, because of the very specific requirements for tissue collection.

Modelling both branched and flat phenotype cells in vitro is vital for effective inhibitor screening. The presence of intra- and inter-tumoural primary culture phenotype heterogeneity emphasises the importance of capturing the breadth of

variation amongst primary cultures in pre-clinical screening assays. This is achievable, because I have developed high content analysis in vitro assays of cell death, cell cycle arrest and cell invasion to permit the rapid assessment of several inhibitor compounds across multiple primary cultures, simultaneously. It may be possible to extend this platform in future to make routine personalised patient-specific assessment of potential agents using primary cultures developed from a patient's own tumour. However, the ultimate goal will be to identify biomarkers that relate the expected primary culture phenotype to the actual tumour tissue and in turn predict therapeutic efficacy. This is necessary because the expansion of primary cultures from tumour tissue is expensive and time consuming, so unlikely to be scalable for widespread clinical use. There are currently no biomarkers that have been demonstrated to have predictive value in the management of patients with glioma [314]. The molecular and genomic variations that I have described in this thesis might have potential in this regard.

I focused my initial compound screen on inhibitors of the PI3 kinase pathway, because this pathway has a central role in both the pathogenesis of gliomas and the normal regulation of neural stem cells, with which glioma stem-like cells are thought to be homologous [126, 127, 148, 280]. I identified that PIK75, an isoform specific inhibitor of the p110α catalytic subunit of PI3 kinase, appeared to have a dose-dependent on-target activity against all the primary cultures examined. Considering the differing molecular and genetic features of the flat, mesenchymal-like cells when compared to my radial-glial-like, branched phenotype cells, I would actually have expected that they might have differing sensitivities to inhibitor compounds. The efficacy of PIK75 across the spectrum of primary cultures tested might therefore indicate action on a pathway that is fundamental to the biology of these tumours. The efficacy and mechanism of action of PIK75 in glioma primary cultures requires further investigation and validation. I detailed how I would achieve this in Chapter 4.

Screening large numbers of inhibitor compounds across a broad spectrum of cultures is a useful way to align inhibitor efficacy with inter-tumoural features, the goal being to predict patient responsiveness in the clinic [315]. However, the phenotypic and molecular heterogeneity observed between primary cultures makes it unlikely that a single inhibitor compound will be identified that can effectively treat all gliomas in the clinic. In future studies I will interrogate whether PIK75 also inhibits invasion of my putative glioma stem-like cells, because compounds that target multiple facets of glioma cell biology are more likely to be efficacious in the clinic [315]. I will also examine the cooperative effect of multiple inhibitors in combination as a strategy to prevent the activation of redundant pathway signalling that is responsible for the development of therapy resistance when single chemotherapeutic agents are used alone [315].

If PIK75, or a related compound, is to progress to early clinical assessment of its efficacy, then we need to establish that it can cross the blood brain barrier, since this restricts the movement of most inhibitor compounds between the blood and the brain. It is not known whether PIK75 can cross the blood brain barrier, but its poor solubility suggests that this might not be the case [267]. An important strategy in drug development to overcome the restrictions of the blood brain barrier is to utilise native cell transport mechanism in the brain to facilitate the uptake of drugs and therefore the recent development of a PIK75 nanosuspension that targets PIK75 uptake to folate receptors is encouraging and supports a rationale for proceeding with in vivo pre-clinical testing [267].

Partly to assist with pre-clinical in vivo compound screening, I attempted to develop a novel GEMM of glioma, based on the hierarchical model of glioma, by targeting floxed *PTEN* and *ERBB2* transgenes to the Oligodendrocyte precursor cell as a potential glioma-initiating cell using a *Cnp* promoter-driven cre recombinase. The goal of this was also to help validate the hierarchical model of glioma formation. Unexpectedly, this GEMM generated mice with peripheral nerve sheath tumours

(PNSTs) rather than gliomas. Further work is therefore needed to validate my hypothesis that the OPC is the glioma-initiating cell and I have outlined some of the steps that this would involve in Chapter 5. Nevertheless, this novel GEMM appears to recapitulate human malignant peripheral nerve sheath tumour development, so it is a potentially valuable resource for interrogating the pathogenesis of this deadly disease and for developing novel therapeutic strategies. My failure to develop a novel GEMM for compound testing in gliomas should not delay the in vivo assessment of PIK75. An alternative strategy, as I discussed in Chapter 4, would be to utilise other existing glioma GEMMs instead.

LIST OF REFERENCES

1. Louis, D.N., et al., *The 2007 WHO classification of tumours of the central nervous system.* Acta neuropathologica, 2007. **114**(2): p. 97-109.
2. Stupp, R., et al., *Radiotherapy plus concomitant and adjuvant temozolomide for glioblastoma.* N Engl J Med, 2005. **352**(10): p. 987-96.
3. Singh, S.K., et al., *Identification of human brain tumour initiating cells.* Nature, 2004. **432**(7015): p. 396-401.
4. Lonn, S., et al., *Incidence trends of adult primary intracerebral tumors in four Nordic countries.* Int J Cancer, 2004. **108**(3): p. 450-5.
5. Radhakrishnan, K., et al., *The trends in incidence of primary brain tumors in the population of Rochester, Minnesota.* Annals of neurology, 1995. **37**(1): p. 67-73.
6. Hess, K.R., K.R. Broglio, and M.L. Bondy, *Adult glioma incidence trends in the United States, 1977-2000.* Cancer, 2004. **101**(10): p. 2293-9.
7. Curran, W.J., Jr., et al., *Recursive partitioning analysis of prognostic factors in three Radiation Therapy Oncology Group malignant glioma trials.* Journal of the National Cancer Institute, 1993. **85**(9): p. 704-10.
8. Hanahan, D. and R.A. Weinberg, *The hallmarks of cancer.* Cell, 2000. **100**(1): p. 57-70.
9. Burger, P.C., et al., *Glioblastoma multiforme and anaplastic astrocytoma. Pathologic criteria and prognostic implications.* Cancer, 1985. **56**(5): p. 1106-11.
10. Kimelberg, H.K. and M. Nedergaard, *Functions of astrocytes and their potential as therapeutic targets.* Neurotherapeutics : the journal of the American Society for Experimental NeuroTherapeutics, 2010. **7**(4): p. 338-53.
11. Bradl, M. and H. Lassmann, *Oligodendrocytes: biology and pathology.* Acta neuropathologica, 2010. **119**(1): p. 37-53.
12. Del Bigio, M.R., *Ependymal cells: biology and pathology.* Acta neuropathologica, 2010. **119**(1): p. 55-73.
13. Doetsch, F., et al., *Subventricular zone astrocytes are neural stem cells in the adult mammalian brain.* Cell, 1999. **97**(6): p. 703-16.
14. Gavin Quigley, D., et al., *Outcome predictors in the management of spinal cord ependymoma.* European spine journal : official publication of the European Spine Society, the European Spinal Deformity Society, and the European Section of the Cervical Spine Research Society, 2007. **16**(3): p. 399-404.
15. Furnari, F.B., et al., *Malignant astrocytic glioma: genetics, biology, and paths to treatment.* Genes Dev, 2007. **21**(21): p. 2683-710.
16. Louis, D.N., E.C. Holland, and J.G. Cairncross, *Glioma classification: a molecular reappraisal.* The American journal of pathology, 2001. **159**(3): p. 779-86.

17. Bauman, G., et al., *Pretreatment factors predict overall survival for patients with low-grade glioma: a recursive partitioning analysis.* International journal of radiation oncology, biology, physics, 1999. **45**(4): p. 923-9.
18. Jenkins, R.B., et al., *A t(1;19)(q10;p10) mediates the combined deletions of 1p and 19q and predicts a better prognosis of patients with oligodendroglioma.* Cancer research, 2006. **66**(20): p. 9852-61.
19. Louis, D.N., *Molecular pathology of malignant gliomas.* Annual review of pathology, 2006. **1**: p. 97-117.
20. Parsons, D.W., et al., *An integrated genomic analysis of human glioblastoma multiforme.* Science, 2008. **321**(5897): p. 1807-12.
21. Ohgaki, H. and P. Kleihues, *Genetic pathways to primary and secondary glioblastoma.* Am J Pathol, 2007. **170**(5): p. 1445-53.
22. Yan, H., et al., *IDH1 and IDH2 mutations in gliomas.* N Engl J Med, 2009. **360**(8): p. 765-73.
23. Yan, H., et al., *IDH1 and IDH2 mutations in gliomas.* The New England journal of medicine, 2009. **360**(8): p. 765-73.
24. Turcan, S., et al., *IDH1 mutation is sufficient to establish the glioma hypermethylator phenotype.* Nature, 2012. **483**(7390): p. 479-83.
25. Little, S.E., et al., *Receptor tyrosine kinase genes amplified in glioblastoma exhibit a mutual exclusivity in variable proportions reflective of individual tumor heterogeneity.* Cancer research, 2012. **72**(7): p. 1614-20.
26. Snuderl, M., et al., *Mosaic amplification of multiple receptor tyrosine kinase genes in glioblastoma.* Cancer cell, 2011. **20**(6): p. 810-7.
27. Verhaak, R.G., et al., *Integrated genomic analysis identifies clinically relevant subtypes of glioblastoma characterized by abnormalities in PDGFRA, IDH1, EGFR, and NF1.* Cancer cell, 2010. **17**(1): p. 98-110.
28. Lei, L., et al., *Glioblastoma models reveal the connection between adult glial progenitors and the proneural phenotype.* PloS one, 2011. **6**(5): p. e20041.
29. Hegi, M.E., et al., *MGMT gene silencing and benefit from temozolomide in glioblastoma.* The New England journal of medicine, 2005. **352**(10): p. 997-1003.
30. Le Mercier, M., et al., *A simplified approach for the molecular classification of glioblastomas.* PloS one, 2012. **7**(9): p. e45475.
31. Brenner, H., *Long-term survival rates of cancer patients achieved by the end of the 20th century: a period analysis.* Lancet, 2002. **360**(9340): p. 1131-5.
32. Dandy, *Removal of right cerebral hemisphere for certain tumors with hemiplegia.* JAMA, 1928. **90**: p. 823.
33. Lefranc, F., J. Brotchi, and R. Kiss, *Possible future issues in the treatment of glioblastomas: special emphasis on cell migration and the resistance of migrating glioblastoma cells to apoptosis.* J Clin Oncol, 2005. **23**(10): p. 2411-22.
34. Lacroix, M., et al., *A multivariate analysis of 416 patients with glioblastoma multiforme: prognosis, extent of resection, and survival.* Journal of neurosurgery, 2001. **95**(2): p. 190-8.

35. Stummer, W., et al., *Fluorescence-guided surgery with 5-aminolevulinic acid for resection of malignant glioma: a randomised controlled multicentre phase III trial.* The lancet oncology, 2006. **7**(5): p. 392-401.
36. Nimsky, C., et al., *Preoperative and intraoperative diffusion tensor imaging-based fiber tracking in glioma surgery.* Neurosurgery, 2005. **56**(1): p. 130-7; discussion 138.
37. Kubben, P.L., et al., *Intraoperative MRI-guided resection of glioblastoma multiforme: a systematic review.* The lancet oncology, 2011. **12**(11): p. 1062-70.
38. Nimsky, C., et al., *Volumetric assessment of glioma removal by intraoperative high-field magnetic resonance imaging.* Neurosurgery, 2004. **55**(2): p. 358-70; discussion 370-1.
39. Mieog, J.S., et al., *Novel intraoperative near-infrared fluorescence camera system for optical image-guided cancer surgery.* Molecular imaging, 2010. **9**(4): p. 223-31.
40. Luciani, A., et al., *Glucose-receptor MR imaging of tumors: study in mice with PEGylated paramagnetic niosomes.* Radiology, 2004. **231**(1): p. 135-42.
41. Schmieder, A.H., et al., *Three-dimensional MR mapping of angiogenesis with alpha5beta1(alpha nu beta3)-targeted theranostic nanoparticles in the MDA-MB-435 xenograft mouse model.* FASEB journal : official publication of the Federation of American Societies for Experimental Biology, 2008. **22**(12): p. 4179-89.
42. Yang, Y.L., et al., *Characteristic autofluorescence for cancer diagnosis and its origin.* Lasers in surgery and medicine, 1987. **7**(6): p. 528-32.
43. advice, N.g., http://guidance.nice.org.uk/IP/893. 2010.
44. Stevens, M.F., et al., *Antitumor activity and pharmacokinetics in mice of 8-carbamoyl-3-methyl-imidazo[5,1-d]-1,2,3,5-tetrazin-4(3H)-one (CCRG 81045; M & B 39831), a novel drug with potential as an alternative to dacarbazine.* Cancer research, 1987. **47**(22): p. 5846-52.
45. Friedman, H.S., T. Kerby, and H. Calvert, *Temozolomide and treatment of malignant glioma.* Clinical cancer research : an official journal of the American Association for Cancer Research, 2000. **6**(7): p. 2585-97.
46. Newlands, E.S., et al., *Temozolomide: a review of its discovery, chemical properties, pre-clinical development and clinical trials.* Cancer treatment reviews, 1997. **23**(1): p. 35-61.
47. Westphal, M., et al., *A phase 3 trial of local chemotherapy with biodegradable carmustine (BCNU) wafers (Gliadel wafers) in patients with primary malignant glioma.* Neuro-oncology, 2003. **5**(2): p. 79-88.
48. Bota, D.A., et al., *Interstitial chemotherapy with biodegradable BCNU (Gliadel) wafers in the treatment of malignant gliomas.* Therapeutics and clinical risk management, 2007. **3**(5): p. 707-15.
49. McGovern, P.C., et al., *Risk factors for postcraniotomy surgical site infection after 1,3-bis (2-chloroethyl)-1-nitrosourea (Gliadel) wafer placement.* Clinical infectious diseases : an official publication of the Infectious Diseases Society of America, 2003. **36**(6): p. 759-65.

50. Chamberlain, M.C., *Bevacizumab for the treatment of recurrent glioblastoma.* Clinical Medicine Insights. Oncology, 2011. **5**: p. 117-29.
51. Sathornsumetee, S. and J.N. Rich, *Designer therapies for glioblastoma multiforme.* Annals of the New York Academy of Sciences, 2008. **1142**: p. 108-32.
52. Friedman, H.S., et al., *Bevacizumab alone and in combination with irinotecan in recurrent glioblastoma.* Journal of clinical oncology : official journal of the American Society of Clinical Oncology, 2009. **27**(28): p. 4733-40.
53. Herper, M., *The Truly Staggering Cost of Inventing New Drugs.* Forbes, 2012. **10/02/12**.
54. Kola, I. and J. Landis, *Can the pharmaceutical industry reduce attrition rates?* Nature reviews. Drug discovery, 2004. **3**(8): p. 711-5.
55. Abbott, N.J., L. Ronnback, and E. Hansson, *Astrocyte-endothelial interactions at the blood-brain barrier.* Nature reviews. Neuroscience, 2006. **7**(1): p. 41-53.
56. Pardridge, W.M., *The blood-brain barrier: bottleneck in brain drug development.* NeuroRx : the journal of the American Society for Experimental NeuroTherapeutics, 2005. **2**(1): p. 3-14.
57. Nowell, P.C., *The clonal evolution of tumor cell populations.* Science, 1976. **194**(4260): p. 23-8.
58. Alison, M.R., S.M. Lim, and L.J. Nicholson, *Cancer stem cells: problems for therapy?* The Journal of pathology, 2011. **223**(2): p. 147-61.
59. Sanai, N., A. Alvarez-Buylla, and M.S. Berger, *Neural stem cells and the origin of gliomas.* The New England journal of medicine, 2005. **353**(8): p. 811-22.
60. Weiss, S., et al., *Is there a neural stem cell in the mammalian forebrain?* Trends in neurosciences, 1996. **19**(9): p. 387-93.
61. Lee, J., et al., *Tumor stem cells derived from glioblastomas cultured in bFGF and EGF more closely mirror the phenotype and genotype of primary tumors than do serum-cultured cell lines.* Cancer Cell, 2006. **9**(5): p. 391-403.
62. Lobo, N.A., et al., *The biology of cancer stem cells.* Annual review of cell and developmental biology, 2007. **23**: p. 675-99.
63. Bonnet, D. and J.E. Dick, *Human acute myeloid leukemia is organized as a hierarchy that originates from a primitive hematopoietic cell.* Nature medicine, 1997. **3**(7): p. 730-7.
64. Dirks, P., *Cancer stem cells: Invitation to a second round.* Nature. **466**(7302): p. 40-1.
65. Fael Al-Mayhani, T.M., et al., *An efficient method for derivation and propagation of glioblastoma cell lines that conserves the molecular profile of their original tumours.* J Neurosci Methods, 2009. **176**(2): p. 192-9.
66. Galli, R., et al., *Isolation and characterization of tumorigenic, stem-like neural precursors from human glioblastoma.* Cancer Res, 2004. **64**(19): p. 7011-21.

67. Pollard, S.M., et al., *Glioma stem cell lines expanded in adherent culture have tumor-specific phenotypes and are suitable for chemical and genetic screens.* Cell Stem Cell, 2009. **4**(6): p. 568-80.
68. Kriegstein, A. and A. Alvarez-Buylla, *The glial nature of embryonic and adult neural stem cells.* Annual review of neuroscience, 2009. **32**: p. 149-84.
69. Gotz, M. and W.B. Huttner, *The cell biology of neurogenesis.* Nature reviews. Molecular cell biology, 2005. **6**(10): p. 777-88.
70. Leclerc, C., I. Neant, and M. Moreau, *The calcium: an early signal that initiates the formation of the nervous system during embryogenesis.* Frontiers in molecular neuroscience, 2012. **5**: p. 3.
71. Salomoni, P. and F. Calegari, *Cell cycle control of mammalian neural stem cells: putting a speed limit on G1.* Trends in cell biology, 2010. **20**(5): p. 233-43.
72. Sanai, N., et al., *Unique astrocyte ribbon in adult human brain contains neural stem cells but lacks chain migration.* Nature, 2004. **427**(6976): p. 740-4.
73. Johansson, C.B., et al., *Neural stem cells in the adult human brain.* Experimental cell research, 1999. **253**(2): p. 733-6.
74. Spalding, K.L., et al., *Dynamics of hippocampal neurogenesis in adult humans.* Cell, 2013. **153**(6): p. 1219-27.
75. Singh, S.K., et al., *Identification of a cancer stem cell in human brain tumors.* Cancer Res, 2003. **63**(18): p. 5821-8.
76. Reya, T., et al., *Stem cells, cancer, and cancer stem cells.* Nature, 2001. **414**(6859): p. 105-11.
77. Lathia, J.D., et al., *The microenvironment of the embryonic neural stem cell: lessons from adult niches?* Dev Dyn, 2007. **236**(12): p. 3267-82.
78. Alvarez-Buylla, A., B. Seri, and F. Doetsch, *Identification of neural stem cells in the adult vertebrate brain.* Brain Res Bull, 2002. **57**(6): p. 751-8.
79. Menn, B., et al., *Origin of oligodendrocytes in the subventricular zone of the adult brain.* J Neurosci, 2006. **26**(30): p. 7907-18.
80. Yuan, X., et al., *Isolation of cancer stem cells from adult glioblastoma multiforme.* Oncogene, 2004. **23**(58): p. 9392-400.
81. Li, Y. and J. Laterra, *Cancer stem cells: distinct entities or dynamically regulated phenotypes?* Cancer research, 2012. **72**(3): p. 576-80.
82. Visvader, J.E., *Cells of origin in cancer.* Nature, 2011. **469**(7330): p. 314-22.
83. Huse, J.T. and E.C. Holland, *Genetically engineered mouse models of brain cancer and the promise of preclinical testing.* Brain Pathol, 2009. **19**(1): p. 132-43.
84. Carpenter, M.K., et al., *In vitro expansion of a multipotent population of human neural progenitor cells.* Experimental neurology, 1999. **158**(2): p. 265-78.
85. Reynolds, B.A. and S. Weiss, *Clonal and population analyses demonstrate that an EGF-responsive mammalian embryonic CNS precursor is a stem cell.* Dev Biol, 1996. **175**(1): p. 1-13.

86. Reynolds, B.A., W. Tetzlaff, and S. Weiss, *A multipotent EGF-responsive striatal embryonic progenitor cell produces neurons and astrocytes.* J Neurosci, 1992. **12**(11): p. 4565-74.
87. Pollard, S.M., et al., *Adherent neural stem (NS) cells from fetal and adult forebrain.* Cerebral cortex, 2006. **16 Suppl 1**: p. i112-20.
88. Dirks, P.B., *Brain tumor stem cells: bringing order to the chaos of brain cancer.* J Clin Oncol, 2008. **26**(17): p. 2916-24.
89. Craig, C.G., et al., *In vivo growth factor expansion of endogenous subependymal neural precursor cell populations in the adult mouse brain.* J Neurosci, 1996. **16**(8): p. 2649-58.
90. Duggal, N., R. Schmidt-Kastner, and A.M. Hakim, *Nestin expression in reactive astrocytes following focal cerebral ischemia in rats.* Brain research, 1997. **768**(1-2): p. 1-9.
91. Ma, Y.H., et al., *Expression of stem cell markers in human astrocytomas of different WHO grades.* Journal of neuro-oncology, 2008. **86**(1): p. 31-45.
92. Lathia JD, H.M., Gallagher J, Gadani SP, Adkins J, Vasanji A, Liu L, Eyler CE, Heddleston JM, Wu Q, Minhas S, Soeda A, Hoeppner DJ, Ravin R, McKay RD, McLendon RE, Corbeil D, Chenn A, Hjelmeland AB, Park DM, Rich JN., *Distribution of CD133 reveals glioma stem cells self-renew through symmetric and asymmetric cell divisions.* Cell Death and Disease, 2012. **2**(9): p. e200.
93. Brescia, P., C. Richichi, and G. Pelicci, *Current strategies for identification of glioma stem cells: adequate or unsatisfactory?* Journal of oncology, 2012. **2012**: p. 376894.
94. Bao, S., et al., *Targeting cancer stem cells through L1CAM suppresses glioma growth.* Cancer Res, 2008. **68**(15): p. 6043-8.
95. Assanah, M., et al., *Glial progenitors in adult white matter are driven to form malignant gliomas by platelet-derived growth factor-expressing retroviruses.* J Neurosci, 2006. **26**(25): p. 6781-90.
96. Hall, P.E., et al., *Integrins are markers of human neural stem cells.* Stem Cells, 2006. **24**(9): p. 2078-84.
97. Lathia, J.D., et al., *Integrin alpha 6 regulates glioblastoma stem cells.* Cell Stem Cell. **6**(5): p. 421-32.
98. Beier, D., et al., *CD133(+) and CD133(-) glioblastoma-derived cancer stem cells show differential growth characteristics and molecular profiles.* Cancer research, 2007. **67**(9): p. 4010-5.
99. Lathia, J.D., et al., *Distribution of CD133 reveals glioma stem cells self-renew through symmetric and asymmetric cell divisions.* Cell death & disease, 2011. **2**: p. e200.
100. Liu, G., et al., *Analysis of gene expression and chemoresistance of CD133+ cancer stem cells in glioblastoma.* Mol Cancer, 2006. **5**: p. 67.
101. Platet, N., et al., *Influence of oxygen tension on CD133 phenotype in human glioma cell cultures.* Cancer Lett, 2007. **258**(2): p. 286-90.
102. Tabu, K., et al., *Promoter hypomethylation regulates CD133 expression in human gliomas.* Cell Res, 2008. **18**(10): p. 1037-46.

103. Yan, X., et al., *A CD133-related gene expression signature identifies an aggressive glioblastoma subtype with excessive mutations.* Proceedings of the National Academy of Sciences of the United States of America, 2011. **108**(4): p. 1591-6.
104. Uchida, N., et al., *Direct isolation of human central nervous system stem cells.* Proceedings of the National Academy of Sciences of the United States of America, 2000. **97**(26): p. 14720-5.
105. deCarvalho, A.C., et al., *Gliosarcoma stem cells undergo glial and mesenchymal differentiation in vivo.* Stem Cells, 2010. **28**(2): p. 181-90.
106. Wang, J., et al., *CD133 negative glioma cells form tumors in nude rats and give rise to CD133 positive cells.* International journal of cancer. Journal international du cancer, 2008. **122**(4): p. 761-8.
107. Cheng, L., et al., *L1CAM regulates DNA damage checkpoint response of glioblastoma stem cells through NBS1.* The EMBO journal, 2011. **30**(5): p. 800-13.
108. Kerr, M.A. and S.C. Stocks, *The role of CD15-(Le(X))-related carbohydrates in neutrophil adhesion.* The Histochemical journal, 1992. **24**(11): p. 811-26.
109. Kahlert, U.D., et al., *CD133/CD15 defines distinct cell subpopulations with differential in vitro clonogenic activity and stem cell-related gene expression profile in in vitro propagated glioblastoma multiforme-derived cell line with a PNET-like component.* Folia neuropathologica / Association of Polish Neuropathologists and Medical Research Centre, Polish Academy of Sciences, 2012. **50**(4): p. 357-68.
110. Hynes, R.O., *Integrins: bidirectional, allosteric signaling machines.* Cell, 2002. **110**(6): p. 673-87.
111. *Cilengitide, Temozolomide, and Radiation Therapy in Treating Patients With Newly Diagnosed Glioblastoma and Methylated Gene Promoter Status (CENTRIC)*. 2013; Available from: http://clinicaltrials.gov/show/NCT00689221.
112. Seidel, S., et al., *A hypoxic niche regulates glioblastoma stem cells through hypoxia inducible factor 2 alpha.* Brain, 2010. **133**(Pt 4): p. 983-95.
113. Studer, L., et al., *Enhanced proliferation, survival, and dopaminergic differentiation of CNS precursors in lowered oxygen.* J Neurosci, 2000. **20**(19): p. 7377-83.
114. Parrinello, S., et al., *Oxygen sensitivity severely limits the replicative lifespan of murine fibroblasts.* Nat Cell Biol, 2003. **5**(8): p. 741-7.
115. Sullivan, M., P. Galea, and S. Latif, *What is the appropriate oxygen tension for in vitro culture?* Mol Hum Reprod, 2006. **12**(11): p. 653.
116. Csete, M., *Oxygen in the cultivation of stem cells.* Ann N Y Acad Sci, 2005. **1049**: p. 1-8.
117. Silver, I. and M. Erecinska, *Oxygen and ion concentrations in normoxic and hypoxic brain cells.* Adv Exp Med Biol, 1998. **454**: p. 7-16.
118. Whittle, I.R., *Assessment of physiological parameters within glioblastomas in awake patients: a prospective clinical study.* . British Journal of Neurosurgery, 2010. **24**(4): p. 447-453.

119. Bertout, J.A., S.A. Patel, and M.C. Simon, *The impact of O2 availability on human cancer.* Nat Rev Cancer, 2008. **8**(12): p. 967-75.
120. Calabrese, C., et al., *A perivascular niche for brain tumor stem cells.* Cancer Cell, 2007. **11**(1): p. 69-82.
121. Heddleston, J.M., et al., *The hypoxic microenvironment maintains glioblastoma stem cells and promotes reprogramming towards a cancer stem cell phenotype.* Cell Cycle, 2009. **8**(20): p. 3274-84.
122. Province, P., *Hypoxia, Angiogenesis and Mechanisms for Invasion of Malignant Gliomas*, in *Evolution of the Molecular Biology of Brain Tumors and the Therapeutic Implications*, P. Lichtor, Editor 2013, InTech.
123. Evans, S.M., et al., *Comparative measurements of hypoxia in human brain tumors using needle electrodes and EF5 binding.* Cancer Res, 2004. **64**(5): p. 1886-92.
124. Acs, G., et al., *Autocrine erythropoietin signaling inhibits hypoxia-induced apoptosis in human breast carcinoma cells.* Cancer Lett, 2004. **214**(2): p. 243-51.
125. Bao, S., et al., *Glioma stem cells promote radioresistance by preferential activation of the DNA damage response.* Nature, 2006. **444**(7120): p. 756-60.
126. Bleau, A.M., et al., *PTEN/PI3K/Akt pathway regulates the side population phenotype and ABCG2 activity in glioma tumor stem-like cells.* Cell Stem Cell, 2009. **4**(3): p. 226-35.
127. Li, J., et al., *PTEN, a putative protein tyrosine phosphatase gene mutated in human brain, breast, and prostate cancer.* Science, 1997. **275**(5308): p. 1943-7.
128. Eyler, C.E. and J.N. Rich, *Survival of the fittest: cancer stem cells in therapeutic resistance and angiogenesis.* J Clin Oncol, 2008. **26**(17): p. 2839-45.
129. Danovi, D., et al., *High content screening of defined chemical libraries using normal and glioma-derived neural stem cell lines.* Methods in enzymology, 2012. **506**: p. 311-29.
130. Kenney-Herbert, E.M., et al., *Glioblastoma cell lines derived under serum-free conditions can be used as an in vitro model system to evaluate therapeutic response.* Cancer letters, 2011. **305**(1): p. 50-7.
131. Brunelle, J.K. and B. Zhang, *Apoptosis assays for quantifying the bioactivity of anticancer drug products.* Drug resistance updates : reviews and commentaries in antimicrobial and anticancer chemotherapy, 2010. **13**(6): p. 172-9.
132. Badr, C.E., T. Wurdinger, and B.A. Tannous, *Functional drug screening assay reveals potential glioma therapeutics.* Assay and drug development technologies, 2011. **9**(3): p. 281-9.
133. Skehan, P., et al., *New colorimetric cytotoxicity assay for anticancer-drug screening.* Journal of the National Cancer Institute, 1990. **82**(13): p. 1107-12.
134. Rixe, O. and T. Fojo, *Is cell death a critical end point for anticancer therapies or is cytostasis sufficient?* Clinical cancer research : an official

journal of the American Association for Cancer Research, 2007. **13**(24): p. 7280-7.
135. Gioeli, D., *The Dynamics of the Cell Signaling Network; Implications for Targeted Therapies*, in *Targeted Therapies: Mechanisms of Resistance,*, D. Gioeli, Editor 2011.
136. Liu, C., et al., *Mosaic analysis with double markers reveals tumor cell of origin in glioma.* Cell, 2011. **146**(2): p. 209-21.
137. Carragher, N., *Advancing high content analysis towards improving clinical efficacy.* European Pharmaceutical Review, 2011. **16**(1): p. 12-16.
138. Wilson, B., L.A. Liotta, and E. Petricoin, 3rd, *Monitoring proteins and protein networks using reverse phase protein arrays.* Disease markers, 2010. **28**(4): p. 225-32.
139. Bickle, M., *The beautiful cell: high-content screening in drug discovery.* Analytical and bioanalytical chemistry, 2010. **398**(1): p. 219-26.
140. Huse, J.T. and E.C. Holland, *Targeting brain cancer: advances in the molecular pathology of malignant glioma and medulloblastoma.* Nature reviews. Cancer, 2010. **10**(5): p. 319-31.
141. Stockhausen, M.T., K. Kristoffersen, and H.S. Poulsen, *The functional role of Notch signaling in human gliomas.* Neuro-oncology, 2010. **12**(2): p. 199-211.
142. Lino, M.M., A. Merlo, and J.L. Boulay, *Notch signaling in glioblastoma: a developmental drug target?* BMC medicine, 2010. **8**: p. 72.
143. Yamanaka, R. and H. Saya, *Molecularly targeted therapies for glioma.* Annals of neurology, 2009. **66**(6): p. 717-29.
144. De Witt Hamer, P.C., *Small molecule kinase inhibitors in glioblastoma: a systematic review of clinical studies.* Neuro-oncology, 2010. **12**(3): p. 304-16.
145. Lino, M.M. and A. Merlo, *PI3Kinase signaling in glioblastoma.* Journal of neuro-oncology, 2011. **103**(3): p. 417-27.
146. Dourdin, N., et al., *Phosphatase and tensin homologue deleted on chromosome 10 deficiency accelerates tumor induction in a mouse model of ErbB-2 mammary tumorigenesis.* Cancer Res, 2008. **68**(7): p. 2122-31.
147. Cheng, J.Q., et al., *The Akt/PKB pathway: molecular target for cancer drug discovery.* Oncogene, 2005. **24**(50): p. 7482-92.
148. Wang, S.I., et al., *Somatic mutations of PTEN in glioblastoma multiforme.* Cancer research, 1997. **57**(19): p. 4183-6.
149. Chakravarti, A., et al., *The prognostic significance of phosphatidylinositol 3-kinase pathway activation in human gliomas.* J Clin Oncol, 2004. **22**(10): p. 1926-33.
150. Furnari, F.B., et al., *Growth suppression of glioma cells by PTEN requires a functional phosphatase catalytic domain.* Proc Natl Acad Sci U S A, 1997. **94**(23): p. 12479-84.
151. Groszer, M., et al., *Negative regulation of neural stem/progenitor cell proliferation by the Pten tumor suppressor gene in vivo.* Science, 2001. **294**(5549): p. 2186-9.

152. Kim, H.S., et al., *Gliomagenesis arising from Pten- and Ink4a/Arf-deficient neural progenitor cells is mediated by the p53-Fbxw7/Cdc4 pathway, which controls c-Myc.* Cancer research, 2012. **72**(22): p. 6065-75.
153. Alcantara Llaguno, S., et al., *Malignant astrocytomas originate from neural stem/progenitor cells in a somatic tumor suppressor mouse model.* Cancer cell, 2009. **15**(1): p. 45-56.
154. Vivanco, I., et al., *Differential sensitivity of glioma- versus lung cancer-specific EGFR mutations to EGFR kinase inhibitors.* Cancer discovery, 2012. **2**(5): p. 458-71.
155. Heimberger, A.B., et al., *The natural history of EGFR and EGFRvIII in glioblastoma patients.* Journal of translational medicine, 2005. **3**: p. 38.
156. Lefranc, F. and R. Kiss, *The sodium pump alpha1 subunit as a potential target to combat apoptosis-resistant glioblastomas.* Neoplasia, 2008. **10**(3): p. 198-206.
157. Fenton, T.R., et al., *Resistance to EGF receptor inhibitors in glioblastoma mediated by phosphorylation of the PTEN tumor suppressor at tyrosine 240.* Proceedings of the National Academy of Sciences of the United States of America, 2012. **109**(35): p. 14164-9.
158. Broderick, S.R., et al., *SCCRO promotes glioma formation and malignant progression in mice.* Neoplasia, 2010. **12**(6): p. 476-84.
159. Gallia, G.L., et al., *PIK3CA gene mutations in pediatric and adult glioblastoma multiforme.* Molecular cancer research : MCR, 2006. **4**(10): p. 709-14.
160. Zheng, Z., et al., *Isoform-selective inhibition of phosphoinositide 3-kinase: identification of a new region of nonconserved amino acids critical for p110alpha inhibition.* Molecular pharmacology, 2011. **80**(4): p. 657-64.
161. Fan, Q.W., et al., *A dual PI3 kinase/mTOR inhibitor reveals emergent efficacy in glioma.* Cancer cell, 2006. **9**(5): p. 341-9.
162. Tan, S., Y. Ng, and D.E. James, *Next-generation Akt inhibitors provide greater specificity: effects on glucose metabolism in adipocytes.* The Biochemical journal, 2011. **435**(2): p. 539-44.
163. Kerbel, R.S., *What is the optimal rodent model for anti-tumor drug testing?* Cancer metastasis reviews, 1998. **17**(3): p. 301-4.
164. Gupta, P.B., C.L. Chaffer, and R.A. Weinberg, *Cancer stem cells: mirage or reality?* Nat Med, 2009. **15**(9): p. 1010-2.
165. Kelly, P.N., et al., *Tumor growth need not be driven by rare cancer stem cells.* Science, 2007. **317**(5836): p. 337.
166. Quintana, E., et al., *Efficient tumour formation by single human melanoma cells.* Nature, 2008. **456**(7222): p. 593-8.
167. Rana, M.W., et al., *Heterotransplantation of human glioblastoma multiforme and meningioma to nude mice.* Proceedings of the Society for Experimental Biology and Medicine. Society for Experimental Biology and Medicine, 1977. **155**(1): p. 85-8.
168. Chen, J., R.M. McKay, and L.F. Parada, *Malignant glioma: lessons from genomics, mouse models, and stem cells.* Cell, 2012. **149**(1): p. 36-47.

169. Sakariassen, P.O., et al., *Angiogenesis-independent tumor growth mediated by stem-like cancer cells.* Proceedings of the National Academy of Sciences of the United States of America, 2006. **103**(44): p. 16466-71.
170. Wang, J., et al., *A reproducible brain tumour model established from human glioblastoma biopsies.* BMC cancer, 2009. **9**: p. 465.
171. Sharpless, N.E. and R.A. Depinho, *The mighty mouse: genetically engineered mouse models in cancer drug development.* Nature reviews. Drug discovery, 2006. **5**(9): p. 741-54.
172. Ryding, A.D., M.G. Sharp, and J.J. Mullins, *Conditional transgenic technologies.* The Journal of endocrinology, 2001. **171**(1): p. 1-14.
173. Holland, E.C., *A mouse model for glioma: biology, pathology, and therapeutic opportunities.* Toxicol Pathol, 2000. **28**(1): p. 171-7.
174. Henriquez, N.V., et al., *Comparative expression analysis reveals lineage relationships between human and murine gliomas and a dominance of glial signatures during tumor propagation in vitro.* Cancer research, 2013. **73**(18): p. 5834-44.
175. Jacques, T.S., et al., *Combinations of genetic mutations in the adult neural stem cell compartment determine brain tumour phenotypes.* The EMBO journal, 2010. **29**(1): p. 222-35.
176. de Vries, N.A., et al., *Rapid and robust transgenic high-grade glioma mouse models for therapy intervention studies.* Clinical cancer research : an official journal of the American Association for Cancer Research, 2010. **16**(13): p. 3431-41.
177. Phillips, H.S., et al., *Molecular subclasses of high-grade glioma predict prognosis, delineate a pattern of disease progression, and resemble stages in neurogenesis.* Cancer cell, 2006. **9**(3): p. 157-73.
178. Casper, K.B. and K.D. McCarthy, *GFAP-positive progenitor cells produce neurons and oligodendrocytes throughout the CNS.* Mol Cell Neurosci, 2006. **31**(4): p. 676-84.
179. Marino, S., et al., *Induction of medulloblastomas in p53-null mutant mice by somatic inactivation of Rb in the external granular layer cells of the cerebellum.* Genes & development, 2000. **14**(8): p. 994-1004.
180. Lendahl, U., L.B. Zimmerman, and R.D. McKay, *CNS stem cells express a new class of intermediate filament protein.* Cell, 1990. **60**(4): p. 585-95.
181. Dahlstrand, J., M. Lardelli, and U. Lendahl, *Nestin mRNA expression correlates with the central nervous system progenitor cell state in many, but not all, regions of developing central nervous system.* Brain Res Dev Brain Res, 1995. **84**(1): p. 109-29.
182. Wiese, C., et al., *Nestin expression--a property of multi-lineage progenitor cells?* Cell Mol Life Sci, 2004. **61**(19-20): p. 2510-22.
183. Suzuki, S., et al., *The neural stem/progenitor cell marker nestin is expressed in proliferative endothelial cells, but not in mature vasculature.* The journal of histochemistry and cytochemistry : official journal of the Histochemistry Society, 2010. **58**(8): p. 721-30.

184. Ligon, K.L., et al., *The oligodendroglial lineage marker OLIG2 is universally expressed in diffuse gliomas.* J Neuropathol Exp Neurol, 2004. **63**(5): p. 499-509.
185. Lindberg, N., et al., *Oligodendrocyte progenitor cells can act as cell of origin for experimental glioma.* Oncogene, 2009. **28**(23): p. 2266-75.
186. Shoshan, Y., et al., *Expression of oligodendrocyte progenitor cell antigens by gliomas: implications for the histogenesis of brain tumors.* Proc Natl Acad Sci U S A, 1999. **96**(18): p. 10361-6.
187. Sugiarto, S., et al., *Asymmetry-defective oligodendrocyte progenitors are glioma precursors.* Cancer cell, 2011. **20**(3): p. 328-40.
188. Kondo, T. and M. Raff, *Oligodendrocyte precursor cells reprogrammed to become multipotential CNS stem cells.* Science, 2000. **289**(5485): p. 1754-7.
189. Peters, A. and C. Sethares, *Oligodendrocytes, their progenitors and other neuroglial cells in the aging primate cerebral cortex.* Cereb Cortex, 2004. **14**(9): p. 995-1007.
190. Belachew, S., et al., *Postnatal NG2 proteoglycan-expressing progenitor cells are intrinsically multipotent and generate functional neurons.* J Cell Biol, 2003. **161**(1): p. 169-86.
191. Ffrench-Constant, C. and M.C. Raff, *Proliferating bipotential glial progenitor cells in adult rat optic nerve.* Nature, 1986. **319**(6053): p. 499-502.
192. Warf, B.C., J. Fok-Seang, and R.H. Miller, *Evidence for the ventral origin of oligodendrocyte precursors in the rat spinal cord.* The Journal of neuroscience : the official journal of the Society for Neuroscience, 1991. **11**(8): p. 2477-88.
193. Levine, J.M., R. Reynolds, and J.W. Fawcett, *The oligodendrocyte precursor cell in health and disease.* Trends in neurosciences, 2001. **24**(1): p. 39-47.
194. Shoshan, Y., et al., *Expression of oligodendrocyte progenitor cell antigens by gliomas: implications for the histogenesis of brain tumors.* Proceedings of the National Academy of Sciences of the United States of America, 1999. **96**(18): p. 10361-6.
195. Chekenya, M. and G.J. Pilkington, *NG2 precursor cells in neoplasia: functional, histogenesis and therapeutic implications for malignant brain tumours.* Journal of neurocytology, 2002. **31**(6-7): p. 507-21.
196. Wolswijk, G. and M. Noble, *Cooperation between PDGF and FGF converts slowly dividing O-2Aadult progenitor cells to rapidly dividing cells with characteristics of O-2Aperinatal progenitor cells.* J Cell Biol, 1992. **118**(4): p. 889-900.
197. Jackson, E.L., et al., *PDGFR alpha-positive B cells are neural stem cells in the adult SVZ that form glioma-like growths in response to increased PDGF signaling.* Neuron, 2006. **51**(2): p. 187-99.
198. Heidaran, M.A., et al., *Role of alpha beta receptor heterodimer formation in beta platelet-derived growth factor (PDGF) receptor activation by PDGF-AB.* The Journal of biological chemistry, 1991. **266**(30): p. 20232-7.

199. Guha, A., et al., *Expression of PDGF and PDGF receptors in human astrocytoma operation specimens supports the existence of an autocrine loop.* Int J Cancer, 1995. **60**(2): p. 168-73.
200. Varela, M., et al., *EGF-R and PDGF-R, but not bcl-2, overexpression predict overall survival in patients with low-grade astrocytomas.* J Surg Oncol, 2004. **86**(1): p. 34-40.
201. Dai, C. and E.C. Holland, *Glioma models.* Biochimica et biophysica acta, 2001. **1551**(1): p. M19-27.
202. Lappe-Siefke, C., et al., *Disruption of Cnp1 uncouples oligodendroglial functions in axonal support and myelination.* Nat Genet, 2003. **33**(3): p. 366-74.
203. Spurrier, B., S. Ramalingam, and S. Nishizuka, *Reverse-phase protein lysate microarrays for cell signaling analysis.* Nature protocols, 2008. **3**(11): p. 1796-808.
204. Tibes, R., et al., *Reverse phase protein array: validation of a novel proteomic technology and utility for analysis of primary leukemia specimens and hematopoietic stem cells.* Molecular Cancer Therapeutics, 2006. **5**(10): p. 2512-21.
205. Goebbels, S., et al., *Elevated phosphatidylinositol 3,4,5-trisphosphate in glia triggers cell-autonomous membrane wrapping and myelination.* J Neurosci. **30**(26): p. 8953-64.
206. Andrechek, E.R., et al., *Gene expression profiling of neu-induced mammary tumors from transgenic mice reveals genetic and morphological similarities to ErbB2-expressing human breast cancers.* Cancer research, 2003. **63**(16): p. 4920-6.
207. Suzuki, A., et al., *T cell-specific loss of Pten leads to defects in central and peripheral tolerance.* Immunity, 2001. **14**(5): p. 523-34.
208. Spencer, S.L., et al., *Modeling somatic evolution in tumorigenesis.* PLoS computational biology, 2006. **2**(8): p. e108.
209. Clarke, L. and D. van der Kooy, *Low oxygen enhances primitive and definitive neural stem cell colony formation by inhibiting distinct cell death pathways.* Stem Cells, 2009. **27**(8): p. 1879-86.
210. Ernst, A., et al., *Genomic and expression profiling of glioblastoma stem cell-like spheroid cultures identifies novel tumor-relevant genes associated with survival.* Clinical cancer research : an official journal of the American Association for Cancer Research, 2009. **15**(21): p. 6541-50.
211. De Witt Hamer, P.C., et al., *The genomic profile of human malignant glioma is altered early in primary cell culture and preserved in spheroids.* Oncogene, 2008. **27**(14): p. 2091-6.
212. Griffero, F., et al., *Different response of human glioma tumor-initiating cells to epidermal growth factor receptor kinase inhibitors.* The Journal of biological chemistry, 2009. **284**(11): p. 7138-48.
213. Draberova, E., et al., *Class III beta-tubulin is constitutively coexpressed with glial fibrillary acidic protein and nestin in midgestational human fetal*

astrocytes: implications for phenotypic identity. Journal of neuropathology and experimental neurology, 2008. **67**(4): p. 341-54.
214. Pinkel, D., et al., *High resolution analysis of DNA copy number variation using comparative genomic hybridization to microarrays.* Nature genetics, 1998. **20**(2): p. 207-11.
215. Stankiewicz, P. and J.R. Lupski, *Structural variation in the human genome and its role in disease.* Annual review of medicine, 2010. **61**: p. 437-55.
216. Huang da, W., B.T. Sherman, and R.A. Lempicki, *Systematic and integrative analysis of large gene lists using DAVID bioinformatics resources.* Nature protocols, 2009. **4**(1): p. 44-57.
217. Huang da, W., B.T. Sherman, and R.A. Lempicki, *Bioinformatics enrichment tools: paths toward the comprehensive functional analysis of large gene lists.* Nucleic acids research, 2009. **37**(1): p. 1-13.
218. Sun, T., et al., *Olig bHLH proteins interact with homeodomain proteins to regulate cell fate acquisition in progenitors of the ventral neural tube.* Current biology : CB, 2001. **11**(18): p. 1413-20.
219. Zeisberg, M. and E.G. Neilson, *Biomarkers for epithelial-mesenchymal transitions.* The Journal of clinical investigation, 2009. **119**(6): p. 1429-37.
220. Olar, A. and K.D. Aldape, *Biomarkers classification and therapeutic decision-making for malignant gliomas.* Current treatment options in oncology, 2012. **13**(4): p. 417-36.
221. Gritti, A., et al., *Epidermal and fibroblast growth factors behave as mitogenic regulators for a single multipotent stem cell-like population from the subventricular region of the adult mouse forebrain.* J Neurosci, 1999. **19**(9): p. 3287-97.
222. Ricci-Vitiani, L., et al., *Mesenchymal differentiation of glioblastoma stem cells.* Cell death and differentiation, 2008. **15**(9): p. 1491-8.
223. Soleimani, M. and S. Nadri, *A protocol for isolation and culture of mesenchymal stem cells from mouse bone marrow.* Nature protocols, 2009. **4**(1): p. 102-6.
224. Pallini, R., et al., *Cancer stem cell analysis and clinical outcome in patients with glioblastoma multiforme.* Clinical cancer research : an official journal of the American Association for Cancer Research, 2008. **14**(24): p. 8205-12.
225. Dutt, A. and R. Beroukhim, *Single nucleotide polymorphism array analysis of cancer.* Current opinion in oncology, 2007. **19**(1): p. 43-9.
226. Szerlip, N.J., et al., *Intratumoral heterogeneity of receptor tyrosine kinases EGFR and PDGFRA amplification in glioblastoma defines subpopulations with distinct growth factor response.* Proceedings of the National Academy of Sciences of the United States of America, 2012. **109**(8): p. 3041-6.
227. Gunther, H.S., et al., *Glioblastoma-derived stem cell-enriched cultures form distinct subgroups according to molecular and phenotypic criteria.* Oncogene, 2008. **27**(20): p. 2897-909.
228. Clavreul, A., et al., *Isolation of a new cell population in the glioblastoma microenvironment.* Journal of neuro-oncology, 2012. **106**(3): p. 493-504.

229. McKeever, P.E., et al., *Products of cells from gliomas: IX. Evidence that two fundamentally different mechanisms change extracellular matrix expression by gliomas.* Journal of neuro-oncology, 1995. **24**(3): p. 267-80.
230. Gibbons, H.M., et al., *Cellular composition of human glial cultures from adult biopsy brain tissue.* Journal of neuroscience methods, 2007. **166**(1): p. 89-98.
231. Park, T.I., et al., *Adult human brain neural progenitor cells (NPCs) and fibroblast-like cells have similar properties in vitro but only NPCs differentiate into neurons.* PloS one, 2012. **7**(6): p. e37742.
232. Estes, M.L., et al., *Characterization of adult human astrocytes derived from explant culture.* Journal of neuroscience research, 1990. **27**(4): p. 697-705.
233. Norton, W.T., et al., *Pure astrocyte cultures derived from cells isolated from mature brain.* Glia, 1988. **1**(6): p. 403-14.
234. Yung, W.K., M. Luna, and A. Borit, *Vimentin and glial fibrillary acidic protein in human brain tumors.* Journal of neuro-oncology, 1985. **3**(1): p. 35-8.
235. Bhowmick, N.A., E.G. Neilson, and H.L. Moses, *Stromal fibroblasts in cancer initiation and progression.* Nature, 2004. **432**(7015): p. 332-7.
236. Yang, J. and R.A. Weinberg, *Epithelial-mesenchymal transition: at the crossroads of development and tumor metastasis.* Developmental cell, 2008. **14**(6): p. 818-29.
237. WE, D., *Removal of right cerebral hemisphere for certain tumors with hemiplegia.* JAMA : the journal of the American Medical Association, 1928. **90**(11): p. 823-825.
238. Kitange, G.J., et al., *Induction of MGMT expression is associated with temozolomide resistance in glioblastoma xenografts.* Neuro-oncology, 2009. **11**(3): p. 281-91.
239. Amberger-Murphy, V., *Glioma invasion: mechanism, modulation and future possibilities.* Acta neurochirurgica, 2003. **145**(8): p. 613-4.
240. Friedrich, J., et al., *Spheroid-based drug screen: considerations and practical approach.* Nature protocols, 2009. **4**(3): p. 309-24.
241. Chakravarti, A., et al., *The prognostic significance of phosphatidylinositol 3-kinase pathway activation in human gliomas.* Journal of clinical oncology : official journal of the American Society of Clinical Oncology, 2004. **22**(10): p. 1926-33.
242. Rasheed, B.K., et al., *Molecular pathogenesis of malignant gliomas.* Current opinion in oncology, 1999. **11**(3): p. 162-7.
243. Wiencke, J.K., et al., *Methylation of the PTEN promoter defines low-grade gliomas and secondary glioblastoma.* Neuro-oncology, 2007. **9**(3): p. 271-9.
244. GraphPad. *50% of what? How exactly are IC50 and EC50 defined?* ; Available from: http://www.graphpad.com/support/faqid/1356/.
245. Vlahos, C.J., et al., *A specific inhibitor of phosphatidylinositol 3-kinase, 2-(4-morpholinyl)-8-phenyl-4H-1-benzopyran-4-one (LY294002).* The Journal of biological chemistry, 1994. **269**(7): p. 5241-8.

246. Gharbi, S.I., et al., *Exploring the specificity of the PI3K family inhibitor LY294002.* The Biochemical journal, 2007. **404**(1): p. 15-21.
247. Dumont, F.J. and Q. Su, *Mechanism of action of the immunosuppressant rapamycin.* Life sciences, 1996. **58**(5): p. 373-95.
248. Malagu, K., et al., *The discovery and optimisation of pyrido[2,3-d]pyrimidine-2,4-diamines as potent and selective inhibitors of mTOR kinase.* Bioorganic & medicinal chemistry letters, 2009. **19**(20): p. 5950-3.
249. Ashley, D.M., et al., *In vitro sensitivity testing of minimally passaged and uncultured gliomas with TRAIL and/or chemotherapy drugs.* British journal of cancer, 2008. **99**(2): p. 294-304.
250. Rubinstein, L.V., et al., *Comparison of in vitro anticancer-drug-screening data generated with a tetrazolium assay versus a protein assay against a diverse panel of human tumor cell lines.* Journal of the National Cancer Institute, 1990. **82**(13): p. 1113-8.
251. Gal, H., et al., *A rapid assay for drug sensitivity of glioblastoma stem cells.* Biochemical and biophysical research communications, 2007. **358**(3): p. 908-13.
252. Cen, H., et al., *DEVD-NucView488: a novel class of enzyme substrates for real-time detection of caspase-3 activity in live cells.* FASEB journal : official publication of the Federation of American Societies for Experimental Biology, 2008. **22**(7): p. 2243-52.
253. Roth, B.L., et al., *Bacterial viability and antibiotic susceptibility testing with SYTOX green nucleic acid stain.* Applied and environmental microbiology, 1997. **63**(6): p. 2421-31.
254. Latt, S.A., et al., *Recent developments in the detection of deoxyribonucleic acid synthesis by 33258 Hoechst fluorescence.* The journal of histochemistry and cytochemistry : official journal of the Histochemistry Society, 1975. **23**(7): p. 493-505.
255. Hans, F. and S. Dimitrov, *Histone H3 phosphorylation and cell division.* Oncogene, 2001. **20**(24): p. 3021-7.
256. Keen, N. and S. Taylor, *Aurora-kinase inhibitors as anticancer agents.* Nature reviews. Cancer, 2004. **4**(12): p. 927-36.
257. Ivkovic, S., et al., *Direct inhibition of myosin II effectively blocks glioma invasion in the presence of multiple motogens.* Molecular biology of the cell, 2012. **23**(4): p. 533-42.
258. Hennigan, R.F., K.L. Hawker, and B.W. Ozanne, *Fos-transformation activates genes associated with invasion.* Oncogene, 1994. **9**(12): p. 3591-600.
259. Kaufman, L.J., et al., *Glioma expansion in collagen I matrices: analyzing collagen concentration-dependent growth and motility patterns.* Biophysical journal, 2005. **89**(1): p. 635-50.
260. Lamszus, K., et al., *Scatter factor promotes motility of human glioma and neuromicrovascular endothelial cells.* International journal of cancer. Journal international du cancer, 1998. **75**(1): p. 19-28.

261. Heese, O., et al., *Neural stem cell migration toward gliomas in vitro.* Neuro-oncology, 2005. **7**(4): p. 476-84.
262. *clinicaltrials.gov.*
263. Vivanco, I. and C.L. Sawyers, *The phosphatidylinositol 3-Kinase AKT pathway in human cancer.* Nature reviews. Cancer, 2002. **2**(7): p. 489-501.
264. Samuels, Y., et al., *High frequency of mutations of the PIK3CA gene in human cancers.* Science, 2004. **304**(5670): p. 554.
265. Martin, R.M., H. Leonhardt, and M.C. Cardoso, *DNA labeling in living cells.* Cytometry. Part A : the journal of the International Society for Analytical Cytology, 2005. **67**(1): p. 45-52.
266. Torbett, N.E., et al., *A chemical screen in diverse breast cancer cell lines reveals genetic enhancers and suppressors of sensitivity to PI3K isoform-selective inhibition.* The Biochemical journal, 2008. **415**(1): p. 97-110.
267. Talekar, M., et al., *Phosphatidylinositol 3-kinase inhibitor (PIK75) containing surface functionalized nanoemulsion for enhanced drug delivery, cytotoxicity and pro-apoptotic activity in ovarian cancer cells.* Pharmaceutical research, 2012. **29**(10): p. 2874-86.
268. Dagia, N.M., et al., *A preferential p110alpha/gamma PI3K inhibitor attenuates experimental inflammation by suppressing the production of proinflammatory mediators in a NF-kappaB-dependent manner.* American journal of physiology. Cell physiology, 2010. **298**(4): p. C929-41.
269. Smirnova, T., et al., *Phosphoinositide 3-kinase signaling is critical for ErbB3-driven breast cancer cell motility and metastasis.* Oncogene, 2012. **31**(6): p. 706-15.
270. Sheridan, R.P. and S.K. Kearsley, *Why do we need so many chemical similarity search methods?* Drug discovery today, 2002. **7**(17): p. 903-11.
271. Ovcharenko, D., et al., *High-throughput RNAi screening in vitro: from cell lines to primary cells.* RNA, 2005. **11**(6): p. 985-93.
272. Zhou, F.X., J. Bonin, and P.F. Predki, *Development of functional protein microarrays for drug discovery: progress and challenges.* Combinatorial chemistry & high throughput screening, 2004. **7**(6): p. 539-46.
273. Antony, A.C., *Folate receptors.* Annual review of nutrition, 1996. **16**: p. 501-21.
274. Barbu, E., et al., *The potential for nanoparticle-based drug delivery to the brain: overcoming the blood-brain barrier.* Expert opinion on drug delivery, 2009. **6**(6): p. 553-65.
275. Hu, B., et al., *Angiopoietin-2 induces human glioma invasion through the activation of matrix metalloprotease-2.* Proceedings of the National Academy of Sciences of the United States of America, 2003. **100**(15): p. 8904-9.
276. Demuth, T. and M.E. Berens, *Molecular mechanisms of glioma cell migration and invasion.* Journal of neuro-oncology, 2004. **70**(2): p. 217-28.
277. Mihaliak, A.M., et al., *Clinically relevant doses of chemotherapy agents reversibly block formation of glioblastoma neurospheres.* Cancer letters, 2010. **296**(2): p. 168-77.

278. Huszthy, P.C., et al., *In vivo models of primary brain tumors: pitfalls and perspectives.* Neuro-oncology, 2012. **14**(8): p. 979-93.
279. Schmid, R.S., M. Vitucci, and C.R. Miller, *Genetically engineered mouse models of diffuse gliomas.* Brain research bulletin, 2011.
280. Penninger, J.M. and J. Woodgett, *Stem cells. PTEN--coupling tumor suppression to stem cells?* Science, 2001. **294**(5549): p. 2116-8.
281. Hennighausen, L., *Mouse models for breast cancer.* Breast cancer research : BCR, 2000. **2**(1): p. 2-7.
282. Andrechek, E.R., et al., *Amplification of the neu/erbB-2 oncogene in a mouse model of mammary tumorigenesis.* Proceedings of the National Academy of Sciences of the United States of America, 2000. **97**(7): p. 3444-9.
283. *Comprehensive genomic characterization defines human glioblastoma genes and core pathways.* Nature, 2008. **455**(7216): p. 1061-8.
284. Andersson, U., et al., *Epidermal growth factor receptor family (EGFR, ErbB2-4) in gliomas and meningiomas.* Acta Neuropathol, 2004. **108**(2): p. 135-42.
285. Aguirre, A., et al., *A functional role for EGFR signaling in myelination and remyelination.* Nat Neurosci, 2007. **10**(8): p. 990-1002.
286. Park, S.K., et al., *The erbB2 gene is required for the development of terminally differentiated spinal cord oligodendrocytes.* The Journal of cell biology, 2001. **154**(6): p. 1245-58.
287. Schmid, R.S., et al., *Neuregulin 1-erbB2 signaling is required for the establishment of radial glia and their transformation into astrocytes in cerebral cortex.* Proceedings of the National Academy of Sciences of the United States of America, 2003. **100**(7): p. 4251-6.
288. Stemmer-Rachamimov, A.O., et al., *Comparative pathology of nerve sheath tumors in mouse models and humans.* Cancer research, 2004. **64**(10): p. 3718-24.
289. Gregorian, C., et al., *PTEN dosage is essential for neurofibroma development and malignant transformation.* Proc Natl Acad Sci U S A, 2009. **106**(46): p. 19479-84.
290. Anghileri, M., et al., *Malignant peripheral nerve sheath tumors: prognostic factors and survival in a series of patients treated at a single institution.* Cancer, 2006. **107**(5): p. 1065-74.
291. Baehring, J.M., R.A. Betensky, and T.T. Batchelor, *Malignant peripheral nerve sheath tumor: the clinical spectrum and outcome of treatment.* Neurology, 2003. **61**(5): p. 696-8.
292. Ducatman, B.S., et al., *Malignant peripheral nerve sheath tumors. A clinicopathologic study of 120 cases.* Cancer, 1986. **57**(10): p. 2006-21.
293. McCaughan, J.A., et al., *Further evidence of the increased risk for malignant peripheral nerve sheath tumour from a Scottish cohort of patients with neurofibromatosis type 1.* J Med Genet, 2007. **44**(7): p. 463-6.
294. Brems, H., et al., *Mechanisms in the pathogenesis of malignant tumours in neurofibromatosis type 1.* Lancet Oncol, 2009. **10**(5): p. 508-15.

295. Erlandson, R.A. and J.M. Woodruff, *Peripheral nerve sheath tumors: an electron microscopic study of 43 cases.* Cancer, 1982. **49**(2): p. 273-87.
296. Keng, V.W., et al., *Conditional Inactivation of Pten with EGFR Overexpression in Schwann Cells Models Sporadic MPNST.* Sarcoma, 2012. **2012**: p. 620834.
297. Nonaka, D., L. Chiriboga, and B.P. Rubin, *Differential expression of S100 protein subtypes in malignant melanoma, and benign and malignant peripheral nerve sheath tumors.* Journal of cutaneous pathology, 2008. **35**(11): p. 1014-9.
298. Trapp, B.D., et al., *Cellular and subcellular distribution of 2',3'-cyclic nucleotide 3'-phosphodiesterase and its mRNA in the rat central nervous system.* Journal of neurochemistry, 1988. **51**(3): p. 859-68.
299. Talbott, J.F., et al., *Schwann cell-like differentiation by adult oligodendrocyte precursor cells following engraftment into the demyelinated spinal cord is BMP-dependent.* Glia, 2006. **54**(3): p. 147-59.
300. Sprinkle, T.J., *2',3'-cyclic nucleotide 3'-phosphodiesterase, an oligodendrocyte-Schwann cell and myelin-associated enzyme of the nervous system.* Critical reviews in neurobiology, 1989. **4**(3): p. 235-301.
301. Yuan, X., et al., *Expression of the green fluorescent protein in the oligodendrocyte lineage: a transgenic mouse for developmental and physiological studies.* Journal of neuroscience research, 2002. **70**(4): p. 529-45.
302. Holtkamp, N., et al., *EGFR and erbB2 in malignant peripheral nerve sheath tumors and implications for targeted therapy.* Neuro Oncol, 2008. **10**(6): p. 946-57.
303. Atanasoski, S., et al., *ErbB2 signaling in Schwann cells is mostly dispensable for maintenance of myelinated peripheral nerves and proliferation of adult Schwann cells after injury.* J Neurosci, 2006. **26**(7): p. 2124-31.
304. Dey, N., et al., *The protein phosphatase activity of PTEN regulates SRC family kinases and controls glioma migration.* Cancer Res, 2008. **68**(6): p. 1862-71.
305. Holland, E.C., et al., *Combined activation of Ras and Akt in neural progenitors induces glioblastoma formation in mice.* Nature genetics, 2000. **25**(1): p. 55-7.
306. Gregorian, C., et al., *PTEN dosage is essential for neurofibroma development and malignant transformation.* Proceedings of the National Academy of Sciences of the United States of America, 2009. **106**(46): p. 19479-84.
307. Mayes, D.A., et al., *Perinatal or adult Nf1 inactivation using tamoxifen-inducible PlpCre each cause neurofibroma formation.* Cancer research, 2011. **71**(13): p. 4675-85.
308. Michalski, J.P., et al., *The proteolipid protein promoter drives expression outside of the oligodendrocyte lineage during embryonic and early postnatal development.* PloS one, 2011. **6**(5): p. e19772.
309. Klugmann, M., et al., *Assembly of CNS myelin in the absence of proteolipid protein.* Neuron, 1997. **18**(1): p. 59-70.

310. Brossier, N.M. and S.L. Carroll, *Genetically engineered mouse models shed new light on the pathogenesis of neurofibromatosis type I-related neoplasms of the peripheral nervous system.* Brain research bulletin, 2011.
311. Bottillo, I., et al., *Germline and somatic NF1 mutations in sporadic and NF1-associated malignant peripheral nerve sheath tumours.* The Journal of pathology, 2009. **217**(5): p. 693-701.
312. Slamon, D.J., et al., *Use of chemotherapy plus a monoclonal antibody against HER2 for metastatic breast cancer that overexpresses HER2.* The New England journal of medicine, 2001. **344**(11): p. 783-92.
313. Shao, C., et al., *Bystander signaling between glioma cells and fibroblasts targeted with counted particles.* International journal of cancer. Journal international du cancer, 2005. **116**(1): p. 45-51.
314. von Deimling, A., A. Korshunov, and C. Hartmann, *The next generation of glioma biomarkers: MGMT methylation, BRAF fusions and IDH1 mutations.* Brain pathology, 2011. **21**(1): p. 74-87.
315. Carragher, N.O., V.G. Brunton, and M.C. Frame, *Combining imaging and pathway profiling: an alternative approach to cancer drug discovery.* Drug discovery today, 2012. **17**(5-6): p. 203-14.

Appendix 1. The table summarises the experiments presented in Chapter 3 and the primary culture each experiment was performed on.

Summary of experiments for Chapter 3	L	M	N	O	P	Q	R	S	T	U	V	X	Y	Z	AA	BB	CC	DD	EE
Successful expansion of primary culture (Table 3.1)	X	X	X	X	X				X	X	X	X	X	X	X	X	X	X	X
Tumours from which multiple biopsies were taken															X	X	X	X	X
Comparison of oxygen/media conditions (Table 3.2)					X	X	X	X	X	X									
Comparison of substrate conditions (Table 3.3)	X	X	X	X	X	X	X	X	X	X									
Enrichment of CD133 cell fraction (Tables 3.5-3.6)	X	X	X	X	X														
Tumour grown in normoxic and hypoxic conditions					X	X	X	X	X	X				X	X	X	X	X	
Growth **and senescence** characterisation (Figure 3.7)					**X**							X					**X**	X	**X**
Assessment of clonogenicity (Table 3.9)					X							X					X	X	X
Immunofluorescence:stem cell markers (Table 3.10)		X			X				X		X	X		X	X	X	X	X	
DNA copy number changes (Figures 3.10-3.14)	X	X		X								X			X	X	X	X	X
Gene expression: clustering (Figure 3.15)																X	X	X	
Gene expression– RT PCR (Figures 3.16-3.17)					X							X			X	X	X	X	X
Heterotopic xenotransplantation												X							
Orthotopic xenotransplantation					X							X					X	X	
Primary culture cell phenotype	Branched	Branched	Branched	Branched	Branched				Branched	Branched	Flat	Branched	Flat	Flat	Flat	Flat/branched	Flat	Branched	Flat/branched

Appendix 2. The table summarises the experiments presented in Chapter 3 and the primary culture each experiment was performed on.

Summary of experiments for Chapter 4	L	M	N	O	P	Q	R	S	T	U	V	X	Y	Z	AA	BB	CC	DD	EE
Assessment of PTEN status (Table 4.1)	X	X		X							X	X	X		X	X	X	X	X
PI3 kinase pathway inhibitor screen (Table 4.3)	X	X	X	X	X					X		X		X					
Neurosphere inhibitor assay												X							
PIK75 Apoptotic cell death assay (Figure 4.5)					X							X					X	X	X
PIK75 Sytox Green cell death assay (Figure 4.6)					X							X						X	
PIK75 Cell cycle assay (Figure 4.7)												X					X	X	X
PIK75 phospho-histone H3 assay (Figure 4.8)					X							X						X	
KU63794/ Barasertib assay (Figures 4.9-4.11)					X							X					X	X	X
Barasertib cell cycle assay (Figure 4.12)					X							X						X	
Barasertib phospho-histone assay (Figure 4.13)					X							X						X	
PIK75 PI3 kinase signaling assay (Figures 4.14)					X												X	X	
Glioma cell invasion assays					X							X					X	X	X
C-met inhibitor assays					X							X					X	X	X
Primary culture cell phenotype	Branched	Branched	Branched	Branched	Branched				Branched	Branched	Flat	Branched	Flat	Flat	Flat	Flat/branched	Flat	Branched	Flat/branched